THE PRESSURE, VOLUME, TEMPERATURE, AND COMPOSITION PROPERTIES OF LIQUID n-ALKANE MIXTURES AT ELEVATED PRESSURES

A Dissertation

Presented to

the Faculty of the Graduate School

University of Missouri

In Partial Fulfillment

of the Requirements for the Degree

Doctor of Philosophy

---

by

Phillip Sidney Snyder

August 1969

Jack Winnick, Dissertation Supervisor

ACKNOWLEDGEMENT

The author wishes to express his sincere appreciation to Dr. Jack Winnick of the Chemical Engineering Department for his assistance during the course of this project. To Mr. Joseph Twenter, and the men of the Science Instrument shop for construction of part of the experimental apparatus.

The author also wishes to express his gratitude to the University of Missouri Computer Research Center and the Engineering Computer Center for the use of their facilities, the National Science Foundation for financial support through grant NSF GK-1303, and the National Aeronautics and Space Administration for a NASA Traineeship.

Special thanks go to my devoted wife Linda and my twin sons Tom and John without whose understanding and patience this project might never have been completed.

TABLE OF CONTENTS

CHAPTER PAGE

CHAPTER PAGE

LIST OF FIGURES

FIGURE PAGE

FIGURE PAGE

FIGURE PAGE

FIGURE PAGE

FIGURE PAGE

LIST OF TABLES

CHAPTER I

INTRODUCTION

Chemical engineers and chemists have long been in search of a general equation of state. Given the equation of state and appropriate thermodynamic relationships it is possible to accurately predict isothermal changes in heat capacity, enthalpy, entropy and fugacity, activity coefficients, latent heat of vaporization, vapor pressure, and vapor-liquid equilibrium in mixtures. To date it has not been found.

One attempt to write a specific equation of state has been made for chlorodifluoromethane (36), for example, to densities up to 2.3 times the critical density. This equation of state has 44 constants, making it impractical for general use and at very best cumbersome to work with.

A logical limitation on an equation of state would be to require that it be valid for one phase only. This requires a different equation for each of the gas, liquid, and solid phases.

The gas phase is characterized by low density and molecular encounters that mainly occur between only two molecules at one time, has been described by simple

equations of state (i.e. the ideal gas law and first order corrections such as those of the van der Walls equations of state). This is the starting point for more detailed and accurate equations of state to describe the gas phase of real gases. Some of these are based upon kinetic theory (9,44) and statistical thermodynamics (29). This has lead to highly successful equations of state such as the virial equation.

The solid phase with its high degree of spatial ordering and the small amplitudes of the thermal motions can also be described by an equation of state. As in the case of the gas phase this allows a starting point for more detailed theories and accurate equations of state. Some are based, for example, upon the "integrated linear theory of finite strains" (39).

For the liquid phase there appears to be no obvious element of simplicity comparable to those for the gas and solid phases. In the liquid state one is faced with long range disorder and multi-molecular interactions.

The least restrictive liquid theory is based on the radial distribution function (18,25). The successful Percus-Yevick equation of state falls into this catagory. There are other equations based on the radial distribution function theory. The major short coming of the radial distribution function type theories is that they

require experimental x-ray scattering data from which the radial distribution function is determined. It is difficult if not impossible to interpret this data for polyatomic molecules without making major assumptions.

Scaled particle theory, a new liquid theory, was proposed by Reiss (47) in 1959. To date it has been applied mainly to spherical molecules and liquid metals. It has met with some success, but has not as yet been tested for cases where pressure was allowed to vary.

More restrictive liquid theories assume either a solid-like or gas-like model. The more successful have been based on a lattice-like structure, as is used in the various lattice theories of the liquid state (4). This assumption of the liquid structure essentially means that the liquid is being considered as a superheated solid. This theory works best in the high pressure, high density and low temperature region of the liquid phase or near the freezing curve.

The other assumption is that the liquid is a super cooled gas (46). These theories work best at high temperature and low density. The major short coming of these two classes of liquid theories is that they are successful only for spherical molecules with essentially central force fields such as Argon, Neon and, Methane for example.

The "Significant Structure Theory" of Eyring (20) predicts liquid properties to within 10% in many cases (34,35). Existing liquid p-v-T data is sufficiently refined to test its p-v-T predictions completely (61).

To be able to consider industrially more interesting molecules, but still simple compared to those with hydrogen bonding and/or polar fields, it is necessary to make even more restrictive assumptions, such as those of the Corresponding States Principle (31). The basic assumptions, detailed by Leland and Chappelear (32), exclude molecules with hydrogen bonding and molecules light enough for quantum effects to become important. The major problem with the Corresponding States Principle is that in some cases the predicted properties are nearly exact, but in others they may err as much as 10%. There seems to be no method short of taking experimental data to determine the accuracy of the prediction using these correlations.

To obtain predictive methods of greater accuracy than those listed above with the exception of Scaled particle theory, as it has not been tested, it is necessary to restrict the theory to one type or class of compounds such as the normal paraffins. This has been done by Flory (21) and Prausnitz (42) in their liquid partition function models. Both of these theories require some experimental

data to determine what are called characteristic or reducing parameters. The Prausnitz theory (42) was found to work very well for simple liquids and over moderate pressure ranges. The Flory theory was tested by Sims and Winnick (58) for n-Decane, n-Dodecane, n-Tetradecane, n-Hexadecane, and several binary mixtures and found to correlate their atmospheric density data as a function of temperature to within experimental error.

Thus there appear to be three possible method of predicting liquid p-v-T data with high accuracy. That is: the Scaled particle theory, the Prausnitz partition function theory, and the Flory partition function theory. One of the most stringent tests that can be applied to an equation of state is to determine the isothermal compressibility equation from it because the isothermal compressibility equation requires a derivative of the equation of state. Using the Prausnitz and Flory partition function theories for the isothermal compressibility this requires the second derivative of the partition function. Each of these theories requires some data to determine the free parameters, the effective spherical radius in the Scaled particle theory and characteristic parameters in the Prausnitz and Flory theories. Once the parameters are

determined the equations can be used to predict values of the isothermal compressibility, the isothermal changes in heat capacity, enthalpy, entropy and fugacity, activity coefficients, latent heat of vaporization, vapor pressure, and vapor-liquid equilibrium in mixtures.

To test the isothermal compressibility predictions very accurate experimental p-v-T data are necessary to test these predictions. To provide the most severe test the p-v-T data should be for the widest possible range of temperature and pressure. It is also desirable that the data be available for more than one compound and preferably for a homologous series.

CHAPTER II

THEORIES TESTED

The three liquid theories to be tested and the mixing rules are considered in this chapter. In the case of the Prausnitz partition function theory the assumptions basic to the derivation are presented. Then the configurational partition function, the equation of state, and the isothermal compressibility equation are presented. Following this the basic assumptions of the Flory configurational partition function theory is considered in the light of how its basic assumptions differ from those of the Prausnitz configurational partition function theory. Then the configurational partition function, the equation of state, and the isothermal compressibility equation are presented. For the Scaled particle theory the assumptions basic to the derivation are presented. Then the equation of state and isothermal compressibility equation are presented. In the last section the mixing rules are considered.

I. PRAUSNITZ PARTITION FUNCTION

The Prausnitz configurational partition function, Q_p, is based on the cell theory of liquids. The functional form of Ψ^N and exp(-E/kT) are modified by assumptions to the standard cell theory configurational partition function (4);

$$Q = \Psi^N \exp(-E/kT). \qquad \text{(II-1)}$$

The assumptions are:

1. Ψ^N can be written as the product of a function of volume only $f_1(\tilde{V})$ and a function of volume and temperature only $f_2(\tilde{V},\tilde{T})$ (60).
2. $f_1(\tilde{V})$ can be functionally written as $(\tilde{V}^{1/3}-1.)$ (1,19,23,45).
3. $f_2(\tilde{V},\tilde{T})$ can be assumed to be $f_2(\tilde{T})$ due to the small variation in liquid density relative to the gas (53).
4. $f_2(\tilde{T})$ can be written as $\left(\frac{0.4}{3\tilde{T}^2}\right)$. This is based upon analysis of existing experimental heat capacity data.
5. That E in the exp(-E/kT) can be assumed to be a function of volume only (53). That is:

$$E = E(V) = P^* V^* \tilde{E}(\tilde{V}) = \frac{P^* V^*}{\tilde{V}} . \qquad \text{(II-2)}$$

6. That the characteristic parameters P*, V*, T* are temperature independent due to their relationship to the molecular parameters (55).
7. In addition to the above assumptions made by Prausnitz, one more is added here: that the partition function and all the assumptions apply to the normal paraffins.

The Prausnitz configurational partition function, Q_p, developed using the above assumptions is given in equation II-3. Its development has been presented in the literature (43,52,53).

$$Q_p = \left[V^{*\frac{1}{3}} \left(\tilde{V}^{\frac{1}{3}} - 1\right) \exp\left(\frac{0.4}{3\tilde{T}^2}\right)\right]^{3Nc} \exp\left(\frac{P^* V^*}{kT} \frac{1}{\tilde{V}}\right). \qquad \text{(II-3)}$$

where: V* is the characteristic volume, P* is the characteristic pressure, T* is the characteristic temperature, $\tilde{V}$ is the reduced volume defined in equation II-4, $\tilde{P}$ is the reduced pressure defined in equation II-4, and $\tilde{T}$ is the reduced temperature defined in equation II-4, c is a parameter related to the departure from spherical symmetry (that is, the departure from non-central force fields).

$$\tilde{V} = V/V^*$$
$$\tilde{P} = P/P^*$$
$$\tilde{T} = T/T^* \qquad \text{(II-4)}$$

The equation of state based upon II-1 is:

$$\frac{10.\,\tilde{P}\,\tilde{V}}{\tilde{T}} = \frac{\tilde{V}^{\frac{1}{3}}}{\tilde{V}^{\frac{1}{3}}-1.} - \frac{10.}{\tilde{V}\,\tilde{T}} \qquad \text{(II-5)}$$

and the isothermal compressibility is:

$$\tilde{\beta} = \beta P^{*} = \frac{\tilde{V}^{\frac{1}{3}} - 1.}{\tilde{P}\left(\tilde{V}^{\frac{1}{3}} - 2/3.\right) - \tilde{V}^{-2}\left(\tilde{V}^{\frac{1}{3}} - 4/3.\right)} \,. \qquad \text{(II-6)}$$

II. FLORY PARTITION FUNCTION

The Flory configurational partition function is identical to the Prausnitz configurational partition function except for the term $(\exp \frac{0.4}{3\tilde{T}^{2}})^{3Nc}$.

There are two basic differences in assumptions which lead to the difference in the configurational partition functions of Flory and Prausnitz. These are:

1. The Prausnitz assumption four is changed to: $f_2(T) = 1$.
2. The Prausnitz assumption six is changed to: P*, V*, T* are not temperature independent due to their relationship to the segment parameters (21).

The first assumption means that the Flory configurational partition function, Q_f, will always give configurational heat capacities equal to zero. This limits its application to the p-v-T properties.

The second difference between these theories is that Prausnitz assumes that the characteristic parameters are related to molecular contributions and molecular parameters and thus are temperature independent. Flory assumes that the characteristic parameters are related to segment contributions and segment parameters and that they are not temperature independent (21).

The Flory configurational partition function, Q_f, developed using the above assumptions is given in equation II-7, and its development has been presented by Flory (21,22).

$$Q_f = \left[V^{*1/3} \left(\tilde{V}^{1/3} - 1. \right) \cdot 1. \right]^{3Nc} \exp\left(\frac{P^* V^*}{kT} \frac{1}{\tilde{V}} \right) \qquad \text{(II-7)}$$

Where c is the number of external degrees of freedom per segment.

The equation of state based upon equation II-7 is:

$$\frac{10.\tilde{P}\tilde{V}}{\tilde{T}} = \frac{\tilde{V}^{1/3}}{\tilde{V}^{1/3} - 1.} - \frac{10.}{\tilde{V}\tilde{T}} \qquad \text{(II-8)}$$

and the isothermal compressibility is

$$\tilde{\beta} = \beta P^* = \frac{\tilde{V}^{1/3} - 1.}{\tilde{P}(\tilde{V}^{1/3} - 2/3.) - \tilde{V}^{-2}(\tilde{V}^{1/3} - 4/3.)} \quad . \tag{II-9}$$

Since equations II-5 and II-8 are identical it becomes a matter of testing the second basic difference, discussed above. That is what significance is attached to the characteristic parameters and how they are evaluated.

III. SCALED PARTICLE THEORY

The assumptions involved in developing the Scaled particle theory equation of state are:

1. The particles are spherically symmetric with central force fields.
2. The particles interact with an effective rigid sphere potential.
3. The work, W(r), required to produce the cavity can be approximated by $W(r) = k_o + K_1 r + K_2 r^2 + K_3 r^3$ (50), where r is the cavity radius.
4. The effective hard sphere radius, A, is not a function of pressure.
5. The assumption that the equation of state given by II-10 is valid for the n-paraffins has already been made by Mayer (37) and has been shown to be reasonably valid at atmospheric pressure.

The scaled particle theory equation of state developed using these assumptions is given by equation II-10, and its development has been presented in the literature (48, 49, 50).

$$\frac{\pi A^3 P}{6kT} = \frac{y(1. + y + y^2)}{(1. - y^3)} . \qquad \text{(II-10)}$$

where: P is the pressure, k is the Boltzmann constant, T is the absolute temperature, A is the effective hard sphere radius, and y is a reduced volume defined in equation II-11.

$$y = \frac{\pi A^3 N}{6V} . \qquad \text{(II-11)}$$

where: N is Avogardro's number, and V is the volume.

The isothermal compressibility is obtained from equation II-10:

$$\beta = \frac{V(1. - y)^4}{RT(1. + 2y)^2} . \qquad \text{(II-12)}$$

IV. MIXING RULES

Prausnitz Mixing Rules

Prausnitz (42) proposed a set of mixing rules based upon a modification of the geometric mean rule. These mixing rules require the second virial coefficients for the mixture to evaluate the parameter his modification introduces. Since these data are not available for the mixtures studied in this work the Prausnitz mixing rules will not be considered.

Flory Mixing Rules

Flory (22) proposes a mixing rule based upon the assumption that any two mixtures or a mixture and a compound which have identical numbers of each type of segments present should have the same physical properties and thus the same characteristic parameters. In the case of the n-paraffins there are two types of segments; end segments which are $-CH_3$ groups and $-CH_2-$ groups which are middle segments. As an illustrative example consider a 0.5 mole fraction mixture of n-Decane and n-Tetradecane. n-Decane has two end segments and eight central segments while n-Tetradecane has two end segments and twelve central segments. For a 0.5 mole fraction mixture n-Decane contributes one end segment and four central segments while n-Tetradecane contributes one end segment and six

central segments. Thus the resulting mixture has two end segments and ten central segments and would be expected to have the same physical properties as n-Dodecane. Flory's mixing rule is basically a segment fraction mixing rule.

Scaled Particle Theory

To date no mixing rules have been presented for scaled particle theory.

CHAPTER III

LITERATURE DATA

Accurate experimental data for pure components and their mixtures are necessary to test the above liquid state theories and mixing rule. To define more precisely what accuracy is required of the data, consider the following: When a liquid normal paraffin is subjected to 50,000 psi at room temperature the maximum change in volume that occurs will be about 20%. That is, the relative volume would be 0.80000. If the relative volume is known to ± 0.001, then the change in relative volume would be known only to ± 0.5%. At lower pressures the accuracy would be even lower. Sims (58) reported that at 65.°C for the system n-Decane and n-Hexadecane the maximum change in volume on mixing is + 0.5%. Thus to be able to test the three liquid theories and the mixing rule the data must be accurate to ± 0.0002 in the relative volume. The data should be available over a broad range of temperature and pressure to provide the most stringent test. Data for the normal paraffins found in the literature are listed below.

I. LIQUID P-V-T DATA

The data cited below are listed in chronological order. In addition to the compounds the temperature and pressure range are also given.

Bridgman

Bridgman (7) reported PVT data for n-pentane, n-hexane, n-heptane, n-octane, and n-decane at 0.0, 50,0, and 95°C up to the freezing pressure or 10,000 kg/cm^2, which ever came first on each isotherm. These data are reported to four significant digits, but considering calibration techniques available when the data were taken it is unlikely that the claimed absolute accuracy was obtained. It is more likely that the data was precise to four significant digits, accurate to three.

Eduljee

Eduljee *et al.* (17) reported data for n-hexane, n-heptane, and n-octane at 0.0, 25.0, 40.0, and 60°C up to the freezing pressure or 5000 atmospheres, which ever came first on each isotherm. They also reported Tait coefficients (59) for eight binary mixtures and two ternary mixtures but the experimental data are not included. A detailed error analysis of the experimental method (see

Appendix G) indicates the data are accurate to three significant digits with ± 0.0004 precision. The data are reported to four significant digits.

Cutler and McMickle

Cutler and McMickle (10) reported data for n-dodecane, n-pentadecane, and n-octadecane at 37.8, 60.0, 79.4, 98.9, 115.0, 135.0°C up to the freezing pressure on each isotherm. Cutler (11) reports that the slide wire used in their sylphon bellows piezometer was non-linear by ± 2%, but the wire was considered to be uniform and thus the average resistance per unit length was used. As can be seen from the error analysis in Appendix B an error of 2% in the linearity of the slide wire would mean that at best the data could be accurate to three significant digits.

Doolittle

Doolittle (14) reported smoothed data for n-heptane, n-nonane, n-undecane, n-tridecane, n-heptadecane, n-eicosane, n-tricontane, and n-tetracontane at 30.0, 50.0, 100.0, 150.0, 200.0, 250.0, and 300.0°C up to the freezing pressure or 3000 bars, which ever came first on each isotherm. It should be noted that the data reported are generated from a fit of the Hudleston equation to the raw data (13). It should also be noted that the technique was such that the initial weight of sample was not known to

better than 0.1% (15). These factors limit the absolute accuracy of the data to three significant digits. To obtain the fourth digit Doolittle used the initial sample volume as an adjustable parameter in the Hudleston equation and back calculated from the data the initial sample volume and thus its weight (16).

Boelhouwer

Boelhouwer (5) reported data for n-Heptane, n-octane, n-nonane, n-dodecane, and n-hexadecane at 30.0, 60.0, 90.0, 120.0°C up to the freezing pressure or 1200 kg/cm^2, which ever came first at a given temperature. This data is reported to four significant digits. Boelhouwer reports his relative volume data is absooute to 0.04%. The pressure range is such that the minimum relative volume obtainable is 0.9000 nominal. Thus the change in volume is known to 0.4%. As indicated above this is insufficient accuracy. Boelhouwer reports no mixture data.

Shavers

Shavers (57) reported PVT data for n-hexane at 50.0, 75.0, 100.0, 125.0, 150.0, 175.0, 200.0, 225.0°C up to 1000 atmospheres. Shavers reports the experimental reproducibility, rather than the actual measure-

ment errors, in his volume measurements. Using actual measurement errors his data are accurate to ± 0.1% at the high temperature end and ± 0.2% at the low temperature end. The data are reported to four significant digits.

II. CONCLUSIONS

All of the pure component data reported are of insufficient accuracy, or for too limited a temperature range, has been smoothed via the Hudelston equation, or is over too small a pressure range to provide a valid test for the liquid theories considered in Chapter II.

The one set of mixture data reported is of insufficient accuracy to allow the study of mixtures. That is, the phenomena being observed is of the same magnitude as the experimental uncertainty.

Thus the only course left open is to conduct a high accuracy experimental investigation to determine the desired data using the best experimental techniques and apparatus available. The apparatus and techniques used are described below.

CHAPTER IV

EQUIPMENT

To compress a liquid by 20% requires about 50,000 psi pressure. This is an extreme pressure even when compared to those normally encountered in most high-pressure laboratories studying gas properties. To obtain useful liquid p-v-T data such pressure and above must be obtained on a routine basis. The volume changes which occur must be accurately measured. Such operating conditions and measurements require specialized equipment. Yet in the field of high-pressure research there are almost as many experimental techniques as there are investigators. Each technique has its advantages and its weak points. To decide which technique or combination of techniques to use the following criteria were established:

1. The technique must be applicable over a wide range of temperature and pressure.
2. The technique, with suitable calibration, must be capable of determining absolute values of the change in volume with pressure.

3. The technique, with suitable calibration, must be capable of giving high accuracy results.

4. The measuring technique must be rapid.

All of the techniques reviewed, i.e. those used by the investigators in Chapter III (5,7,10,14,17,57) and others (2,3,24,62), were found lacking in at least one of the four requirements given above, see Table I, with the exception of those of Bridgman, Winnick, and Cutler and McMickle.

It was decided that with some modification of the technique and improved calibration procedures that a combination of these methods could provide the best technique to satisfy all four of the requirements listed above. The equipment and procedures are described below. Appendix E should be consulted for details of the apparatus design.

I. P-V-T CELL

In order to measure the change in volume as a function of pressure for the pure components and mixtures considered, the sylphon bellows technique originated by Bridgman (7) was chosen. In this study, the change in volume was determined by direct resistance difference measurements rather than potential differences used by

TABLE I

CHOICE OF TECHNIQUE

Investigator and Reference	Requirements				Deficiency Soluble
	Wide Range	Absolute Values	Accuracy	Rapidity	
Bridgman (7)	Yes	Yes	Medium	Yes	Yes
Eduljee (17)	No	Yes	Medium	No	No
Cutler and McMickle (10)	Yes	Yes	Medium	Yes	Yes
Doolittle (14)	Yes	Yes	Medium-Low	Yes	No
Boelhouwer (5)	No	Yes	High-Medium	Yes	No
Shavers (57)	No	Yes	Medium	Yes	No
Gibson (24)	No	Yes	Medium	No	No
Adams (2)	No	Yes	Medium	No	No
Amagat (3)	No	Yes	High	Yes	No
Winnick (62)	Yes	No	High	Yes	Yes

other investigators. The calibration techniques were improved as described in Chapter 5 and Appendix C.

The operation of the P-V-T cell can be described with the aid of Figure 1. The liquid sample is contained in the bellows, B, mounted securely to the retainer, R, at the point P. A piece of very fine Karma wire, S, whose resistance per length has been determined (see Appendix C), is attached to the bellows and as the bellows contracts with pressure it is drawn past the fixed contact, C, mounted on the fixed ring, T. Using the calibrations described in Appendix C the change in volume of the bellows can be calculated from the change in resistance across E_1, E_2, and E_3.

Figures 2 and 3 show the piezometer and the high pressure enclosure. Table II is the listing of the numbers in Figures 2 and 3.

The liquid sample is placed in the bellows, 7, and the bellows is sealed by an allen screw and ball bearing, 3. One end of the bellows is affixed to the retainer, 5, the other end is free. A short section of calibrated Karma wire, 9, is attached to the free end of the bellows, 8, by an allen screw, 24. The other end of the Karma wire is attached to two flexible lead wires which go out of

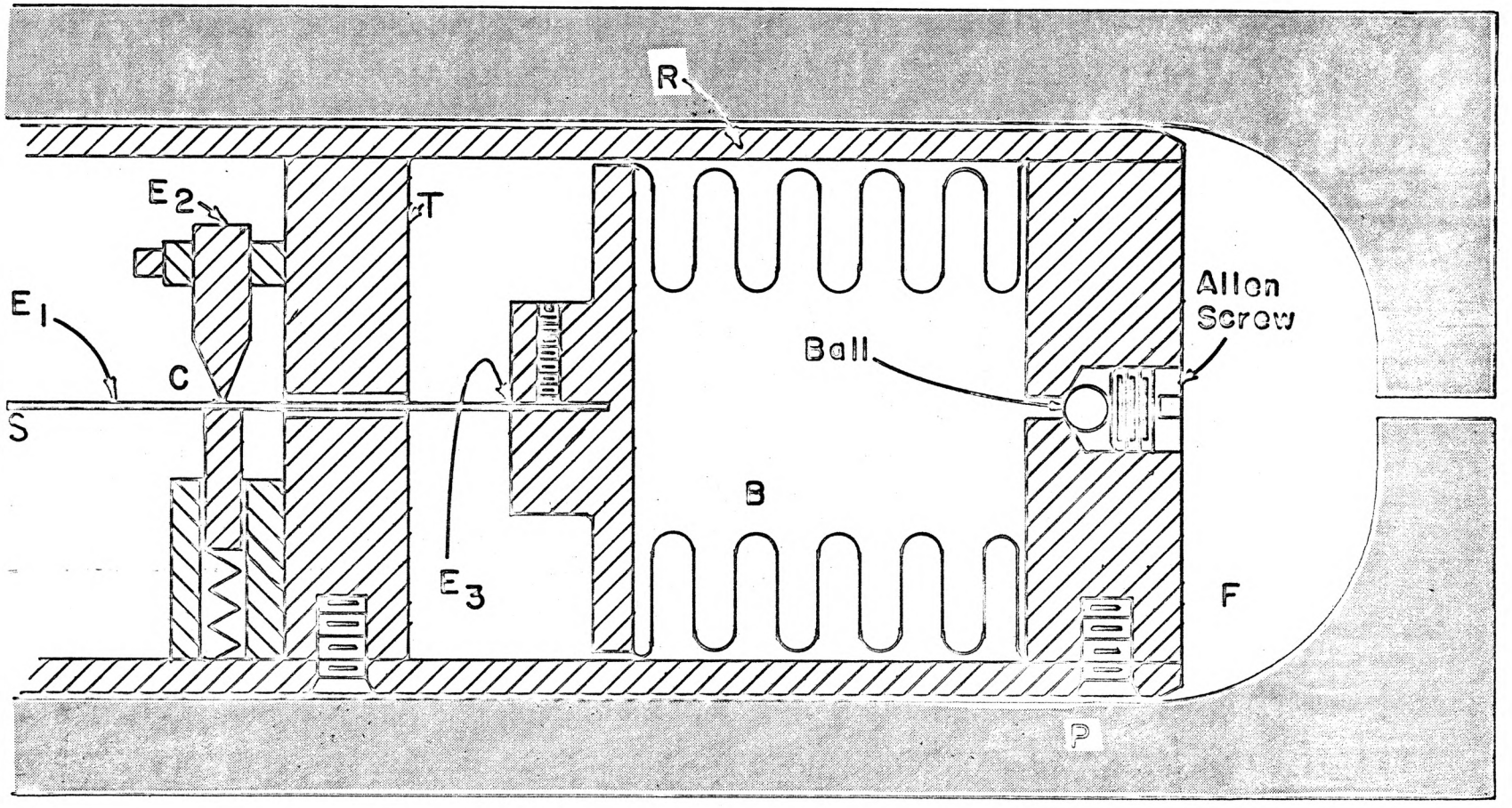

FIGURE 1. BELLOWS DETAIL

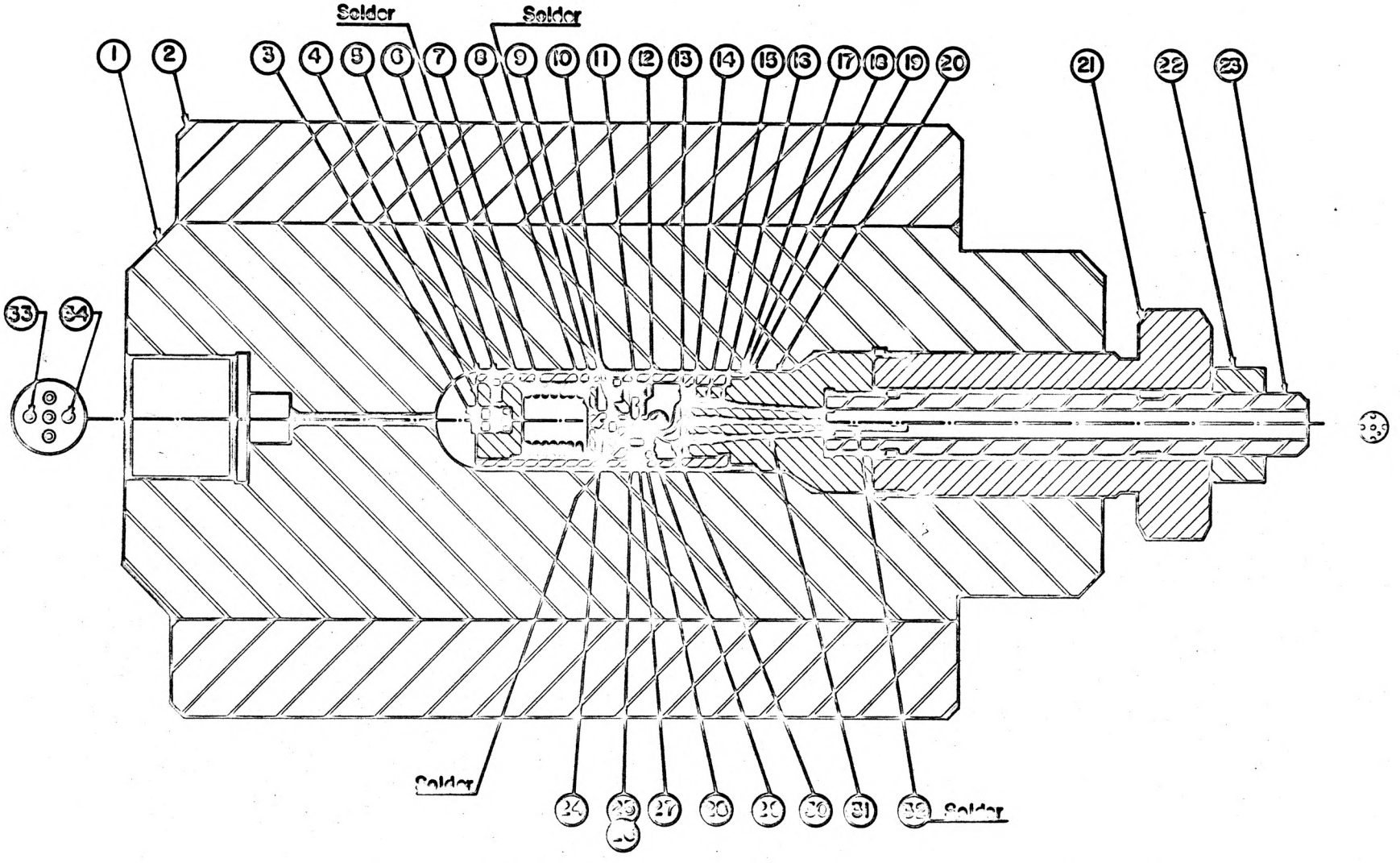

FIGURE 2 . PVT CELL (Courtesy Harwood Engineering Company)

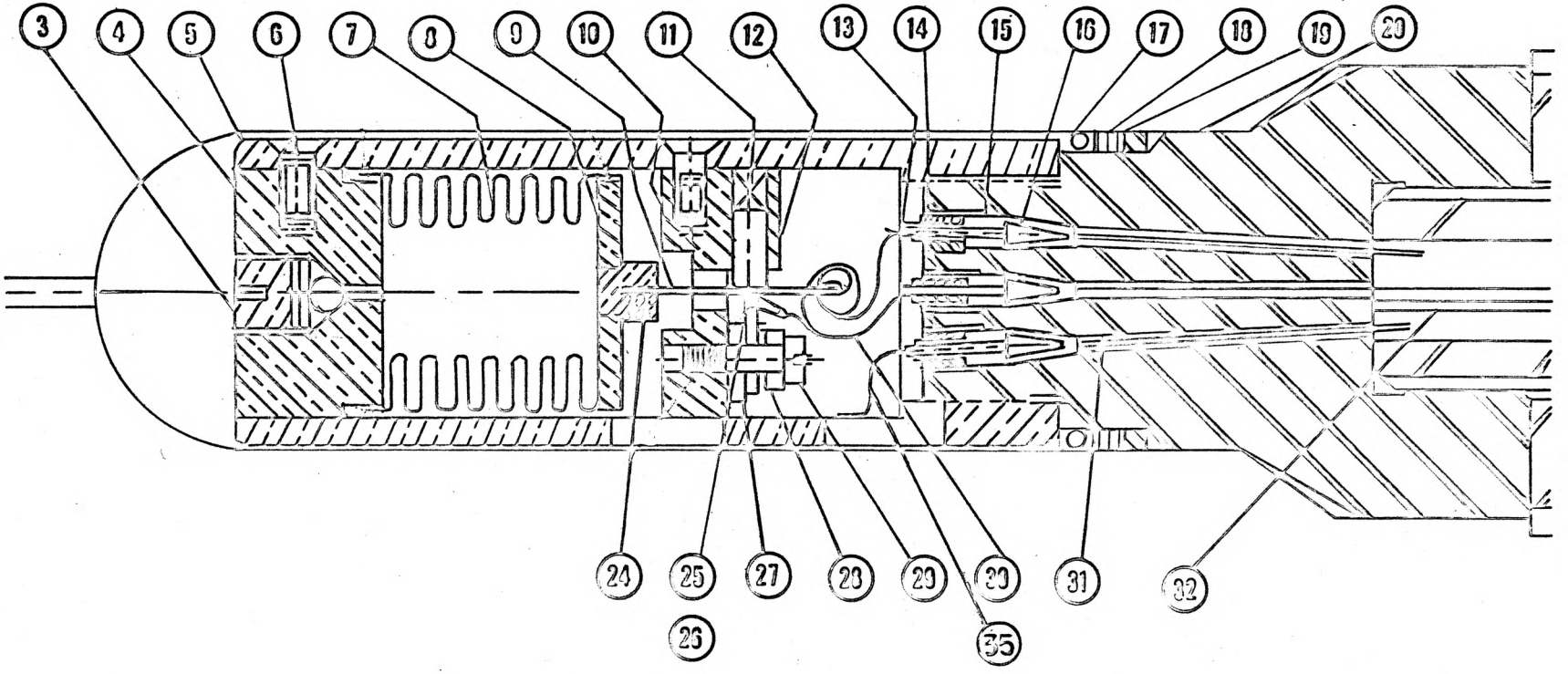

FIGURE 3. Enlargement of Bellows Area (Courtesy Harwood Engineering Company)

TABLE II

LISTING OF BALLOONS

1	Vessel
2	Sleeve
3	Cap screw
4	Front bellows end plate
5	Retainer
6	Set screws
7	Syphon bellows
8	Rear bellows end plate
9	Karma wire
10	Fixed connection housing
11	Spring
12	Teflon piston
13	Electrical connection
14	Teflon insulator
15	Unsupported area seal
16	Unsupported area seal
17	O-ring
18	Lead washer
19	Steel ring
20	Closure
21	Drive plug
22	Nut
23	Closure bolt
24	Set screw
25	Fixed contact
26	Fixed contact insulator
27	Insulating spacer
28	Insulating spacer
29	Insulating spacer
30	Electrical leads
31	Electrical leads
32	Ground
33	Electrical lead
34	Electrical lead

the pressure vessel led through teflon insulators, 14. The Karma slide wire is held against the fixed contact, 25, by a spring, 11, and Teflon plunger, 12. One lead wire from the fixed contact was also led out of the cell. One of the two lead wires attached to the end of the Karma wire and the lead attached to the fixed contact form half of the measuring circuit for determination of the change in bellows length with increasing hydrostatic load. The other half consisted of the cell ground lead, 32, and the lead wire, 35, which is attached to the retainer, 5. Using this measurement circuit it is possible to eliminate all contact and lead wire resistance, it resembles the circuit of a four lead platinum resistance thermometer.

The high pressure seals were of the Bridgman unsupported area type (8). The seal was formed by the rubber, 17, lead, 18, and steel, 19, o-rings.

The cavity around the bellows, within the P-V-T cell, was filled with pressure transmitting fluid composed of five parts petroleum ether to two parts SAE 10 oil. This mixture was chosen because it would not freeze before any of the liquid samples. The oil also provided some lubrication to prolong the life of the valves and the piston intensifier. As pressure was applied to the

transmitting fluid the bellows contracted to equilibrate the pressure inside and out. The design of the bellows was such that the contraction was longitudinal along its axis (7). As the bellows contracted the Karma slide wire was pulled past the fixed contact changing the resistance between the fixed contact and either end of the slide wire. The change in volume was determined from the cross sectional area of the bellows and the unit length* of the Karma slide wire.

II. MEASURING BRIDGE

A Mueller G-2 bridge with a high-sensitivity lamp and scale type galvanometer were used to determine: the change in volume with increasing hydrostatic load via slide wire, the system pressure above 50,000 psi via manganin cell, and the P-V-T cell temperature via platinum resistance thermometer. A four position mercury contact commutator allowed four different measurement circuits to be attached to the Mueller bridge without rewiring between measurements. A schematic of the bridge is shown in Figure 4. All measurement circuits were wired

---

*Note: The term unit length is defined here to mean the number of centimeters of slide wire that are required to obtain a resistance of one ohm absolute at 25.0°C (i.e. cm/ohm). The symbol Ω will be used for unit length.

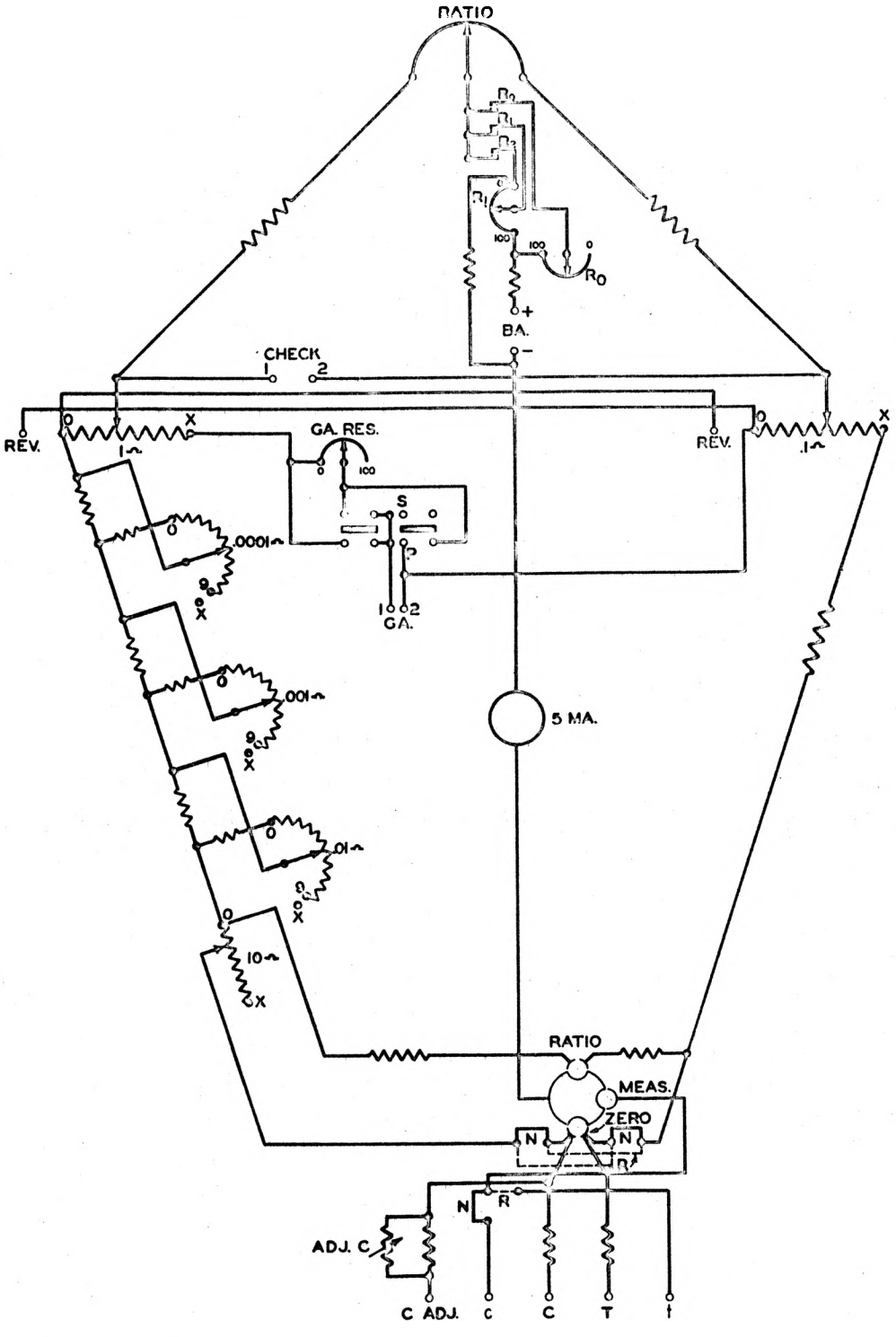

FIGURE 4. Schematic Diagram of the Bridge Circuit

in the manner of the four lead Platinum resistance thermometer so that lead wire resistances were eliminated by cancellation.

III. PRESSURE MEASUREMENT

The experimental pressure system is shown in Figure 5. There were three different pressure measuring devices employed. Each device was used over a specific range. The three were: a 0-1500 psi Heise gauge, a 0-50,000 psi Heise gauge, and a Manganin cell.

0-1500 psi Heise Gauge

The 0-1500 psi Heise gauge was used to provide accurate pressure values in the low pressure range. This gauge is accurate to ± 0.1% of full scale, and has thermal compensation for ambient temperature variations of -25. to +125.°F.

0-50,000 psi Heise Gauge

The 0-50,000 psi Heise Gauge was the primary pressure measuring device above 1500 psi and up to 50,000 psi. It is accurate to ± 0.1% of full scale. The gauge had a thermal compensator to allow for ambient temperature variations from -25. to +125.°F.

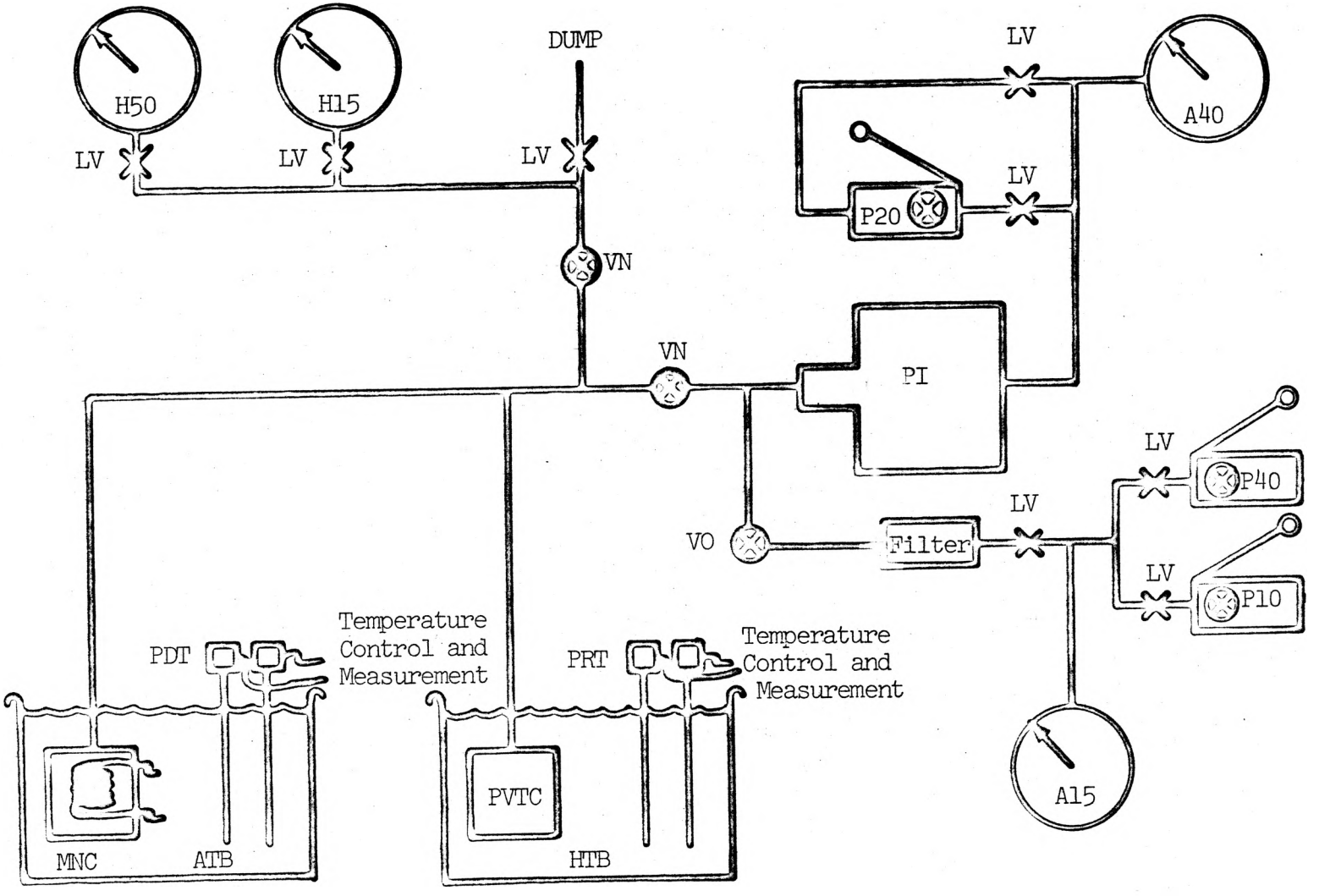

FIGURE 5 . Experimental Apparatus

Manganin Cell

The Manganin cell was used for pressure measurements above 50,000 psi. It is designed for service up to 200,000 psi. The Manganin cell was maintained at 25.00 $\pm$ 0.01°C during calibration as described in Chapter 5 and Appendix C, and during the measurements.

The cell resistance was first measured at atmospheric pressure P_o prior to the start of a run. The cell resistance was then measured at each pressure. The difference between these two resistances at P and at P_o times the cell pressure coefficient provided the system pressure.

IV. PRESSURE APPLICATION

The system pressure was provided by three hydraulic handjacks and the piston intensifier shown in Figure 5. The 0-10,000 psi Blackhawk handjack was used to provide system pressure up to 9000 psi. This handjack was also used to reverse the intensifier. Above 9000 psi and below 200,000 psi either the 0-20,000 psi or the 0-40,000 psi handjack was used to drive the piston intensifier to provide the system pressure. The intensifier is of Harwood Engineering Company design and has an area ratio of 17:1.

V. TEMPERATURE CONTROL AND MEASUREMENT

The P-V-T cell temperature was controlled by the Hallikainen constant temperature bath, Figure 5, to within ± 0.002°C on each isotherm. The Hallikainen bath had a nickel resistance thermometer with a sensitivity of 0.001°C. A Hallikainen Thermotrol with three control modes: on-off, proportional, and integral controlled the bath temperature. The integral mode provided the most accurate control in this application. The bath temperature was monitored by a Platinum resistance thermometer.

The Manganin cell was maintained at 25.00 ± 0.01°C in the AMINCO bath shown in Figure 5. The bath controller sensing element was a Mercury contact thermometer. The bath was monitored with a five degree range Philadelphia differential thermometer. At 25.00°C it read 2.37.

CHAPTER V

CALIBRATION

To determine the absolute change in volume as a function of pressure; the fiducial density, $\rho_{o,t}$, the sample weight w, the cross sectional area of the bellows $A_{p,t}$, and the change in length of the bellows with pressure ΔL_B are required for the basic data reduction equation:

$$\frac{\Delta V}{V_o} = \frac{\Delta L_B \cdot A_{p,t} \cdot \rho_{o,t}}{w} \quad . \tag{V-1}$$

Where $\Delta V/V_o$ is the compression or change in relative volume. The fiducial densities were determined by Harrison (27), Sims (58), and Lin (33). The sample weight was measured by differential weighing. The cross sectional area of the bellows was unknown but was calibrated to sufficient accuracy as described in Appendix B. The change in length of the bellows with pressure was determined by measuring the change in resistance (see Chapter IV). This change was converted to change in length by knowing the slide wire unit length. The slide wire unit length was given by the manufacturer, but not to sufficient accuracy.

The manganin cell pressure transducer was calibrated against a secondary pressure standard in order to obtain its pressure coefficient.

A consistancy check using the normal Heptane data of other investigators was made. The results of this check are reported in the final section of this chapter.

I. P-V-T CELL CALIBRATIONS

Two calibrations were required for the P-V-T cell. Determination of the cross sectional area of the bellows was accomplished in a two step procedure, using a fluid displacement technique. The other was determination of the slide wire unit length.

Bellows Cross Sectional Area Calibration

The bellows calibration procedure adopted requires two steps. The fluid displacement technique used requires a capillary tube of very accurately known uniformity and cross sectional area. Thus prior to the calibration to determine the cross sectional area of the bellows it was necessary to calibrate a capillary tube.

Capillary Tube Calibration. The capillary tube radius and uniformity were determined so that the capillary tube cross sectional area could be calculated. The mercury thread weight technique was used (30).

Apparatus. The capillary calibration apparatus is shown in Figure 6. The capillary was maintained at $25.00 \pm 0.005^{\circ}C$ during the course of the calibration by circulating distilled water in the flow loop indicated by arrows in Figure 6. One cathetometer was used to measure the mercury thread inside the capillary tube.

Procedure. Prior to actual calibration the most uniform of a group of ten capillary tubes was chosen for calibration. Then the tube was cleaned with hot chromic acid and vacuum dried.

The calibration involved measuring the lengths A-B, B-C, and C-D shown in Figure 7 of a thread of mercury inside the capillary tube, with the tube mounted vertically. Once the measurements had been made at one position the mercury thread was moved up the tube and measured again. This was repeated until measurements had been taken at forty points spaced along the length of the tube at about two centimeter intervals. Following this the thread was removed and weighed.

The procedure was followed for two mercury threads, one that was one cm. length nominal and the other two cm. nominal.

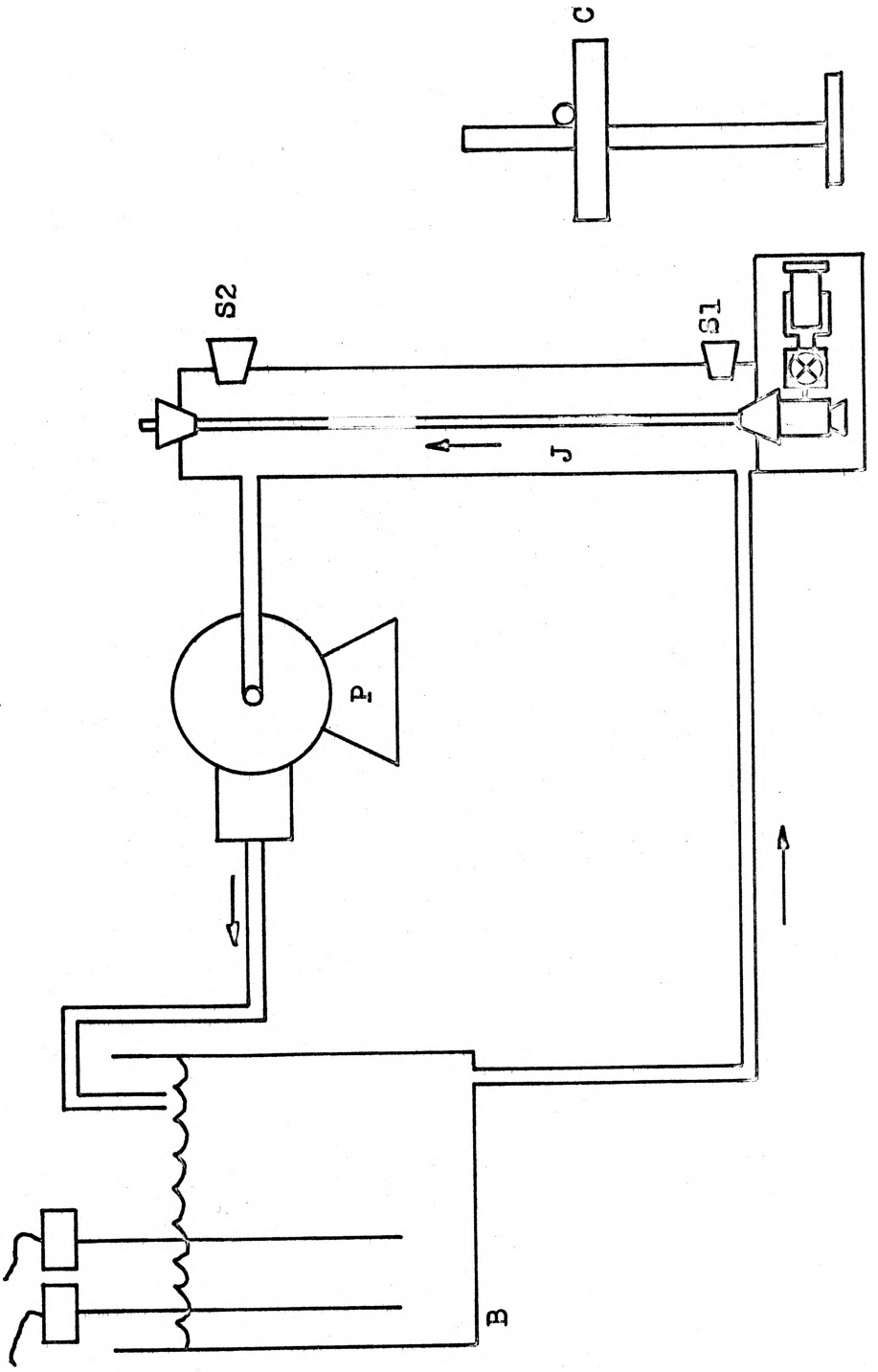

FIGURE 6. Capillary Calibration Apparatus

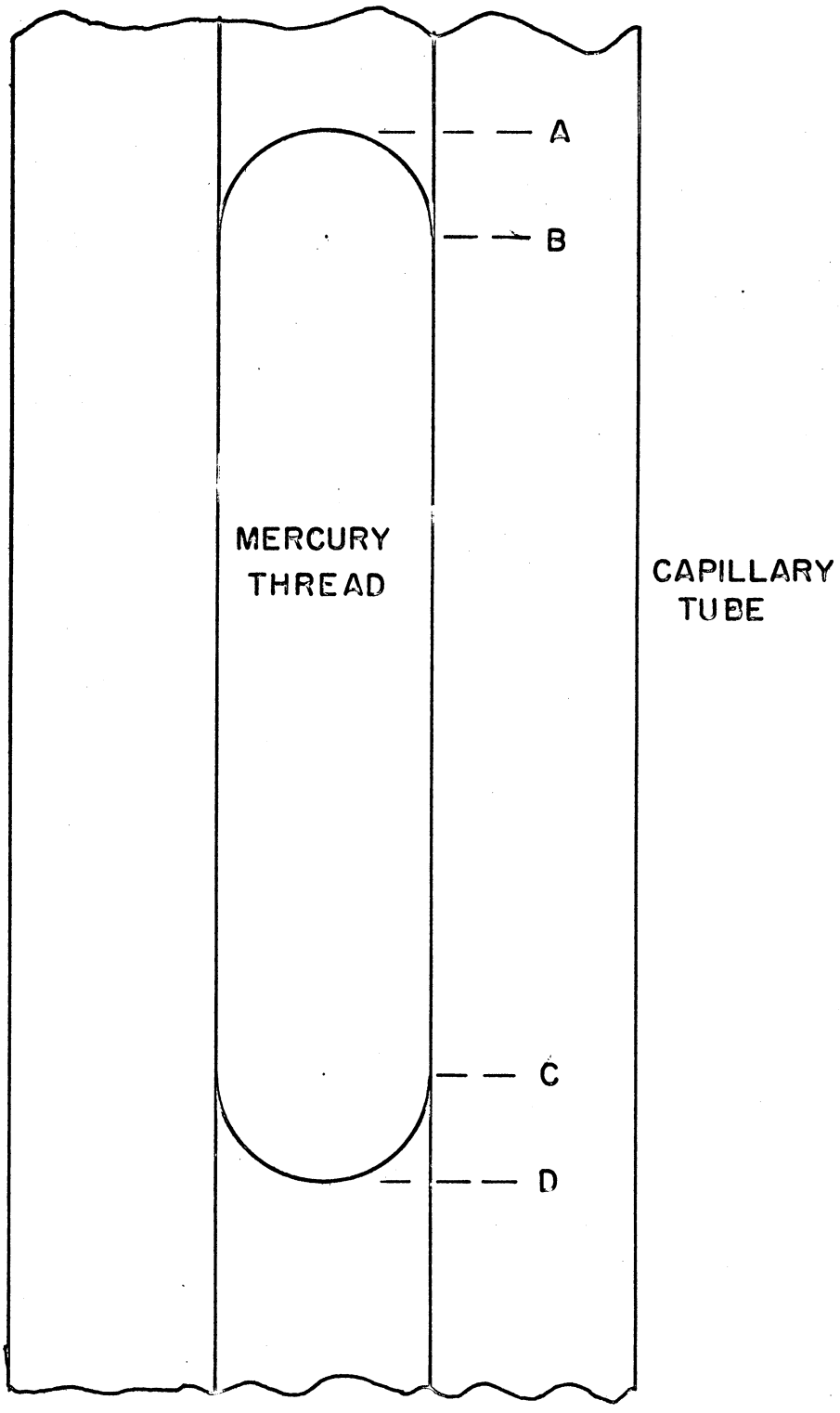

FIGURE 7. Hypothetical Mercury Thread

Results. The one cm. mercury thread weighed 0.51263 gm. while the two cm. weighed 0.90526 gm. The density of mercury at 25.00°C was taken as 13.5336348 gm/cc (40). Using the above two thread lengths the capillary tube radius was calculated to be 0.100320 ± 0.000035 cm. The capillary tube was found to be uniform to within ± 0.000035 cm. over its entire length. (See Appendices B and C).

Bellows Calibration. With the capillary tube cross sectional area and uniformity known it was then possible to determine the cross sectional area of the bellows and uniformity.

Apparatus. The apparatus used was essentially that used during the capillary calibration with the following changes: the bellows was attached to the capillary tube and driven by a precision micrometer. An additional cathetometer was used to measure the free end, of the bellows,displacements. The apparatus is shown in Figure 8.

Procedure. Prior to calibrating the bellows was filled with water. Then it was attached to the capillary tube and aligned so that the flat face on the bellows' free end was parallel to the flat face on the micrometer driver arrangement. Next initial readings were taken with the two cathetometers of the bellows' free end

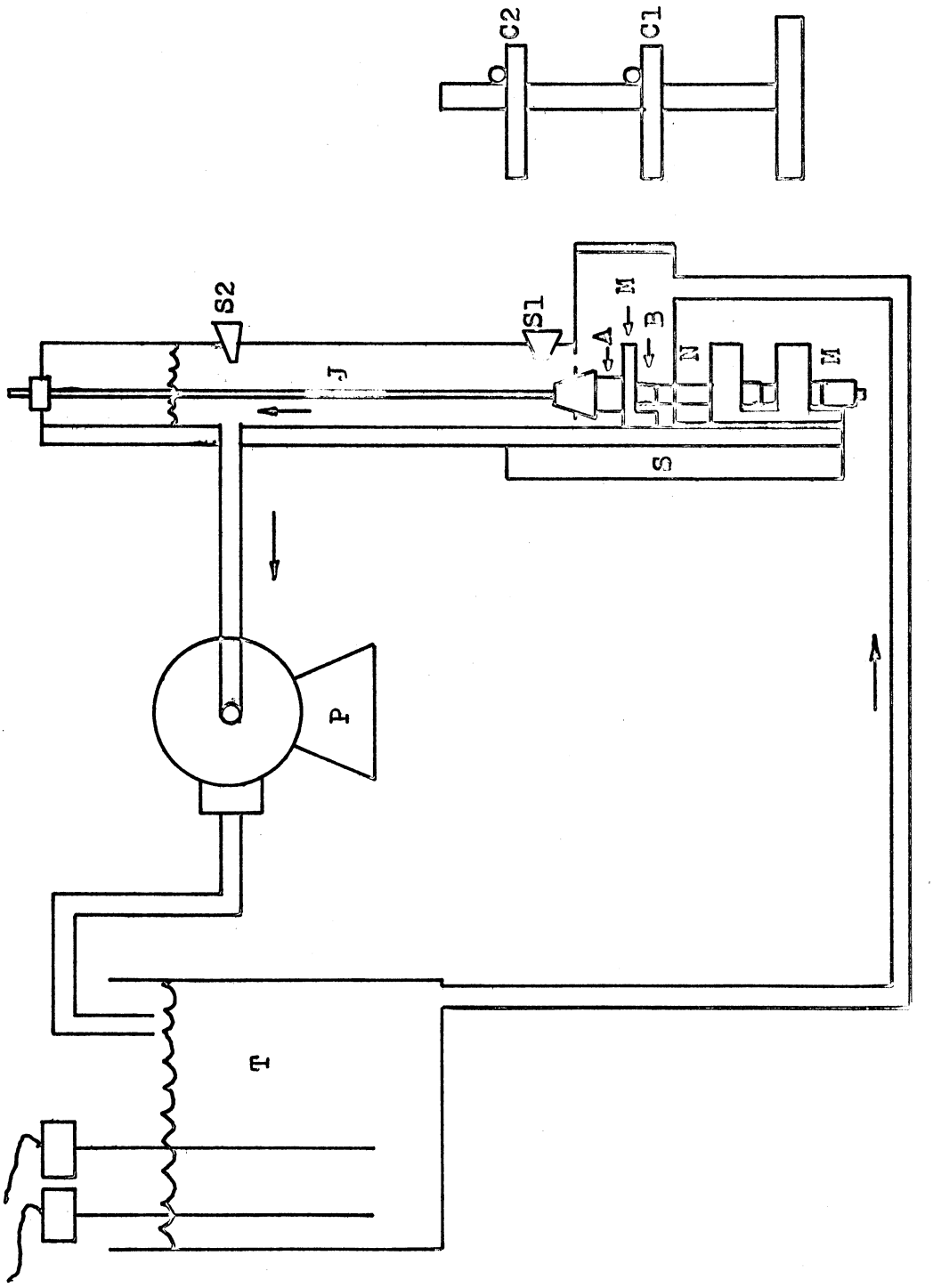

FIGURE 8. Bellows Calibration Apparatus

position and the water meniseus in the capillary tube. Then a displacement of the bellows' free end was made and a new set of readings taken. This procedure was repeated until a total displacement of 0.25 in. was made in the bellows' free end.

Results. With the capillary tube cross sectional area known, the bellows' free end displacement, and the liquid displacement up the capillary tube caused by the bellows' free end displacements known the bellows' cross sectional area can be calculated from:

$$A_{o,o} = A_c \frac{\Delta L_c}{\Delta L_B} \qquad \text{(V-1)}$$

The cross sectional area is 1.9815 ± 0.0011 cm^2. The uniformity was within $\pm$ 0.0011 cm^2.

Slide Wire Unit Length. The determination of the slide wire unit length required only that the resistance of an accurately known length of slide wire be known. The error analysis in Appendix B set the accuracy required.

Apparatus. The apparatus for the unit length determination shown in Figure 9, consisted of an optically flat surface over which the wire was held in slight tension by two springs and an upper piece which served as a holder and spacer for two knife edges.

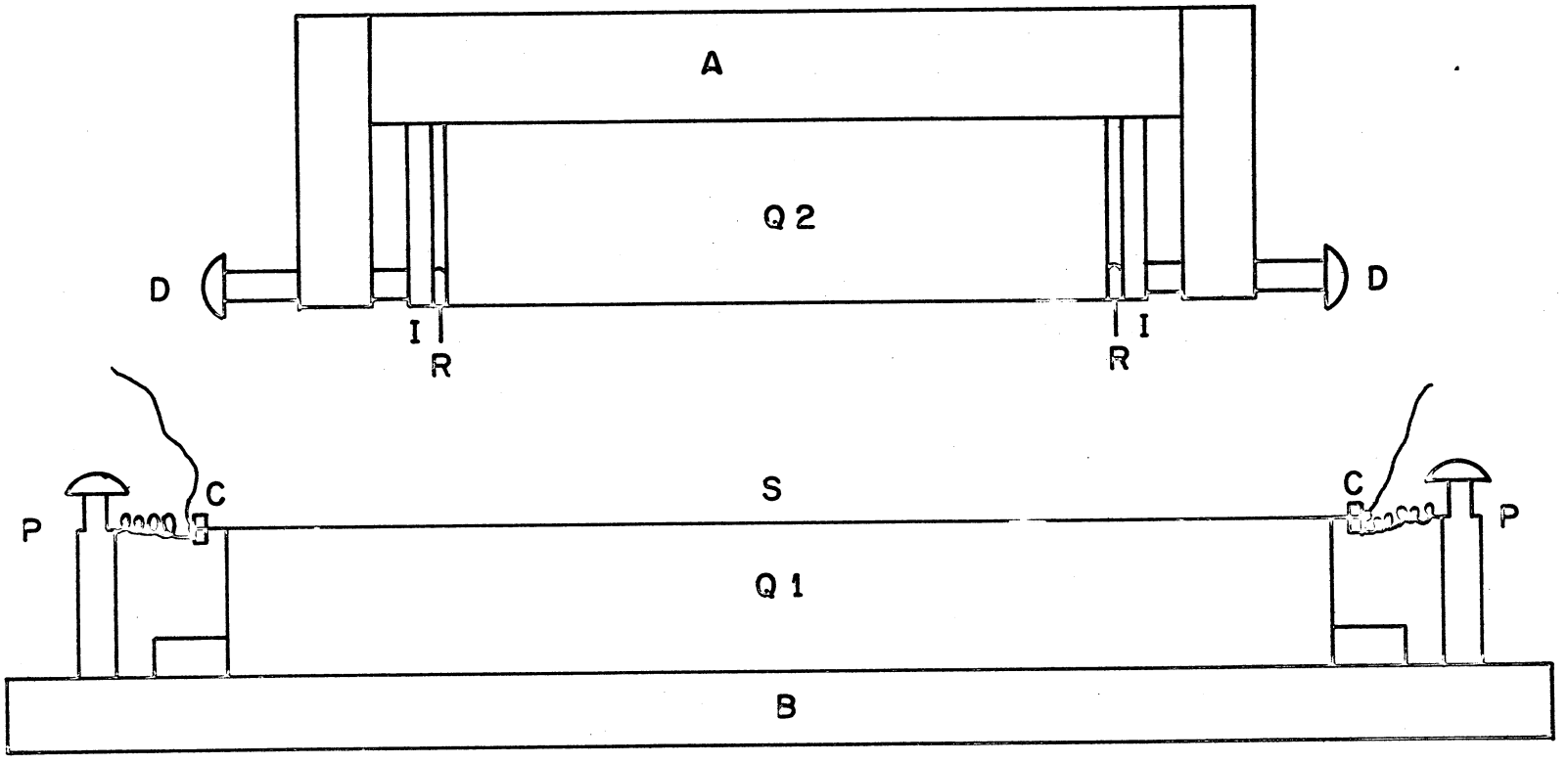

FIGURE 9. Slide Wire Calibration Apparatus

Procedure. The knife edges in Figure 9 were lowered onto the slide wire which was being held on the optically flat surface. Then in the manner used with a four lead Platinum resistance thermometer the resistance between the knife edges was measured with the Mueller G-2 bridge. Then the distance between the scratches, which the knife edges left on the slide wire, was measured with the cathetometer. With these two quantities known the unit length of the slide wire was calculable.

Results. The slide wire unit length for three different sections of Karma wire, all cut from the same spool in a sequential manner, was found to be 3.87800 $\pm$0.00002 cm/ohm.

II. MANGANIN CELL CALIBRATION

The Manganin cell was calibrated against an AMINCO dead weight tester. The range of calibration was 0-100,000 psig. It was used as the pressure measurement device above 50,000 psi.

Apparatus

The Manganin cell was attached to the AMINCO dead weight tester via 100,000 psi test line. The Manganin cell was maintained at 25.00 $\pm$ 0.01°C in an AMINCO temperature bath. The apparatus is shown in Figure 10.

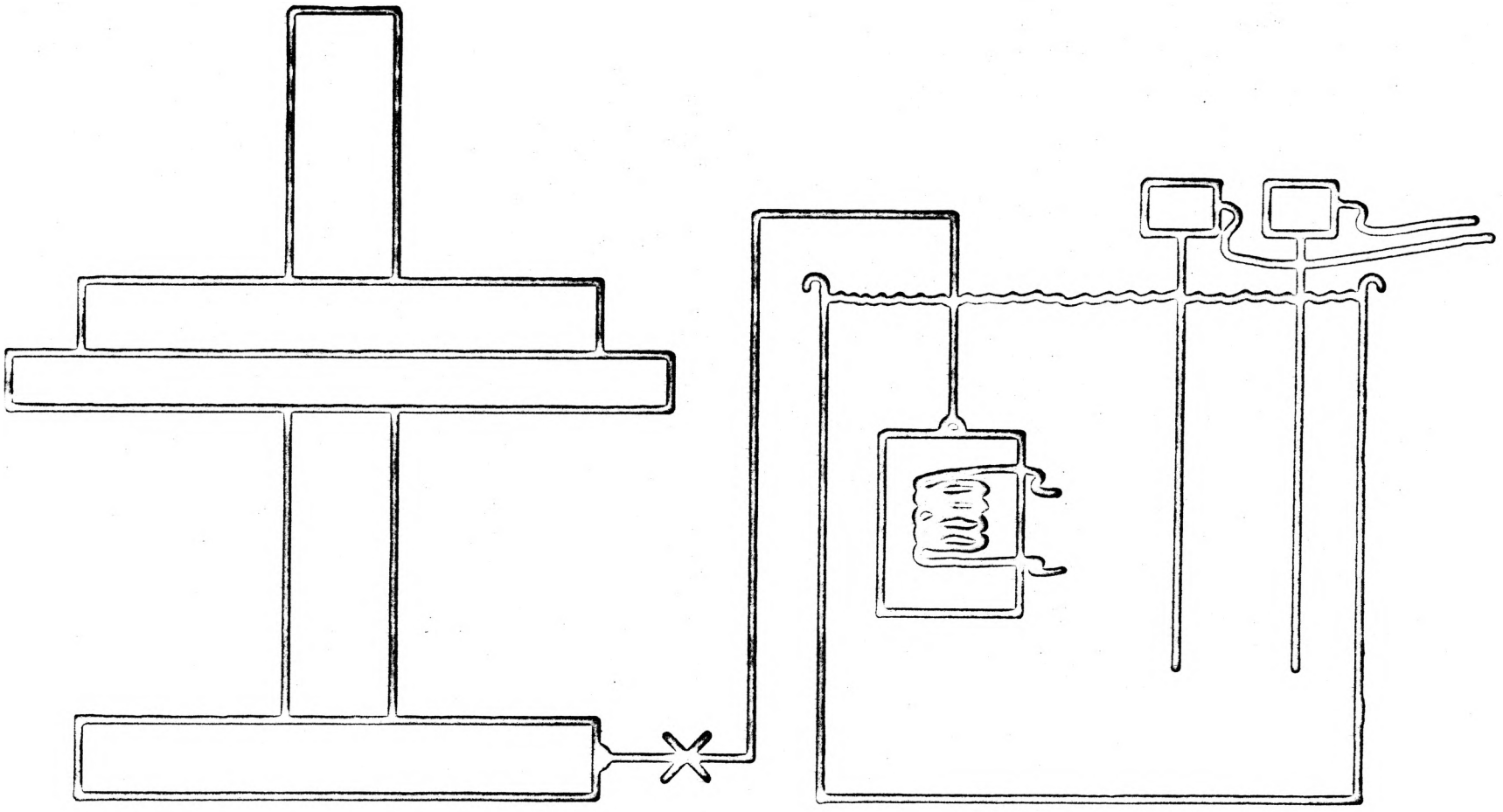

FIGURE 10. Manganin Cell Calibration Apparatus

Procedure

The zero point resistance at atmospheric pressure was determined with the Mueller G-2 bridge. Then with a load applied to the dead weight tester the pressure was increased until the piston floated. At this point the unit was at a known pressure ± 50 psi. Again the resistance of the cell was determined. This procedure was repeated at 5000 psi intervals between 10,000 and 100,000 psi.

Results

The Manganin cell pressure coefficient was found to be 58260. ± 100. psi/ohm.

III. N-HEPTANE CONSISTENCY

With all calibrations complete it was decided to make a series of experimental runs on n-Heptane at 30.0, 40.0, 50.0, 60.0°C to allow a check with other investigators. At 30.0°C the data of Boelhouwer (5) and Doolittle (14) were combined and compared with the experimental values for n-Heptane. Similarly at 40.0°C the data of Eduljee (17), at 50.0°C the data of Doolittle, and at 60.0°C the data of Boelhouwer and Eduljee. In all cases the single and combined data sets were found to be within their

estimated experimental error of the data taken in this study. It should be noted that this was done only as a consistancy check, since the calibrations described above make all data taken in this study absolute.

CHAPTER VI

DATA REDUCTION AND RESULTS

The primary quantities measured during the experimentation were; resistance of the slide wire segment between bellows and contact, and resistance of the manganin pressure transducer. Conversion of the raw change in resistance between the bellows and the fixed contact data to compression and relative volume data requires: the fiducial density, the sample weight, the slide wire resistivity, and the bellows' cross sectional area. The bellows' change in length is determined from the change in resistance between the bellows and the fixed contact multiplied by the slide wire unit length. Detailed data reduction is covered in Appendix A. Raw change in resistance data is tabulated in Appendix F.

The second section covers conversion of Manganin cell reading to pressure. The last section of this chapter contains a tabulation of the compression and relative volume versus pressure results.

I. VOLUME MEASUREMENT REDUCTION

Conversion of the resistance change data to compressions (56) is accomplished through the use of equation A-1:

$$\frac{\Delta V}{V_o} \qquad \frac{\Delta L_B \cdot A_{p,t} \cdot \rho_{o,t}}{w} \tag{VI-1}$$

The change in volume ΔV accounts for the product $\Delta L_B \cdot A_{p,t}$ which is the bellows change in length multiplied by the bellows' cross sectional area. The initial volume, V_o, is the sample weight w divided by the fiducial density $\rho_{o,t}$.

The two terms which make up the change in volume part of VI-1 are a composite of several terms which include temperature and pressure corrections. The terms which make up the initial volume part of VI-1 are directly measured experimental quantities and require no corrections. The composite terms are considered below.

Bellows Change in Length. The change in bellows' length is calculated from the measured slide wire resistance change multiplied by the slide wire unit length:

$$\Delta L_B = \Omega \cdot (R_{a,p} - R_{a,o}) + C_p . \tag{VI-2}$$

Where: Ω is the slide wire unit length(defined in Chapter V), $R_{a,p} - R_{a,o}$ is change in slide wire resistance between the bellows and fixed contact with pressure and C_p is a symbolic representation for the pressure correction. The pressure correction is due to the difference in compressibility of the Karma slide wire and the Brass carrier to which the bellows and fixed contact are attached. This arrangement can be seen in Figure 1 . This correction is additive and is detailed in Appendix A. The correction is:

$$C_p = L_{br,p} - L_{ka,p} \quad . \tag{VI-3}$$

Where: $L_{br,p}$ is the uncompressed length of the brass carrier which when compressed corresponds to the slide wire length between the fixed contact and bellows, and $L_{ka,p}$ is the uncompressed length of Karma slide wire which when compressed corresponds to the slide wire length between the fixed contact and bellows.

Bellows' Cross Sectional Area. The bellows cross sectional area at atmospheric pressure and 25.00°C., $A_{o,o}$, is a calibration constant. There are two corrections that must be made to this quantity. One is due to thermal expansion at temperatures other than 25.00°C and one is due to its compression due to pressure.

The correction due to thermal expansion is:

$$A_{o,t} = A_{o,o} \left(1.0 + 2.0\, \alpha_{br} \left(t - 25.00\right)\right). \qquad \text{(VI-4)}$$

Where: $A_{o,t}$ is the new bellows' cross sectional area at temperature t, and α_{br} is the linear coefficient of thermal expansion for brass. The value of α_{br} used is $19.1 \times 10^{-6}/^{o}C$ (26).

The correction due to compression is:

$$A_{P,o} = A_{o,o} \left(1.0 - \frac{2.0}{3.0} \left(A_{br} \cdot P - B_{br} \cdot P^{2}\right)\right). \qquad \text{(VI-5)}$$

Where: $A_{P,o}$ is the new bellows' cross sectional area at pressure P, and A_{br} and B_{br} are best fit constants, as determined by Bridgman (7), for the relative compression of Brass.

Equation VI-1 With Correction. Equation VI-1, with the correction from above, can be written:

$$\frac{\Delta V}{V_o} = \Omega \cdot \left(R_{a,P} - R_{a,o}\right) + \left(L_{br,P} - L_{ka,P}\right) \cdot A_{o,o} \cdot \left(1.0 + 2.0\, \alpha_{br} \cdot \left(t - 25.00\right)\right) \cdot \left(1.0 - \frac{2.0}{3.0} \left(A_{br} \cdot P - B_{br} \cdot P^{2}\right)\right) \cdot \rho_{o,t} / W. \qquad \text{(VI-6)}$$

II. PRESSURE MEASUREMENT REDUCTION

For isotherms on which the pressure exceeded 50,000 psi it was necessary to use the Manganin cell. The procedure was to measure the cell's resistance, $R_{Mn,o}$, at one atmosphere pressure prior to starting the isotherm and then to measure the cell's resistance, $R_{Mn,p}$, at the pressure in question. The difference in these two resistance values multiplied by the Manganin cell pressure coefficient (see Chapter V), gives the system pressure, or

$$P = \left(R_{Mn,p} - R_{Mn,o} \right) \cdot 58260 \frac{psi}{ohm} . \qquad (VI-7)$$

III. RAW RELATIVE VOLUME DATA

The raw resistance data of Appendix F has been converted to relative volumes without smoothing. The relative volume is the compression determined by using equation VI-6 subtracted from 1.00000.

The following table contains compression and relative volume data versus pressure for all of the systems and mixtures run. That is: isotherms of 25.00, 45.00, 65.00, and 85.00°C for pure n-Decane, n-Dodecane,

n-Tetradecane, and n-Hexadecane; binary mixtures of 0.5000 mole fraction n-Decane and n-Tetradecane and of n-Dodecane and n-Hexadecane; and a ternary mixture of 0.6000 mole fraction n-Decane with 0.2000 mole fraction each of n-Tetradecane and n-Hexadecane.

TABLE III

N-DECANE AT 25.00 DEG. C.

DENSITY = .72580 GM./C.C. SAMPLE WEIGHT = 2.07530 GM.

COMPRESSION (CC/CC)	RELATIVE VOLUME	P (PSI)	P (PATM)
0.0	1.00000	14.7	1.0
0.00211	0.99789	292.7	19.9
0.00402	0.99598	523.7	35.6
0.00754	0.99246	1006.7	68.5
0.01021	0.98979	1401.7	95.4
0.01377	0.98623	1994.7	135.7
0.02196	0.97804	3194.7	217.4
0.02959	0.97041	4524.7	307.9
0.03823	0.96177	6094.7	414.7
0.04560	0.95440	7584.7	516.1
0.05235	0.94765	9024.7	614.1
0.05891	0.94109	10594.7	719.6
0.06508	0.93492	12064.7	821.0
0.07040	0.92960	13584.7	924.4
0.07576	0.92424	15034.7	1023.0
0.08080	0.91920	16534.7	1125.1
0.08635	0.91365	18014.7	1225.8
0.09145	0.90855	19994.7	1360.6
0.09803	0.90197	22014.7	1498.0
0.10522	0.89478	25194.7	1714.4
0.11246	0.88754	27994.7	1904.9
0.11874	0.88126	31014.7	2110.4
0.12518	0.87482	33954.7	2310.5

TABLE III (CONTINUED)

N-DECANE AT 45.00 DEG. C.

DENSITY = .71059 GM./C.C. SAMPLE WEIGHT = 2.07530 GM.

COMPRESSION (CC/CC)	RELATIVE VOLUME	P (PSI)	(PATM)
0.0	1.00000	14.7	1.0
0.00268	0.99732	300.7	20.5
0.00428	0.99572	460.7	31.3
0.00890	0.99110	1024.7	69.7
0.01287	0.98713	1474.7	100.3
0.01625	0.98375	2014.7	137.1
0.02400	0.97600	3044.7	207.2
0.03392	0.96608	4584.7	312.0
0.04242	0.95758	5984.7	407.2
0.05142	0.94858	7614.7	518.1
0.05852	0.94148	9064.7	616.8
0.06599	0.93401	10594.7	725.7
0.07200	0.92800	12074.7	821.6
0.07822	0.92178	13614.7	926.4
0.08427	0.91573	15114.7	1028.5
0.09002	0.90998	16794.7	1142.8
0.09437	0.90563	18064.7	1229.2
0.10343	0.89657	21084.7	1434.7
0.11214	0.88786	24014.7	1634.1
0.12033	0.87967	27184.7	1849.8
0.12721	0.87279	30064.7	2045.8
0.13340	0.86660	33054.7	2249.2
0.13987	0.86013	36014.7	2450.6
0.14495	0.85386	39014.7	2654.8
0.15051	0.84949	41884.7	2850.1
0.15535	0.84465	44994.7	3061.7
0.16085	0.83915	48114.7	3274.0
0.16291	0.83709	49492.6	3367.8
0.17068	0.82932	54389.7	3701.0

TABLE III (CONTINUED)

N-DECANE AT 65.00 DEG. C.

DENSITY = .69512 GM./C.C. SAMPLE HEIGHT = 2.07530 GM.

COMPRESSION (CC/CC)	RELATIVE VOLUME	P (PSI)	(PATM)
0.0	1.00000	14.7	1.0
0.00292	0.99708	327.7	22.3
0.00544	0.99456	492.7	33.5
0.01014	0.98986	1009.7	68.7
0.01493	0.98507	1444.7	98.3
0.01984	0.98016	2094.7	142.5
0.02727	0.97273	3084.7	209.9
0.03803	0.96197	4534.7	308.6
0.04761	0.95239	5994.7	407.9
0.05729	0.94271	7604.7	517.5
0.06519	0.93481	9084.7	618.2
0.07355	0.92645	10594.7	726.4
0.07965	0.92035	12114.7	824.4
0.08564	0.91436	13474.7	916.9
0.09210	0.90790	15039.7	1023.4
0.09867	0.90133	16794.7	1142.8
0.10324	0.89676	17994.7	1224.5
0.11297	0.88703	21004.7	1429.3
0.12282	0.87718	24034.7	1635.5
0.13020	0.86980	27104.7	1844.4
0.13819	0.86181	30144.7	2051.2
0.14531	0.85469	33194.7	2258.8
0.15071	0.84929	36024.7	2451.3
0.15658	0.84214	39204.7	2667.7
0.16232	0.83768	42064.7	2862.3
0.16711	0.83289	45084.7	3067.8
0.17239	0.82761	48014.7	3267.2
0.17894	0.82106	52594.5	3578.8
0.18511	0.81489	56553.3	3848.2
0.18790	0.81210	58781.7	3999.8
0.19600	0.80400	64661.3	4399.9
0.20366	0.79634	71077.8	4836.5

TABLE III (CONTINUED)

N-DECANE AT 85.00 DEG. C.

DENSITY = .67945 GM./C.C. SAMPLE WEIGHT = 2.07530 GM.

COMPRESSION (CC/CC)	RELATIVE VOLUME	P (PSI)	P (PATM)
0.0	1.00000	14.7	1.0
0.00330	0.99670	301.7	20.5
0.00551	0.99449	529.7	36.0
0.01045	0.98955	994.7	67.7
0.01574	0.98426	1436.7	97.8
0.01979	0.98021	1996.7	135.7
0.03119	0.96881	3114.7	211.9
0.03897	0.96103	4024.7	273.9
0.04658	0.95342	5144.7	350.1
0.05276	0.94724	6134.7	417.4
0.05913	0.94087	7054.7	480.0
0.06553	0.93447	8034.7	550.1
0.07702	0.92298	10184.7	693.0
0.08175	0.91825	11064.7	752.9
0.08624	0.91376	12044.7	819.6
0.09166	0.90834	13044.7	887.6
0.09574	0.90426	14134.7	961.8
0.09969	0.90031	15034.7	1023.0
0.10211	0.89789	15664.7	1065.9
0.10770	0.89230	17014.7	1157.8
0.11201	0.88799	18134.7	1234.0
0.11524	0.88476	19064.7	1297.3
0.11840	0.88160	20134.7	1370.1
0.12236	0.87730	21034.7	1431.3
0.12741	0.87259	22934.7	1560.6
0.13449	0.86551	25014.7	1702.1
0.13969	0.86031	27244.7	1853.9
0.14509	0.85491	29054.7	1977.0
0.15022	0.84978	31284.7	2128.8
0.15615	0.84385	33814.7	2300.9
0.15937	0.84063	35164.7	2392.8
0.16390	0.83610	37014.7	2518.7
0.16676	0.83324	38954.7	2650.7
0.17169	0.82831	40984.7	2788.8
0.17414	0.82586	43144.7	2935.8
0.17942	0.82144	45064.7	3066.5
0.18132	0.81868	46934.7	3193.7
0.18530	0.81470	49039.7	3336.9
0.18992	0.81008	52798.8	3592.7
0.19730	0.80270	57108.2	3886.0
0.20158	0.79842	61031.4	4152.9

TABLE III (CONTINUED)

N-DECANE AT 85.00 DEG. C.

COMPRESSION (CC/CC)	RELATIVE VOLUME	P (PSI)	(PATM)
0.20158	0.79842	61031.4	4152.9
0.21106	0.78894	68585.5	4666.9
0.21314	0.78686	68989.1	4694.4
0.21859	0.78141	74013.0	5036.3
0.21961	0.78039	75713.8	5152.0
0.23959	0.76041	95128.1	6473.1

TABLE III (CONTINUED)

N-DODECANE AT 25.00 DEG. C.

DENSITY = .74490 GM./C.C. SAMPLE WEIGHT = 2.18552 GM.

COMPRESSION (CC/CC)	RELATIVE VOLUME	P (PSI)	(PATM)
0.0	1.00000	14.7	1.0
0.00183	0.99817	252.7	17.2
0.00399	0.99601	425.7	29.0
0.00593	0.99407	999.7	68.0
0.00916	0.99084	1462.7	99.5
0.01203	0.98797	1974.7	134.4
0.01819	0.98181	3014.7	205.1
0.02646	0.97354	4524.7	307.9
0.03403	0.96597	5984.7	407.2
0.04110	0.95890	7544.7	513.4
0.04786	0.95214	9054.7	616.1
0.05369	0.94631	10594.7	718.2
0.05975	0.94025	12034.7	818.9
0.06487	0.93513	13614.7	926.4
0.07020	0.92980	15024.7	1022.4
0.07468	0.92532	16604.7	1129.9
0.07958	0.92042	18024.7	1226.5
0.08347	0.91653	19484.7	1325.9
0.08860	0.91140	21014.7	1430.0

TABLE III (CONTINUED)

N-DODECANE AT 45.00 DEG. C.

DENSITY = .73030 GM./C.C. SAMPLE WEIGHT = 2.18552 GM.

COMPRESSION (CC/CC)	RELATIVE VOLUME	P (PSI)	P (PATM)
0.0	1.00000	14.7	1.0
0.00202	0.99798	253.7	17.3
0.00415	0.99585	532.7	36.2
0.00792	0.99208	1012.7	68.9
0.01157	0.98843	1446.7	98.4
0.01423	0.98577	2014.7	137.1
0.02317	0.97683	3094.7	210.6
0.03039	0.96961	4514.7	307.2
0.03872	0.96128	6014.7	409.3
0.04640	0.95360	7544.7	513.4
0.05321	0.94679	9014.7	613.4
0.06015	0.93985	10594.7	717.5
0.06579	0.93421	11994.7	816.2
0.07180	0.92820	13594.7	925.1
0.07738	0.92262	15094.7	1027.1
0.08272	0.91728	16654.7	1133.3
0.08719	0.91281	18054.7	1228.5
0.09330	0.90670	20074.7	1366.0
0.09892	0.90108	21994.7	1496.6
0.10748	0.89252	25284.7	1720.5
0.11386	0.88614	27974.7	1903.6
0.11829	0.88171	30014.7	2042.4
0.12275	0.87725	32014.7	2178.5

TABLE III (CONTINUED)

N-DODECANE AT 65.00 DEG. C.

DENSITY = .71563 GM./C.C. SAMPLE HEIGHT = 2.18552 GM.

COMPRESSION (CC/CC)	RELATIVE VOLUME	P (PSI)	(PATM)
0.0	1.00000	14.7	1.0
0.00191	0.99809	294.7	20.1
0.00380	0.99620	530.7	36.1
0.00807	0.99193	1040.7	70.8
0.01112	0.98888	1398.7	95.2
0.01605	0.98395	2014.7	137.1
0.02332	0.97668	3064.7	208.5
0.03369	0.96631	4584.7	312.0
0.04323	0.95677	6064.7	412.7
0.05100	0.94900	7564.7	514.7
0.05850	0.94150	9094.7	618.9
0.06572	0.93428	10594.7	716.8
0.07239	0.92761	12064.7	821.0
0.07831	0.92169	13664.7	929.8
0.08365	0.91635	15044.7	1023.7
0.08922	0.91078	16604.7	1129.9
0.09457	0.90543	18064.7	1229.2
0.10051	0.89949	20014.7	1361.9
0.10684	0.89316	22114.7	1504.8
0.11456	0.88544	24964.7	1698.7
0.12319	0.87681	28104.7	1912.4
0.12910	0.87090	31064.7	2113.8
0.13592	0.86408	34104.7	2320.7
0.14154	0.85777	36924.7	2512.6
0.14766	0.85234	40114.7	2729.6
0.15261	0.84739	42994.7	2925.6
0.15820	0.84180	46114.7	3137.9
0.16286	0.83714	49004.7	3334.6
0.16753	0.83247	51917.4	3532.8

TABLE III (CONTINUED)

N-DODECANE AT 85.00 DEG. C.

DENSITY = .70082 GM./C.C. SAMPLE WEIGHT = 2.18552 GM.

COMPRESSION (CC/CC)	RELATIVE VOLUME	P (PSI)	(PATM)
0.0	1.00000	14.7	1.0
0.00305	0.99695	311.7	21.2
0.00596	0.99404	548.7	37.3
0.01049	0.98951	1037.7	70.6
0.01464	0.98536	1459.7	99.3
0.01936	0.98064	2034.7	138.5
0.02844	0.97156	3114.7	211.9
0.03905	0.96095	4544.7	309.2
0.04851	0.95149	5964.7	405.9
0.05868	0.94132	7544.7	513.4
0.06595	0.93405	9034.7	614.8
0.07376	0.92624	10594.7	718.2
0.08087	0.91913	12064.7	821.0
0.08684	0.91316	13464.7	916.2
0.09374	0.90626	15064.7	1025.1
0.10505	0.89495	18134.7	1234.0
0.11113	0.88887	20134.7	1370.1
0.11770	0.88230	21994.7	1496.6
0.12622	0.87378	25144.7	1711.0
0.13427	0.86573	28114.7	1913.1
0.14097	0.85903	31144.7	2119.3
0.14770	0.85230	33924.7	2308.4
0.15340	0.84660	37094.7	2524.1
0.16011	0.84214	39934.7	2717.4
0.16473	0.83527	42994.7	2925.6
0.17004	0.82916	46034.7	3132.5
0.17520	0.82480	48974.7	3332.5
0.18560	0.81440	56202.9	3824.4
0.19228	0.80772	60461.6	4114.1

TABLE III (CONTINUED)

N-HEXADECANE AT 25.00 DEG. C.

DENSITY = .75888 GM./C.C. SAMPLE WEIGHT = 2.24803 GM.

COMPRESSION (CC/CC)	RELATIVE VOLUME	P (PSI)	(PATM)
0.0	1.00000	14.7	1.0
0.00048	0.99952	129.7	8.8
0.00238	0.99762	337.7	23.0
0.00342	0.99658	484.7	33.0
0.00630	0.99370	1030.7	70.1
0.01003	0.98997	1447.7	98.5
0.01212	0.98788	2054.7	139.8
0.01591	0.98409	2534.7	172.5
0.01779	0.98221	3064.7	208.5
0.02182	0.97818	3564.7	242.6
0.02291	0.97709	4064.7	276.6
0.02630	0.97370	4450.7	311.3
0.02740	0.97260	5044.7	343.3
0.03087	0.96913	5564.7	378.7
0.03187	0.96813	6074.7	413.4
0.03565	0.96435	6544.7	445.3
0.03694	0.96306	7044.7	479.4
0.04010	0.95990	7474.7	508.6
0.04092	0.95908	7984.7	543.3
0.04436	0.95564	8584.7	584.2
0.04904	0.95096	9594.7	652.9

TABLE III (CONTINUED)

N-HEXADECANE AT 45.00 DEG. C.

DENSITY = .74477 GM./C.C. SAMPLE WEIGHT = 2.24803 GM.

COMPRESSION (CC/CC)	RELATIVE VOLUME	P (PSI)	P (PATM)
0.0	1.00000	14.7	1.0
0.00189	0.99811	176.7	11.9
0.00266	0.99734	344.7	23.5
0.00403	0.99597	561.7	38.2
0.00774	0.99226	1096.7	74.6
0.01079	0.98921	1429.7	97.3
0.01411	0.98589	2054.7	139.8
0.01751	0.98249	2564.7	174.5
0.02037	0.97963	3084.7	209.9
0.02354	0.97646	3624.7	246.6
0.02601	0.97399	4044.7	275.2
0.02913	0.97087	4450.7	310.6
0.03090	0.96910	5024.7	341.9
0.04123	0.95877	7084.7	482.1
0.04580	0.95420	7964.7	542.0
0.05039	0.94961	9154.7	622.9
0.05490	0.94510	10014.7	681.5
0.05832	0.94168	11114.7	756.3
0.06299	0.93701	12054.7	820.3
0.06643	0.93357	13164.7	895.8
0.07011	0.92989	14004.7	953.0
0.07305	0.92695	15084.7	1026.4
0.07713	0.92287	15994.7	1088.4
0.07937	0.92027	16964.7	1154.4
0.08330	0.91670	18034.7	1227.2
0.08702	0.91298	19014.7	1293.9
0.08955	0.91045	20034.7	1363.3
0.09239	0.90761	21244.7	1445.6
0.09484	0.90516	22054.7	1500.7
0.09762	0.90238	22984.7	1564.0
0.10101	0.89899	24084.7	1638.9

TABLE III (CONTINUED)

N-HEXADECANE AT 65.00 DEG. C.

DENSITY = .73057 GM./C.C. SAMPLE WEIGHT = 2.24803 GM.

COMPRESSION (CC/CC)	RELATIVE VOLUME	P (PSI)	(PATM)
0.0	1.00000	14.7	1.0
0.00137	0.99863	199.7	13.6
0.00397	0.99603	507.7	34.5
0.00829	0.99171	1055.7	71.8
0.01570	0.98430	2094.7	142.5
0.02235	0.97765	3104.7	211.3
0.02878	0.97122	4034.7	274.5
0.03402	0.96598	5024.7	341.9
0.03958	0.96042	6014.7	409.3
0.04574	0.95426	7134.7	485.5
0.05032	0.94968	7994.7	544.0
0.05574	0.94426	9058.7	622.9
0.05998	0.94002	10054.7	684.2
0.06438	0.93562	11044.7	751.5
0.06809	0.93191	12034.7	818.9
0.07224	0.92776	13094.7	891.0
0.07565	0.92435	14024.7	954.3
0.07992	0.92008	15084.7	1026.4
0.08327	0.91673	16084.7	1094.5
0.08689	0.91311	17214.7	1171.4
0.08995	0.91005	18064.7	1229.2
0.09302	0.90698	19154.7	1303.4
0.09628	0.90372	20104.7	1368.0
0.09924	0.90074	21154.7	1439.5
0.10239	0.89761	22134.7	1506.2
0.10459	0.89541	23034.7	1567.4
0.10801	0.89199	24084.7	1638.9
0.11038	0.88962	25084.7	1706.9
0.11299	0.88701	26044.7	1772.2
0.11464	0.88536	27114.7	1845.0
0.11790	0.88210	28094.7	1911.7
0.11967	0.88033	29114.7	1981.1
0.12255	0.87745	30134.7	2050.5
0.12389	0.87611	31124.7	2117.9
0.12642	0.87358	32034.7	2179.8
0.12864	0.87196	33084.7	2251.3
0.13100	0.86900	34114.7	2321.4
0.13295	0.86705	35064.7	2386.0
0.13527	0.86473	36004.7	2450.0

TABLE III (CONTINUED)

N-HEXADECANE AT 85.00 DEG. C.

DENSITY = .71625 GM./C.C. SAMPLE WEIGHT = 2.24803 GM.

COMPRESSION (CC/CC)	RELATIVE VOLUME	P (PSI)	P (PATM)
0.0	1.00000	14.7	1.0
0.00112	0.99888	139.7	9.5
0.00543	0.99457	566.7	38.6
0.00914	0.99086	1005.7	68.4
0.01343	0.98657	1466.7	99.8
0.01738	0.98262	1994.7	135.7
0.02620	0.97380	3166.7	215.3
0.03214	0.96786	4039.7	274.9
0.03908	0.96092	5064.7	344.6
0.04483	0.95517	6054.7	412.0
0.05577	0.94423	8024.7	546.0
0.06112	0.93888	9058.7	616.8
0.06650	0.93350	10114.7	688.3
0.07083	0.92917	11044.7	751.5
0.07538	0.92462	12114.7	824.4
0.07902	0.92098	13014.7	885.6
0.08307	0.91693	14154.7	963.2
0.08691	0.91309	15064.7	1025.1
0.09103	0.90897	16144.7	1098.6
0.09433	0.90567	17024.7	1158.5
0.09804	0.90196	18114.7	1232.6
0.10154	0.89846	19084.7	1298.6
0.10452	0.89548	20214.7	1375.5
0.10772	0.89292	21074.7	1434.0
0.11219	0.88781	23174.7	1576.9
0.11923	0.88077	25014.7	1702.1
0.12370	0.87630	27014.7	1838.2
0.12992	0.87008	29114.7	1981.1
0.13425	0.86575	31214.7	2124.0
0.13905	0.86095	33014.7	2246.5
0.14240	0.85760	35234.7	2397.6
0.14724	0.85276	37014.7	2518.7
0.15038	0.84962	39039.7	2656.5
0.15507	0.84493	41024.7	2791.6
0.15848	0.84152	43154.7	2936.5
0.16379	0.83774	45114.7	3069.9
0.16355	0.83645	47104.7	3205.3
0.16840	0.83160	49044.7	3337.3
0.17090	0.82910	50709.3	3450.5
0.17475	0.82525	53192.9	3619.5

TABLE III (CONTINUED)

N-TETRADECANE AT 25.00 DEG. C.

DENSITY = .76968 GM./C.C. SAMPLE WEIGHT = 2.26350 GM.

COMPRESSION (CC/CC)	RELATIVE VOLUME	P (PSI)	P (PATM)
0.0	1.00000	14.7	1.0
0.00139	0.99861	91.7	6.2
0.00185	0.99815	164.7	11.2
0.00252	0.99748	244.7	16.7
0.00350	0.99650	312.7	21.3
0.00359	0.99641	395.7	26.9
0.00414	0.99586	470.7	32.0
0.00496	0.99504	646.7	44.0
0.00478	0.99522	688.7	46.9
0.00608	0.99392	770.7	52.4
0.00592	0.99408	871.7	59.3
0.00705	0.99295	934.2	63.7
0.00717	0.99283	1070.7	72.9
0.00904	0.99096	1230.7	83.7
0.00818	0.99182	1237.7	84.2
0.01059	0.98941	1516.7	103.2
0.01028	0.98972	1734.7	118.0
0.01333	0.98667	2084.7	141.9
0.01292	0.98708	2184.7	148.7
0.01609	0.98391	2564.7	174.5
0.01811	0.98189	2994.7	203.8
0.01762	0.98238	3194.7	217.4
0.02101	0.97899	3514.7	239.2
0.02346	0.97496	4064.7	276.6

TABLE III (CONTINUED)

N-TETRADECANE AT 45.00 DEG. C.

DENSITY = .75586 GM./C.C. SAMPLE WEIGHT = 2.26350 GM.

COMPRESSION (CC/CC)	RELATIVE VOLUME	P (PSI)	P (PATM)
0.0	1.00000	14.7	1.0
0.00085	0.99915	152.7	10.4
0.00152	0.99848	274.7	18.7
0.00412	0.99588	548.7	37.3
0.00637	0.99363	1034.7	70.4
0.01273	0.98727	1984.7	135.1
0.01915	0.98085	3094.7	210.6
0.02479	0.97521	4044.7	275.2
0.02898	0.97102	5064.7	344.6
0.03430	0.96570	6024.7	410.0
0.03888	0.96112	7144.7	486.2
0.04379	0.95621	8034.7	548.8
0.04740	0.95260	9114.7	620.2
0.05155	0.94845	10014.7	681.5
0.05560	0.94440	11084.7	754.3
0.05961	0.94039	12084.7	822.3
0.06214	0.93786	13084.7	890.4
0.06628	0.93372	14094.7	959.1
0.06865	0.93135	15034.7	1023.0
0.07387	0.92613	16014.7	1089.7

TABLE III (CONTINUED)

N-TETRADECANE AT 65.00 DEG. C.

DENSITY = .74202 GM./C.C. SAMPLE WEIGHT = 2.26350 GM.

COMPRESSION (CC/CC)	RELATIVE VOLUME	P (PSI)	(PATM)
0.0	1.00000	14.7	1.0
0.00093	0.99907	108.7	7.4
0.00163	0.99837	215.7	14.7
0.00421	0.99579	484.7	33.0
0.00729	0.99271	1005.7	68.4
0.01443	0.98557	2034.7	138.5
0.02131	0.97869	3114.7	211.9
0.02715	0.97285	4014.7	273.2
0.03215	0.96785	5034.7	342.6
0.03810	0.96190	6014.7	409.3
0.04290	0.95710	7114.7	484.1
0.04851	0.95149	8034.7	548.8
0.05240	0.94760	9114.7	620.2
0.05679	0.94321	10034.7	682.8
0.06119	0.93881	11194.7	761.8
0.06465	0.93535	12034.7	818.9
0.06783	0.93217	13044.7	887.6
0.07285	0.92715	14044.7	955.7
0.07627	0.92373	15134.7	1029.9
0.07958	0.92042	16014.7	1089.7
0.08548	0.91452	18134.7	1234.0
0.09297	0.90703	20124.7	1369.4
0.09800	0.90200	22184.7	1509.6
0.10348	0.89683	24064.7	1637.5
0.10831	0.89169	26254.7	1786.5
0.11328	0.88672	28024.7	1907.0
0.11780	0.88220	30064.7	2045.8

TABLE III (CONTINUED)

N-TETRADECANE AT 85.00 DEG. C.

DENSITY = .72810 GM./C.C. SAMPLE WEIGHT = 2.26350 GM.

COMPRESSION (CC/CC)	RELATIVE VOLUME	P (PSI)	P (PATM)
0.0	1.00000	14.7	1.0
0.00076	0.99924	55.7	3.8
0.00207	0.99793	132.7	9.0
0.00467	0.99533	534.7	36.4
0.00864	0.99136	939.7	63.9
0.01652	0.98348	2084.7	141.9
0.02453	0.97547	3094.7	210.6
0.03268	0.96732	4504.7	306.5
0.03741	0.96259	5064.7	344.6
0.04251	0.95749	6074.7	413.4
0.04835	0.95165	7114.7	484.1
0.05296	0.94704	8034.7	551.5
0.05879	0.94121	9174.7	624.3
0.06247	0.93753	10094.7	686.9
0.06829	0.93171	11024.7	750.2
0.07080	0.92920	12114.7	824.4
0.07578	0.92422	13114.7	892.4
0.07890	0.92110	14114.7	960.4
0.08332	0.91668	15194.7	1033.9
0.08798	0.91202	16584.7	1128.5
0.09389	0.90611	18014.7	1225.8
0.09973	0.90027	20094.7	1367.4
0.10691	0.89309	22114.7	1504.8
0.11163	0.88902	24164.7	1644.3
0.11778	0.88222	26134.7	1778.4
0.12161	0.87839	28114.7	1913.1
0.12670	0.87330	30104.7	2048.5
0.13221	0.86779	32154.7	2188.0
0.13533	0.86467	34214.7	2328.2
0.13990	0.86010	36194.7	2462.9
0.14345	0.85655	38234.7	2601.7
0.14770	0.85230	40094.7	2728.3
0.15079	0.84921	42084.7	2863.7

TABLE III (CONTINUED)

MIXTURE 0.5000 MOLE FRACTION N-DECANE AND N-TETRADECANE
AT 25.00 DEG. C.

DENSITY = .74490 GM./C.C. SAMPLE WEIGHT = 2.18239 GM.

COMPRESSION (CC/CC)	RELATIVE VOLUME	P (PSI)	(PATM)
0.0	1.00000	14.7	1.0
0.00089	0.99911	258.7	17.3
0.00223	0.99777	545.7	37.1
0.00535	0.99465	1036.7	70.5
0.00840	0.99160	1456.7	99.1
0.01113	0.98887	2014.7	137.1
0.01495	0.98505	2594.7	176.6
0.01702	0.98298	3064.7	208.5
0.02018	0.97982	3524.7	239.8
0.02208	0.97792	4024.7	273.9
0.02604	0.97396	4594.7	312.6
0.03030	0.96970	5474.7	377.3
0.03637	0.96363	6594.7	448.7
0.03963	0.96037	7554.7	514.1
0.04494	0.95506	8604.7	585.5
0.04767	0.95233	9494.7	646.1
0.05286	0.94714	10544.7	717.5
0.05601	0.94399	11564.7	786.9
0.06017	0.93983	12524.7	852.3
0.06317	0.93683	13534.7	921.0
0.06755	0.93245	14564.7	991.1
0.07033	0.92967	15554.7	1058.4
0.07425	0.92575	16624.7	1131.2
0.07664	0.92417	17384.7	1183.0
0.07979	0.92021	18484.7	1257.8

TABLE III (CONTINUED)

MIXTURE 0.5000 MOLE FRACTION N-DECANE AND N-TETRADECANE
AT 45.00 DEG. C.

DENSITY = .73030 GM./C.C. SAMPLE WEIGHT = 2.18239 GM.

COMPRESSION (CC/CC)	RELATIVE VOLUME	P (PSI)	(PATM)
0.0	1.00000	14.7	1.0
0.00163	0.99837	249.7	17.0
0.00400	0.99600	488.7	33.3
0.00773	0.99227	999.7	68.0
0.01137	0.98863	1445.7	98.4
0.01533	0.98467	2024.7	137.8
0.02182	0.97818	3094.7	210.6
0.02968	0.97032	4474.7	304.5
0.03883	0.96117	6044.7	411.3
0.04536	0.95464	7414.7	504.5
0.05335	0.94665	9004.7	612.7
0.05973	0.94027	10594.7	723.6
0.06615	0.93385	12094.7	823.0
0.07184	0.92816	13704.7	932.5
0.07680	0.92320	14964.7	1018.3
0.08200	0.91799	16614.7	1130.6
0.08736	0.91264	18084.7	1230.6
0.09565	0.90435	21034.7	1431.3
0.10406	0.89594	23994.7	1632.7
0.11117	0.88883	27014.7	1838.2
0.11952	0.88048	30094.7	2047.8

TABLE III (CONTINUED)

MIXTURE 0.5000 MOLE FRACTION N-DECANE AND N-TETRADECANE
AT 65.00 DEG. C.

DENSITY = .71563 GM./C.C. SAMPLE WEIGHT = 2.18239 GM.

COMPRESSION (CC/CC)	RELATIVE VOLUME	P (PSI)	(PATM)
0.0	1.00000	14.7	1.0
0.00208	0.99792	263.7	17.9
0.00416	0.99584	479.7	32.6
0.00880	0.99120	1031.7	70.2
0.01273	0.98727	1490.7	101.4
0.01585	0.98415	1994.7	135.1
0.02481	0.97519	3144.7	214.0
0.03483	0.96517	4484.7	305.2
0.05149	0.94851	7624.7	518.8
0.05875	0.94125	9024.7	614.1
0.06589	0.93411	10614.7	722.3
0.07292	0.92708	12130.7	823.0
0.07822	0.92178	13634.7	927.8
0.08421	0.91579	15084.7	1026.4
0.08921	0.91079	16624.7	1131.2
0.09534	0.90466	18144.7	1234.7
0.10070	0.89930	21124.7	1437.4
0.10751	0.89249	22054.7	1500.7
0.11540	0.88460	25284.7	1720.5
0.12289	0.87711	27944.7	1901.5
0.12924	0.87076	31144.7	2119.3
0.13740	0.86260	34134.7	2322.7
0.14400	0.85600	37114.7	2525.5
0.14864	0.84996	40054.7	2725.6
0.15347	0.84653	43014.7	2927.0
0.15951	0.84049	46014.7	3131.1

TABLE III (CONTINUED)

MIXTURE 0.5000 MOLE FRACTION N-DECANE AND N-TETRADECANE
AT 85.00 DEG. C.

DENSITY = .70082 GM./C.C. SAMPLE WEIGHT = 2.18239 GM.

COMPRESSION (CC/CC)	RELATIVE VOLUME	P (PSI)	(PATM)
0.0	1.00000	14.7	1.0
0.00099	0.99901	144.7	9.8
0.00161	0.99839	225.7	15.4
0.00239	0.99761	265.7	18.1
0.00251	0.99749	306.7	20.9
0.00386	0.99614	394.7	26.9
0.00488	0.99512	520.7	35.4
0.00634	0.99366	616.7	42.0
0.00738	0.99262	717.7	48.8
0.00818	0.99182	818.7	55.7
0.00972	0.99028	938.7	63.9
0.01016	0.98984	1046.2	70.9
0.01046	0.98954	1042.7	71.0
0.01302	0.98698	1267.7	86.3
0.01503	0.98497	1490.7	101.4
0.01872	0.98128	2014.7	137.1
0.02737	0.97263	3064.7	208.5
0.03806	0.96194	4524.7	307.9
0.04955	0.95045	6134.7	417.4
0.05897	0.94103	7624.7	518.8
0.06524	0.93476	9014.7	613.4
0.07324	0.92676	10704.7	728.4
0.08029	0.91971	12114.7	824.4
0.08666	0.91246	13614.7	926.4
0.09305	0.90695	15164.7	1031.9
0.09706	0.90294	16644.7	1132.6
0.10357	0.89643	18024.7	1226.5
0.10995	0.89005	20184.7	1373.5
0.11736	0.88264	22194.7	1510.3
0.12161	0.87839	24034.7	1635.5
0.12798	0.87202	26024.7	1770.9
0.13507	0.86493	29244.7	1990.0
0.14266	0.85734	32014.7	2178.5
0.14814	0.85186	35094.7	2388.0
0.15607	0.84393	37944.7	2582.0
0.15989	0.84011	41084.7	2795.6
0.16777	0.83223	43994.7	2993.7
0.17043	0.82957	46954.7	3195.1
0.17685	0.82315	49914.7	3396.5
0.17981	0.82019	52868.9	3597.5
0.18529	0.81471	55989.7	3809.9

TABLE III (CONTINUED)

MIXTURE 0.5000 MOLE FRACTION N-DECANE AND N-TETRADECANE
AT 85.00 DEG. C.

COMPRESSION (CC/CC)	RELATIVE VOLUME	P (PSI)	(PATM)
0.18529	0.81471	55989.7	3809.9
0.18913	0.81087	58787.6	4000.2
0.19365	0.80635	62381.4	4244.8

TABLE III (CONTINUED)

MIXTURE 0.5000 MOLE FRACTION N-DODECANE AND N-HEXADECANE
AT 25.00 DEG. C.

DENSITY = .75888 GM./C.C. SAMPLE WEIGHT = 2.23155 GM.

COMPRESSION (CC/CC)	RELATIVE VOLUME	P (PSI)	(PATM)
0.0	1.00000	14.7	1.0
0.00165	0.99835	258.7	17.6
0.00366	0.99634	505.7	34.4
0.00525	0.99475	752.7	51.2
0.00695	0.99305	1066.7	72.6
0.00776	0.99224	1244.7	84.7
0.00964	0.99036	1485.7	101.1
0.01211	0.98789	1994.7	135.7
0.01564	0.98436	2584.7	175.9
0.01777	0.98223	3014.7	205.1
0.02020	0.97980	3514.7	239.2
0.02285	0.97715	3990.2	271.1
0.02554	0.97446	4534.7	308.6
0.02817	0.97183	5064.7	344.6
0.03078	0.96922	5584.7	380.0
0.03324	0.96676	6044.7	411.3
0.03526	0.96474	6564.7	446.7
0.03771	0.96229	7064.7	480.7
0.03941	0.96059	7524.7	512.0
0.04185	0.95815	8084.7	550.1

TABLE III (CONTINUED)

MIXTURE 0.5000 MOLE FRACTION N-DODECANE AND N-HEXADECANE
AT 45.00 DEG. C.

DENSITY = .74477 GM./C.C. SAMPLE WEIGHT = 2.23155 GM.

COMPRESSION (CC/CC)	RELATIVE VOLUME	P (PSI)	(PATM)
0.0	1.00000	14.7	1.0
0.00244	0.99756	265.7	18.1
0.00448	0.99552	513.7	35.0
0.00924	0.99076	1262.7	85.9
0.01040	0.98960	1450.7	98.7
0.01428	0.98572	1984.7	135.1
0.02168	0.97832	3134.7	213.3
0.02562	0.97438	4044.7	275.2
0.03079	0.96921	4984.7	339.2
0.03653	0.96347	6024.7	410.0
0.04245	0.95754	7114.7	484.1
0.04616	0.95384	8034.7	548.8
0.05068	0.94932	9094.7	618.9
0.05507	0.94493	10064.7	684.9
0.05889	0.94111	11084.7	754.3
0.06308	0.93692	12084.7	822.3
0.06646	0.93354	13064.7	889.0
0.07017	0.92983	14084.7	958.4
0.07331	0.92669	14984.7	1019.6
0.07633	0.92367	15914.7	1082.9
0.07984	0.92016	17044.7	1159.8
0.08283	0.91717	18014.7	1225.8

TABLE III (CONTINUED)

MIXTURE 0.5000 MOLE FRACTION N-DODECANE AND N-HEXADECANE
AT 65.00 DEG. C.

DENSITY = .73057 GM./C.C. SAMPLE WEIGHT = 2.23155 GM.

COMPRESSION (CC/CC)	RELATIVE VOLUME	P (PSI)	(PATM)
0.0	1.00000	14.7	1.0
0.00157	0.99843	252.7	17.2
0.00405	0.99594	514.7	35.0
0.00787	0.99213	1009.7	68.7
0.01097	0.98903	1426.7	97.1
0.01491	0.98509	2014.7	137.1
0.02251	0.97749	3064.7	208.5
0.03150	0.96850	4524.7	307.9
0.04027	0.95973	6014.7	409.3
0.04817	0.95183	7574.7	515.4
0.05572	0.94428	9074.7	617.5
0.06164	0.93836	10594.7	720.9
0.06788	0.93212	11934.7	812.1
0.07390	0.92610	13584.7	924.4
0.07902	0.92098	14964.7	1018.3
0.08512	0.91488	16614.7	1130.6
0.08975	0.91025	17954.7	1221.7
0.09631	0.90369	20114.7	1368.7
0.10171	0.89829	22014.7	1498.0
0.10726	0.89274	24104.7	1640.2
0.11171	0.88829	25764.7	1753.2
0.11952	0.88048	28974.7	1971.6
0.12632	0.87368	31874.7	2168.9

TABLE III (CONTINUED)

MIXTURE 0.5000 MOLE FRACTION N-DODECANE AND N-HEXADECANE
AT 85.00 DEG. C.

DENSITY = .71625 GM./C.C. SAMPLE HEIGHT = 2.23155 GM.

COMPRESSION (CC/CC)	RELATIVE VOLUME	P (PSI)	(PATM)
0.0	1.00000	14.7	1.0
0.00158	0.99842	250.7	17.1
0.00492	0.99508	534.7	36.4
0.00874	0.99126	1014.7	69.0
0.01269	0.98731	1434.7	97.6
0.01732	0.98268	2024.7	137.8
0.02488	0.97512	3024.7	205.8
0.03533	0.96467	4554.7	309.9
0.04427	0.95573	5934.7	403.8
0.05365	0.94635	7604.7	517.5
0.06152	0.93848	9064.7	616.8
0.06862	0.93138	10594.7	718.9
0.07552	0.92448	12124.7	825.0
0.08174	0.91826	13654.7	929.1
0.08684	0.91316	14964.7	1018.3
0.09265	0.90735	16664.7	1134.0
0.09779	0.90221	18044.7	1227.9
0.10414	0.89586	20124.7	1369.4
0.11012	0.88988	22004.7	1497.3
0.11647	0.88353	24194.7	1646.3
0.12147	0.87853	26014.7	1770.2
0.12645	0.87355	28124.7	1913.8
0.13122	0.86878	30054.7	2045.1
0.13798	0.86167	33054.7	2249.2
0.14414	0.85586	35914.7	2443.8
0.15009	0.84991	39154.7	2664.3
0.15518	0.84482	42194.7	2871.2
0.16133	0.83867	45214.7	3076.7
0.16584	0.83416	48044.7	3269.2

TABLE III (CONTINUED)

MIXTURE 0.6000 MOLE FRACTION N-DECANE, 0.2000 MOLE FRACTION N-TETRADECANE AND N-HEXADECANE AT 25.00 DEG. C.

DENSITY = .74490 GM./C.C. SAMPLE WEIGHT = 2.14735 GM.

COMPRESSION (CC/CC)	RELATIVE VOLUME	P (PSI)	P (ATM)
0.0	1.00000	14.7	1.0
0.00188	0.99812	246.7	16.7
0.00341	0.99659	513.7	35.0
0.00726	0.99274	1012.7	68.9
0.00950	0.99050	1473.7	100.3
0.01305	0.98695	2014.7	137.1
0.01898	0.98102	3034.7	206.5
0.02507	0.97493	4054.7	275.9
0.03032	0.96968	5174.7	352.1
0.03554	0.96446	6034.7	410.6
0.03882	0.96118	6944.7	472.6
0.04486	0.95514	8034.7	550.8
0.04855	0.95145	9064.7	616.8
0.05318	0.94682	10114.7	688.3
0.05643	0.94357	11054.7	752.2
0.06088	0.93912	12054.7	820.3
0.06383	0.93617	13034.7	887.0
0.06769	0.93231	14014.7	953.6
0.07046	0.92954	15074.7	1025.8
0.07337	0.92663	15814.7	1076.1
0.07710	0.92290	16964.7	1154.4

TABLE III (CONTINUED)

MIXTURE 0.6000 MOLE FRACTION N-DECANE, 0.2000 MOLE FRACTION N-TETRADECANE AND N-HEXADECANE AT 45.00 DEG. C.

DENSITY = .73030 GM./C.C. SAMPLE WEIGHT = 2.14735 GM.

COMPRESSION (CC/CC)	RELATIVE VOLUME	P (PSI)	(PATM)
0.0	1.00000	14.7	1.0
0.00201	0.99799	272.7	18.6
0.00519	0.99481	544.7	37.1
0.00842	0.99158	985.7	67.1
0.01127	0.98873	1432.7	97.5
0.01470	0.98530	2024.7	137.8
0.02176	0.97824	3094.7	210.6
0.03114	0.96886	4534.7	308.6
0.03774	0.96226	5924.7	403.2
0.04755	0.95245	7614.7	518.1
0.05389	0.94611	9084.7	618.2
0.06099	0.93901	10594.7	723.6
0.06628	0.93372	12014.7	817.5
0.07305	0.92695	13694.7	931.9
0.07747	0.92253	15014.7	1021.7
0.08341	0.91659	16614.7	1130.6
0.08728	0.91272	18014.7	1225.8
0.09496	0.90504	20194.7	1374.2
0.09959	0.90041	22034.7	1499.4
0.10526	0.89474	24054.7	1636.8
0.10975	0.89025	26154.7	1779.7
0.11431	0.88569	27914.7	1899.5
0.11853	0.88147	30004.7	2041.7

TABLE III (CONTINUED)

MIXTURE 0.6000 MOLE FRACTION N-DECANE, 0.2000 MOLE FRACTION N-TETRADECANE AND N-HEXADECANE AT 65.00 DEG. C.

DENSITY = .71563 GM./C.C. SAMPLE WEIGHT = 2.14735 GM.

COMPRESSION (CC/CC)	RELATIVE VOLUME	P (PSI)	(PATM)
0.0	1.00000	14.7	1.0
0.00269	0.99731	261.7	17.8
0.00454	0.99546	463.7	31.6
0.00926	0.99074	1002.7	68.2
0.01768	0.98232	2014.7	137.1
0.02451	0.97549	2954.7	201.1
0.03440	0.96560	4534.7	308.6
0.04330	0.95670	6044.7	411.3
0.05117	0.94883	7314.7	497.7
0.05967	0.94033	9054.7	616.1
0.06690	0.93310	10544.7	717.5
0.07216	0.92784	12130.7	821.0
0.07965	0.92035	13614.7	926.4
0.08474	0.91526	15014.7	1021.7
0.09042	0.90958	16614.7	1130.6
0.09524	0.90476	17974.7	1223.1
0.10223	0.89777	20174.7	1372.8
0.10773	0.89227	22004.7	1497.3
0.11415	0.88585	24174.7	1645.0
0.11835	0.88165	25914.7	1763.4
0.12427	0.87573	28214.7	1919.9
0.12843	0.87157	29974.7	2039.6
0.13571	0.86429	33294.7	2265.6
0.14086	0.85777	36014.7	2450.6
0.14750	0.85250	39134.7	2662.9
0.15291	0.84709	42344.7	2881.4
0.15590	0.84410	43814.7	2981.4
0.15927	0.84073	45944.7	3126.3

TABLE III (CONTINUED)

MIXTURE 0.6000 MOLE FRACTION N-DECANE, 0.2000 MOLE FRACTION N-TETRADECANE AND N-HEXADECANE AT 85.00 DEG. C.

DENSITY = .70082 GM./C.C. SAMPLE HEIGHT = 2.14735 CM.

COMPRESSION (CC/CC)	RELATIVE VOLUME	P (PSI)	(PATM)
0.0	1.00000	14.7	1.0
0.00250	0.99750	251.7	17.1
0.00589	0.99411	593.7	40.4
0.00983	0.99017	996.7	67.8
0.01422	0.98578	1406.7	95.7
0.01863	0.981[illegible]	2024.7	137.8
0.02678	0.97322	2964.7	201.7
0.03964	0.96036	4684.7	318.8
0.04861	0.95139	6034.7	410.6
0.05804	0.94196	7604.7	517.5
0.06649	0.93351	9174.7	624.3
0.07394	0.92606	10594.7	720.9
0.08078	0.91922	12114.7	824.4
0.08682	0.91318	13614.7	926.4
0.09273	0.90727	15014.7	1021.7
0.09891	0.90109	16594.7	1129.2
0.10403	0.89597	18114.7	1232.6
0.11088	0.88912	20114.7	1368.7
0.11709	0.88291	22084.7	1502.8
0.12314	0.87686	24164.7	1644.3
0.12829	0.87171	26024.7	1770.9
0.13648	0.86352	29264.7	1991.3
0.14312	0.85688	32014.7	2178.5
0.15004	0.84996	35124.7	2390.1
0.15531	0.84469	37974.7	2584.0
0.16141	0.83859	41064.7	2794.3
0.16647	0.83353	43934.7	2989.6
0.17156	0.82844	46834.7	3186.9
0.17627	0.82373	49764.7	3386.3
0.17992	0.82008	52077.9	3543.7
0.18505	0.81495	55966.4	3808.3
0.18618	0.81382	56734.4	3860.5
0.19249	0.80751	61510.5	4185.5

CHAPTER VII

THEORIES TESTED

Prior to the actual testing of the theories considered in Chapter II it was necessary to find a method to analytically represent the data within experimental error. This was accomplished by using the Tait equation (59).

The characteristic parameters for the Prausnitz partition function were determined in the manner suggested by Prausnitz and the characteristic parameters for the Flory partition function were determined in the manner suggested by Flory. The characteristic parameters were also determined in both cases using the assumptions given in Chapter II concerning their temperature dependence. This determination was accomplished using the Tait equation and a least squares regression analysis on the respective isothermal compressibility equations and equations of state.

The Flory mixing rule is considered and the results for the two binary mixtures and one ternary mixture are compared with the Flory mixing rule results.

The next section considers the isothermal compressibility predicted by the Scaled particle theory versus that obtained via the Tait equation. The Scaled Particle effective spherical radius, A, used in the predictions was determined via regression analysis on the isothermal compressibility.

The last section contains a comparison of the three liquid theories for a representative case, n-Dodecane.

I. TAIT EQUATION

The Tait equation which many other investigators have used was found to fit the present data to within experimental error. The Tait coefficient J could not be considered temperature independent nor a universal constant for data of the accuracy of that taken in this study.

Data Representation

To provide a smooth representation of the data with the Tait equation it was necessary to allow both J and L to be functions of temperature and compound or composition, but independent of pressure. The Tait equation is

$$-\left(\frac{\partial V}{\partial P}\right)_{T,N_i} = \frac{J}{P+L} \quad . \qquad \text{(VII-1)}$$

There is no theoretical relationship known between the equation of state for a liquid and the Tait coefficients J and L. The functional form of the equation is such that L is the pressure at which the isothermal compressibility goes to one-half of the zero point value.

Figures 11 thru 17 show the experimental compression data for all seven pures and mixtures as a function of temperature and pressure. The experimental points appear to be directly on the smoothed Tait curve for each system.

To see the difference in the smoothed curve and experimental data it is necessary to plot differences in compression versus pressure. Representative plots are shown in Figures 18 thru 21.

The values of J and L to be used for the twenty-eight isotherms are listed in Table IV. Figures 22 and 23 are plots of L versus temperature and J versus temperature for the twenty-eight isotherms. Table V contains the key to the compound or mixture code used in this work. That is: A is used for n-Decane, B for n-Dodecane, C for n-Tetradecane, D for n-Hexadecane, FU for the n-Decane and n-Tetradecane binary mixture, IU for the n-Dodecane and n-Hexadecane binary mixture, and T1 for the ternary mixture.

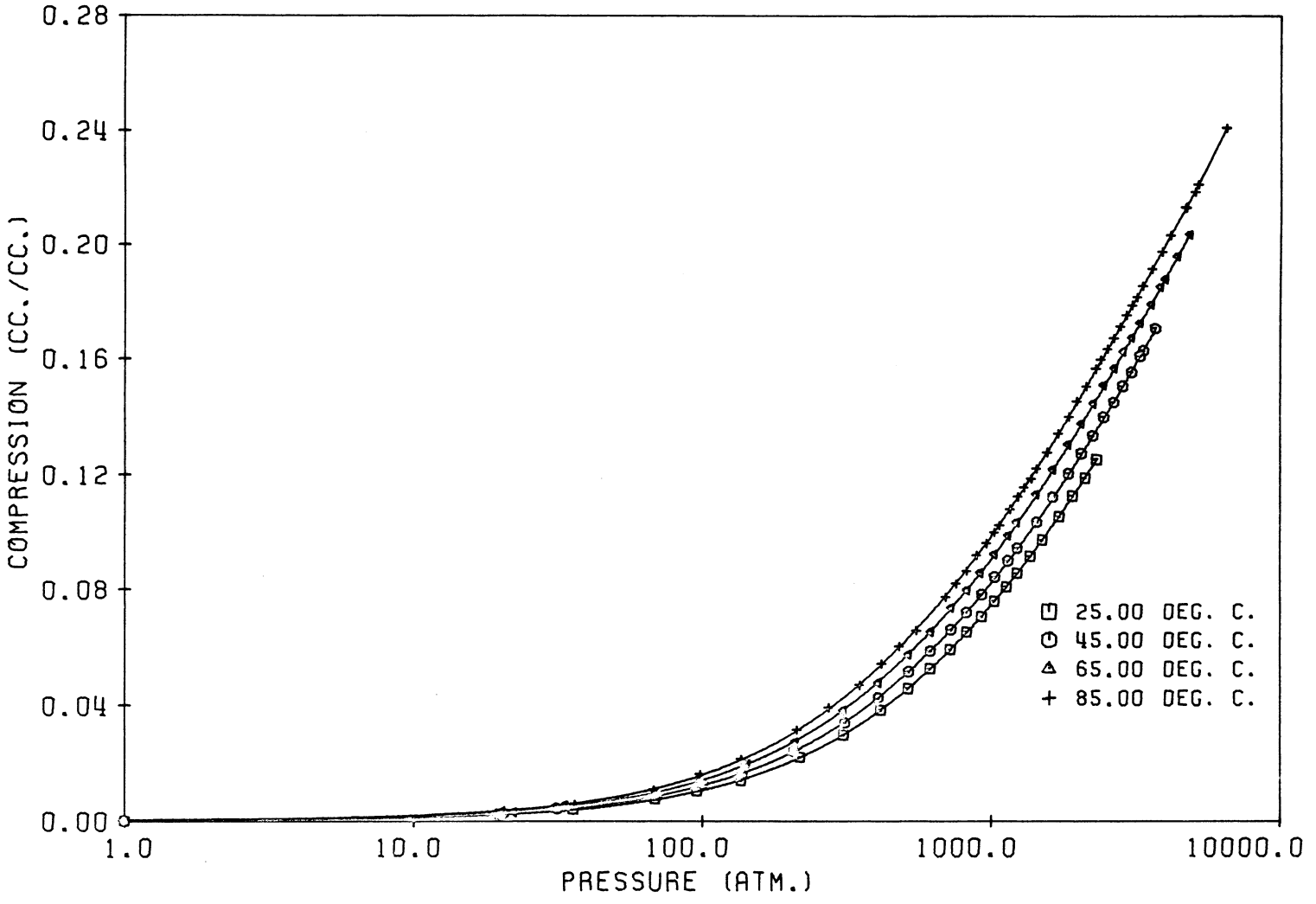

FIGURE 11
RAW COMPRESSION DATA VERSUS PRESSURE FOR
NORMAL DECANE

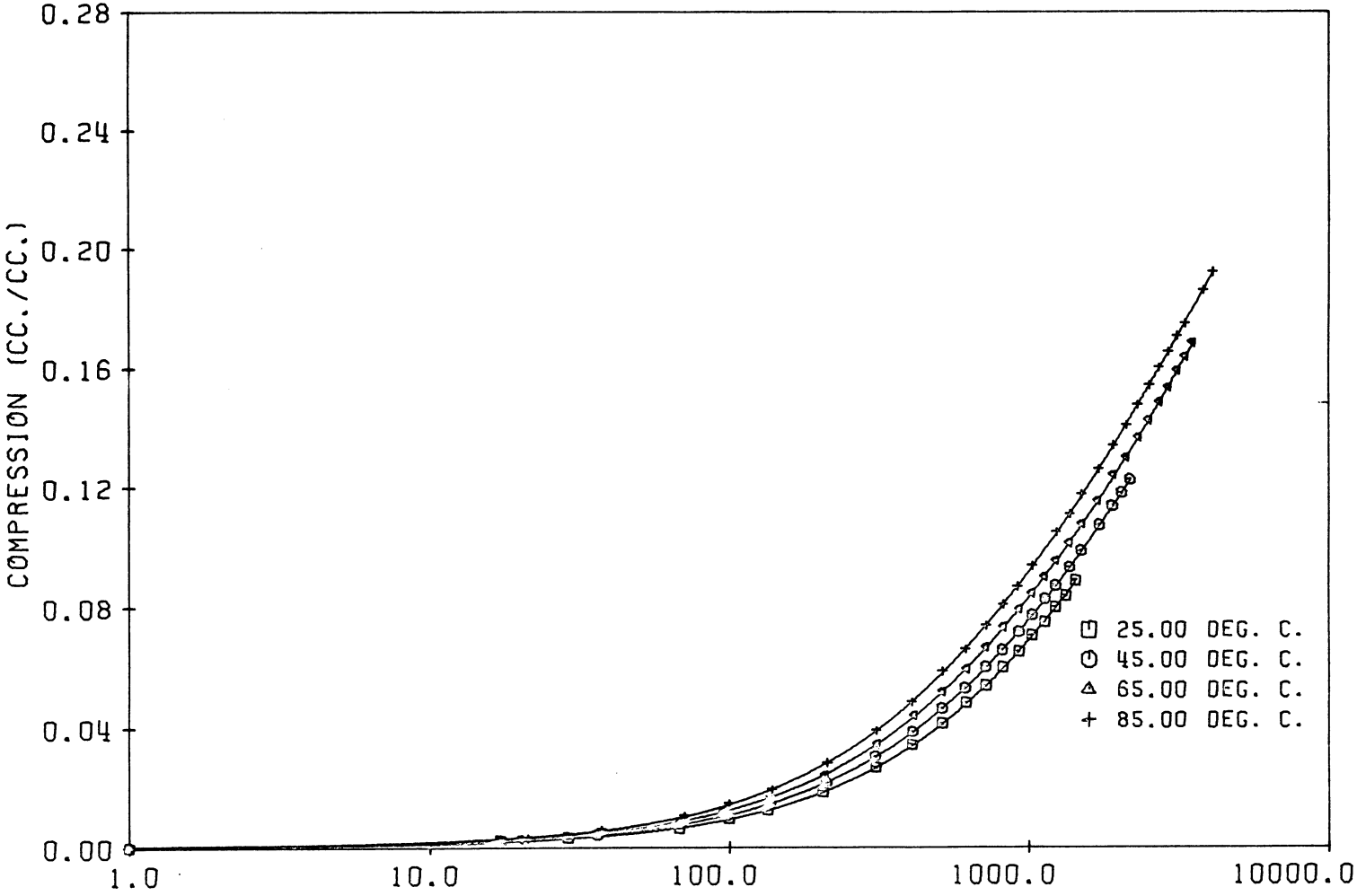

FIGURE 12

RAW COMPRESSION DATA VERSUS PRESSURE FOR NORMAL DODECANE

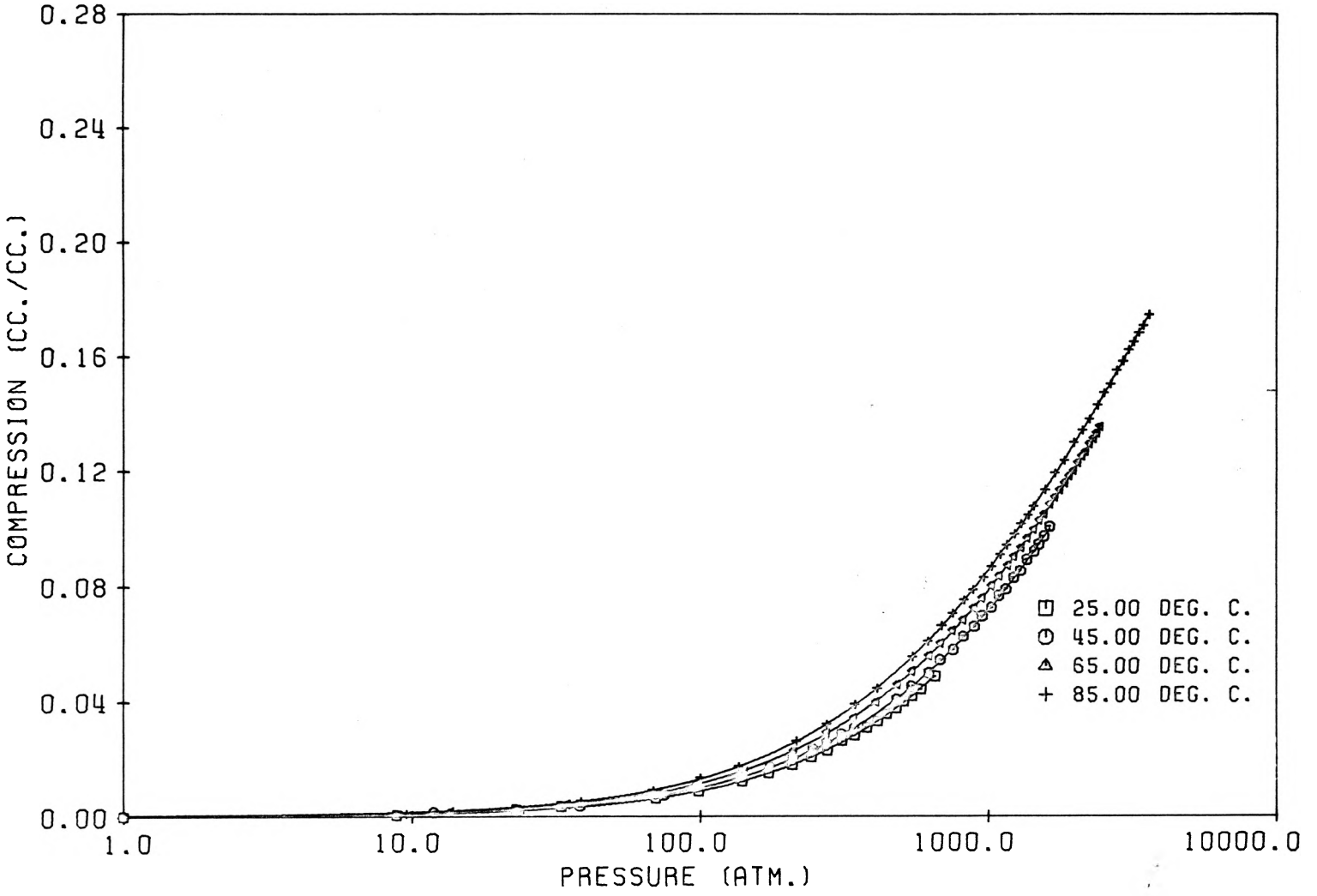

FIGURE 13

RAW COMPRESSION DATA VERSUS PRESSURE FOR NORMAL TETRADECANE

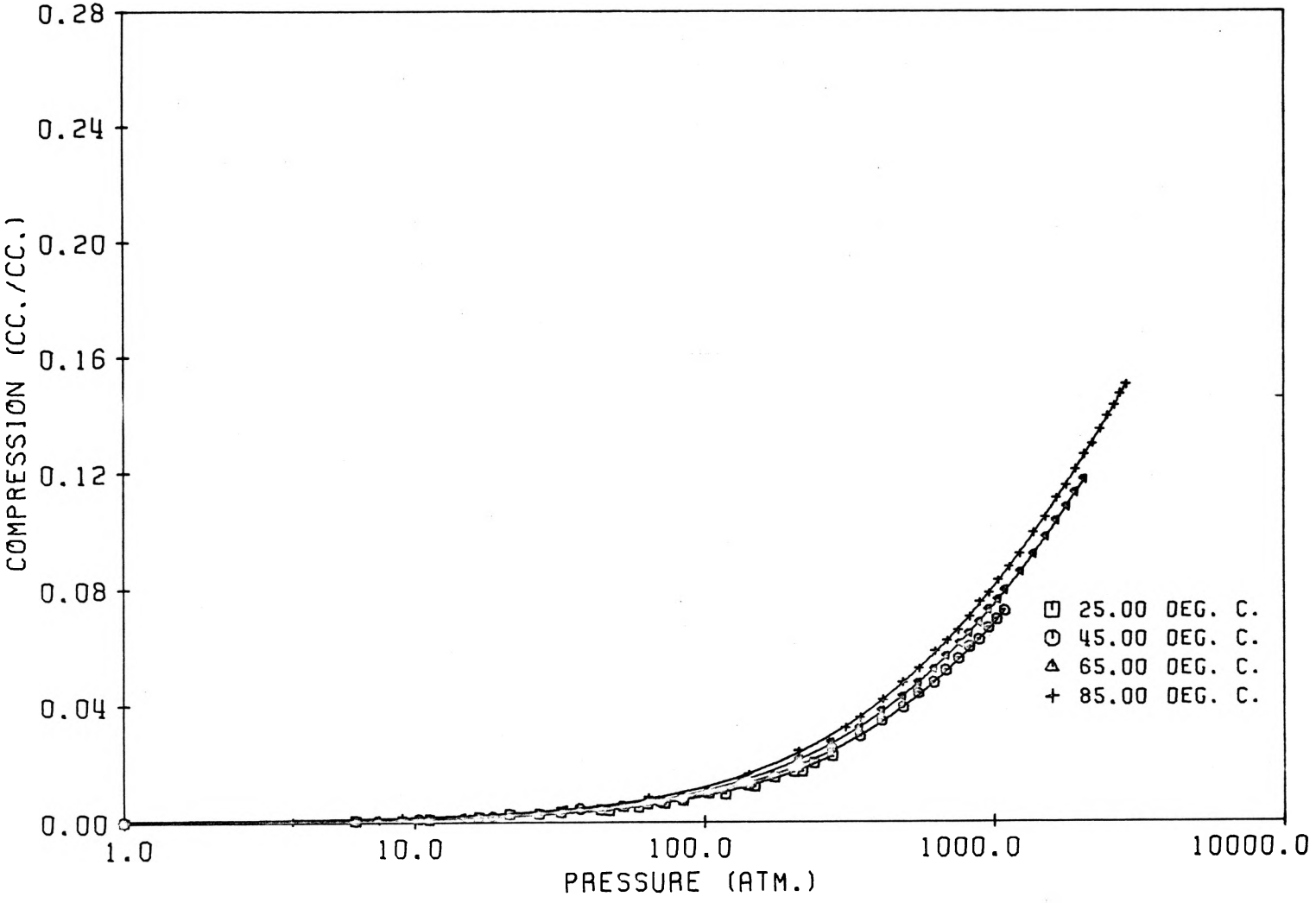

FIGURE 14

RAW COMPRESSION DATA VERSUS PRESSURE FOR NORMAL HEXADECANE

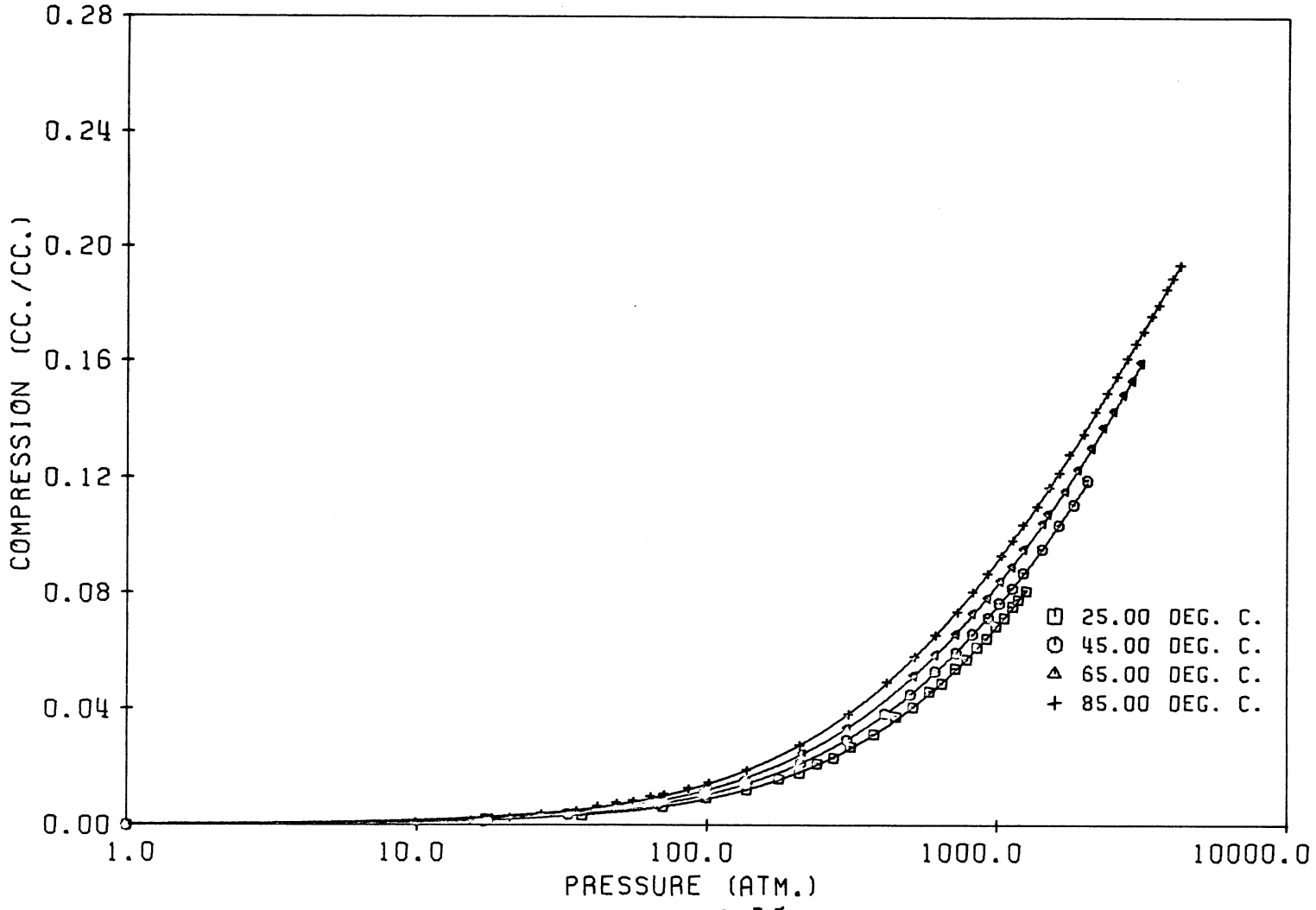

FIGURE 15

RAW COMPRESSION DATA VERSUS PRESSURE FOR
0.5000 M.F. N-DECANE AND N-TETRADECANE

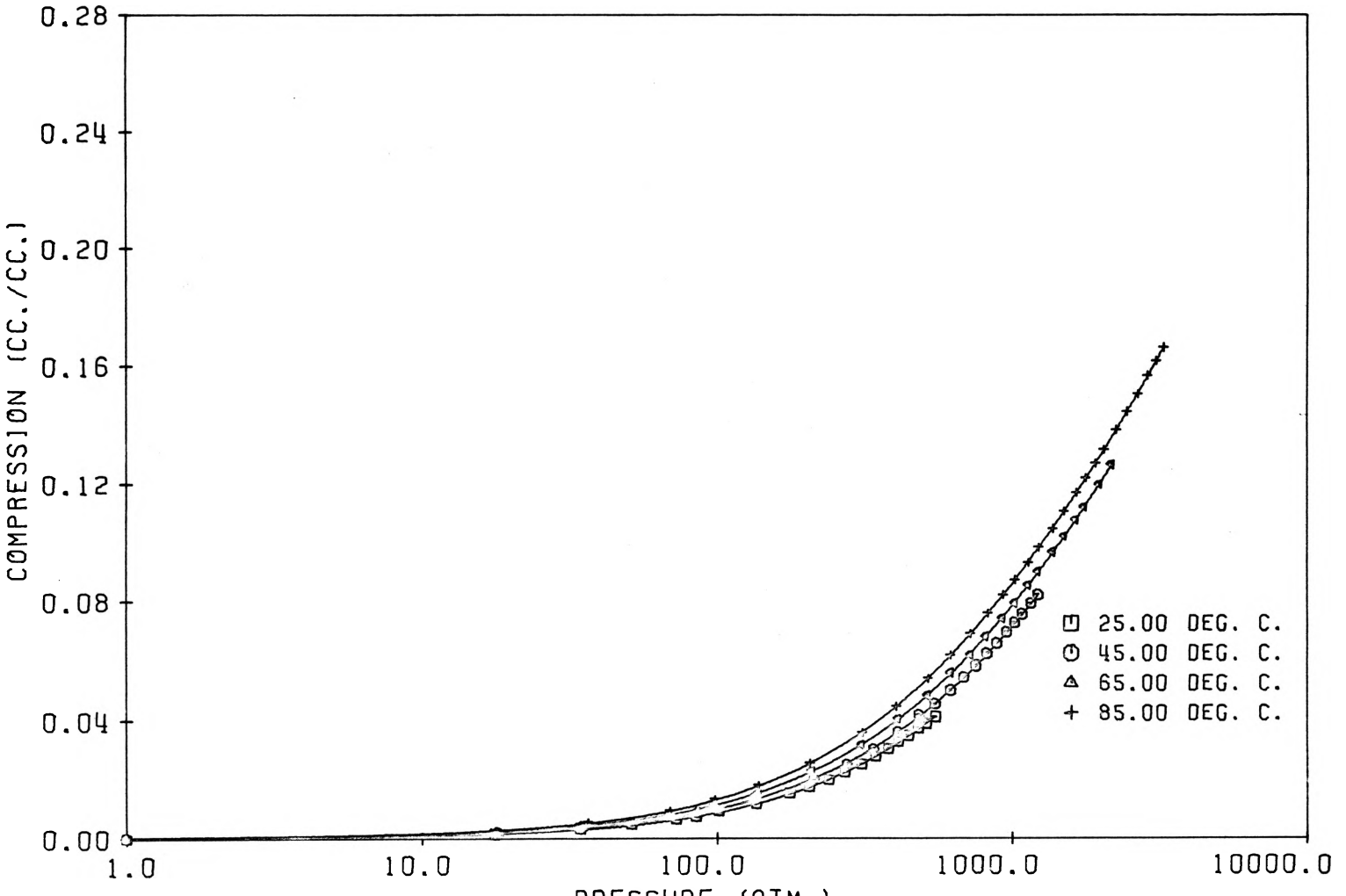

FIGURE 16

RAW COMPRESSION DATA VERSUS PRESSURE FOR
0.5000 M.F. N-DODECANE AND N-HEXADECANE

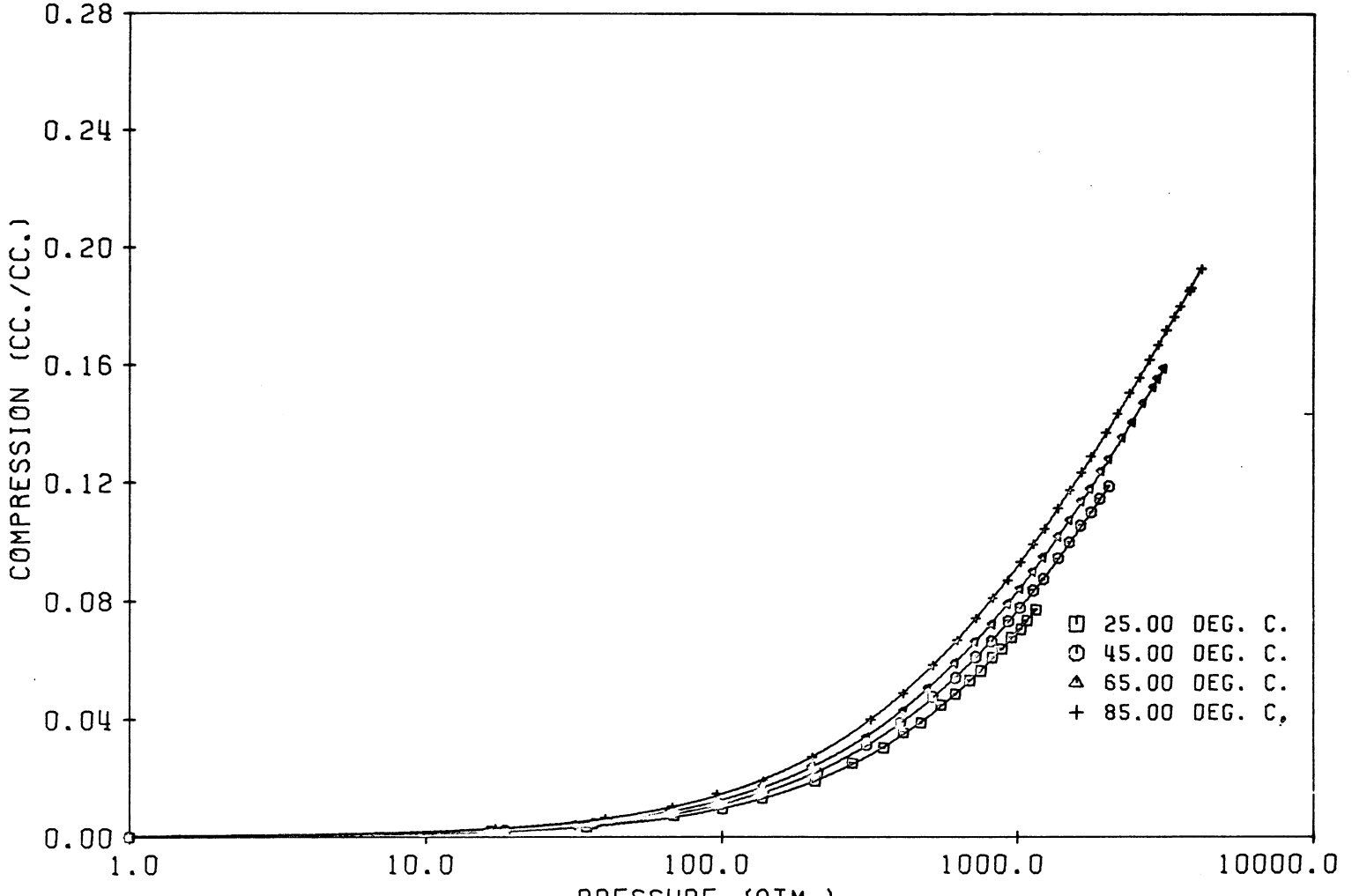

FIGURE 17

RAW COMPRESSION DATA VERSUS PRESSURE FOR
0.600 M.F. N-C10 AND 0.200 M.F. N-C14 AND N-C16

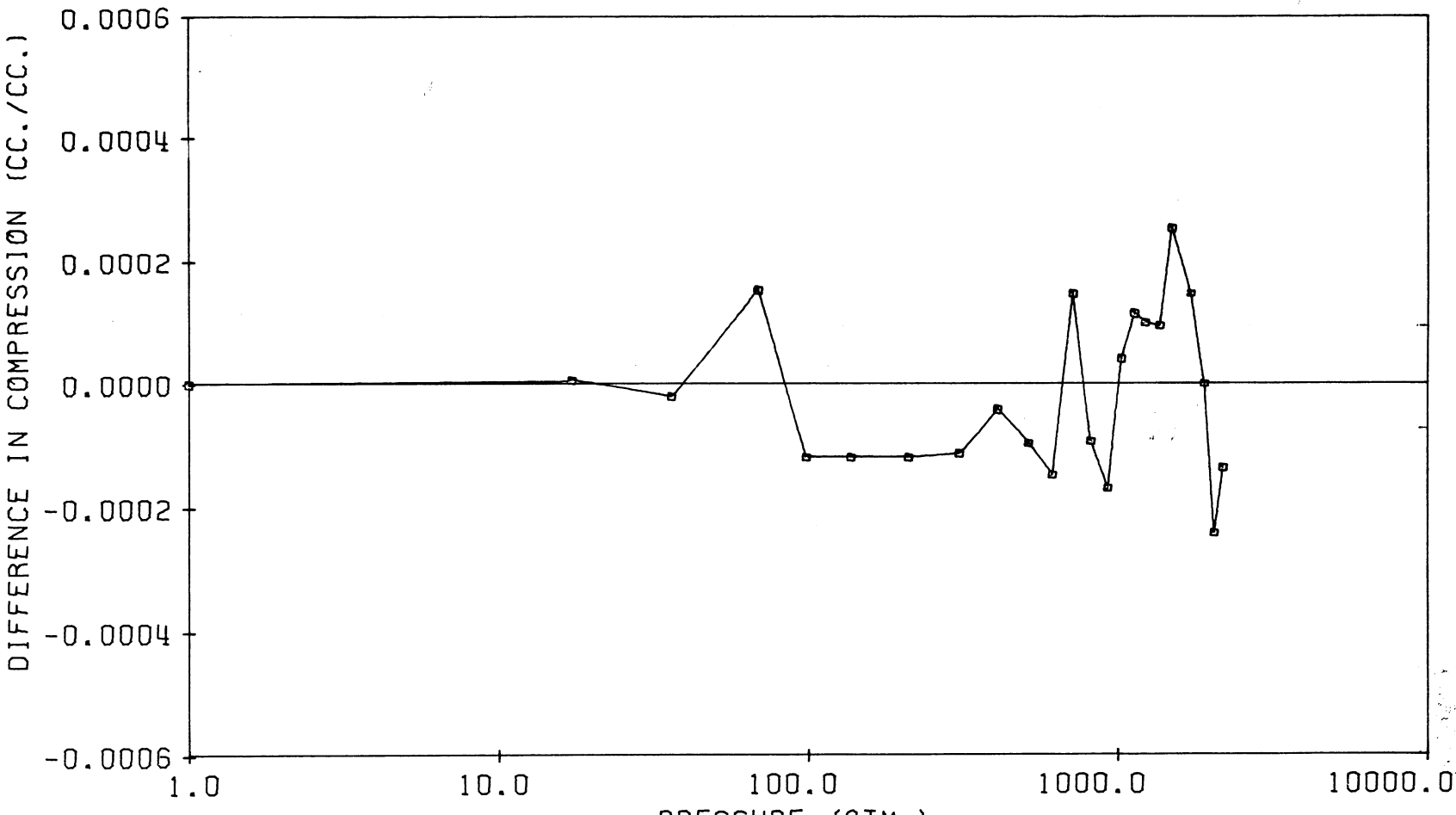

FIGURE 18

DIFFERENCE IN RAW AND SMOOTHED COMPRESSION DATA
VERSUS PRESSURE FOR
NORMAL DODECANE AT 45.0 DEG. C.

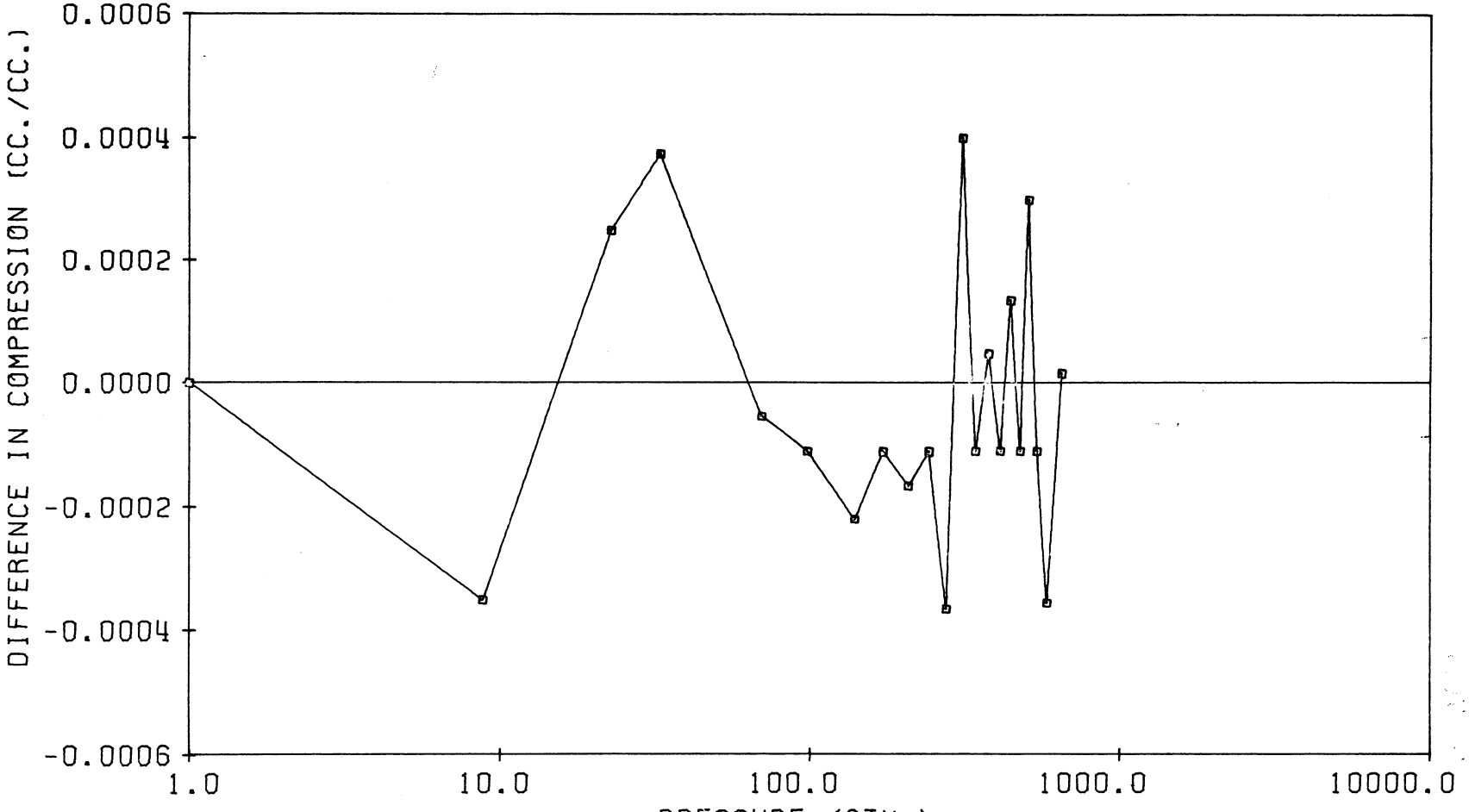

FIGURE 19

DIFFERENCE IN RAW AND SMOOTHED COMPRESSION DATA
VERSUS PRESSURE FOR
NORMAL TETRADECANE AT 25.0 DEG. C.

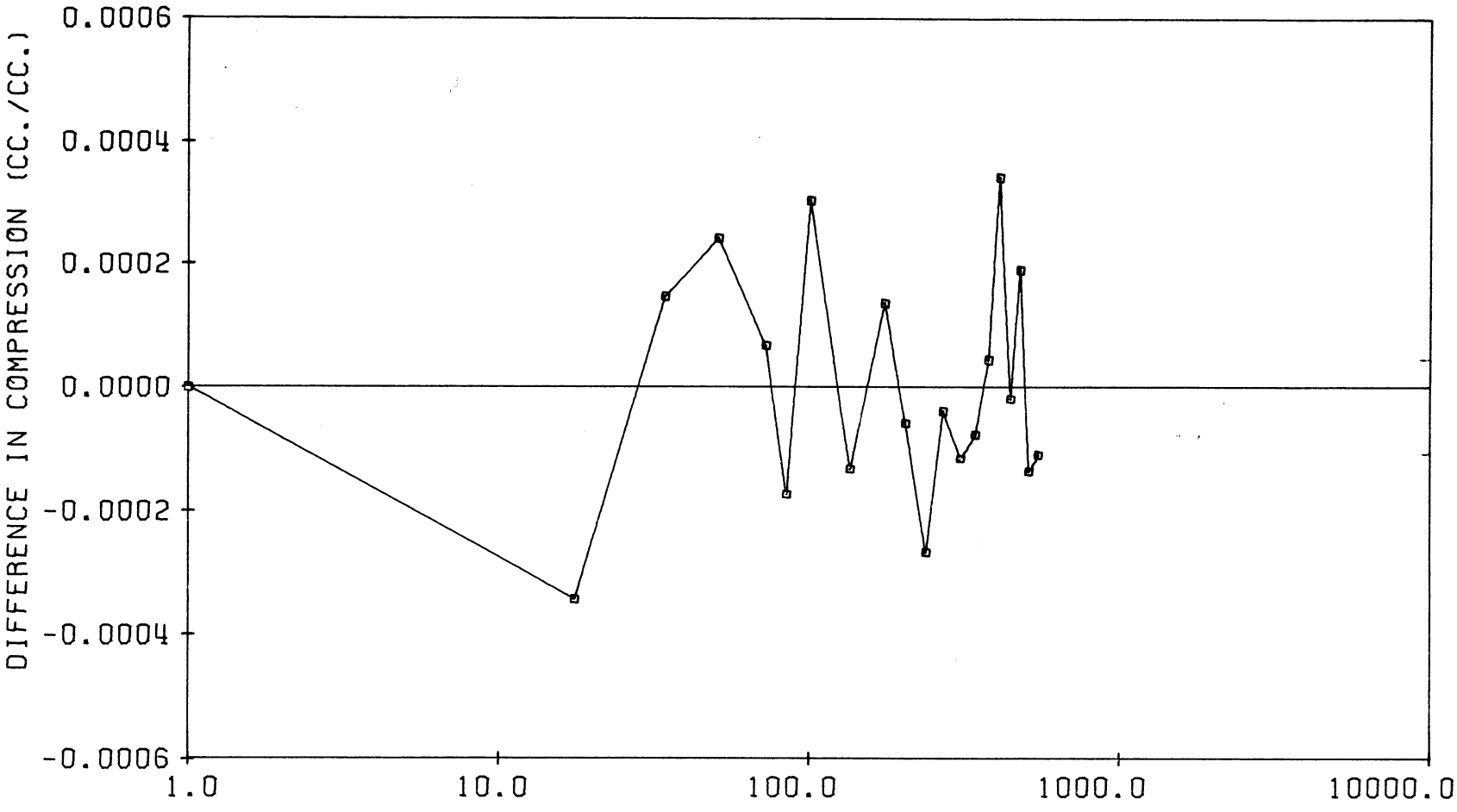

FIGURE 20

DIFFERENCE IN RAW AND SMOOTHED COMPRESSION DATA
VERSUS PRESSURE FOR
MIXTURE 0.5000 MOLE FRACTION N-DODECANE AND N-HEXADECANE AT 25.0 DEG.C .

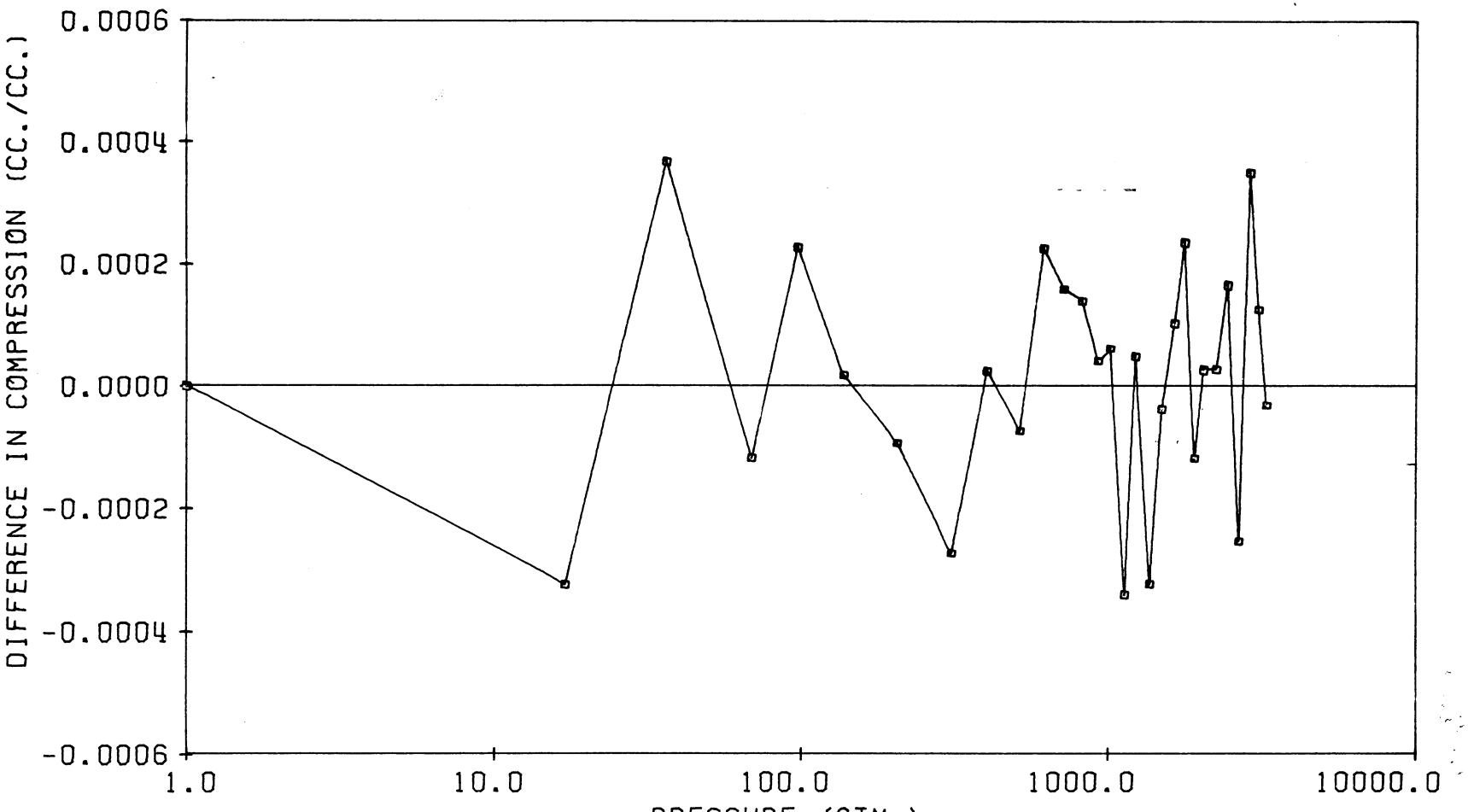

FIGURE 21

DIFFERENCE IN RAW AND SMOOTHED COMPRESSION DATA
VERSUS PRESSURE FOR
MIXTURE 0.5000 MOLE FRACTION N-DODECANE AND N-HEXADECANE AT 85.0 DEG.C .

TABLE IV

TAIT COEFFICIENTS J AND L

Compound or Mixture	t (°C)	L (atm.)	J (cc/cc)
n-Decane	25.0	824.	.094226
	45.0	719.	.094093
	65.0	617.	.093828
	85.0	518.	.092502
n-Dodecane	25.0	874.	.091248
	45.0	775.	.092041
	65.0	680.	.092312
	85.0	589.	.092774
n-Tetradecane	25.0	913.	.089818
	45.0	822.	.091570
	65.0	732.	.092188
	85.0	645.	.092742
n-Hexadecane	25.0	950.	.084001
	45.0	868.	.089023
	65.0	780.	.091520
	85.0	696.	.092650
0.5000 mole fraction n-Decane and n-Tetradecane	25.0	885.	.088416
	45.0	780.	.091890
	65.0	687.	.092751
	85.0	598.	.092790
0.5000 mole fraction n-Dodecane and n-Hexadecane	25.0	921.	.089205
	45.0	834.	.091445
	65.0	740.	.092454
	85.0	652.	.092732
0.6000 mole fraction n-Decane and 0.2000 mole fraction n-Tetradecane and n-Hexadecane	25.0	870.	.091479
	45.0	768.	.092073
	65.0	674.	.09281
	85.0	586.	.092372

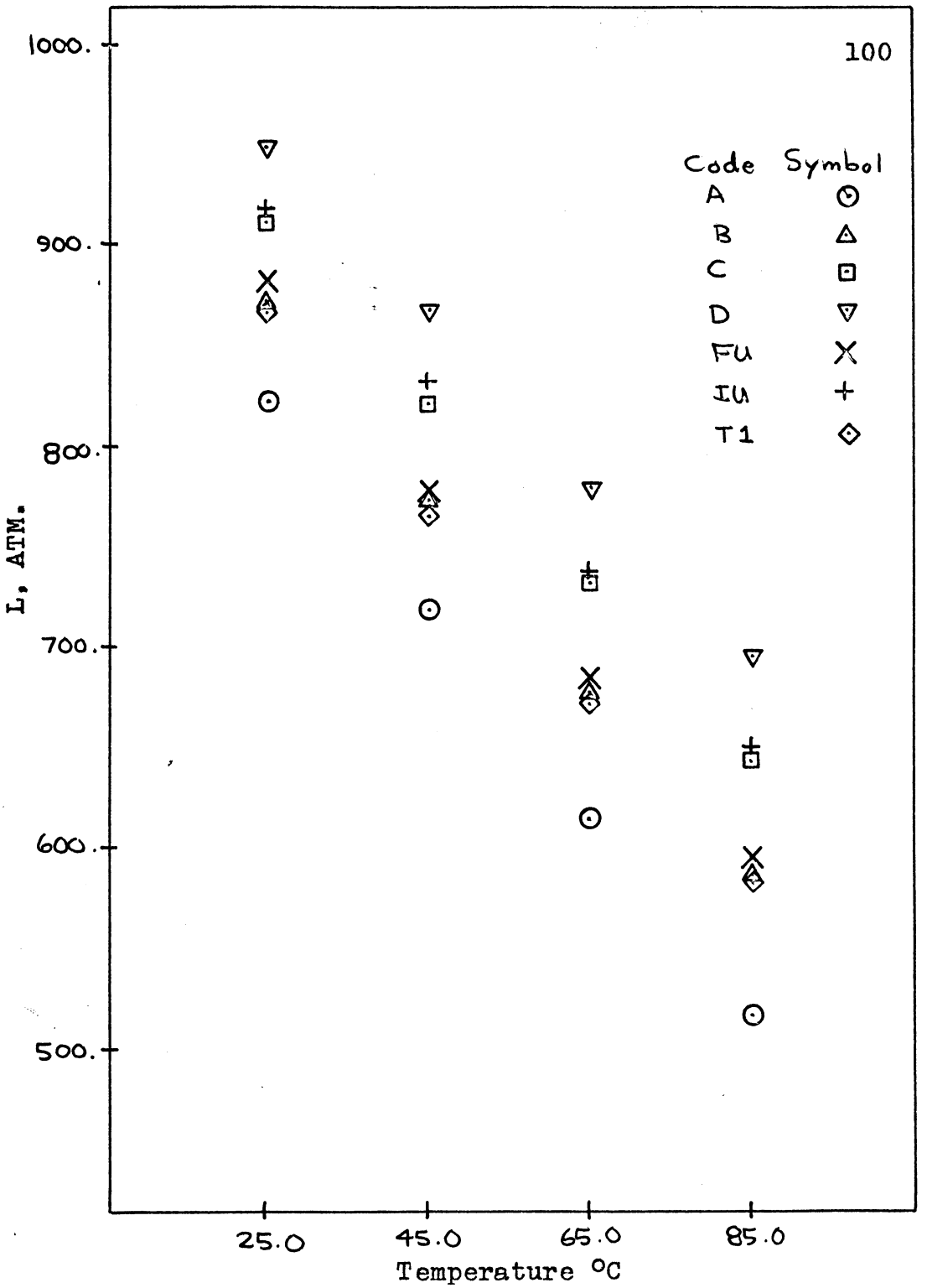

FIGURE 22

TAIT COEFFICIENT L VS. TEMPERATURE

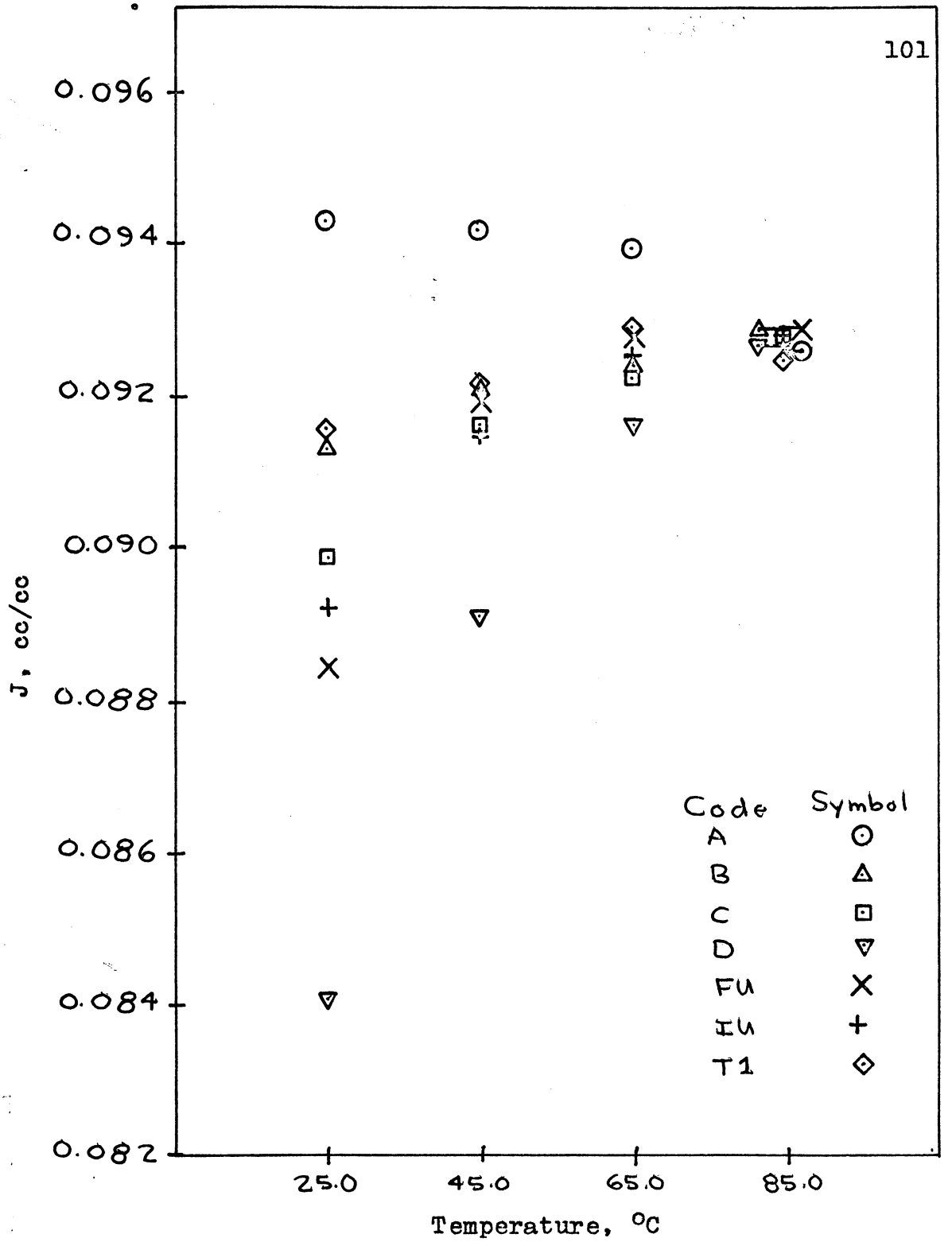

FIGURE 23

TAIT COEFFICIENT J VS. TEMPERATURE

TABLE V

COMPOUND AND MIXTURE CODE KEY

Code	Compound or Mixture
A	n-Decane
B	n-Dodecane
C	n-Tetradecane
D	n-Hexadecane
FU	0.5000 mole fraction mixture of n-Decane and n-Tetradecane
IU	0.5000 mole fraction mixture of n-Dodecane and n-Hexadecane
T1	0.6000 mole fraction mixture of n-Decane with 0.2000 mole fraction n-Tetradecane and n-Hexadecane

Temperature Independence and Universality of J

The contention that the Tait coefficient J is a universal constant and independent of temperature has long been in the literature (10,57). To test this contention all twenty-eight isotherms were analyzed by a least squares procedure which chose the "best" value of J, and the "best" L for each isotherm. This was a regression analysis of twenty-nine variables. The value of J was found to be 0.093523 cc/cc. The corresponding values of L are listed in Table VI and plotted in Figure 24. Figure 25 shows the difference between the Tait curve and the experimental data when J is assumed to be a constant.

II. THE PRAUSNITZ PARTITION FUNCTION

The characteristic parameters for the Prausnitz partition function were evaluated two ways. The first, as Prausnitz suggests (42). The second by least-square regression analysis on the data using the isothermal compressibility equation and the equation of state. The results of these two methods are compared.

TABLE VI

TAIT COEFFICIENT L FOR UNIVERSAL J

(Universal J = 0.093523 cc/cc for this studies' data)

Compound or Mixture	t (°C)	L (atm.)
n-Decane	25.0	815.
	45.0	704.
	65.0	608.
	85.0	536.
n-Dodecane	25.0	924.
	45.0	793.
	65.0	710.
	85.0	594.
n-Tetradecane	25.0	963.
	45.0	851.
	65.0	760.
	85.0	662.
n-Hexadecane	25.0	827.
	45.0	927.
	65.0	814.
	85.0	711.
0.5000 mole fraction n-Decane and n-Tetradecane	25.0	995.
	45.0	796.
	65.0	700.
	85.0	606.
0.5000 mole fraction n-Dodecane and n-Hexadecane	25.0	963.
	45.0	847.
	65.0	762.
	85.0	666.
0.6000 mole fraction n-Decane and 0.2000 mole fraction n-Tetradecane and n-Hexadecane	25.0	898.
	45.0	785.
	65.0	685.
	85.0	601.

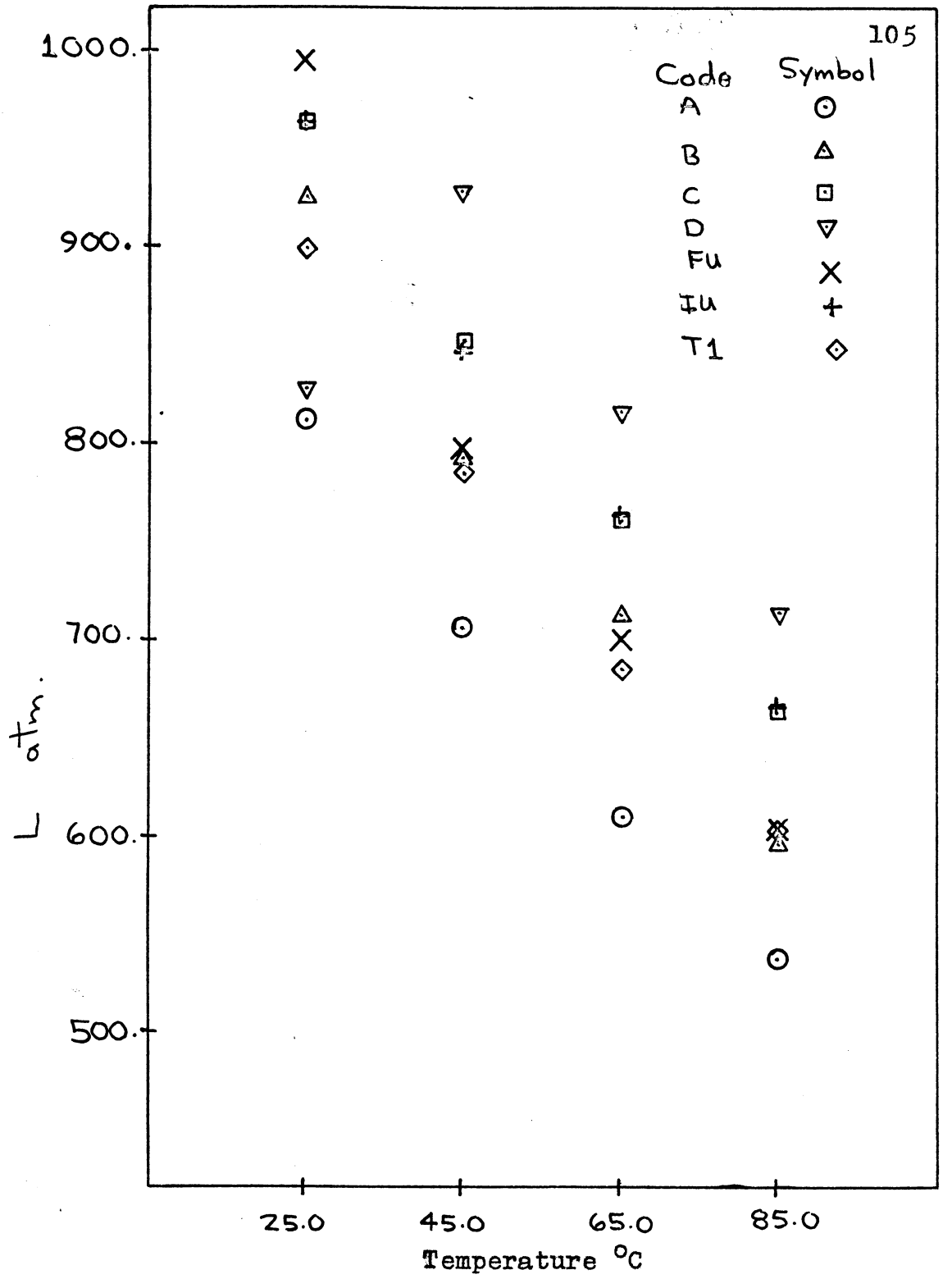

FIGURE 24

TAIT COEFFICIENT L FOR UNIVERSAL J VS. TEMPERATURE

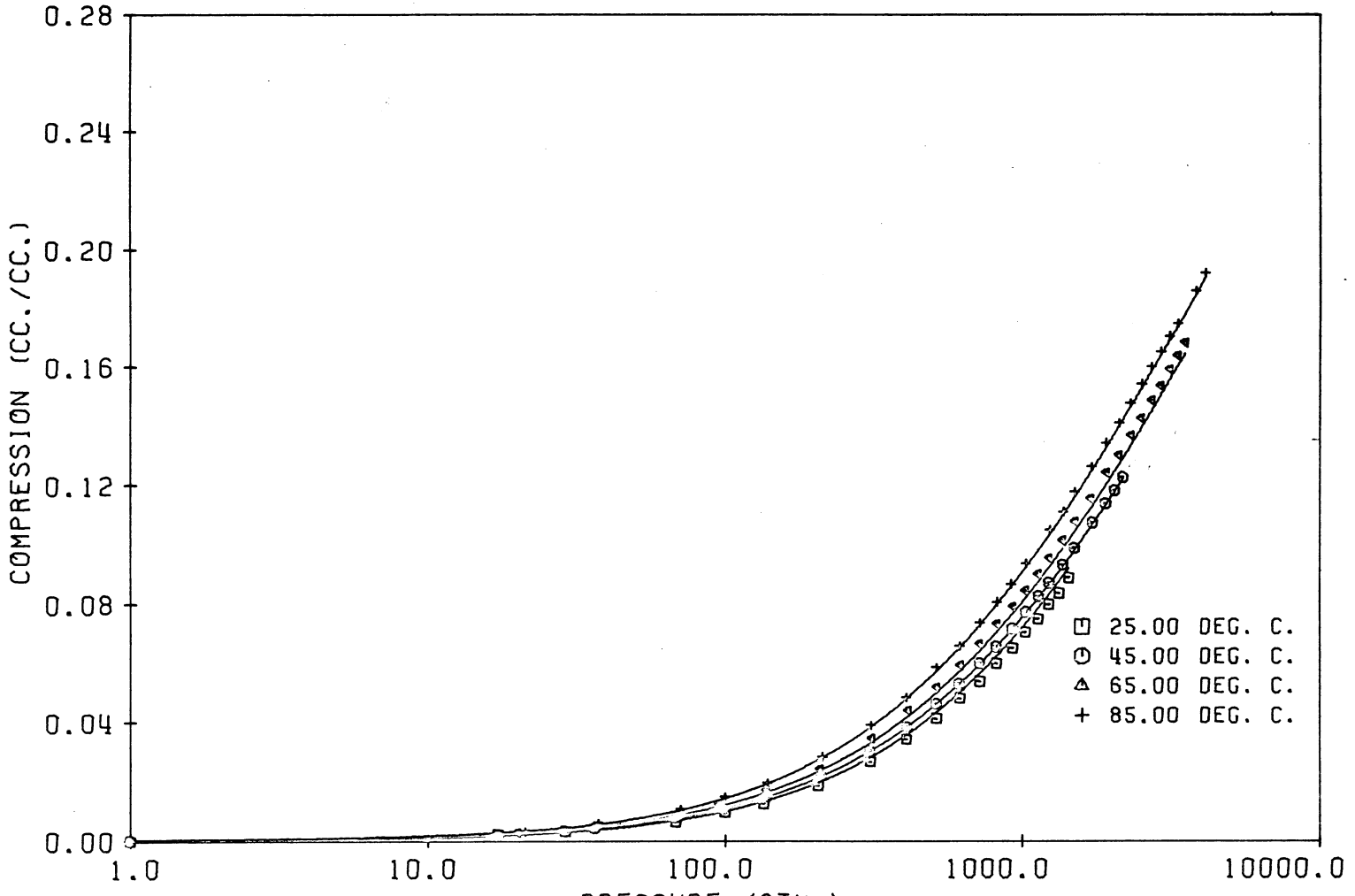

FIGURE 25

RAW COMPRESSION DATA VERSUS PRESSURE FOR
N-DODECANE WITH THE UNIVERSAL J ASSUMPTION

Prausnitz Method

The method suggested by Prausnitz (42) is to determine the characteristic temperature and volume from the p-v-T properties along the vapor-liquid equilibrium curve at saturation. The characteristic pressure is determined from liquid heat capacity data. Computer programs to do this are available in Renon's dissertation (52).

This procedure was carried out only for the pure components as the required data do not exist for the mixtures studied. The results for the pure components are given in Table VII.

Regression Analysis Method

The regression analysis for the characteristic parameters was accomplished in two steps. The first was to least-square fit the Prausnitz isothermal compressibility equation to the Tait smoothed experimental isothermal compressibility data. The computer program BMDX85, described in Appendix D, was used to do this. This step provided the characteristic volume and pressure. The second step was to fit the Prausnitz equation of state to the experimental volume data. The computer program STEPIT, described in Appendix D, was used and this provided the characteristic temperature.

TABLE VII

PRAUSNITZ METHOD CHARACTERISTIC PARAMETERS

Compound	Characteristic		
	Temperature (°K)	Volume (cc/mole)	Pressure (atm.)
n-Decane	529.	157.5	3200.
n-Dodecane	559.	187.0	3080.
n-Tetradecane	584.	216.5	3050.
n-Hexadecane	604.	246.0	3010.

Throughout the regression analysis for the Prausnitz characteristic parameters the assumptions of the Prausnitz partition function, given in Chapter II, were rigidly observed. The results for all seven pure components and mixtures are given in Table VIII.

Comparison of Methods

Figures 26 thru 29 show a representative temperature series for n-Dodecane. The volume is predicted from the equation of state and then the isothermal compressibility is calculated. The temperature series for n-Dodecane shows that the assumption of temperature independence of the characteristic parameters moves the best-fit curve away from the Tait smoothed experimental data curve in such a way as to minimize the overall error. This is also influenced by the pressure range and the number and distribution of data points. In terms of sum of the square residuals the best fit parameters are slightly better than those developed from the method suggested by Prausnitz.

TABLE VIII

PRAUSNITZ BEST FIT CHARACTERISTIC PARAMETERS

Compound	Characteristic Temperature (°K)	Characteristic Volume (cc/mole)	Characteristic Pressure (atm.)
n-Decane	354.	118.9	28890.
n-Dodecane	364.	144.3	24070.
n-Tetradecane	370.	168.5	22200.
n-Hexadecane	391.	200.1	16130.
0.5000 mole fraction n-Decane and n-Tetradecane	365.	143.4	24120.
0.5000 mole fraction n-Dodecane and n-Hexadecane	373.	170.3	20820.
0.6000 mole fraction n-Decane and 0.2000 mole fraction n-Tetradecane and n-Hexadecane	364.	144.3	24000.

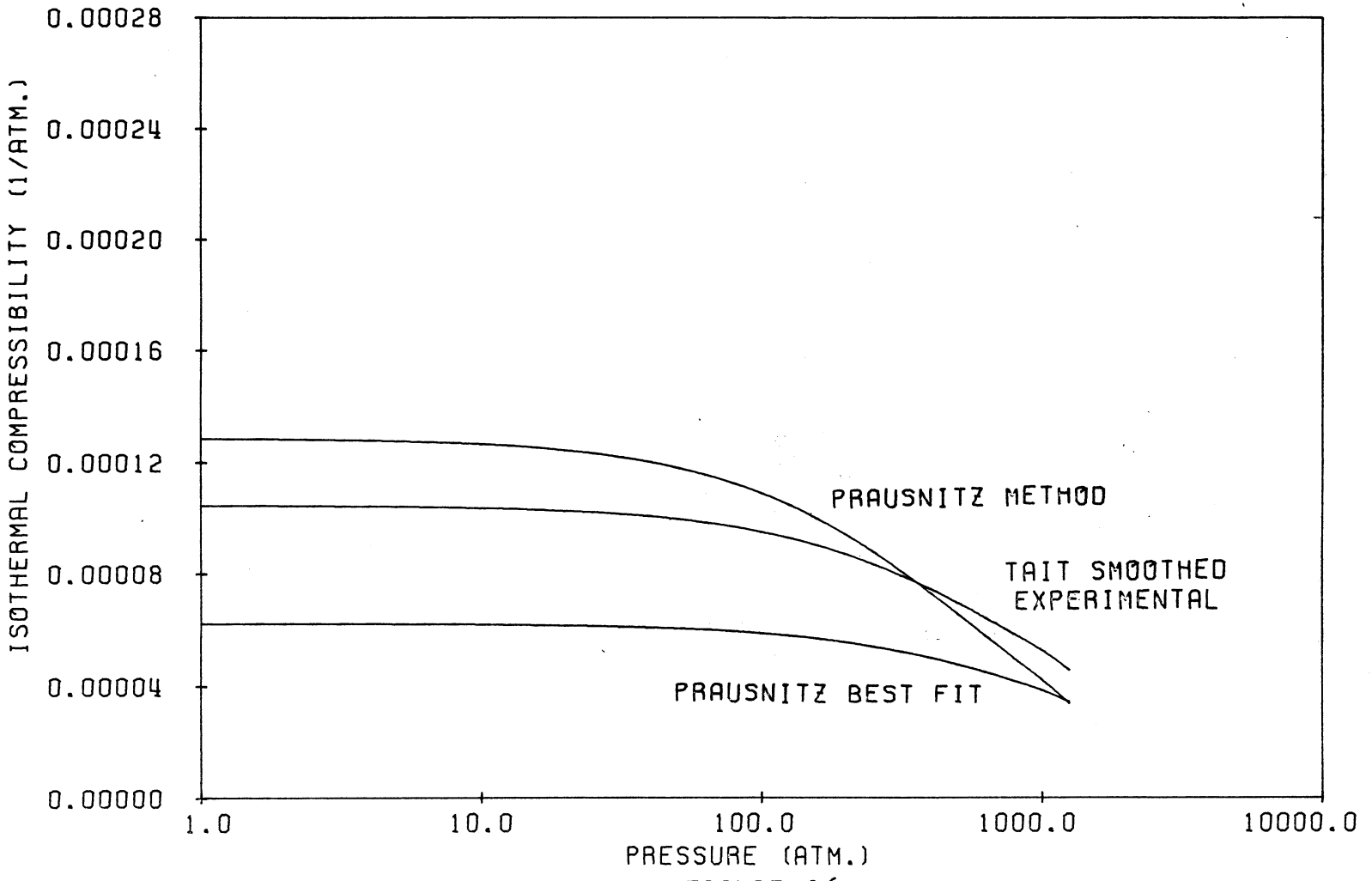

FIGURE 26

SMOOTHED EXPERIMENTAL AND PREDICTED COMPRESSIBILITY
VERSUS PRESSURE FOR
NORMAL DODECANE AT 25.0 DEG. C.

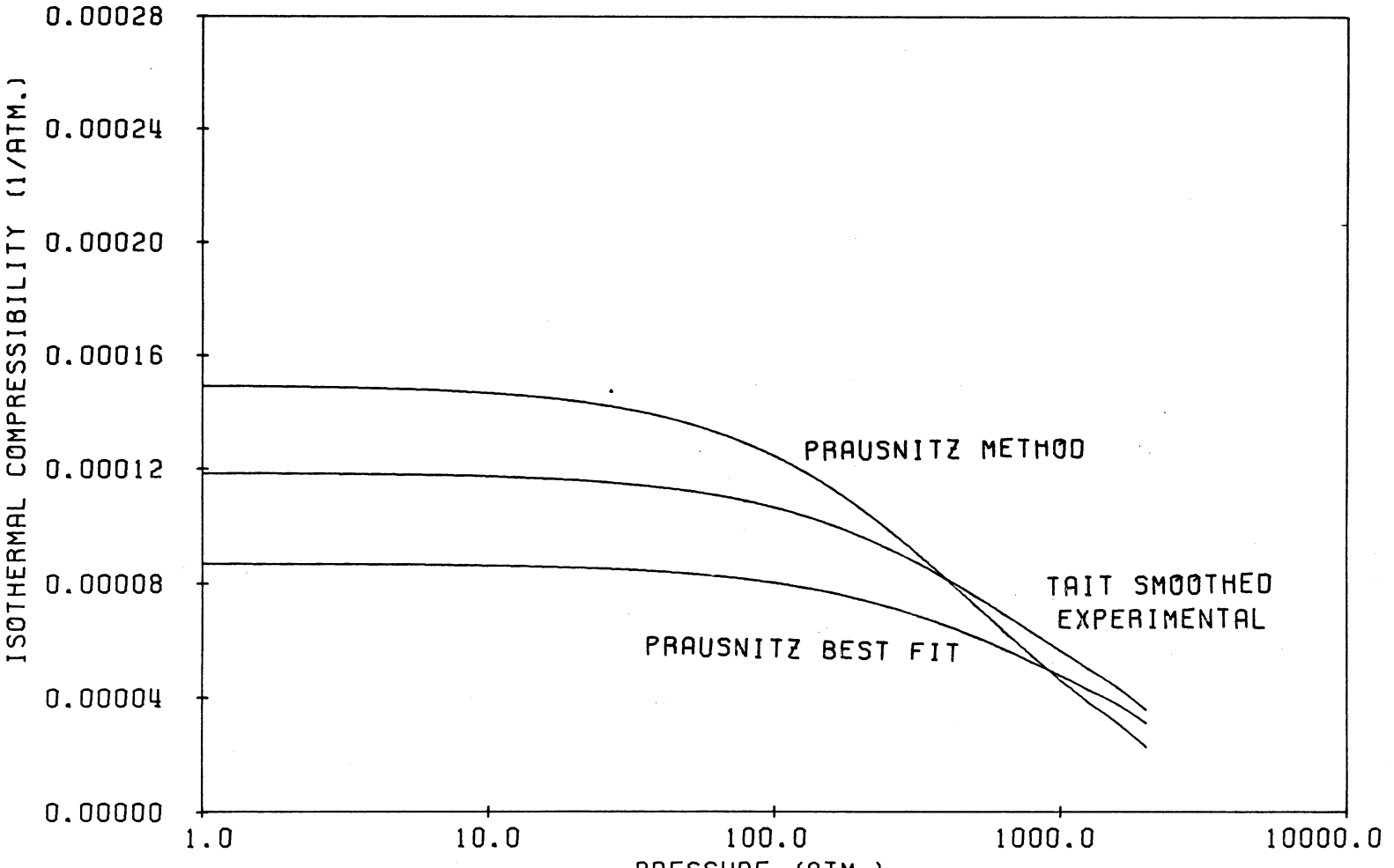

FIGURE 27

SMOOTHED EXPERIMENTAL AND PREDICTED COMPRESSIBILITY
VERSUS PRESSURE FOR
NORMAL DODECANE AT 45.0 DEG. C.

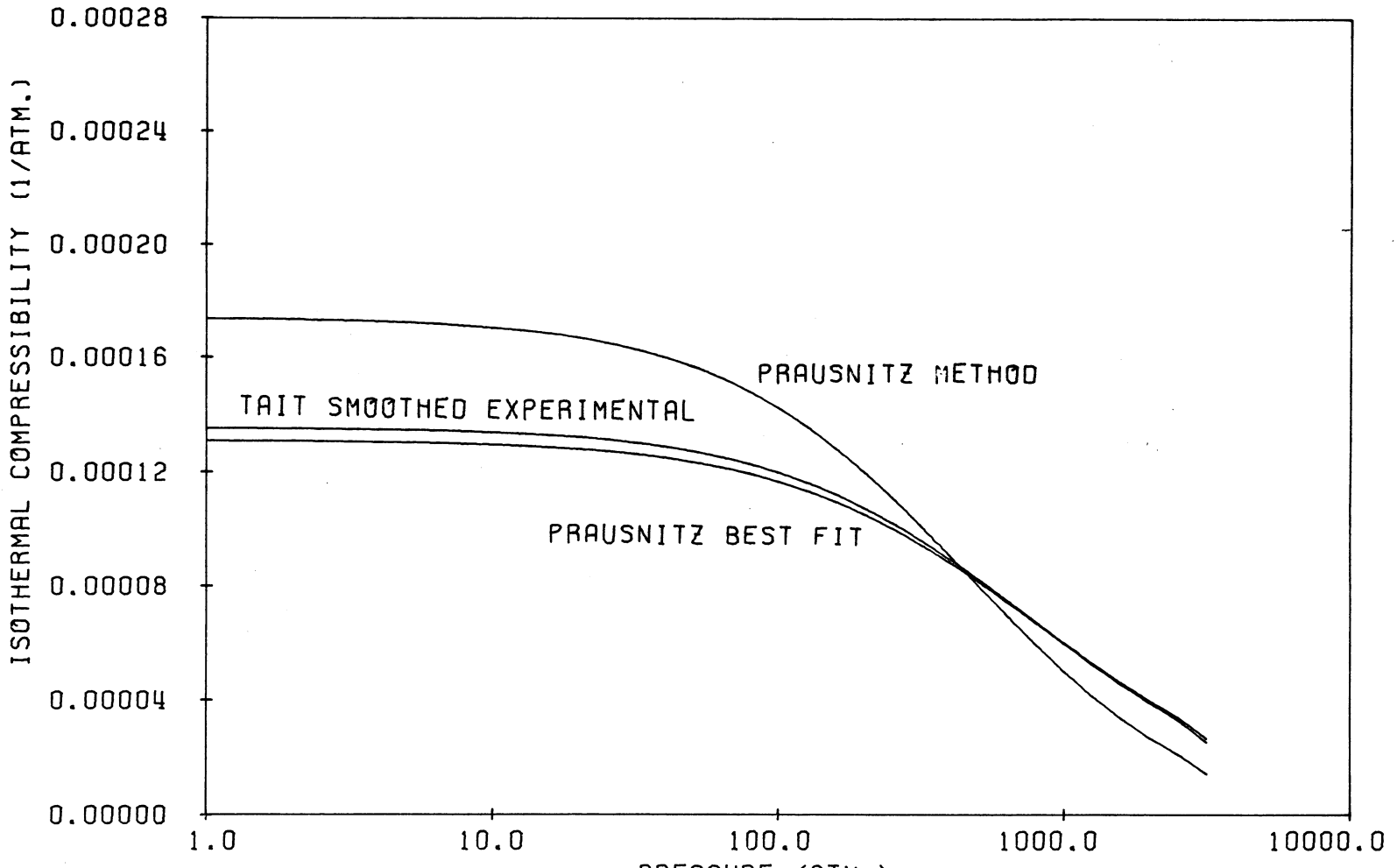

FIGURE 28

SMOOTHED EXPERIMENTAL AND PREDICTED COMPRESSIBILITY
VERSUS PRESSURE FOR
NORMAL DODECANE AT 65.0 DEG. C.

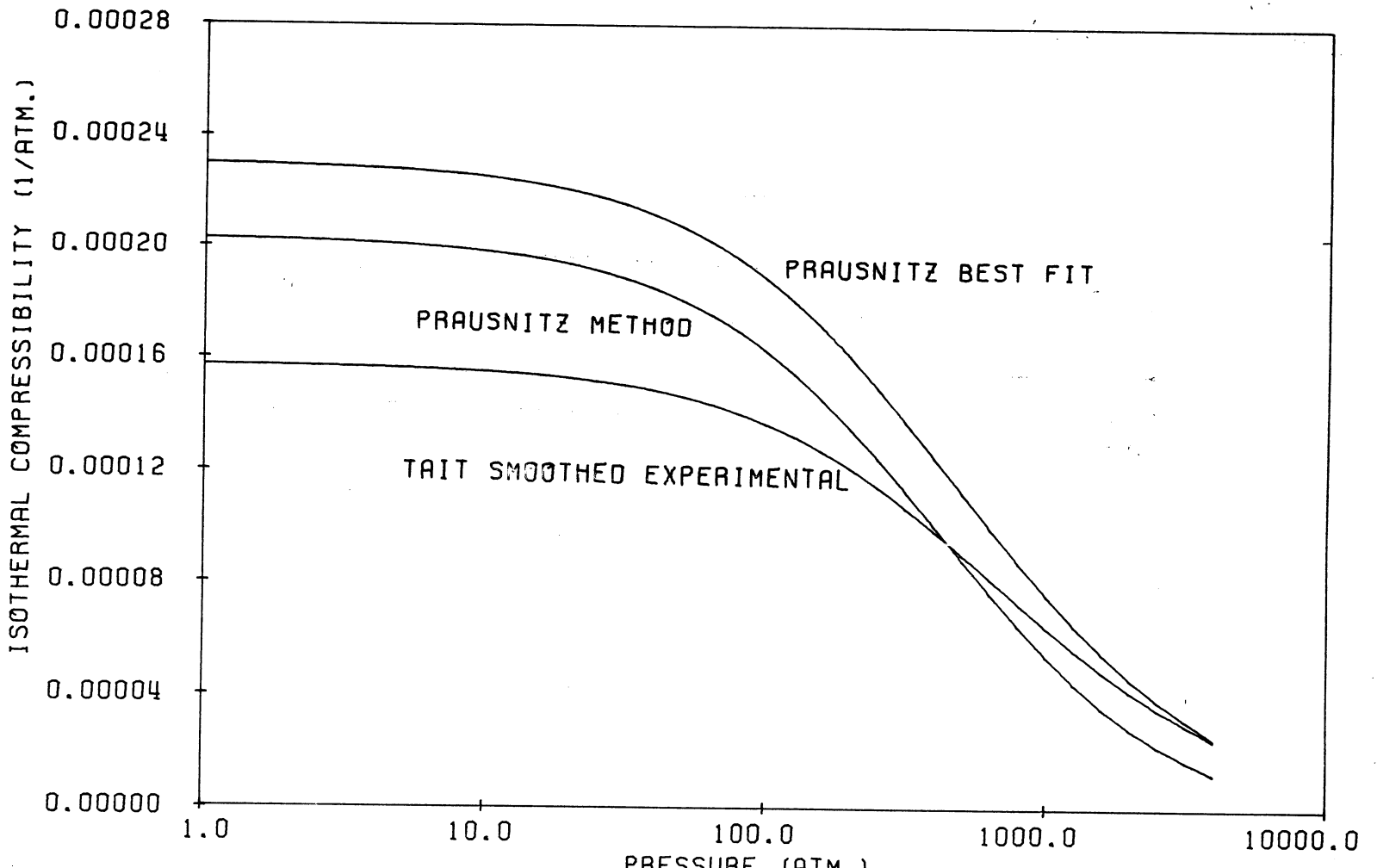

FIGURE 29

SMOOTHED EXPERIMENTAL AND PREDICTED COMPRESSIBILITY
VERSUS PRESSURE FOR
NORMAL DODECANE AT 85.0 DEG. C.

III. THE FLORY PARTITION FUNCTION

The characteristic parameters for the Flory partition function were evaluated in two ways. The first, as Flory suggests (21). The second by least-square regression analysis of the data using the isothermal compressibility equation and the equation of state. The results of these two methods are compared.

Flory Method

Flory (21) suggested that the characteristic volume, temperature and pressure be determined using the initial volume, coefficient of thermal expansion at atmospheric pressure, and the isothermal compressibility at atmospheric pressure. The results of this analysis are given in Table IX and Figures 30 thru 32.

Regression Analysis Method

The regression analysis for the characteristic parameters was accomplished in two steps. Firstly the Flory isothermal compressibility equation was fitted to the Tait smoothed experimental isothermal compressibility data. The computer program BMDX85, described in Appendix D, was used to do this. This provided the characteristic volume and pressure. The second step was to fit the Flory equation of state to the experimental volume data. The

TABLE IX

FLORY'S METHOD CHARACTERISTIC PARAMETERS

Compound or mixture	t (°C)	Characteristic Temperature (°K)	Characteristic Volume (cc/mole)	Characteristic Pressure (atm.)
n-Decane	25.0	511.1	156.0	4297.03
	45.0	519.3	156.8	4271.38
	65.0	525.9	157.6	4214.65
	85.0	531.3	158.2	4127.11
n-Dodecane	25.0	529.1	183.9	4323.33
	45.0	539.7	185.0	4248.47
	65.0	547.8	186.0	4191.28
	85.0	553.9	186.7	4094.61
n-Tetradecane	25.0	546.2	209.2	4261.23
	45.0	555.2	210.0	4226.46
	65.0	562.9	210.8	4206.96
	85.0	569.7	211.5	4147.38
n-Hexadecane	25.0	557.6	243.5	4551.85
	45.0	567.6	244.9	4348.27
	65.0	575.8	246.2	4261.80
	85.0	582.6	247.4	4220.93
0.5000 mole fraction n-Decane and n-Tetradecane	25.0	529.1	183.9	4286.75
	45.0	539.7	185.0	4251.89
	65.0	547.8	186.0	4192.55
	85.0	553.9	186.7	4121.45
0.5000 mole fraction n-Dodecane and n-Hexadecane	25.0	546.2	212.2	4320.61
	45.0	555.2	213.2	4272.21
	65.0	562.9	214.1	4219.61
	85.0	569.7	215.0	4168.69
0.6000 mole fraction n-Decane and 0.2000 mole fraction n-Tetradecane and n-Hexadecane	25.0	529.1	183.9	4299.30
	45.0	539.7	185.0	4225.59
	65.0	547.8	186.0	4174.30
	85.0	553.9	186.7	4105.18

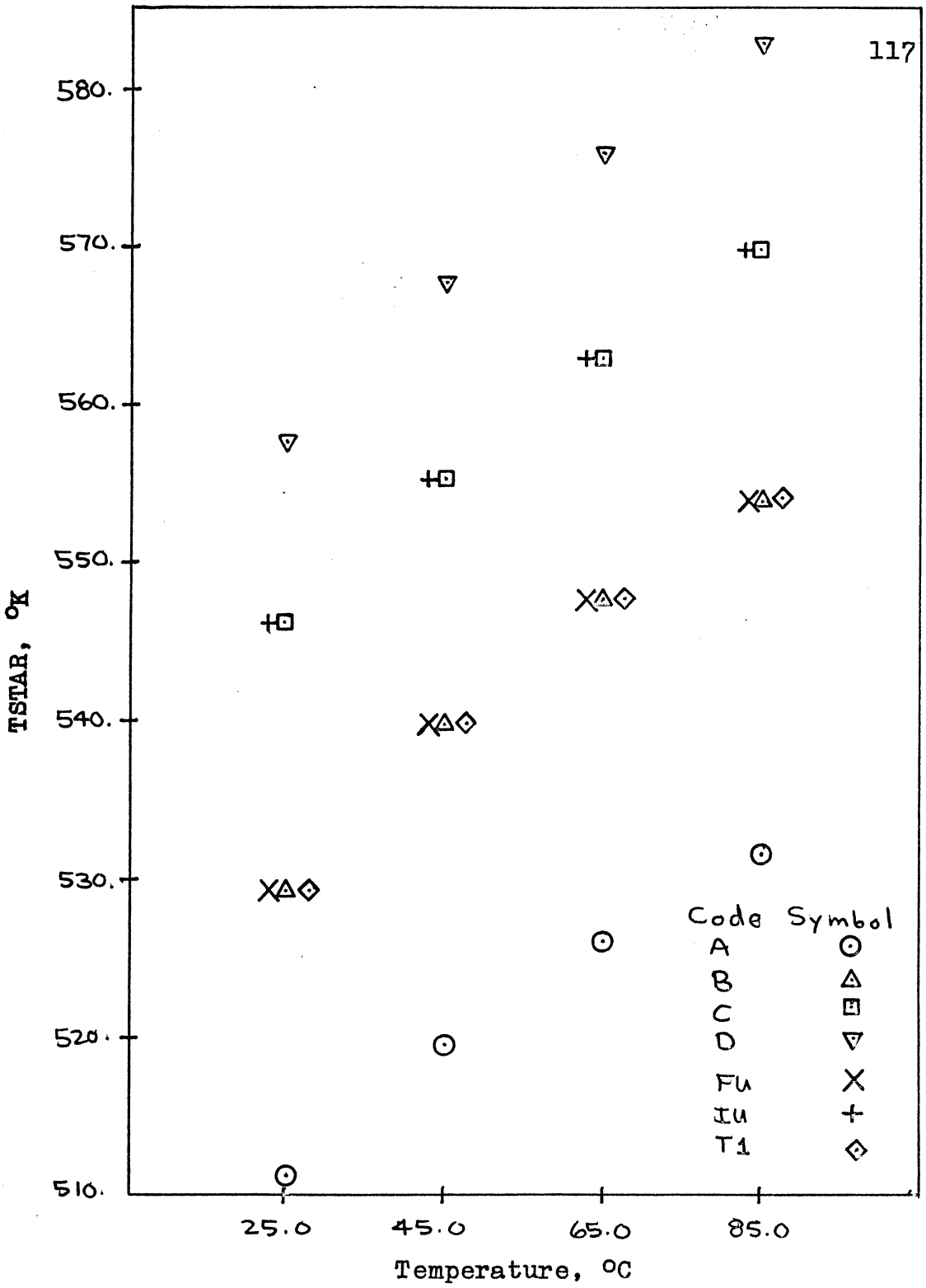

FIGURE 30

FLORY'S CHARACTERISTIC TEMPERATURE VERSUS TEMPERATURE

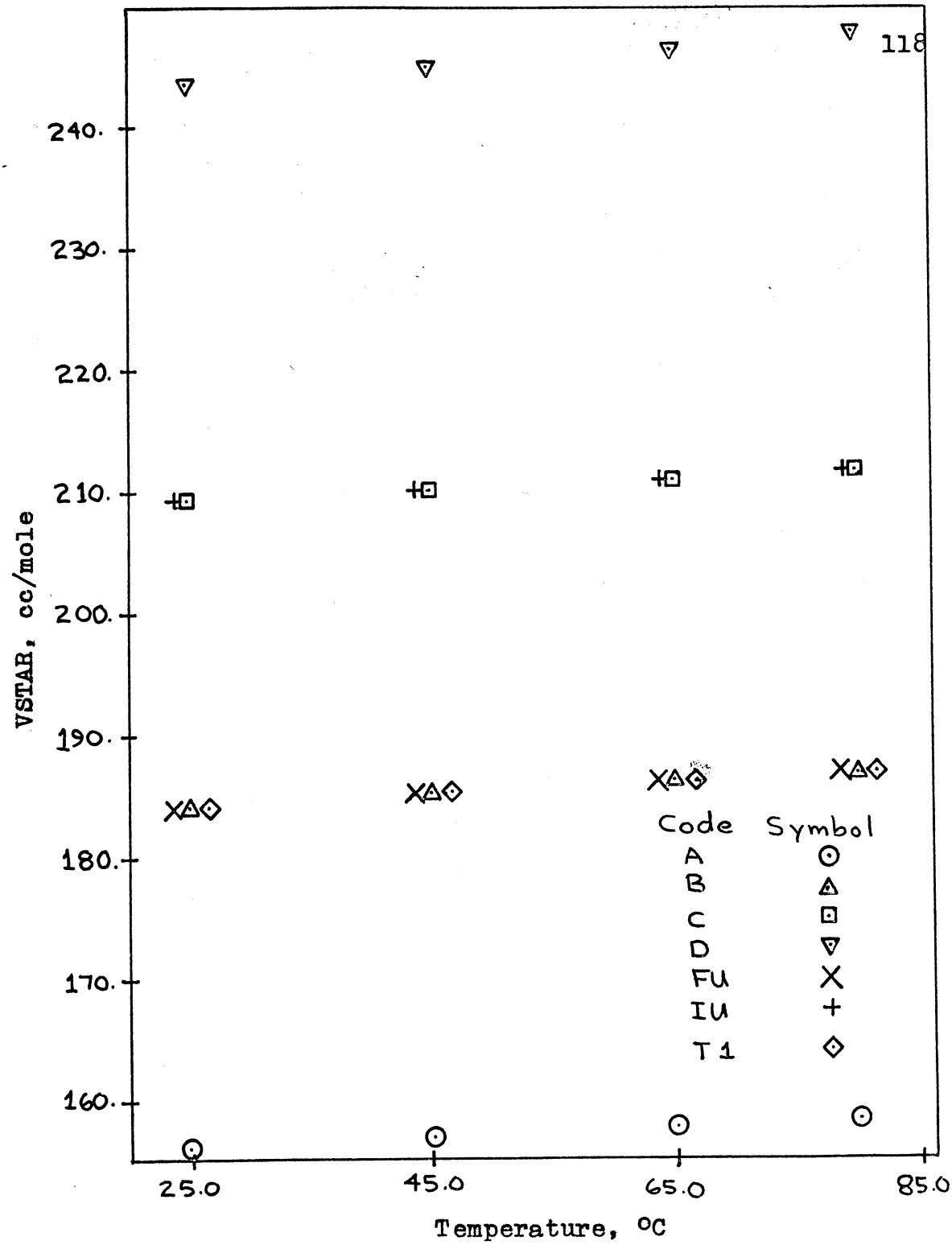

FIGURE 31

FLORY'S CHARACTERISTIC VOLUME VERSUS TEMPERATURE

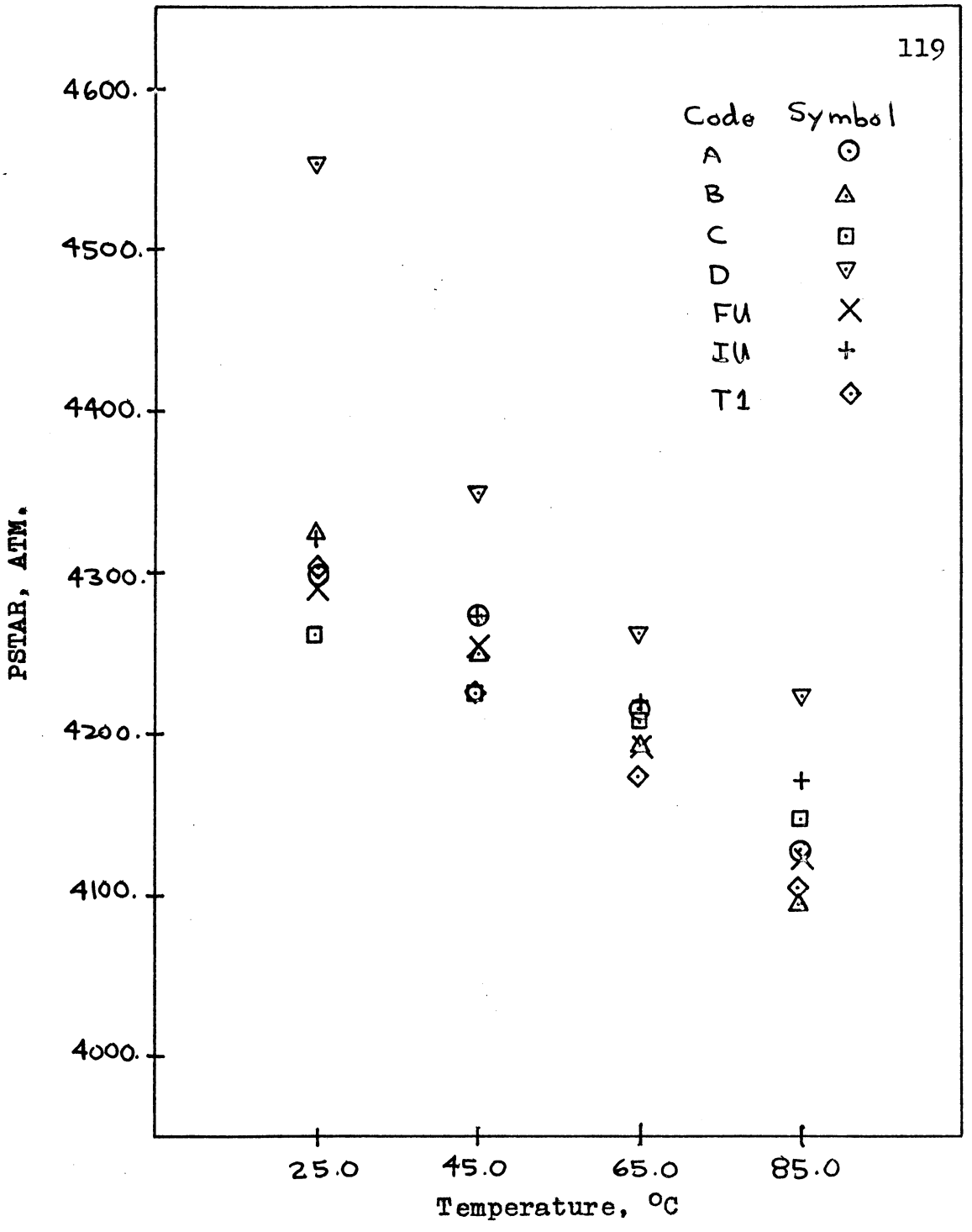

FIGURE 32

FLORY'S CHARACTERISTIC PRESSURE VERSUS TEMPERATURE

computer program STEPIT, described in Appendix D, was used and this provided the characteristic temperature.

Throughout the regression analysis for the Flory characteristic parameters the assumptions of the Flory partition function, given in Chapter II, were rigidly observed. The results are given in Table X and plotted in Figures 33 thru 35.

Comparison of Tables IX and X shows a marked difference between the Flory's method for evaluating the characteristic parameters and the "best fit" characteristic parameters. This is to be expected since the set of parameters evaluated at one end of the pressure range, as the Flory's method does, could not be expected to be the same as those which were evaluated over the extended pressure range of this study.

Comparison of Methods

Figures 36 thru 39 show a representative temperature series for n-Dodecane to allow comparison between theories. The procedure is to predict the volume from the equation of state and then to use this to calculate the isothermal compressibility.

The difference between Tait smoothed experimental isothermal compressibility and the best fit predicted values is well within experimental error. The Flory's

TABLE X

FLORY BEST FIT CHARACTERISTIC PARAMETERS

Compound or mixture	t (°C)	Characteristic Temperature (°K)	Characteristic Volume (cc/mole)	Characteristic Pressure (atm.)
n-Decane	25.0	330.3	123.1	22387.75
	45.0	341.0	121.2	25196.39
	65.0	351.9	119.2	28448.24
	85.0	363.7	117.3	32107.23
n-Dodecane	25.0	343.1	148.8	19444.62
	45.0	351.1	145.9	22301.04
	65.0	360.7	143.3	25323.78
	85.0	370.5	140.3	29109.26
n-Tetradecane	25.0	357.7	175.8	16574.66
	45.0	363.2	172.1	19121.36
	65.0	369.9	168.3	22401.30
	85.0	378.2	164.6	26078.91
n-Hexadecane	25.0	383.0	207.0	13705.03
	45.0	380.7	201.1	16113.16
	65.0	381.8	195.2	19438.79
	85.0	387.5	190.4	22987.42
0.5000 mole fraction n-Decane and n-Tetradecane	25.0	345.0	149.5	18663.25
	45.0	352.3	146.4	21816.86
	65.0	361.5	143.7	24857.41
	85.0	371.5	140.9	28394.67
0.5000 mole fraction n-Dodecane and n-Hexadecane	25.0	361.3	177.1	16023.18
	45.0	364.6	172.7	18946.87
	65.0	371.1	168.9	21951.52
	85.0	379.5	165.4	25380.27
0.6000 mole fraction n-Decane and 0.2000 mole fraction n-Tetradecane and n-Hexadecane	25.0	341.3	148.1	19945.14
	45.0	349.3	145.1	22999.39
	65.0	358.9	142.4	26306.69
	85.0	369.9	140.0	29653.07

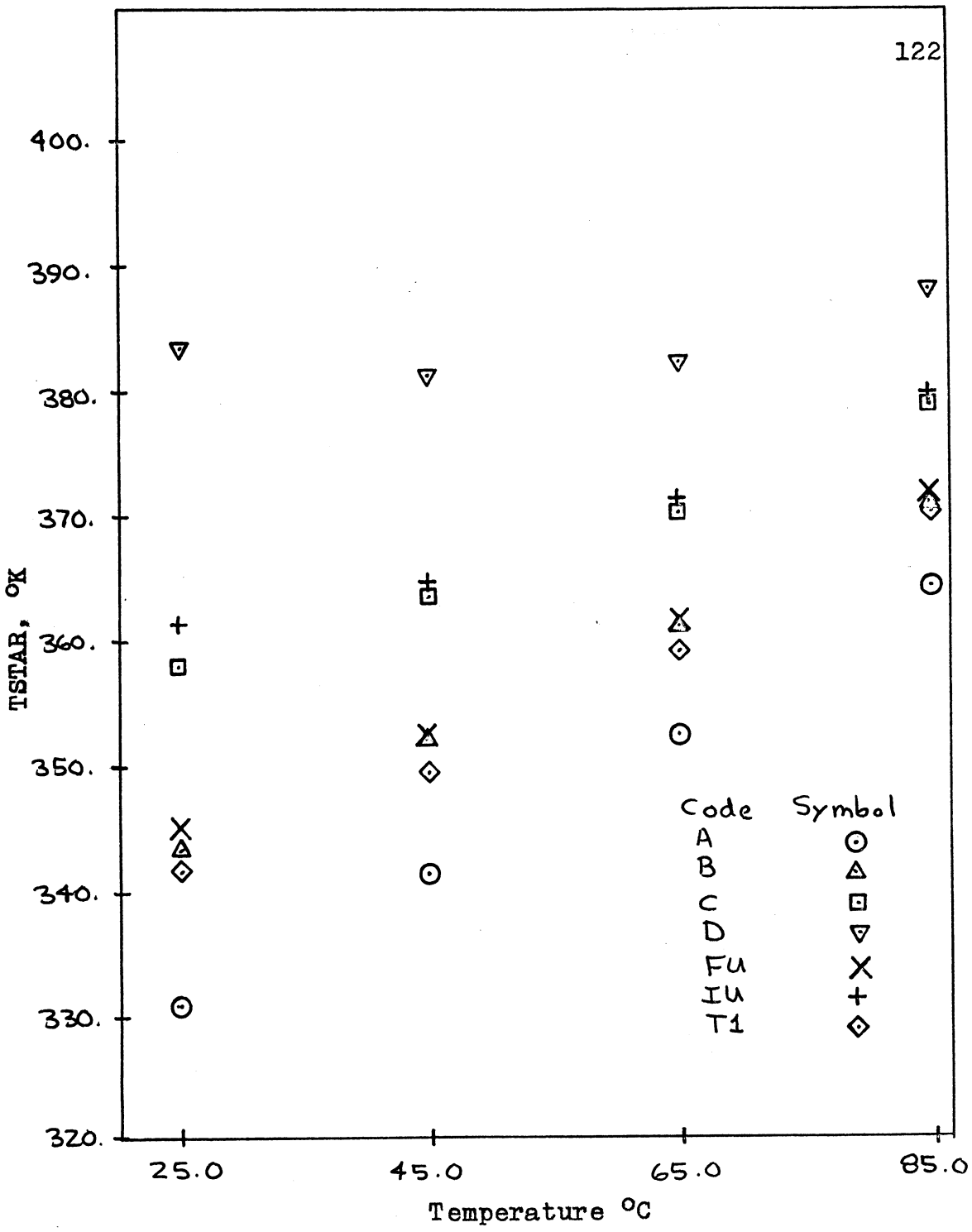

FIGURE 33

FLORY BEST FIT CHARACTERISTIC TEMPERATURE
VERSUS TEMPERATURE

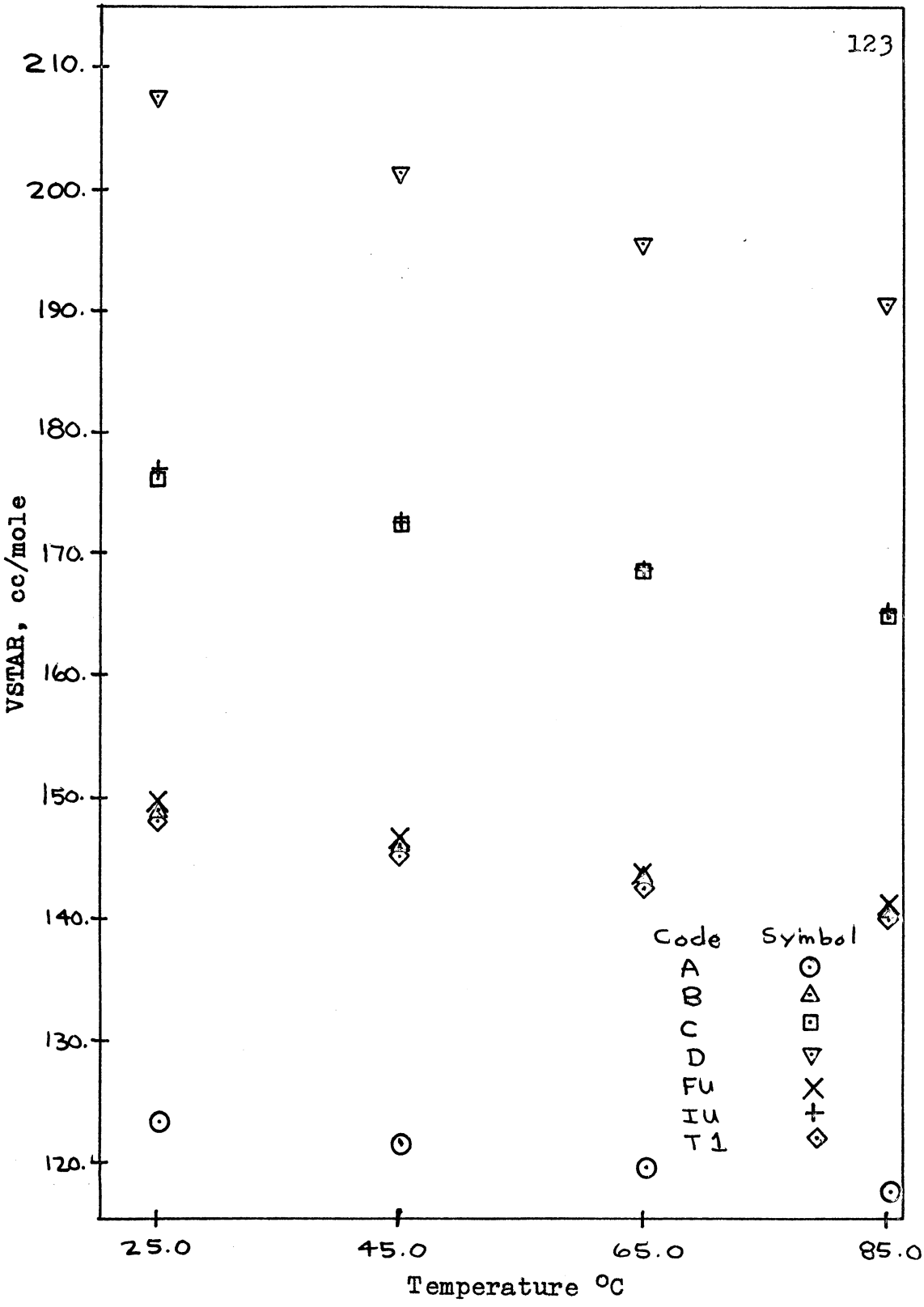

FIGURE 34

FLORY BEST FIT CHARACTERISTIC VOLUME
VERSUS TEMPERATURE

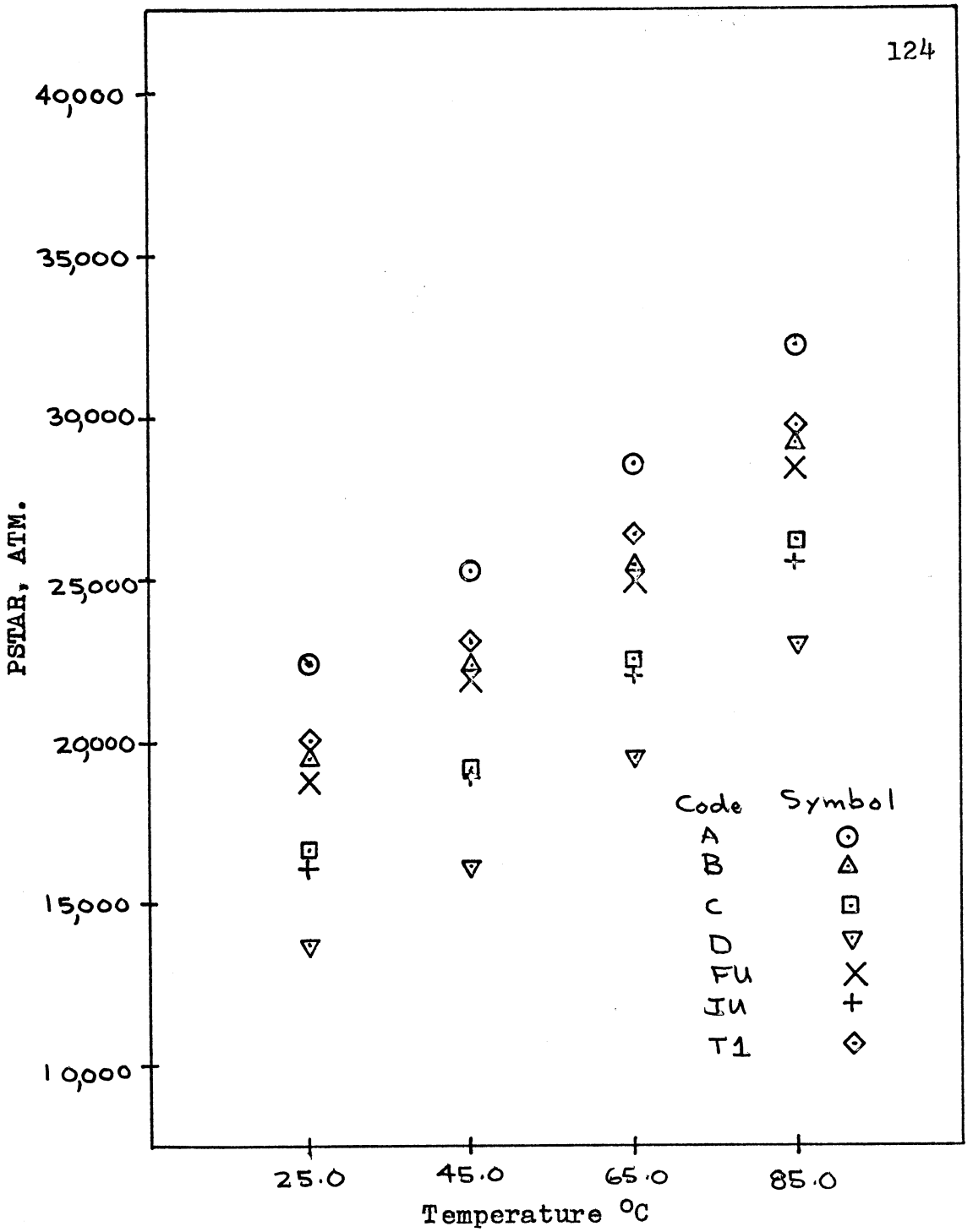

FIGURE 35

FLORY BEST FIT CHARACTERISTIC PRESSURE VERSUS TEMPERATURE

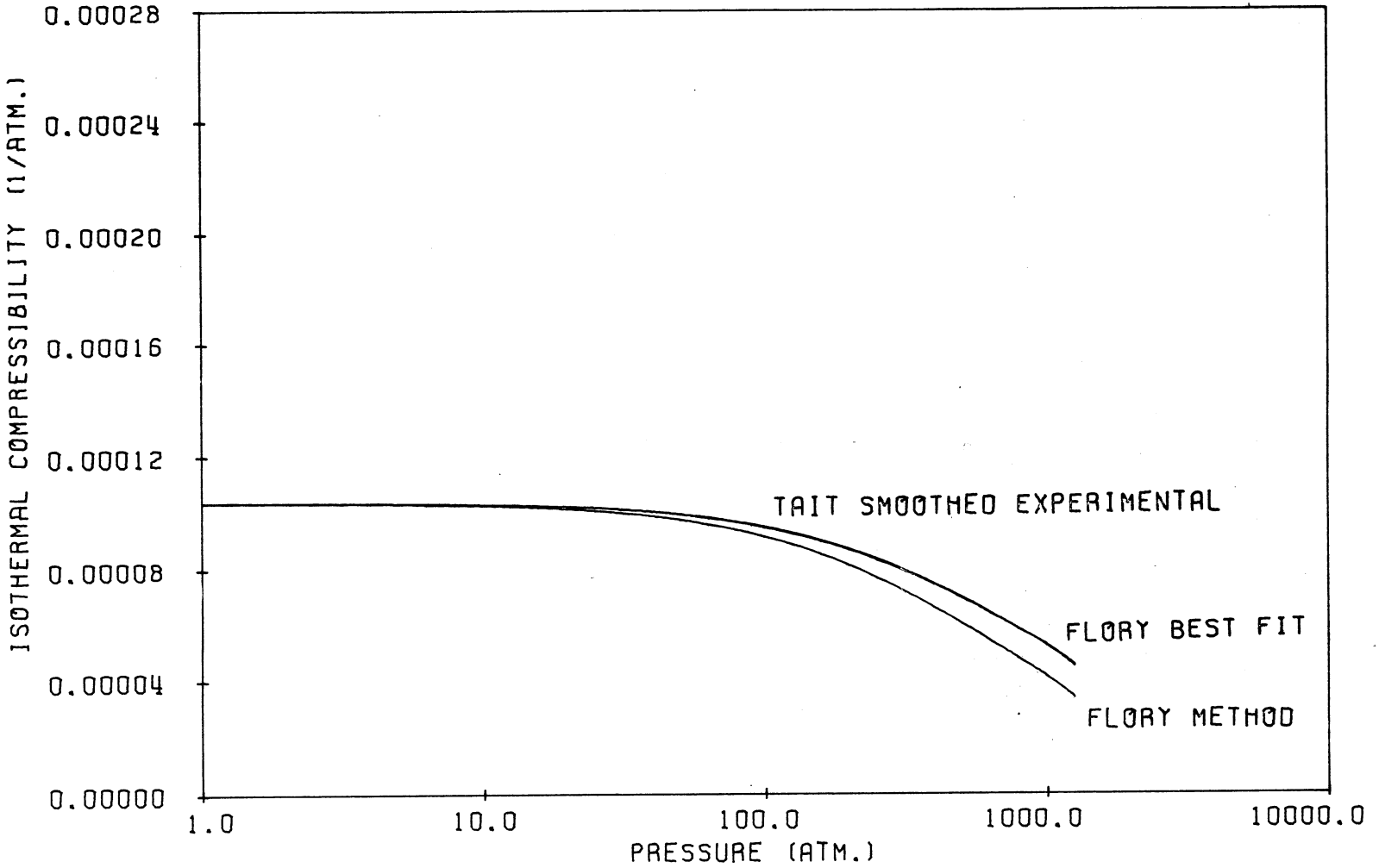

FIGURE 36

SMOOTHED EXPERIMENTAL AND PREDICTED COMPRESSIBILITY
VERSUS PRESSURE FOR
NORMAL DODECANE AT 25.0 DEG. C.

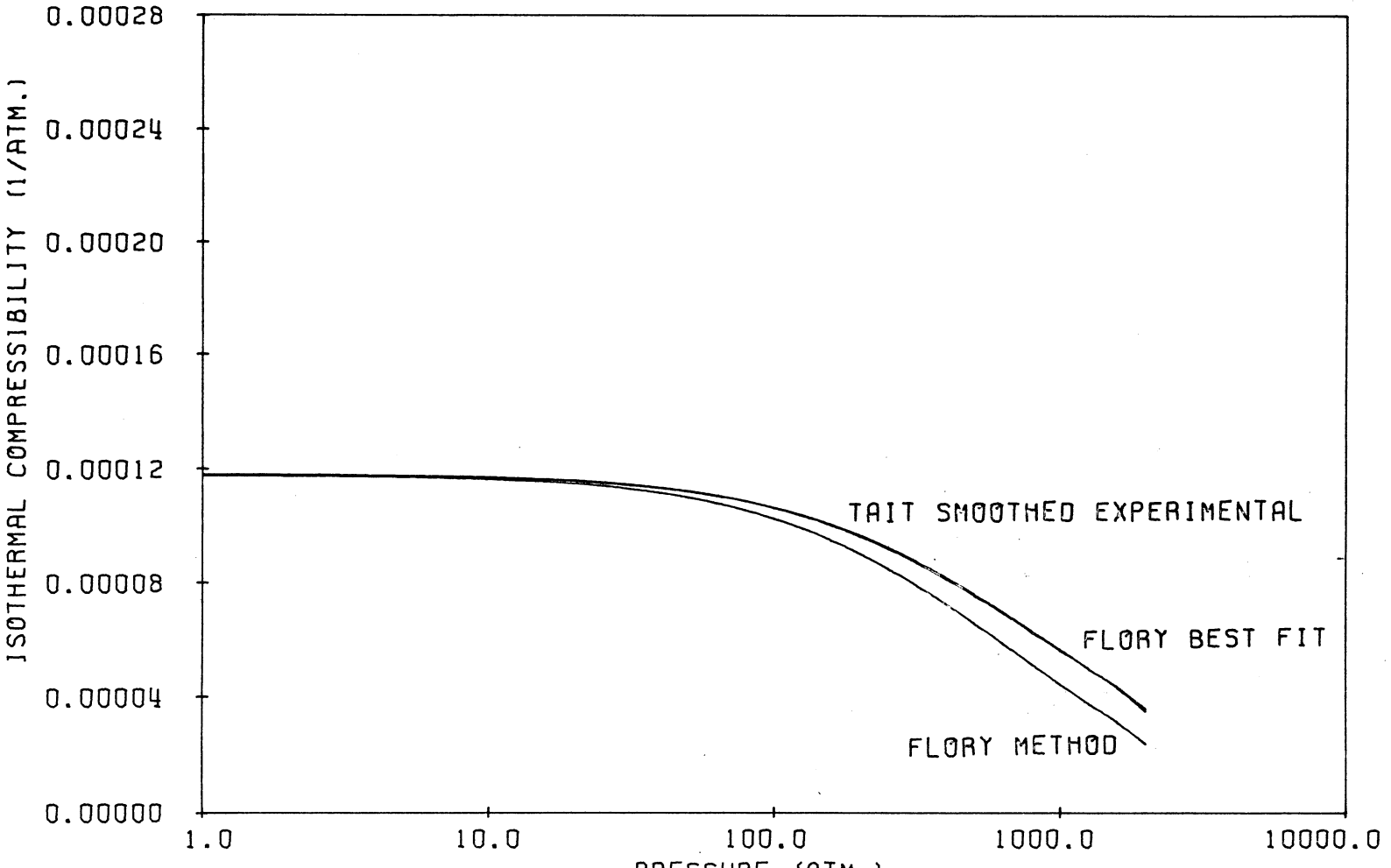

FIGURE 37

SMOOTHED EXPERIMENTAL AND PREDICTED COMPRESSIBILITY
VERSUS PRESSURE FOR
NORMAL DODECANE AT 45.0 DEG. C.

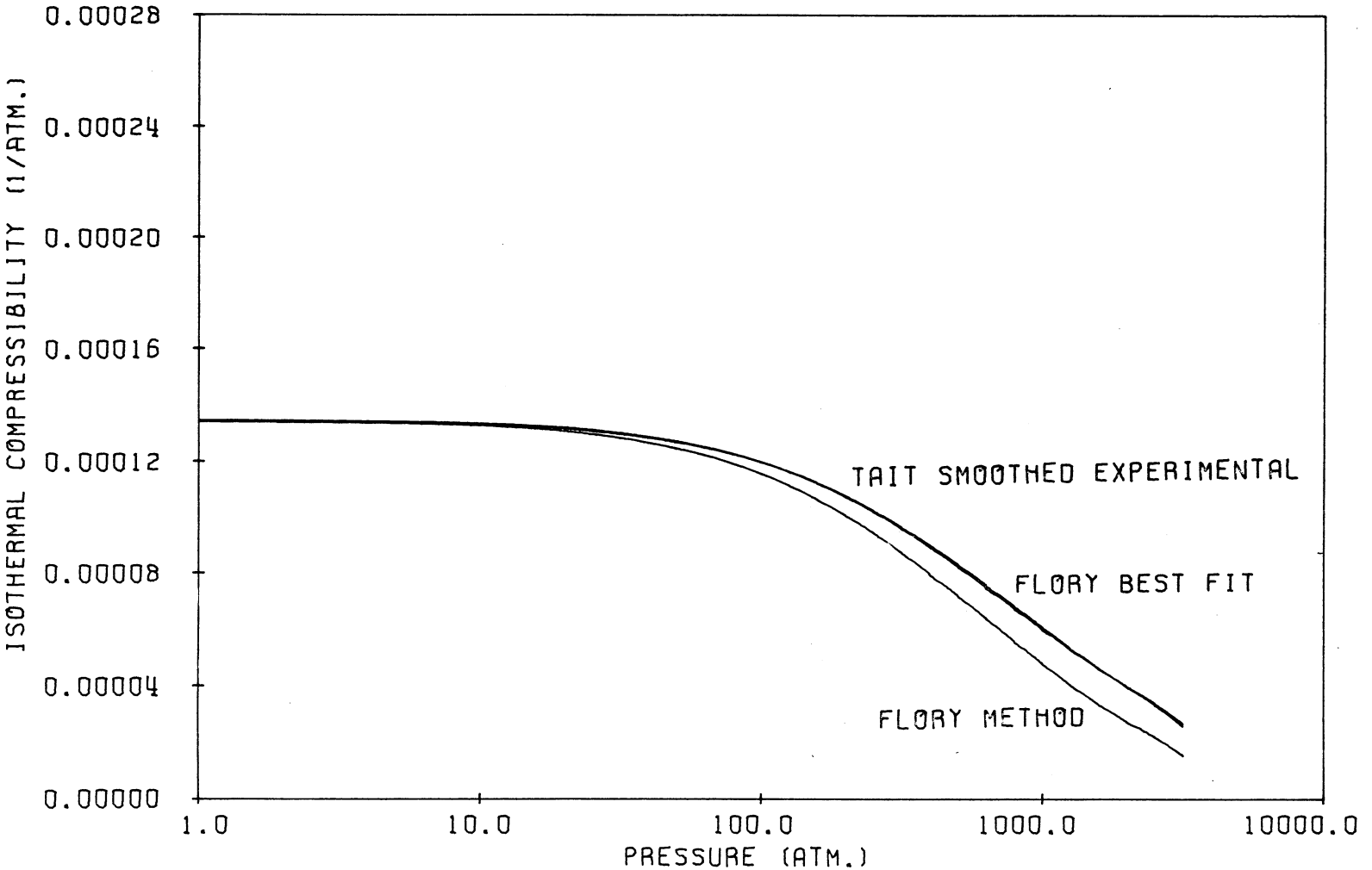

FIGURE 38

SMOOTHED EXPERIMENTAL AND PREDICTED COMPRESSIBILITY
VERSUS PRESSURE FOR
NORMAL DODECANE AT 65.0 DEG. C.

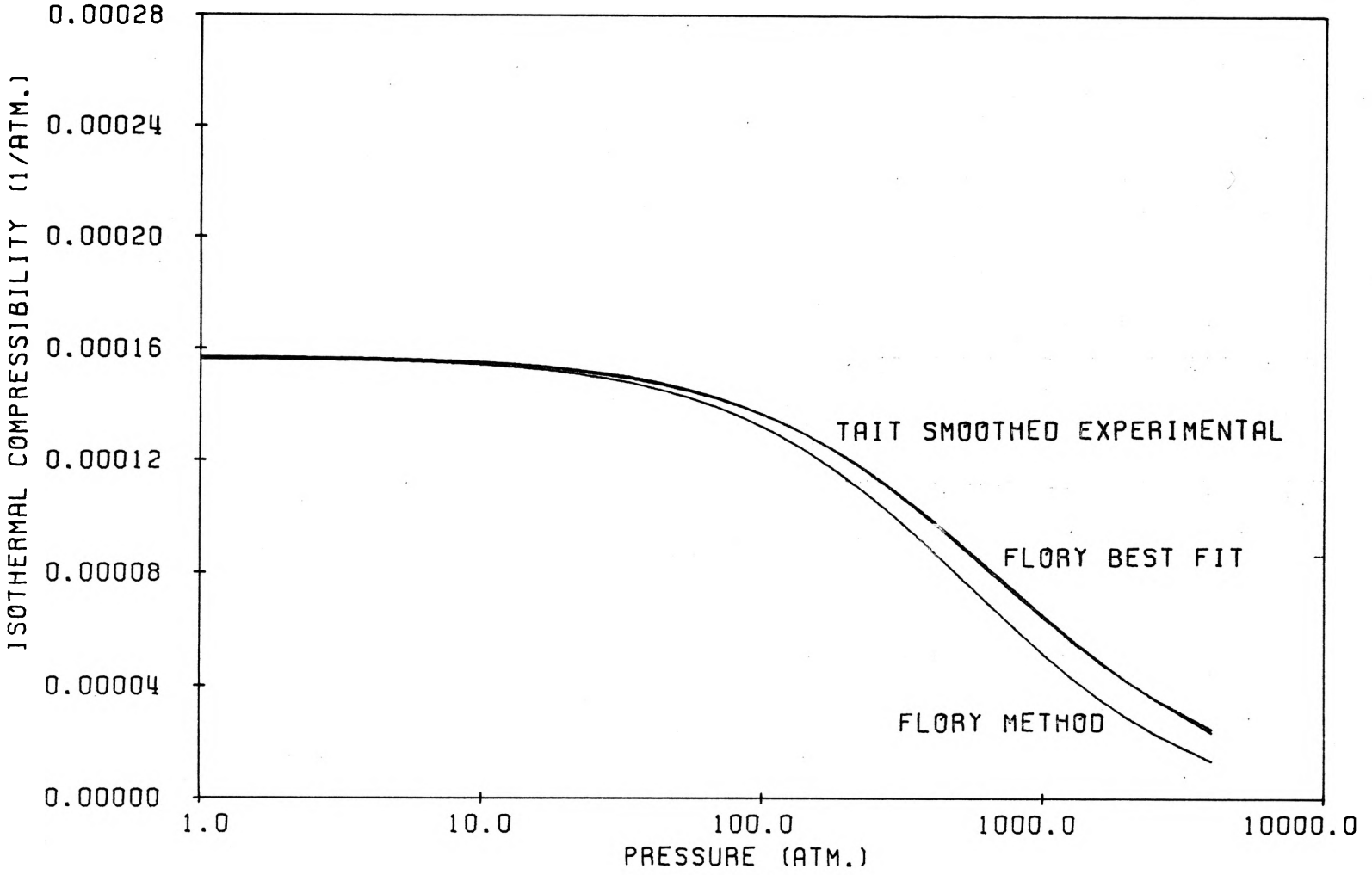

FIGURE 39

SMOOTHED EXPERIMENTAL AND PREDICTED COMPRESSIBILITY
VERSUS PRESSURE FOR
NORMAL DODECANE AT 85.0 DEG. C.

method characteristic parameters predict values of the isothermal compressibility which reproduce the experimental curve up to about 5000 psi in all cases. Above 5000 psi they predict to rapid a decrease in the isothermal compressibility.

IV. FLORY MIXING RULE

The Flory mixing rule (22) has been applied to the best fit and Flory's method pure component characteristic parameters to predict the characteristic parameters for the three mixtures studied. The mixing rule characteristic parameters are given in Tables XI and XII. The mixing rule characteristic parameters were then used to predict the isothermal compressibility for the mixtures studied. A comparison of the predicted and experimental isothermal compressibilities is given in figures 40 thru 47. Only the plots for the binary mixture of 0.5000 mole fraction n-Decane and n-Tetradecane are shown as they are representative of the results for the two binary mixtures studied. Figures 44 thru 47 show the results for the ternary mixture of 0.6000 mole fraction n-Decane and 0.2000 mole fraction n-Tetradecane and n-Hexadecane.

TABLE XI

MIXTURE CHARACTERISTIC PARAMETERS FROM BEST FIT VIA FLORY'S MIXING RULE

Mixture	t (°C)	Characteristic Temperature (°K)	Characteristic Volume (cc/mole)	Characteristic Pressure (atm.)
0.5000 mole fraction n-Decane and n-Tetradecane	25.0	347.6	153.5	18633.1
	45.0	356.0	150.6	21320.1
	65.0	365.6	147.5	24677.1
	85.0	376.2	144.6	28438.7
0.5000 mole fraction n-Dodecane and n-Hexadecane	25.0	363.9	181.8	15716.5
	45.0	367.1	177.2	18315.4
	65.0	373.8	172.7	21625.4
	85.0	382.1	168.7	25320.3
0.6000 mole fraction n-Decane and 0.2000 mole fraction n-Tetradecane and n-Hexadecane	25.0	350.4	157.2	18775.4
	45.0	355.8	153.8	21418.7
	65.0	363.9	150.4	24696.4
	85.0	373.3	147.3	28330.8

TABLE XII

MIXTURE CHARACTERISTIC PARAMETERS FROM FLORY'S METHOD VIA FLORY'S MIXING RULE

Mixture	t (°C)	Characteristic Temperature (°K)	Characteristic Volume (cc/mole)	Characteristic Pressure (atm.)
0.5000 mole fraction n-Decane and n-Tetradecane	25.0	543.4	186.7	4356.2
	45.0	552.1	187.5	4322.8
	65.0	559.9	188.3	4291.3
	85.0	566.5	189.0	4221.8
0.5000 mole fraction n-Dodecane and n-Hexadecane	25.0	559.0	217.7	4565.0
	45.0	568.3	219.0	4397.3
	65.0	576.4	220.1	4318.3
	85.0	583.7	221.1	4259.9
0.6000 mole fraction n-Decane and 0.2000 mole fraction n-Tetradecane and n-Hexadecane	25.0	531.2	191.2	4396.7
	45.0	540.2	192.2	4281.1
	65.0	547.5	193.0	4225.2
	85.0	553.6	193.8	4156.3

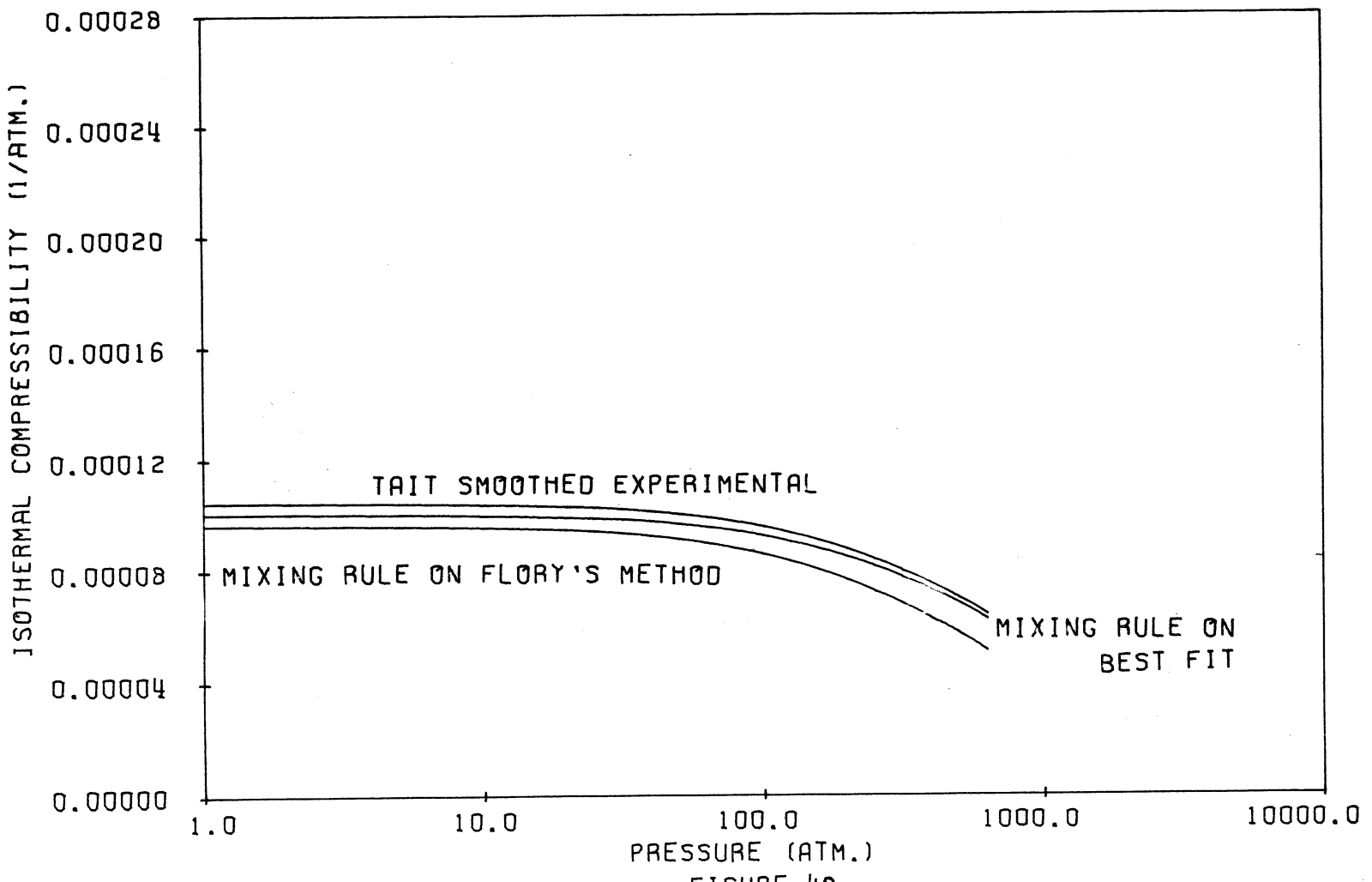

FIGURE 40

SMOOTHED EXPERIMENTAL AND PREDICTED COMPRESSIBILITY
VERSUS PRESSURE FOR
MIXTURE 0.5000 MOLE FRACTION N-DECANE AND N-TETRADECANE AT 25.0 DEG. C.

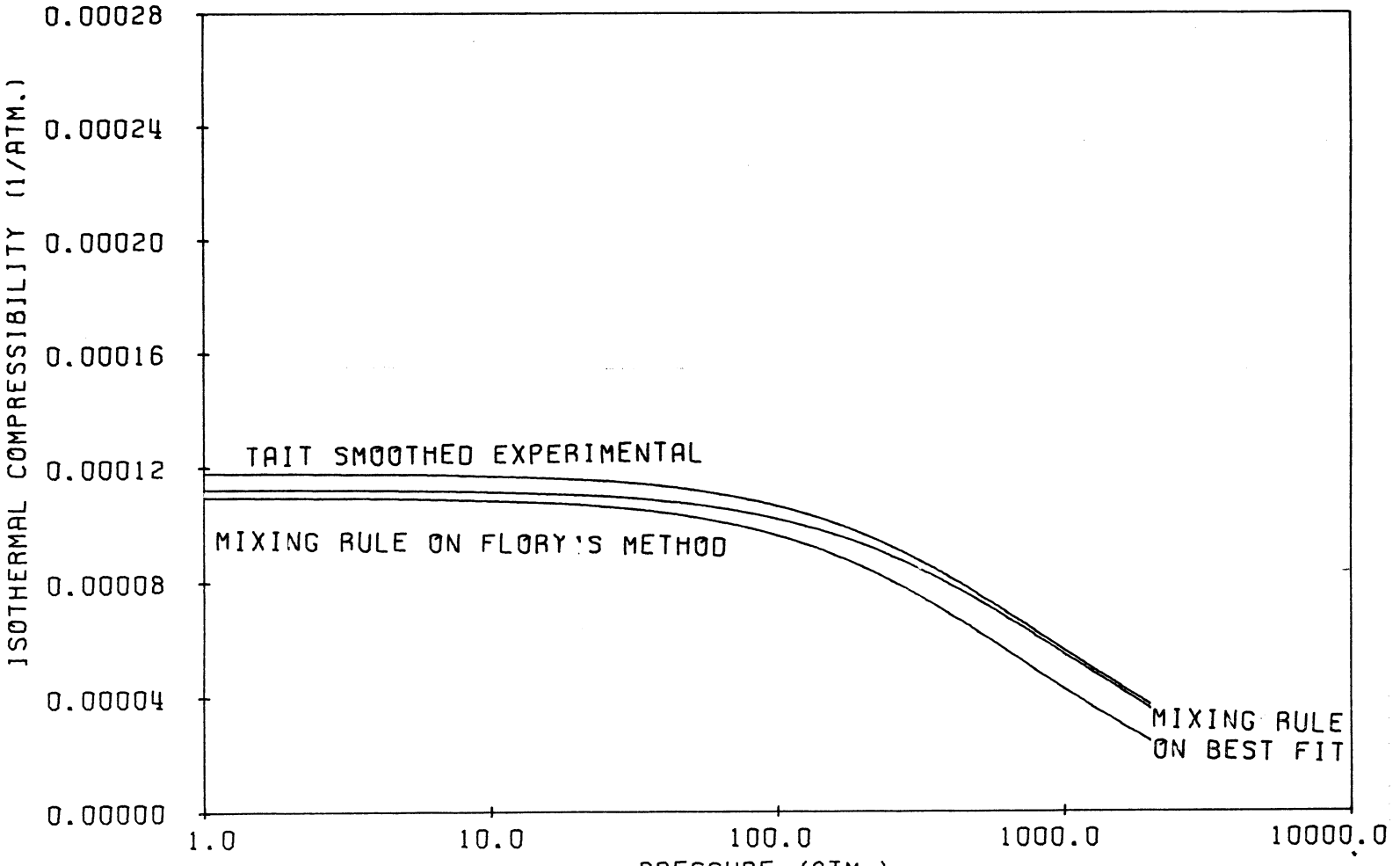

FIGURE 41

SMOOTHED EXPERIMENTAL AND PREDICTED COMPRESSIBILITY
VERSUS PRESSURE FOR
MIXTURE 0.5000 MOLE FRACTION N-DECANE AND N-TETRADECANE AT 45.0 DEG. C.

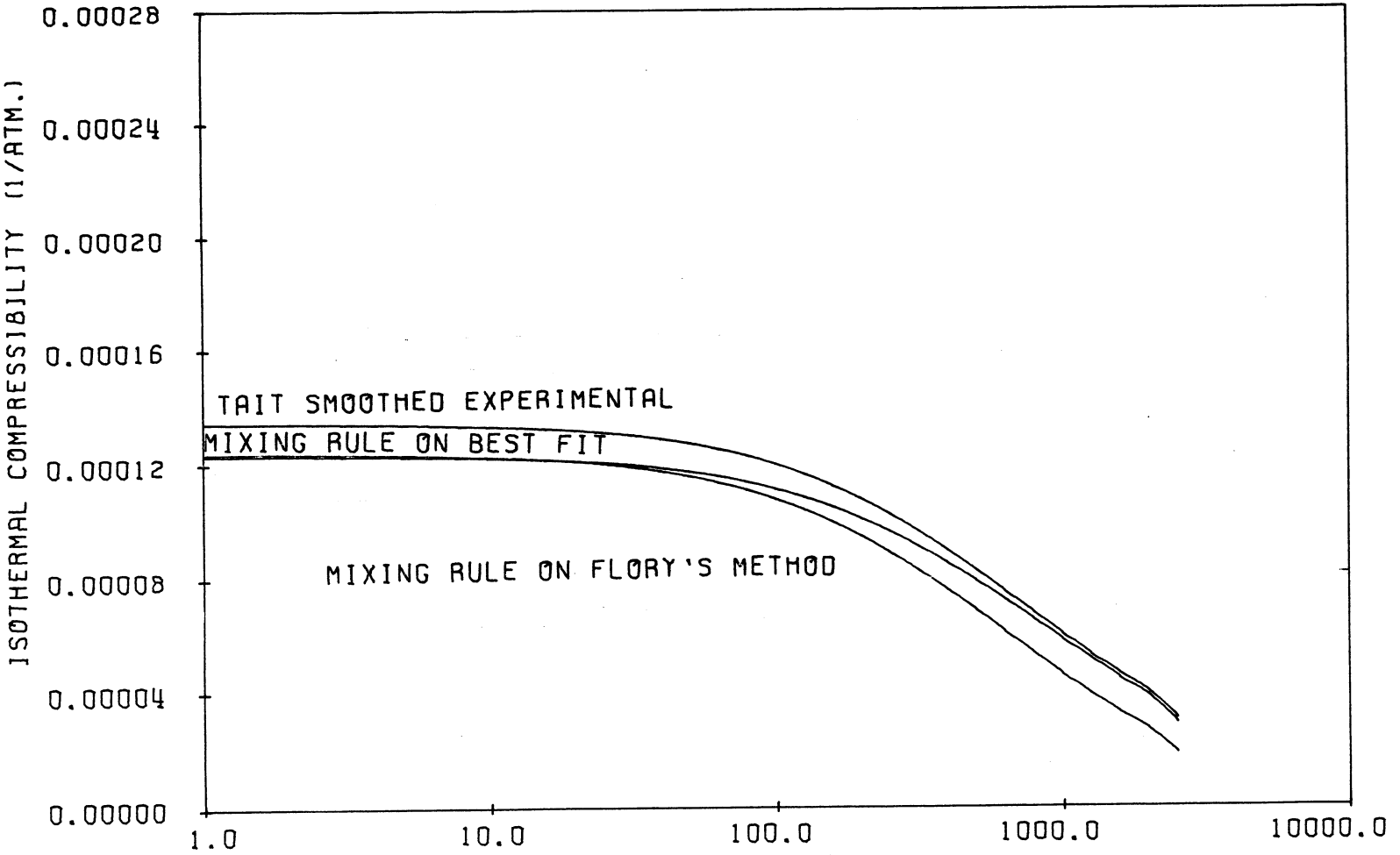

FIGURE 42

SMOOTHED EXPERIMENTAL AND PREDICTED COMPRESSIBILITY VERSUS PRESSURE FOR MIXTURE 0.5000 MOLE FRACTION N-DECANE AND N-TETRADECANE AT 65.0 DEG. C.

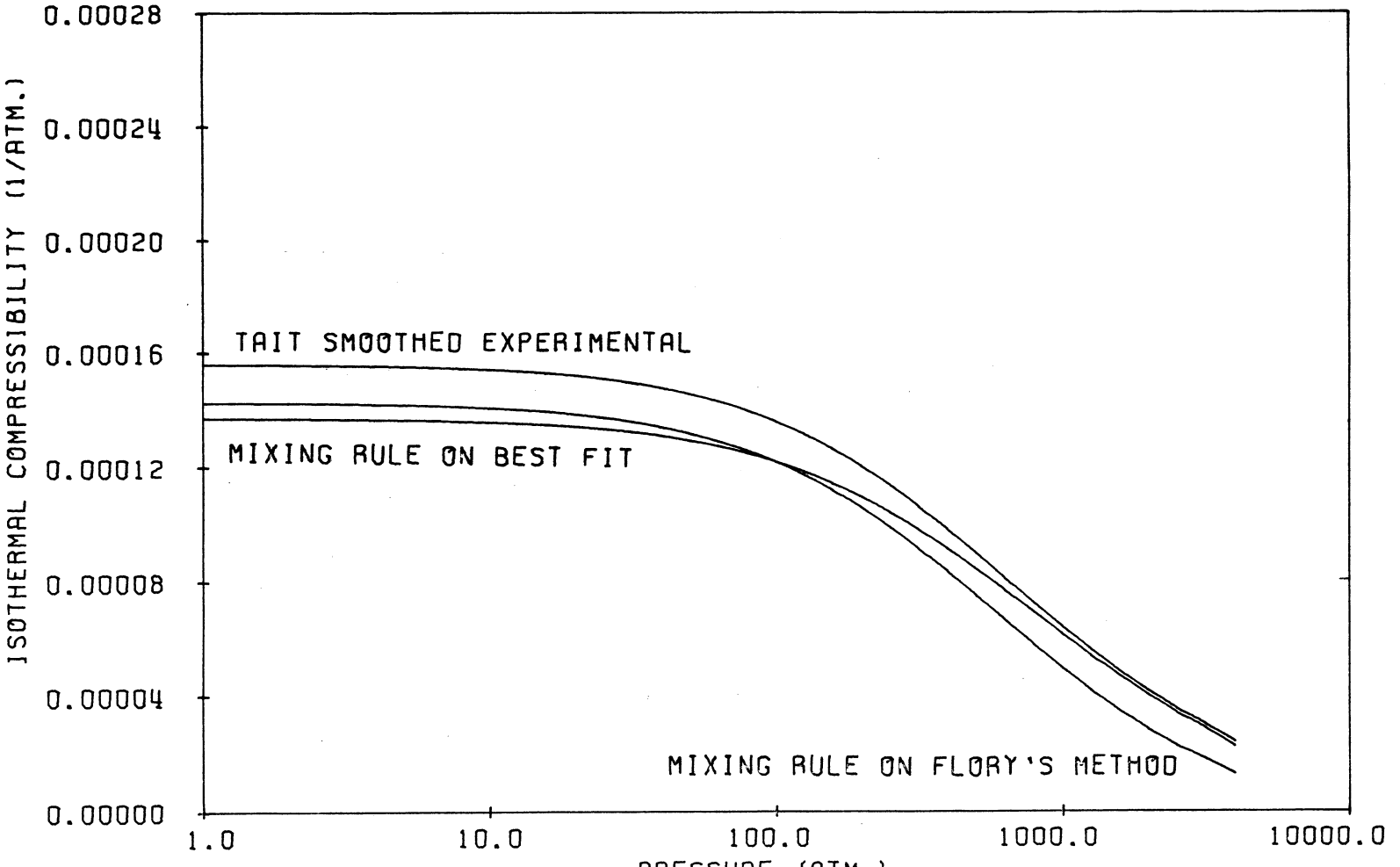

FIGURE 43

SMOOTHED EXPERIMENTAL AND PREDICTED COMPRESSIBILITY
VERSUS PRESSURE FOR
MIXTURE 0.5000 MOLE FRACTION N-DECANE AND N-TETRADECANE AT 85.0 DEG. C.

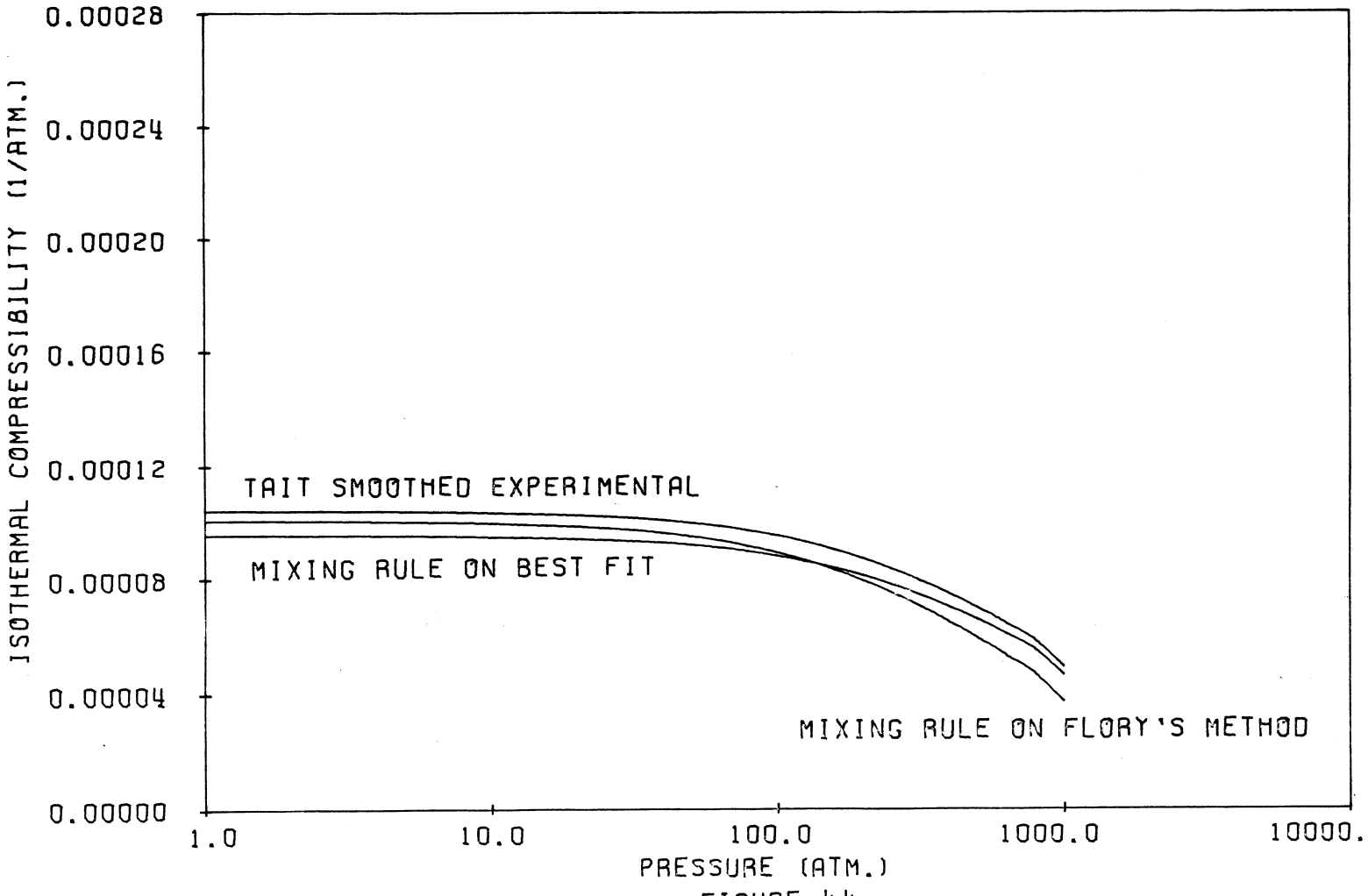

FIGURE 44

SMOOTHED EXPERIMENTAL AND PREDICTED COMPRESSIBILITY VERSUS PRESSURE FOR MIXTURE 0.6000 MOLE FRACTION N-DECANE, 0.2000 MOLE FRACTION N-TETRADECANE AND N-HEXADECANE AT 25.0 D[illegible]

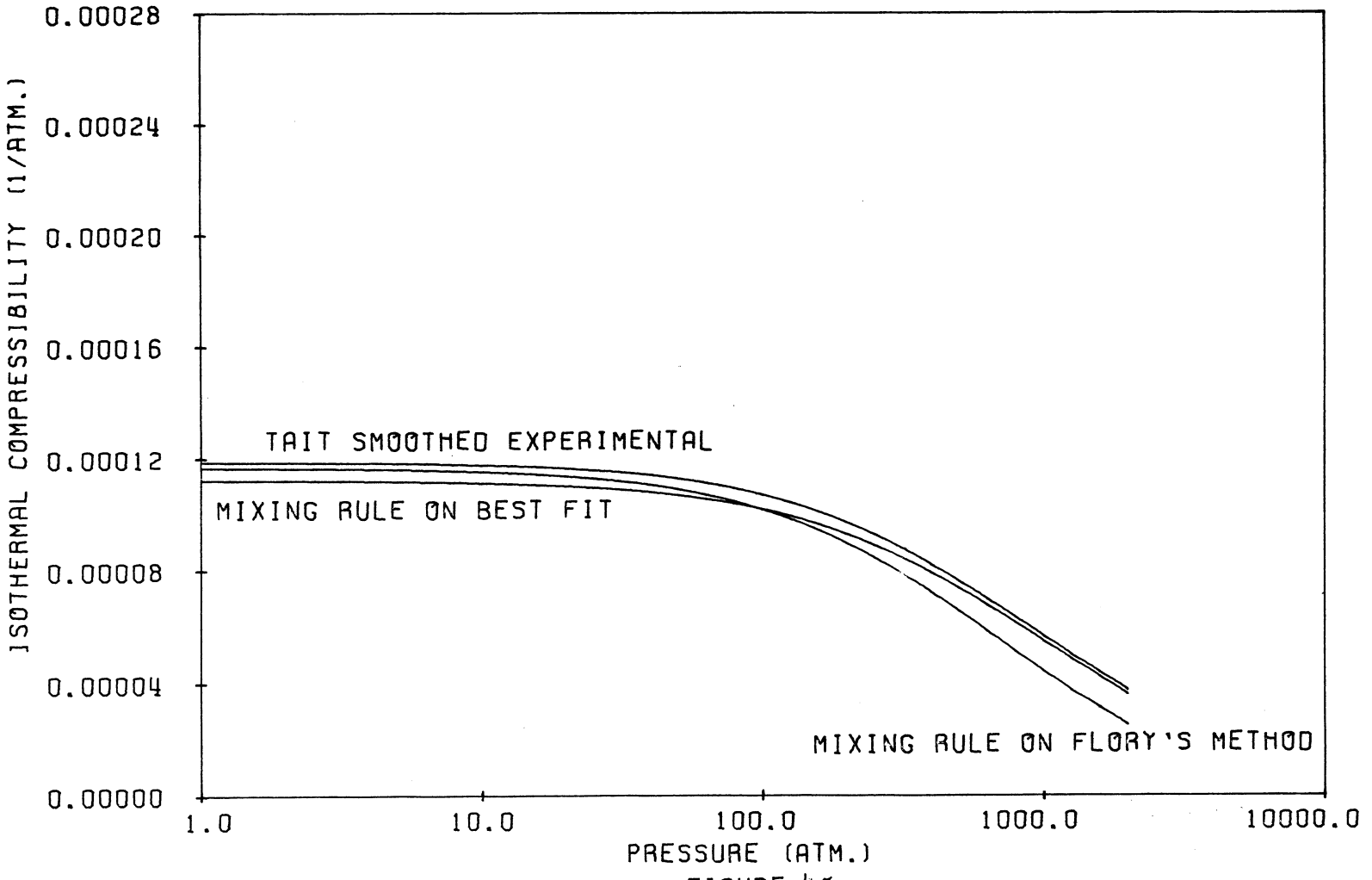

FIGURE 45

SMOOTHED EXPERIMENTAL AND PREDICTED COMPRESSIBILITY VERSUS PRESSURE FOR MIXTURE 0.6000 MOLE FRACTION N-DECANE, 0.2000 MOLE FRACTION N-TETRADECANE AND N-HEXADECANE AT 45.0 DEG. C.

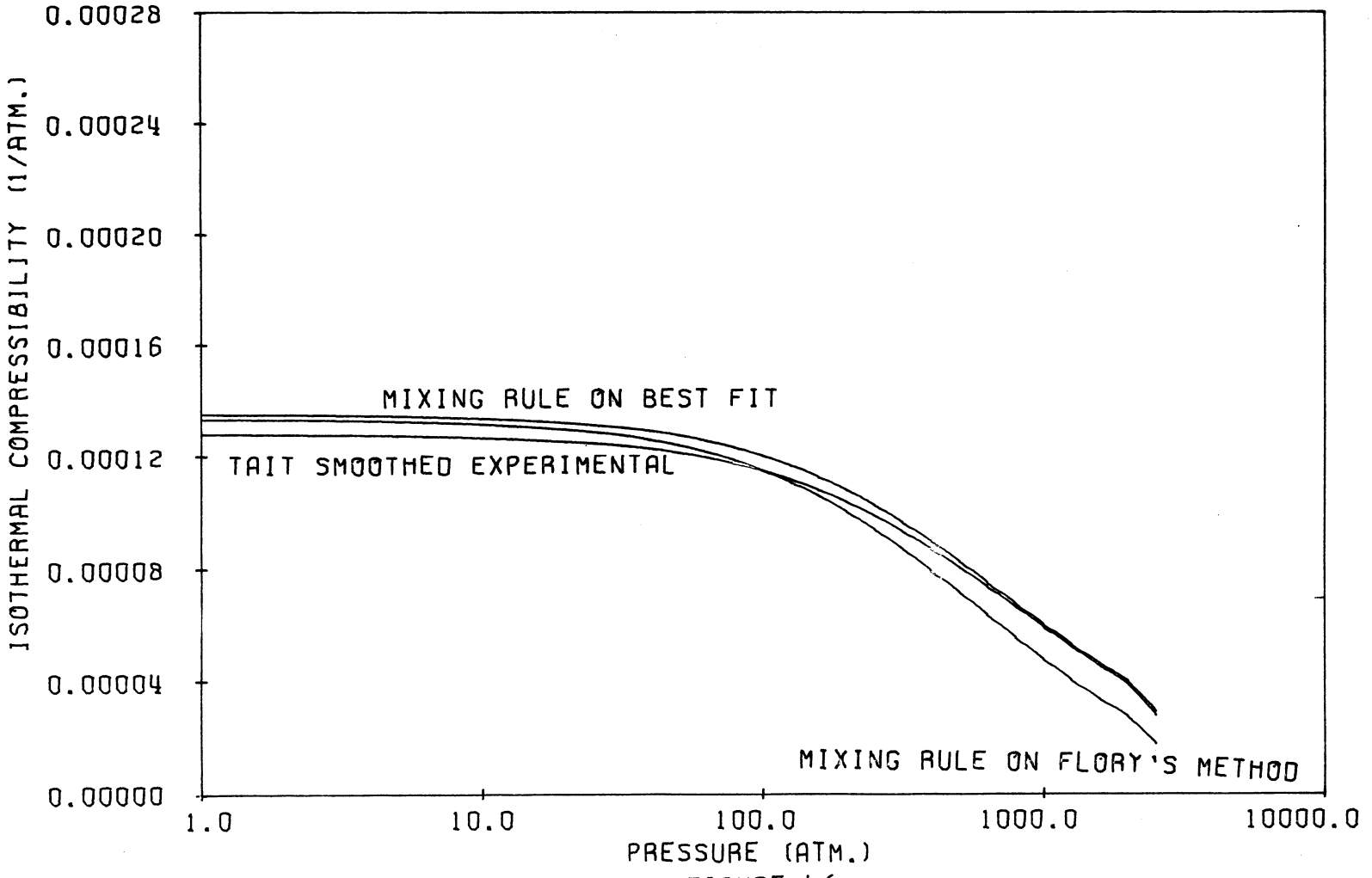

FIGURE 46
SMOOTHED EXPERIMENTAL AND PREDICTED COMPRESSIBILITY VERSUS PRESSURE FOR MIXTURE 0.6000 MOLE FRACTION N-DECANE, 0.2000 MOLE FRACTION N-TETRADECANE AND N-HEXADECANE AT 65.0 DEG. C.

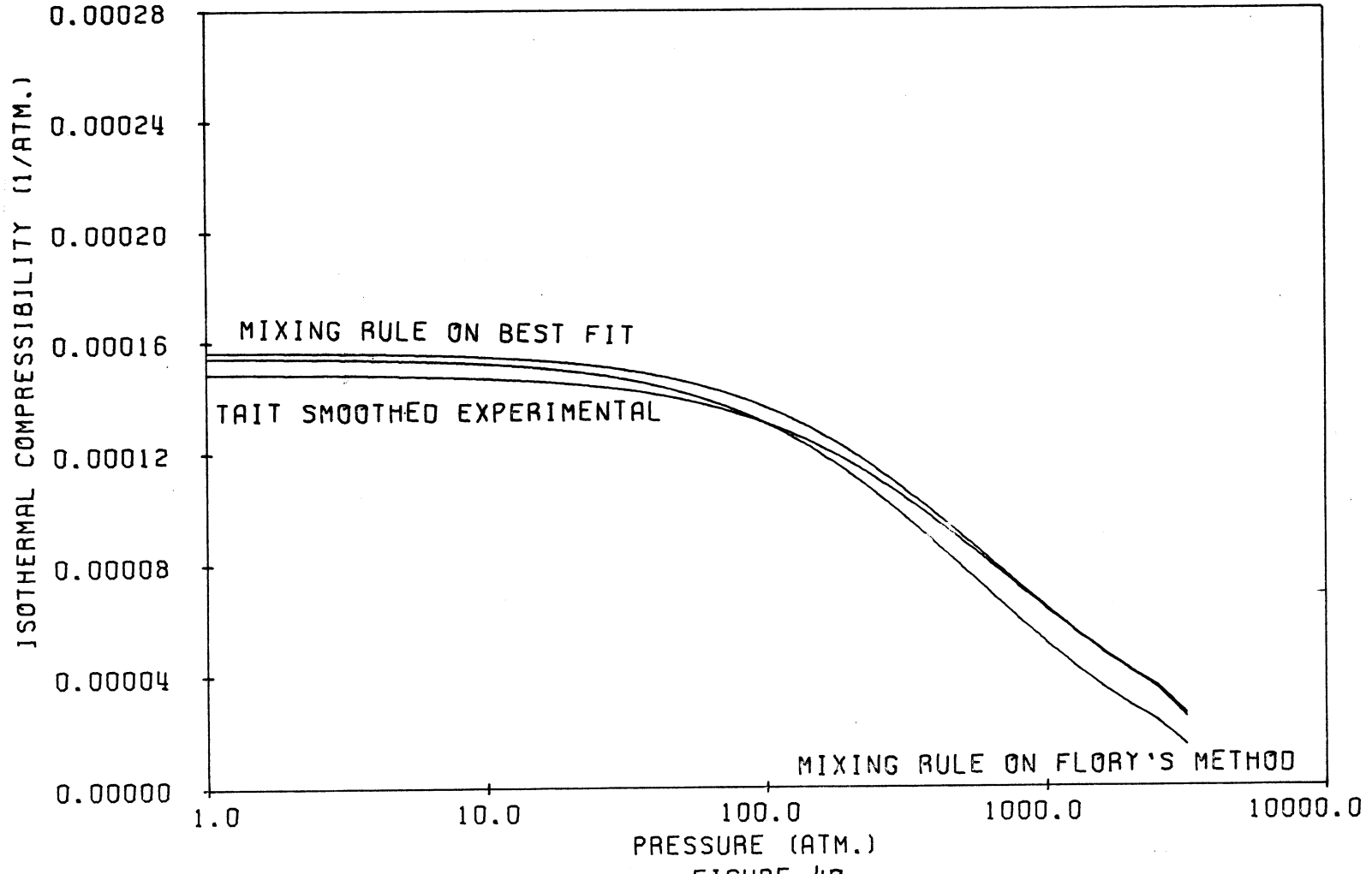

FIGURE 47

SMOOTHED EXPERIMENTAL AND PREDICTED COMPRESSIBILITY VERSUS PRESSURE FOR MIXTURE 0.6000 MOLE FRACTION N-DECANE, 0.2000 MOLE FRACTION N-TETRADECANE AND N-HEXADECANE AT 85.0 DEG. C.

Both the binary and ternary mixing rule results are very good considering that only pure component data was used in predicting the mixture properties.

V. SCALED PARTICLE

The Scaled particle theory isothermal compressibility equation was fit to the Tait smoothed isothermal compressibility data using regression analyais to determine the effective spherical radius parameter A. The results of this work are shown in Table XIII and plotted in Figure 48.

The predicted isothermal compressibility and the Tait smoothed experimental isothermal compressibility are compared in Figures 49 thru 52. These are again the temperature series for n-Dodecane which again was found to be representative.

VI. JOINT COMPARISON

A joint comparison of the Prausnitz, Flory, and Scaled particle theories is presented in Figures 53 thru 56. These figures present the best fit results for each of the three theories for n-Dodecane.

The Flory theory provides the best representation of the data, but it requires three adjustable parameters, each of which is a function of temperature. The Scaled

TABLE XIII

SCALED PARTICLE EFFECTIVE SPHERICAL RADIUS PARAMETER

Compound or mixture	t (°C)	A, ($X10^{+7}$) (cm)
n-Decane	25.0	0.6856
	45.0	0.6838
	65.0	0.6814
	85.0	0.6800
n-Dodecane	25.0	0.7320
	45.0	0.7300
	65.0	0.7283
	85.0	0.7247
n-Tetradecane	25.0	0.7725
	45.0	0.7713
	65.0	0.7708
	85.0	0.7682
n-Hexadecane	25.0	0.8112
	45.0	0.8102
	65.0	0.8083
	85.0	0.8066
0.5000 mole fraction n-Decane and n-Tetradecane	25.0	0.7328
	45.0	0.7298
	65.0	0.7277
	85.0	0.7229
0.5000 mole fraction n-Dodecane and n-Hexadecane	25.0	0.7728
	45.0	0.7716
	65.0	0.7697
	85.0	0.7679
0.6000 mole fraction n-Decane and 0.2000 mole fraction n-Tetradecane and n-Hexadecane	25.0	0.7315
	45.0	0.7299
	65.0	0.7279
	85.0	0.7256

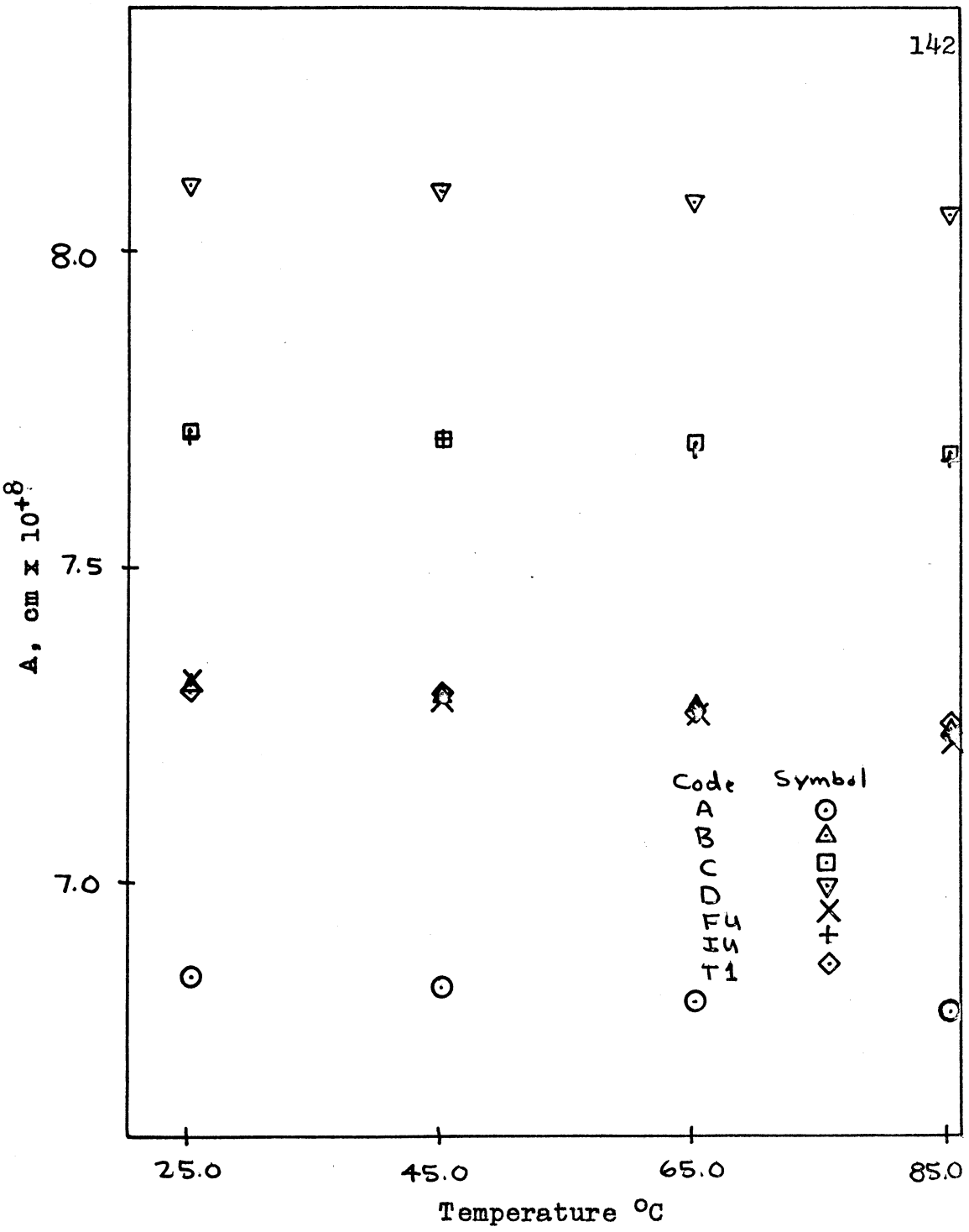

FIGURE 48

SCALED PARTICLE EFFECTIVE SPHERICAL RADIUS PARAMETER A VS. TEMPERATURE

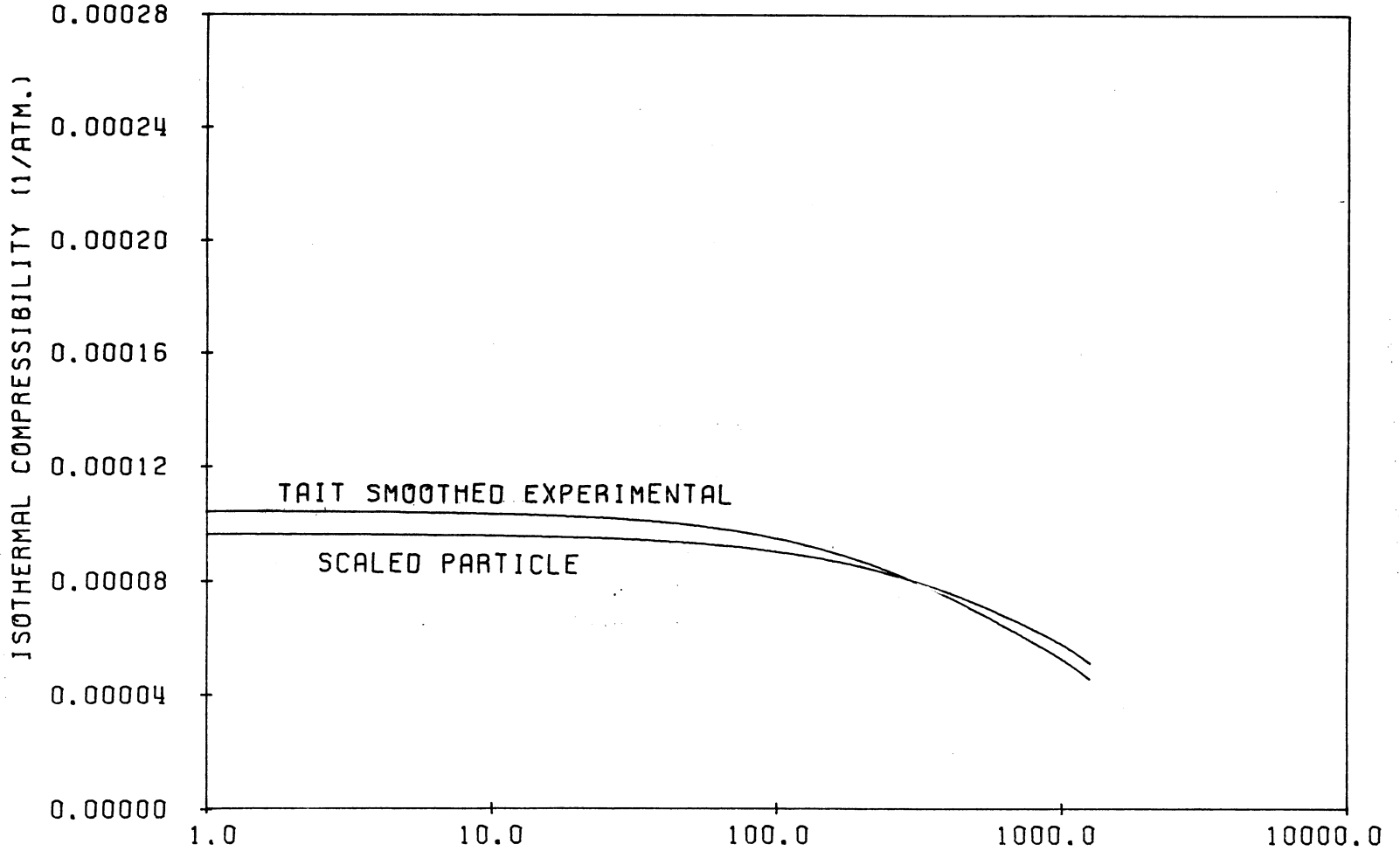

FIGURE 49

SMOOTHED EXPERIMENTAL AND PREDICTED COMPRESSIBILITY
VERSUS PRESSURE FOR
NORMAL DODECANE AT 25.0 DEG. C.

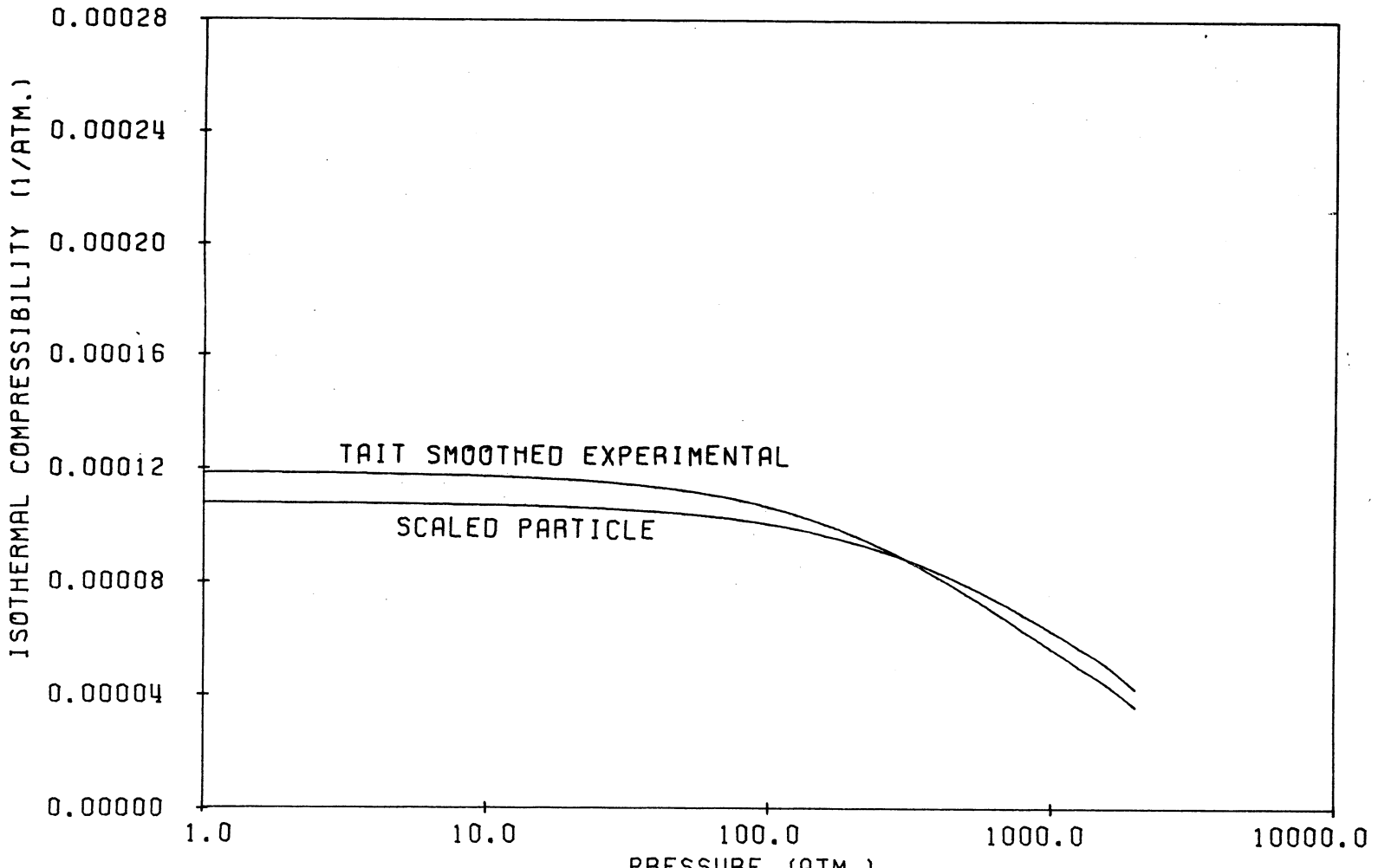

FIGURE 50

SMOOTHED EXPERIMENTAL AND PREDICTED COMPRESSIBILITY
VERSUS PRESSURE FOR
NORMAL DODECANE AT 45.0 DEG. C.

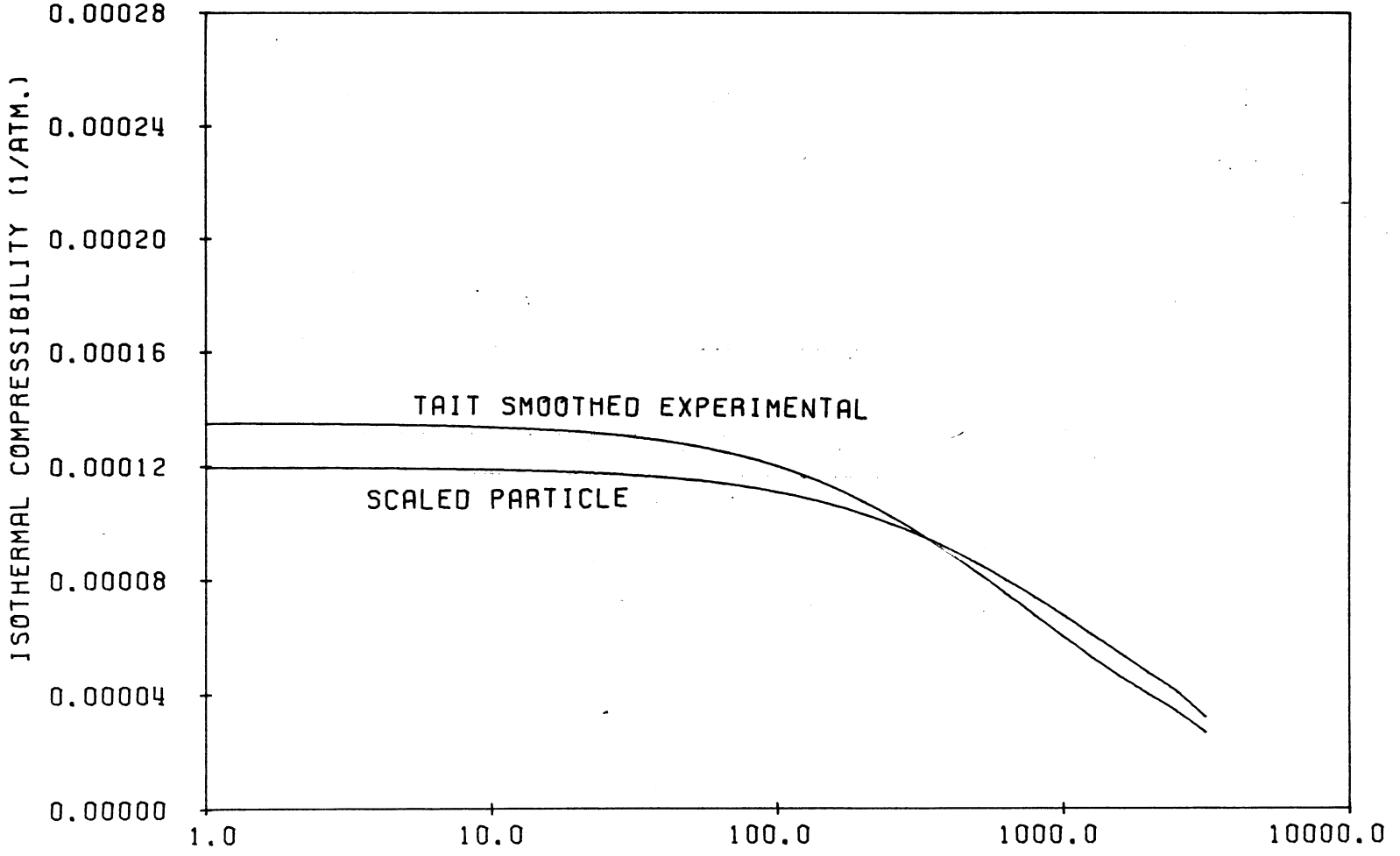

FIGURE 51

SMOOTHED EXPERIMENTAL AND PREDICTED COMPRESSIBILITY
VERSUS PRESSURE FOR
NORMAL DODECANE AT 65.0 DEG. C.

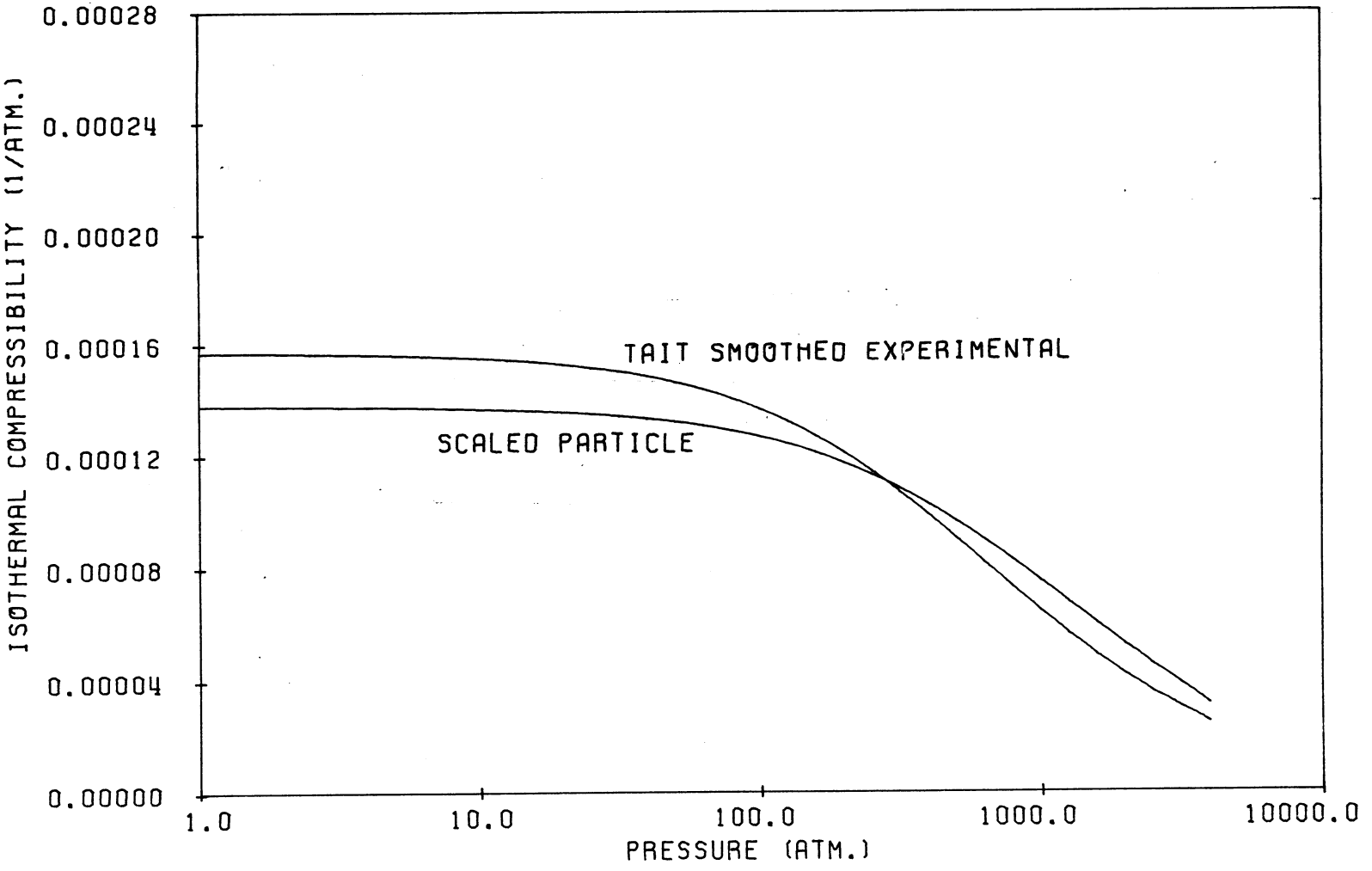

FIGURE 52

SMOOTHED EXPERIMENTAL AND PREDICTED COMPRESSIBILITY
VERSUS PRESSURE FOR
NORMAL DODECANE AT 85.0 DEG. C.

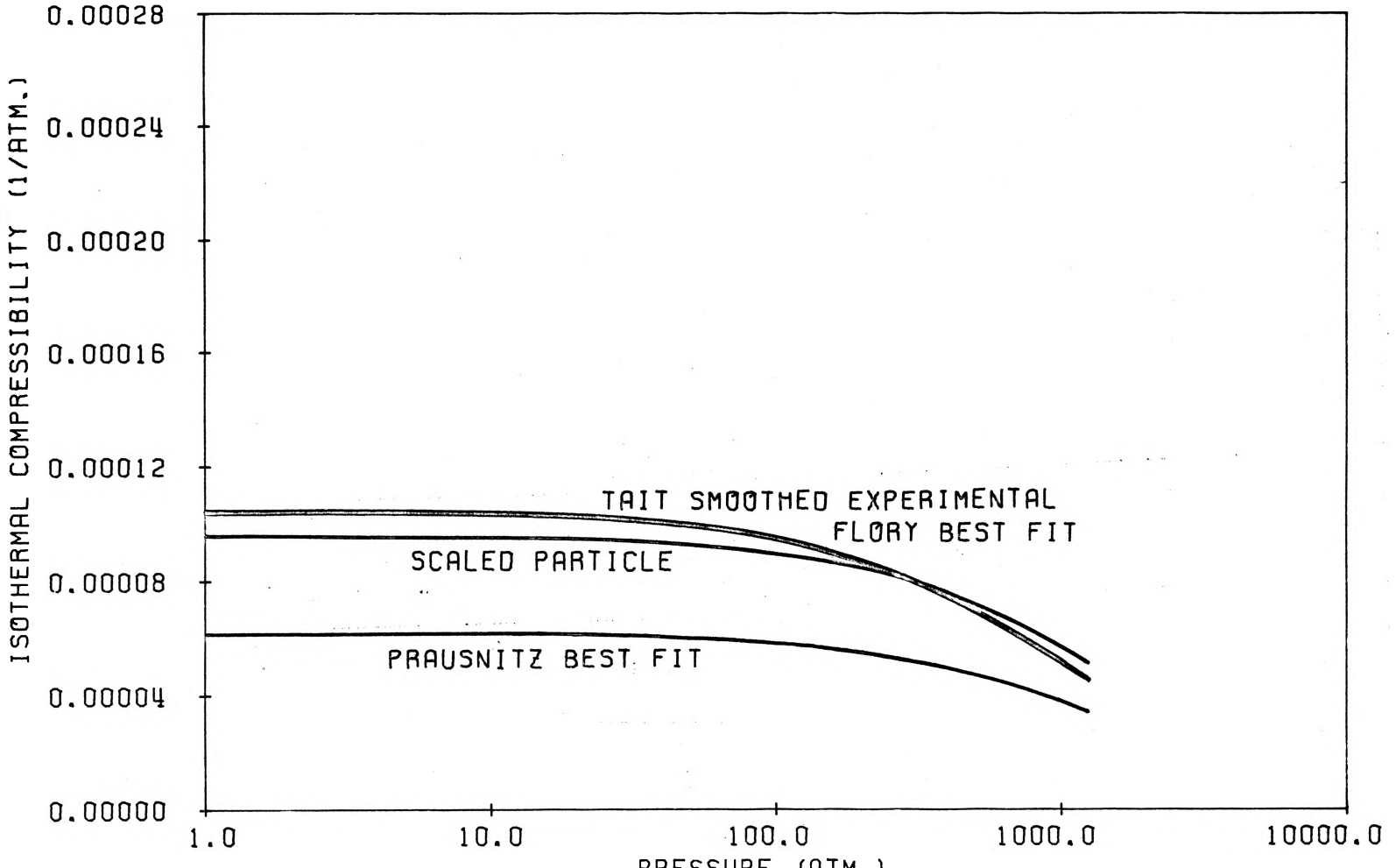

FIGURE 53

SMOOTHED EXPERIMENTAL AND PREDICTED COMPRESSIBILITY
VERSUS PRESSURE FOR
NORMAL DODECANE AT 25.0 DEG. C.

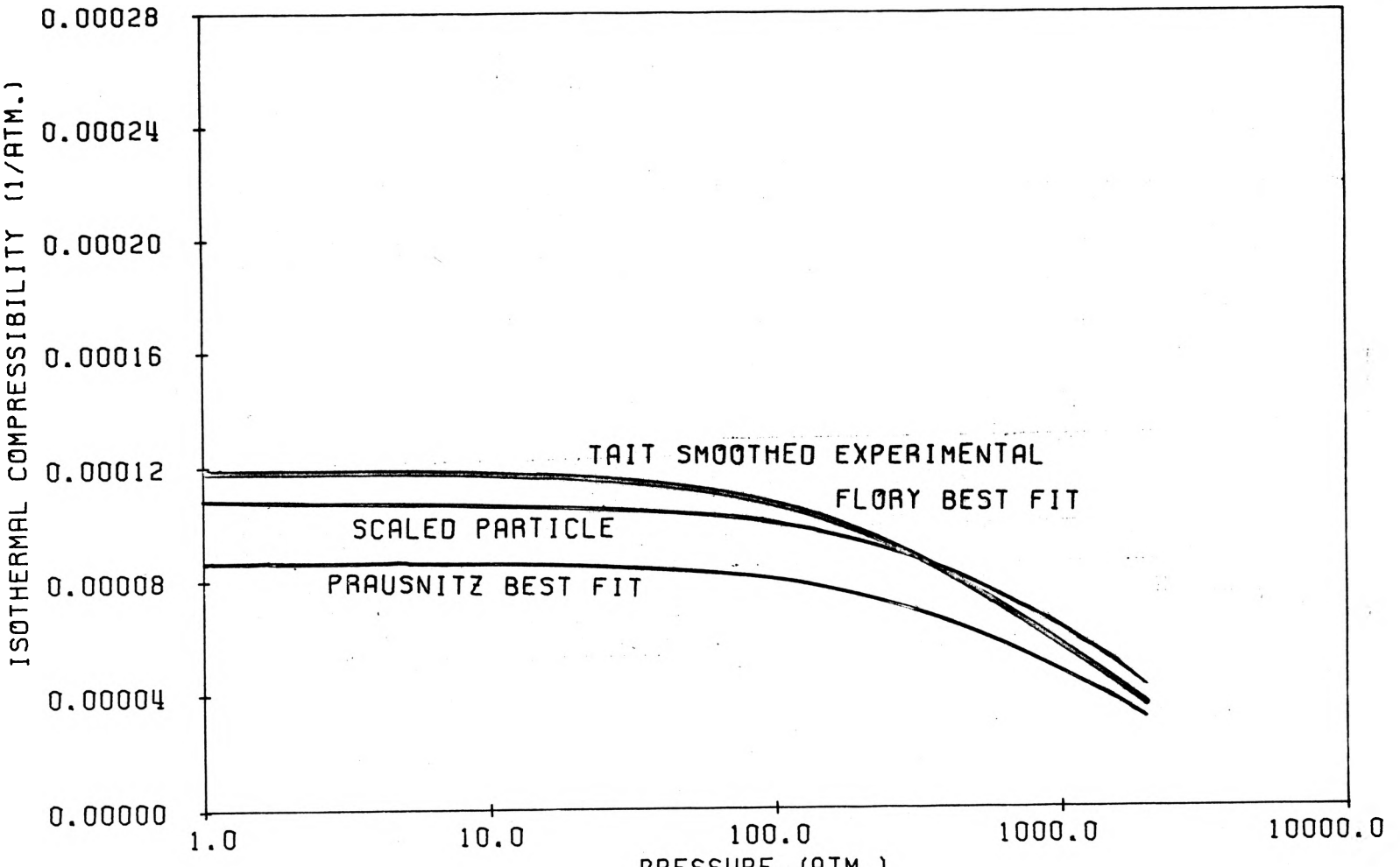

FIGURE 54

SMOOTHED EXPERIMENTAL AND PREDICTED COMPRESSIBILITY
VERSUS PRESSURE FOR
NORMAL DODECANE AT 45.0 DEG. C.

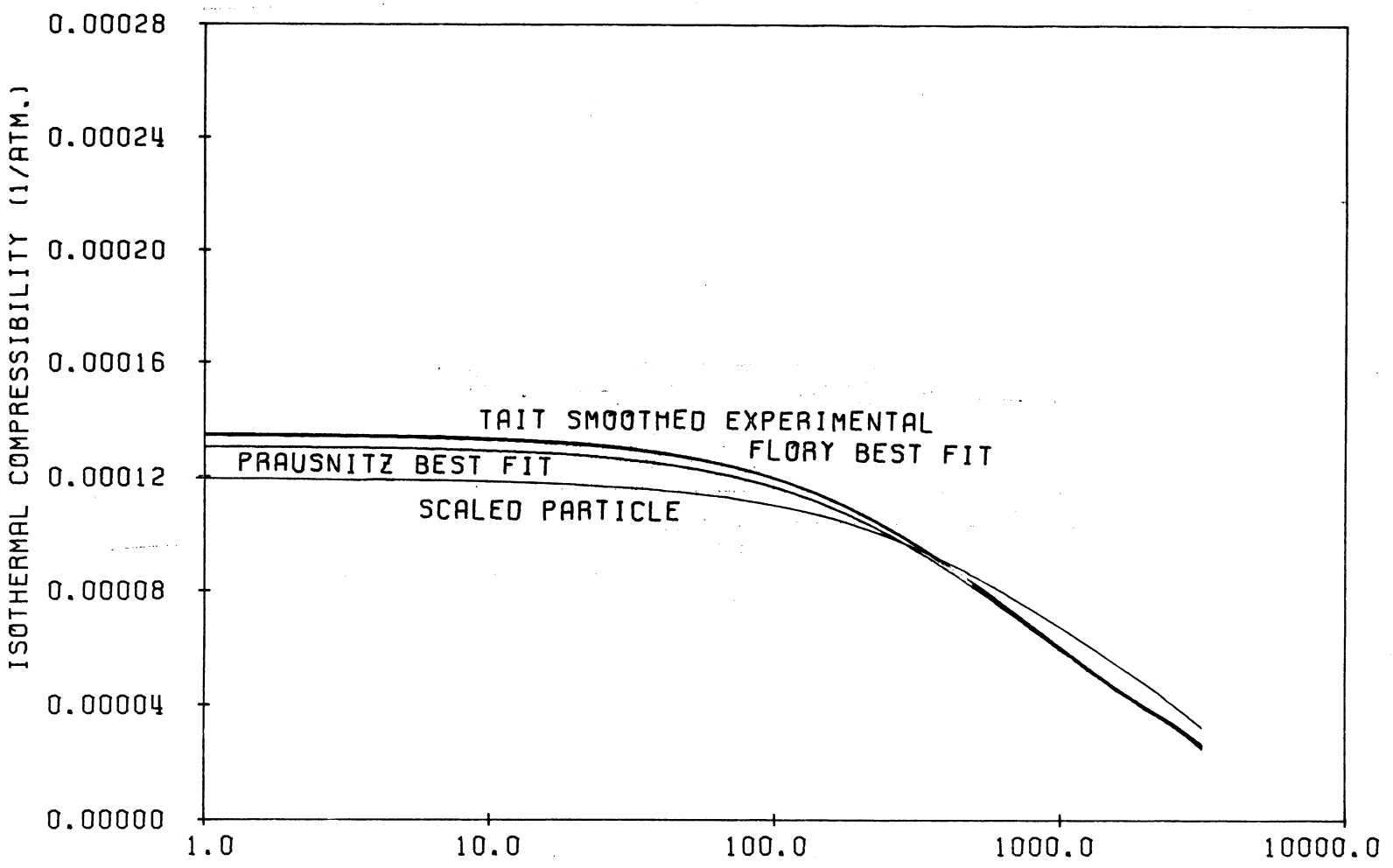

FIGURE 55

SMOOTHED EXPERIMENTAL AND PREDICTED COMPRESSIBILITY
VERSUS PRESSURE FOR
NORMAL DODECANE AT 65.0 DEG. C.

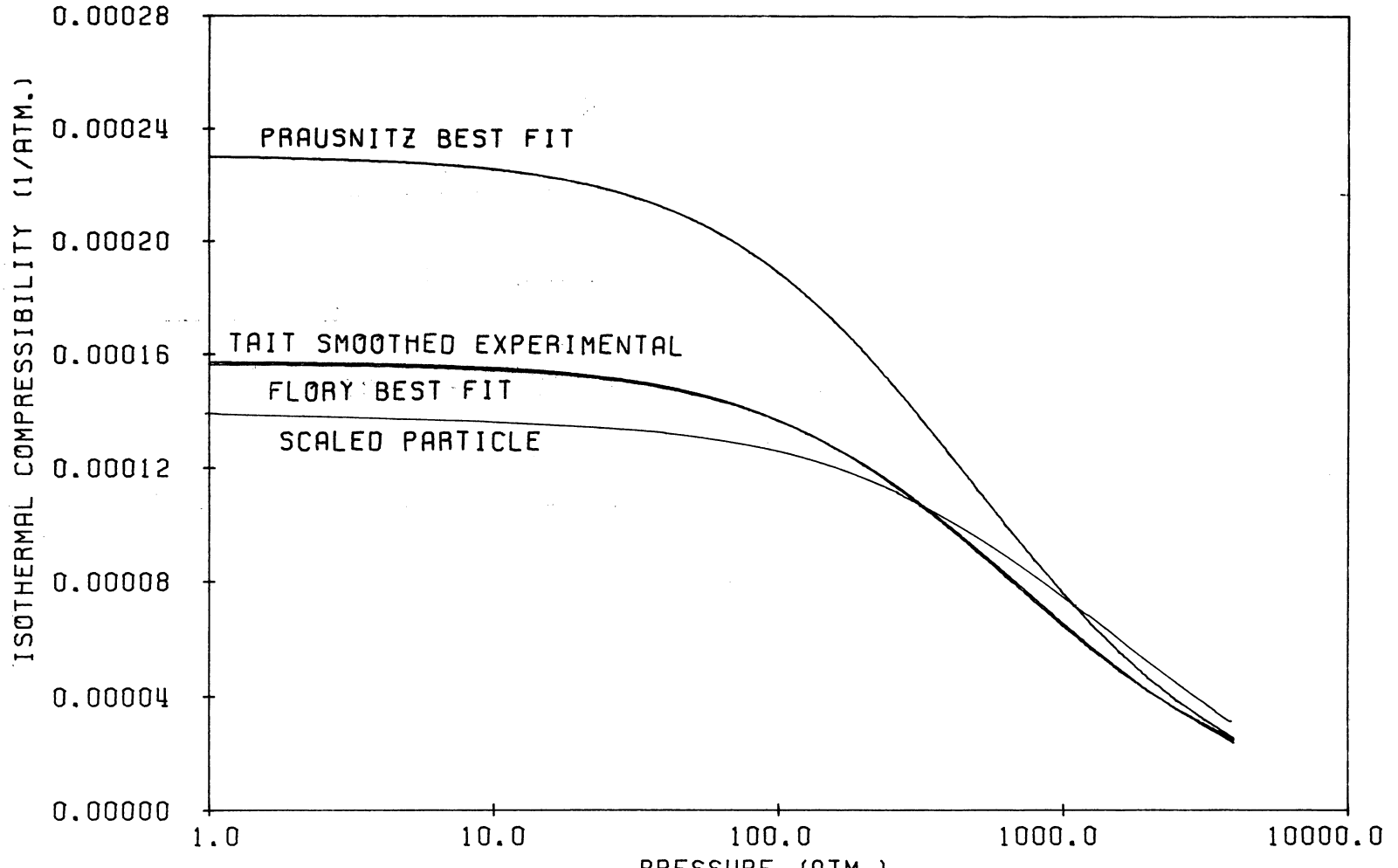

FIGURE 56

SMOOTHED EXPERIMENTAL AND PREDICTED COMPRESSIBILITY
VERSUS PRESSURE FOR
NORMAL DODECANE AT 85.0 DEG. C.

particle theory provides the second best overall representation of the data. It requires only one adjustable parameter which is a function of temperature. The Prausnitz assumption that the characteristic parameters are not a function of temperature proves to be too restrictive in this case.

CHAPTER VIII

CONCLUSIONS, SUMMARY AND RECOMMENDATIONS

I. CONCLUSIONS

Of the Prausnitz, Flory, and Scaled Particle theories only the Flory theory with three parameters per isotherm is flexible enough to allow it to be adjusted to reproduce the data. These parameters appear to vary uniformly (see Figures 33 thru 35). Thus one may assume that interpolation of the parameters would provide a good method of interpolating the experimental data. With data of the present accuracy it is not possible to determine if the Flory Theory can be adjusted to reproduce liquid behavior exactly.

The Scaled particle theory as used probably could be improved by introducing more reaslistic interaction potentials in place of the rigid sphere potential now used. It shows a rather good reproduction of the data, considering it contains only one adjustable parameter, and should receive further work.

The assumptions used by Prausnitz are too restrictive to allow this partition function to fit the experimental data. To relax these assumptions would in effect turn it into the Flory theory.

The Flory theory mixing rule was found to provide a simple and reasonably accurate way of predicting liquid binary and ternary mixture data from pure component liquid data. Further experimental work with mixtures which are more dissimilar will be required to draw any further conclusions concerning the Flory mixing rule. Such a mixture might be 0.5000 mole fraction n-Octane and n-Tetradecane, for example.

II. SUMMARY

An experimental apparatus was built to measure accurate liquid p-v-T data using the sylphon bellows technique. Liquid p-v-T data were taken for n-Decane, n-Dodecane, n-Tetradecane, n-Hexadecane, 0.5000 mole fraction mixtures of n-Decane and n-Tetradecane and of n-Dodecane and n-Hexadecane, and a mixture of 0.6000 mole fraction n-Decane and 0.2000 mole fraction n-Tetradecane and n-Hexadecane at 25.00, 45.00, 65.00, and 85.00°C from atmospheric pressure to the freezing pressure on each isotherm. It was found that the Tait equation represented the experimental data to within experimental error.

The data were used to test three liquid theories and the Flory mixing rule. It was found that the Flory Theory reproduced the experimental data to within experimental error. The Scaled particle theory reproduced the experimental data to within ten times the experimental error. The Prausnitz theory assumptions were found to be too restrictive to represent the data over a wide range of temperature and pressure. The Flory mixing rule provides a reasonably accurate method of predicting binary and ternary liquid p-v-T data using only pure component data, but this procedure requires additional testing.

This study indicates that existing theories can be used to predict liquid properties with reasonable accuracy. Additional work will be required to obtain better predictive methods.

III. RECOMMENDATIONS

It is recommended that the work started in this study be extended in two ways:

1. To increase the temperature range for the samples studied up to the upper limit of the apparatus (150°C).
2. To include n-Hexane and n-Octane for the pure components and to add mixtures of components with chain lengths as dissimilar as possible.

These extensions would allow a more stringent test of the Flory partition function theory and the Flory mixing rule.

NOMENCLATURE

NOMENCLATURE

A	Effective hard sphere radius (Scaled particle theory)	cm.
A	Cross sectional area of the dead weight tester	$in.^2$
A_{br}	Bridgman's best fit linear constant term for relative compression of Brass	1/psi.
A_c	Capillary tube cross sectional area	$cm.^2$
A_{ka}	Bridgman's best fit linear constant term for relative compression of Karma	1/psi.
$A_{p,t}$	Bellows' cross sectional area at pressure P and temperature t	$cm.^2$
b	Dead weight tester's area correction term for pressure on the pistons cross sectional area	/psi.
B_{br}	Bridgman's best fit second order constant term for relative compression of Brass	$1/psi^2$
B_{ka}	Bridgman's best fit second order constant term for relative compression of Karma	1/psi
c	Dead weight tester's area coefficient of thermal expansion	$1/^oC$
c	Prausnitz's parameter related to the departure from non-central force fields	
c	Flory's parameter for the number of external degrees of freedom per segment	
h	Height of the mercury thread in capillary calibration	cm.
J	Tait coefficient	cc/cc.
k	Boltzman constant	
L	Tait coefficient	atm.

$L_{p,t}$	Length of slide wire at pressure P and temperature t between the bellows and fixed contact	cm.
L_p^c	Total length of the slide wire	cm.
ΔL_B	Bellows change in length with pressure	cm.
ΔL_c	Fluid displacement up the capillary tube in the bellows calibration	cm.
M_A	Mass of weights on the dead weight tester pan	lbm.
N	Avagadros number	
P	Pressure	atm.
$\tilde{P}$	Prausnitz or Flory reduced pressure	
P*	Prausnitz of Flory characteristic pressure	atm.
Q_f	Flory configurational partition function	
Q_p	Prausnitz configurational partition function	
r	Scale particle theory cavity radius	cm.
r	Capillary tube radius in capillary tube calibration	
$R_{a,p}$	Slide wire resistance between fixed contact and bellows at pressure P	ohms.
$R_{M_n,P}$	Manganin cell's resistance at pressure P	ohms.
T	Temperature	^oK
$\tilde{T}$	Prausnitz or Flory reduced temperature	
T*	Prausnitz or Flory characteristic temperature	^oK
V	Relative volume	cc/cc
V	Prausnitz or Flory molar volume	cc/mole
$\tilde{V}$	Prausnitz of Flory reduced volume	

V^*	Prausnitz of Flory characteristic volume	cc/mole
ΔV	Change in relative volume	cc/cc
$\frac{\Delta V}{V_o}$	Compression	cc/cc
W	Sample weight	gm.
W(r)	Scaled particle theory work required to produce the spherical cavity	
y	Scaled particle theory reduced volume	

Greek Symbols

α_{br}	Linear coefficient of thermal expansion for brass	$1/^oC$
α_{ka}	Linear coefficient of thermal expansion for karma	$1/^oC$
β	Isothermal compressibility	1/atm.
$\tilde{\beta}$	Prausnitz of Flory reduced isothermal compressibility	
ψ^N	Energy of motion of the molecule in the cell	
Ω	Slide wire unit length	cm/ohm.
ρ_A	Density of air at measurement conditions	gm/cc
ρ_{Hg}	Density of mercury	gm/cc
$\rho_{o,t}$	Fiducial sample density	gm/cc
ρ_w	Dead weight tester's weights density	gm/cc

Superscripts

$\sim$	Prausnitz or Flory reduced property
$*$	Prausnitz of Flory characteristic property

Subscripts

B	Bellows
br	Brass
c	Capillary
ka	Karma
p	At pressure P
t	At temperature t

BIBLIOGRAPHY

BIBLIOGRAPHY

1. Abe, A., Flory, P. J., J. Am. Chem. Soc., 87, 1838 (1965).

2. Adams, L. H., J. Am. Chem. Soc., 53, 3769 (1931).

3. Amagat, E. H., Ann. Chem. et Phys., 29, 68 (1893).

4. Barker, J. A., Lattice Theories of the Liquid State, MacMillan Co., New York, 1963.

5. Boelhouwer, J. M. W., Physica., 26, 1021 (1960).

6. Bridgman, P. W., Proc. Amer. Acad., 58, 166-242 (1923).

7. Bridgman, P. W., Proc. Amer. Acad., 66, 185-233 (1931).

8. Bridgman, P. W., The Physics of High Pressure, G. Bell and Sons, London, 1949.

9. Chapman, S., Cowling, T. G., The Mathematical Theory of Non-Uniform Gases, Cambridge University Press, Cambridge, 1964.

10. Cutler, W. G., McMickle, R. H., Webb, W., Schiessler, R. W., J. Chem. Phys., 29, 727 (1958).

11. Cutler, W. G., Ph.D. Dissertation, Pennsylvania State University (1955).

12. Driver-Harris Bulletin FW 103, Driver-Harris, Inc., Harrison, N.J., p7 (1962).

13. Doolittle, A. K., Simon, I., Cornish, R. M., A.I.Ch.E.J., 6, 160-162 (1960).

14. Ibid., pp. 150.

15. Ibid., pp. 151.

16. Ibid., pp. 153.

17. Eduljee, H. E., Newitt, D. M., Weale, K. E., J. Chem. Soc., 3086 (1951).

18. Egelstaff, P. A., An Introduction to the Liquid State, Academic Press, New York, 1967.

19. Eyring, H., Hirschfelder, J., J. Phys. Chem., 41, 249 (1937).

20. Eyring, H., Ree, T., Hirai, N., Proc. Natl. Acad. Sci. U.S., 44, 683 (1958).

21. Flory, P. J., Orwoll, R. A., Vrij, A., J. Am. Chem. Soc., 86, 3507-9 (1964).

22. Ibid., pp. 3515.

23. Flory, P. J., J. Am. Chem. Soc., 87, 1833 (1965).

24. Gibson, R. E., Loeffler, O. H., J. Am. Chem. Soc., 63, 2287 (1941).

25. Green, H. S., Molecular Theory of Fluids, North-Holland Publishing Co., Amsterdam, 1952.

26. Handbook of Chemistry and Physics, Ed. Charles D. Hadgrman, Chemical Rubber Pub. Co., 43rd Ed., p 2276, (1961-62).

27. Harrison, C., "Volume Change on Mixing of Binary Alkane Mixtures" (M.S. thesis, University of Missouri, 1966). of. also Harrison, C., and Winnick, J., J. Chem. Engr. Data, 12, 176-8 (1967).

28. Hartley, H. O., Technometrics, 3, 269 (1961).

29. Hill, T. L., Statistical Thermodynamics, Addison-Wesley, Reading, 1962.

30. Hyun, K. S., Ph.D. Dissertation, University of Missouri, Columbia, Missouri, 1966.

31. Leland, T. W., Chappelear, P. S., Ind. Eng. Chem. 60 #7, 15-43 (1968).

32. Ibid., pp. 16.

33. Lin, L. Y., private communication.

34. Ma, S. M., Eyring, H., J. Chem. Phys., 42, 1920 (1965).

35. Marchi, R., Liang, K., Eyring, H., Proc. Natl. Acad. Sci. U.S., 52, 1107 (1964).

36. Martin, J. J., Ind. Eng. Chem., 59 #12, 34-52 (1967).

37. Mayer, S. W., J. Chem. Phys., 38 #8, 1803 (1963).

38. Mickley, H.S., Sherwood, T. K., Reed, C. E., Applied Mathematics in Chemical Engineering, 2nd. ed., McGraw-Hill, New York, 1957.

39. Murnaghan, F. D., Proc. Natl. Acad. Sci., 30, 244 (1944).

40. National Bureau of Standards Monograph No. 8.

41. National Bureau of Standards Monograph No. 65.

42. Prausnitz, J. M., Eckert, Renon, H., Ind. Eng. Chem. Fundamentals, 6 #1, 58 (1967).

43. Prausnitz, J. M., O'Connell, J. P., Ind. Eng. Chem., 60 #1, 44 (1968).

44. Present, R. D., Kinetic Theory of Gases, McGraw-Hill, New York, 1958.

45. Prigogine, I., Trappeniers, N., Mathot, V., Discussions Faraday Soc., 15, 93 (1953).

46. Pryde, J. A., The Liquid State, Hutchison Publishers Ltd., London, 1966.

47. Reiss, H., Frisch, H. L., Lebowitz, J. L., J. Chem. Phys., 31, 369 (1959).

48. Reiss, H., Frisch, H. L., Helfand, E., Lebowitz, J. L., J. Chem. Phys., 32 #1, 119 (1960).

49. Reiss, H., Frisch, H. L., Helfand, E., Lebowitz, J. L., J. Chem. Phys., 31 #2, 369 (1959).

50. Reiss, H., Advances in Chemical Physics, 9, 1 (1965).

51. Ibid., pp. 44.

52. Renon, H., Ph.D. Dissertation, University of California, Berkeley, 1966.

53. Renon, H., Eckert, C. A., Prausnitz, J. M., Ind. Eng. Chem. Fundamentals, 6 #1, 52-67 (1967).

54. Ibid., pp. 53.

55. Ibid., pp. 53-54

56. Rowlinson, J. S., Liquids and Liquid Mixtures, Academic Press Inc., New York, 32-38, 1959.

57. Shavers, O. R., Ph.D. Dissertation, University of Houston (1965).

58. Sims, M. J., "Excess Volume of Binary Liquid Mixtures of n-Paraffins" (M.S. Thesis, University of Missouri, 1968) c.f. also Sims, M. J., and Winnick, J., J. Chem. Eng. Data, 14, 164-166, (1969).

59. Tait, P. G., "The Voyage of H.M.S. Challenger", Vol. 2, Part 4, pp. 1-73, H.M.S.O., London, 1888.

60. Wertheim, M. S., J. Chem. Phys., 43, 1370 (1965).

61. Whalley, E., Holder, G. A., Trans. Faraday Soc., 58, 2095 (1962).

62. Winnick, J., Ph.D. Dissertation, The University of Oklahoma, Norman, Oklahoma, 1963.

APPENDICIES

APPENDIX A

DATA REDUCTION

The basic data reduction equation for the p-v-T data is:

$$\frac{\Delta V}{V_o} = \frac{\Delta L_B \cdot A_{p,t} \cdot \rho_{o,t}}{W} \qquad \text{(A-1)}$$

where; $\frac{\Delta V}{V_o}$ is the relative volume change or compression in cc/cc, ΔL_B is the change in length of the bellows, $A_{p,t}$ is the cross sectional area of the bellows at the temperature and pressure of the measurement, $\rho_{o,t}$ is the fiducial density (27, 33, 58), and W is the weight of the sample contained within the bellows. All these values are obtained from experimental measurements.

The calculation of each of the terms in $\Delta V/V_o$ is described below.

1. Calculation of ΔL_B

To determine the chance in length of bellows B in Figure 57, ΔL_B, the resistance of the Karma slide wire, S, between the fixed contact C and bellows B was measured at each pressure, $R_{a,p}$. The change in resistance from the atmospheric pressure value, $R_{a,o}$, times the

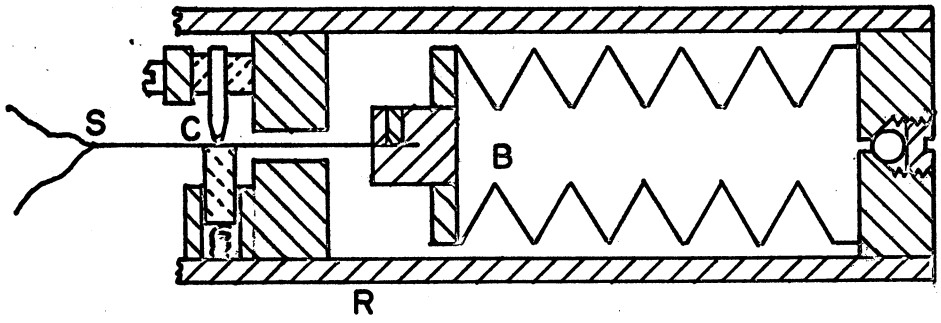

Bellows Area Section

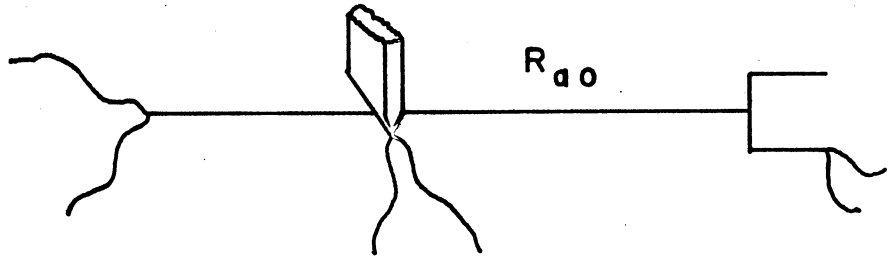

Uncompressed Slide Wire Position

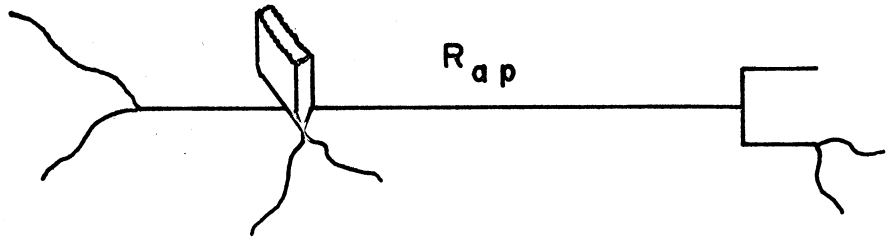

Compressed Slide Wire Position

FIGURE 57. BELLOWS AND SLIDE WIRE ARRANGEMENT

number of cm/ohm, Ω, gave the value of ΔL_B which is corrected for temperature, C_t, and pressure, C_p, effects.

$$\Delta L_B = \Omega \cdot (R_{a,p} - R_{a,o}) + C_p + C_t \qquad \text{(A-2)}$$

The slide wire position before and after pressure application are shown in the second and third views of Figure 57.

a. Pressure Correction

The pressure correction is due to the difference in compressibility of the Brass carrier R and the Karma slide wire S in Figure 57. The measured length of the distance between the bellows B and contact C is given by:

$$L_{a,p} = R_{a,p} \left(\frac{L^c_p}{R_{o,t}} \right) \qquad \text{(A-3)}$$

where; L^c_p is the total length of slide wire S at system pressure, calculated from:

$$L^c_p = R_{o,t} \left(\frac{L_o}{R_{o,t}} \right) \left(1.0 - \frac{1.0}{3.0} \left(A_{ka} \cdot P - B_{ka} \cdot P^2 \right) \right) \qquad \text{(A-4)}$$

where; P is the pressure in psi, L_o is the length of slide wire S at atmospheric pressure, and A_{ka} and B_{ka} are best fit constants at 30.0°C, as determined by Bridgman (6), for the relative compression of Karma. The values of A_{ka} and B_{ka} are

3.87×10^{-8}/psi, and

0.741×10^{-14}/psi^2 respectively.

The temperature effect on A_{ka} and B_{ka} was assumed to be linear over the experimental range, since the only other value reported was at 75.0°C. The variation of A_{ka} with temperature was 0.933×10^{-11}/psi °C and for B_{ka} it was 0.0/psi^2°C.

The true length of the carrier over the slide wire section is related to the measured length at pressure P by:

$$L_{a,P} = L_{br,P}\left(1.0 - \frac{1.0}{3.0}\left(A_{br} \cdot P - B_{br} \cdot P^2\right)\right) \qquad \text{(A-5)}$$

where; A_{br} and B_{br} are the best fit constants, as determined by Bridgman (7), for the relative compression of Brass.

The values of A_{br} and B_{br} are 6.47×10^{-8}/psi, and 3.17×10^{-14}/psi^2 respectively at 30.0°C. The temperature effect on A_{br} and B_{br} was assumed to be linear over the range used. The variation of A_{br} was 0.16×10^{-10}/psi °C and on B_{br} it was -0.688×10^{-16}/psi^2 °C.

The true length of the slide wire is related to the measured length at pressure P by:

$$L_{a,P} = L_{ka,P}\left(1.0 - \frac{1.0}{3.0}\left(A_{ka} \cdot P + B_{ka} \cdot P^2\right)\right). \qquad \text{(A-6)}$$

The correction due to the difference in compression is then:

$$L_{br,P} - L_{ka,P} = R_{a,P}\left(\frac{L_P^c}{R_{o,t}}\right)\left(\frac{1.0}{1.0 - \frac{1.0}{3.0}\left(A_{br}\cdot P - B_{br}\cdot P^2\right)}\right.$$

$$\left. - \frac{1.0}{1.0 - \frac{1.0}{3.0}\left(A_{ka}\cdot P - B_{ka}\cdot P^2\right)}\right) \qquad \text{(A-7)}$$

This correction is additive since the greater compression of the Brass carrier caused the true compression of the same to be reduced by the difference in compression of the Brass carrier and the Karma Slide wire.

b. Temperature Corrections

There are two temperature corrections. The first is the change in total slide wire resistance with temperature. The second is the difference in the coefficient of thermal expansion for the Brass carrier and the Karma slide wire. These corrections were made as follows:

(i) Total Slide Wire Temperature Effect

The change in unit length, Ω, of the Karma slide wire due to the temperature change between isotherms was accounted for by using measured values of $R_{o,t}$. $R_{o,t}$ is the total slide wire resistance at the operating temperature.

(ii) Thermal Expansion Difference

The linear coefficient of thermal expansion for the Brass is $\alpha_{br} = 19.1 \times 10^{-6}/^{o}C$ (26) and for the Karma $\alpha_{ka} = 13.3 \times 10^{-6}/^{o}C$ (12). This correction was made by measuring a new zero point slide wire resistance $R_{a,o}$, between the bellows and fixed contact, on each isotherm.

Thus equation A-2 may be written as:

$$\Delta L_B = \Omega \cdot (R_{a,p} - R_{a,o}) + (L_{br,p} - L_{ka,p}) . \qquad (A-8)$$

2. Calculation of $A_{p,t}$

To determine the bellows cross sectional area $A_{p,t}$ at the operating temperature and pressure two corrections must be made. The first is the thermal expansion of the bellows. The second is the compression of the bellows material under hydrostatic load.

a. Temperature Correction

The temperature correction on the bellows cross sectional area is due to the temperature difference between the temperature at which the cross sectional area was determined (see Appendix C) and the temperature at which the experimental measurements were made. This correction can be written as:

$$A_{o,t} = A_{o,o}\,(1.0 + 2.0\,\alpha_{br}\cdot(t - 25.0))\,. \qquad \text{(A-9)}$$

This correction will increase the cross sectional area as temperature increases.

b. Pressure Correction

As the pressure increased the cross sectional area of the bellows changes. This correction can be written as:

$$A_{P,o} = A_{o,o}\,(1.0 - \tfrac{2.0}{3.0}\,A_{br}\cdot P - B_{br}\cdot P^2))\,. \qquad \text{(A-10)}$$

This will reduce the cross sectional area as pressure increases.

Thus the cross sectional area at the conditions of the measurement can be written as:

$$A_{P,t} = A_{o,o}\,(1.0 + 2.0\,\alpha_{br}\,(t - 25.0))\,(1.0 - \tfrac{2.0}{3.0}\,(A_{br}\cdot P - B_{br}\cdot P^2))\,. \qquad \text{(A-11)}$$

3. Final Form Equation A-1

The final form of equation A-1 is obtained by substituting equations A-8, and A-11 into equation A-1.

$$\frac{\Delta V}{V_o} = \left(Q \left(R_{o,p} - R_{a,o} \right) + \left(L_{br,p} - L_{ka,p} \right) \right.$$

$$\left. - \left(L_{ka,t} - L_{br,t} \right) \right) A_{o,o} \left(1.0 + 2.0 \alpha_{br} \left(t - 25.0 \right) \right)$$

$$\left(1.0 - \frac{2.0}{3.0} \left(A_{br} \cdot P - B_{br} \cdot P^2 \right) \right) \rho_{o,t} / W \; .$$

(A-12)

Equation A-12 was used to obtain the compression measurements (56).

APPENDIX B

ERROR ANALYSIS

The error analysis technique used was that of the National Bureau of Standards type as detailed by Mickley (38).

1. p-v-T Measurements

An error analysis was performed on equation A-1 to determine the absolute accuracy of the measurements of $\frac{\Delta V}{V_o}$.

$$\delta\left(\frac{\Delta V}{V_o}\right) = \frac{\Delta L_B \cdot A_{P,t} \cdot \rho_{o,t}}{W} \left[\frac{\delta \Delta L_B}{\Delta L_B} + \frac{\delta A_{P,t}}{A_{P,t}} + \frac{\delta \rho_{o,t}}{\rho_{o,t}} + \frac{\delta W}{W} \right] \qquad \text{(B-1)}$$

where: ΔL_B is the change in length of the bellows and $\delta \Delta L_B$ is the experimental uncertainty in this measured quantity, $A_{p,t}$ is the cross sectional area of the bellows at temperature t and pressure P and $\delta A_{p,t}$ is the experimental uncertainty in this quantity, $\rho_{o,t}$ is the fiducial point density and $\delta \rho_{o,t}$ is the experimental uncertainty in this measured quantity, W is the weight of the liquid sample which is undergoing compression and δw is the experimental uncertainty in this measured quantity.

Each term in the brackets on the right hand side of equation B-1 will be considered below.

a. Liquid Sample Weight

The absolute uncertainty, δw, can be estimated from the balance. The accuracy of the analytical balance was ± 0.00005 gms. The average hydrocarbon sample weighed approximately 2.25 gms. Thus $\delta W/W$ is estimated to be 2.2×10^{-5}.

b. Fiducial Point Density

The term $\delta\rho_{o,t} / \rho_{o,t}$ is due to the uncertainty of the fiducial point density. The error, $\delta \rho_{o,t}$, in the density determinations of Sims (58), Harrison (27), and Lin (33) is ± 0.00005 gms/cc. The average sample density was approximately 0.70 gms/cc and $\delta\rho_{o,t}/ \rho_{o,t}$ was assigned the value 7.1×10^{-5}.

c. Change in Bellows Length

The term $\delta\Delta L_B / \Delta L_B$ is due to the uncertainty in the measured change in bellows length, from A-8:

$$\delta\Delta L_B = \delta (\Omega (R_{a,P} - R_{a,0}) + (L_{br,P} - L_{ka,P})). \quad \text{(B-2)}$$

The first term on the right side of B-2:

$$\delta(\Omega(R_{a,p}-R_{a,o})) = (R_{a,p}-R_{a,o})\delta\Omega + \Omega(\delta R_{a,p}+\delta R_{a,o}) \qquad \text{(B-3)}$$

The value of Ω was experimentally determined to be 3.8780 $\pm$ 0.000024 cm/ohm. This is detailed in a later section of this Appendix. For a compression of .36 cm, the value of $R_{a,p} - R_{a,o}$ is approximately 0.09 ohm. The uncertainty in resistance measurements was $\pm$ 0.00001 ohms. Substituting these values into B-3 we obtain

$$\delta(\Omega(R_{a,p}-R_{a,o})) = 0.09\,(0.000024) + (4.0)(0.00001)$$

or,

$$\delta(\Omega(R_{a,p}-R_{a,o})) = \pm\ 0.00004 \text{ cm}.$$

The second term on the right hand side of B-2 is evaluated from A-7 and A-4

$$\delta(L_{br,p}-L_{ka,p}) = \delta\left(R_{a,p}\left(\frac{L_o}{R_{o,t}}\right)\left(1.0-\frac{1.0}{3.0}\left(A_{ka}P-B_{ka}\cdot P^2\right)\right)\left(\frac{1.0}{\left(1.0-\frac{1.0}{3.0}\left(A_{br}\cdot P-B_{br}\cdot P^2\right)\right)}-\frac{1.0}{\left(1.0-\frac{1.0}{3.0}\left(A_{ka}\cdot P-B_{ka}P^2\right)\right)}\right)\right) \qquad \text{(B-4)}$$

For ease in discussion, certain terms will be assigned names as follows:

$$C_{ka} = 1.0 - \frac{1.0}{3.0}\left(A_{ka}\cdot P - B_{ka}\cdot P^2\right)$$

$$C_{br} = 1.0 - \frac{1.0}{3.0}\left(A_{br}\cdot P - B_{br}\cdot P^2\right)$$

Recalling that $\Omega = (L_o/R_{o,t})$, then B-4 can be rewritten as:

$$\delta\left(L_{br,p} - L_{ka,p}\right) = \delta\left(\left(R_{a,p}\cdot\Omega\cdot C_{ka}\right)\left(\frac{1.0}{C_{br}} - \frac{1.0}{C_{ka}}\right)\right),$$

or

$$\delta\left(L_{br,p} - L_{ka,p}\right) = R_{a,p}\cdot\Omega\cdot C_{ka}\left(\frac{\delta R_{a,p}}{R_{a,p}} + \frac{\delta\Omega}{\Omega} + \frac{\delta C_{ka}}{C_{ka}} + \frac{\delta C_{br}}{C_{br}}\right) + R_{a,p}\cdot\Omega\left(\frac{\delta R_{a,p}}{R_{a,p}} + \frac{\delta\Omega}{\Omega}\right). \quad \text{(B-5)}$$

When $(R_{a,p} - R_{a,o}) = 0.09$ ohm the value of $R_{a,p}$ is approximately 0.36 ohm. Since $\delta R_{a,p} = \pm 0.00001$ ohm, $\delta R_{a,p}/R_{a,p} = \pm 0.00003$. With $\delta\Omega/\Omega = \pm 0.000006$, and the uncertainty in C_{ka} is,

$$\delta C_{ka} = \frac{1.0}{3.0}\left(\delta A_{ka}\cdot P + \delta B_{ka}\cdot P^2\right). \quad \text{(B-6)}$$

Bridgman (6) determined δA_{ka} to be $\pm$ 0.02 x 10^{-8}/psi and δB_{ka} to be $\pm$ 0.01 x 10^{-14}/psi^2. When $(R_{a,p} - R_{a,o})$ = 0.09 ohm the pressure is approximately 95,000 psi. Substituting into B-6 we obtain:

$$\delta C_{ka} = \frac{1.0}{3.0} \left(0.02 \times 10^{-8} \cdot 0.95 \times 10^{+5} + 0.01 \times 10^{-14} \cdot (0.95 \times 10^{5})^2 \right),$$

or

$$\delta C_{ka} = \pm 0.0000063$$

and C_{ka} has a value of 0.998779.

Similarly using the values of δA_{br} = 0.04 x 10^{-8}/psi and δB_{br} = 0.02 x 10^{-4}/psi^2 as reported by Bridgman (7) we obtain $\delta C_{br} = \pm$ 0.000011 and C_{br} has a value of 0.998005. Thus substituting into B-5 we obtain:

$$\delta (L_{br,p} - L_{ka,p}) = \frac{0.36 \cdot 4.0 \cdot 0.998779}{0.99005} \left(0.00003 + 0.000006 + 0.0000063 + 0.000011 \right) + 0.36 \cdot 4.0 \cdot (0.00003 + .000011)$$

or

$$\delta (L_{br,p} - L_{ka,p}) = \pm 0.00012 \text{ cm.}$$

With all the terms in equation B-2 known it is possible to evaluate $\delta \Delta L_g$:

$\delta \Delta L_B = 0.00004 + .00012$ cm

or

$\delta \Delta L_B = 0.00016$ cm.

d. Cross Sectional Area

The term $A_{p,t}/A_{p,t}$ is due to the uncertainty in the bellows cross sectional area. $\delta A_{p,t}$ is evaluated from equation A-11:

$$\delta A_{p,t} = \delta \left(A_{o,o} \left(1.0 + 2.0 \alpha_{br} (t - 25.0) \right) \left(1.0 - \frac{2.0}{3.0} \left(A_{br} \cdot P - B_{br} \cdot P^2 \right) \right) \right). \quad \text{(B-7)}$$

The $\delta (A_{o,o})$ was found to be ± 0.0012 as described in a later section of this Appendix. The value of $A_{o,o}$ was experimentally determined to be 1.9815 cm^2. The uncertainty in $(1.0 - \frac{2.0}{3.0} (A_{br} P - B_{br} \cdot P^2))$ is twice that of δC_{ka} as determined from equation B-6. Thus $2 \delta C_{ka} = \pm 0.0000126$ and the term $(1.0 - \frac{2.0}{3.0} (A_{br} P - B_{br} \cdot P^2))$, in B-7, has a value of 0.99601 when the pressure is 95,000 psi.

The error in $(1.0 + 2.0 \cdot \alpha_{br} \cdot (t - 25.0))$ is due to the uncertainty in α_{br} which is assumed to be one in the last significant digit reported (26), or $\pm 0.1 \times 10^{-6}/^{o}C$ for $\alpha_{br} = 19.1 \times 10^{-6}/^{o}C$. Then the error in $(1.0 + 2.0 \cdot \alpha_{br} \cdot (t - 25.0))$, at 85.0°C, is $\pm 0.2 \times$

$10^{-6}/^{o}C$ and it has a value of .99760.

Thus substituting into B-7:

$$\delta A_{p,t} = (1.9820)\cdot(0.99601)\cdot(0.99760)\cdot$$

$$\left(\frac{0.0012}{1.9820} + \frac{0.000002}{0.99601} + \frac{0.000013}{0.99760}\right),$$

or

$$\delta A_{p,t} = 0.0012 \text{ cm}^2.$$

e. Evaluation of $\delta \Delta V / V_o$

With all terms in equation B-1 known it is possible to determine $\delta \Delta V / V_o$. Substituting into equation B-1 yields:

$$\delta \frac{\Delta V}{V_o} = \frac{0.36 \cdot 1.98 \cdot 0.7}{2.25} \left[\frac{0.00016}{0.36} + \right.$$

$$\left. \frac{0.0012}{1.98} + 0.000022 + 0.00005 \right],$$

or

$$\delta \frac{\Delta V}{V_o} = 0.0002 \text{ cc/cc}.$$

It should be noted that this experimental uncertainty in $\Delta V / V_o$ is for the worst possible set of conditions, the case where the largest corrections were required and largest experimental errors occurred.

2. Slide Wire Unit Length

The apparatus for determination of Ω, the unit length of the slide wire, is discussed in Appendix C.

The equation for determinating the uncertainty is:

$$\delta(\Omega) = \frac{L}{R}\left(\frac{\delta L}{L} + \frac{\delta R}{R}\right) \qquad \text{(B-8)}$$

The length of wire was approximately 10.cm and the uncertainty in this length was $\pm$ 0.00005 cm. Thus $\delta L / L$ was found to be $\pm 5. \times 10^{-6}$. The measured resistance was approximately 2.5 ohms and the uncertainty in the resistance was $\pm$ 0.00001. ohms, or $\delta R / R$ was $4. \times 10^{-6}$. Substituting into equation B-8 we obtain:

$$\delta(\Omega) = 4.\ (6. \times 10^{-6}) \text{ cm/ohm,}$$

or

$$\delta(\Omega) = 0.000024 \text{ cm/ohm.}$$

3. Capillary Radius

Before determining $\delta A_{o,o}$ it is necessary to determine the uncertainty in the radius of the capillary tube used to calibrate the bellows. The mercury thread weight technique was used as described in Appendix C. The equation used to determine the capillary radius was:

$$w = \sqrt{\frac{w_{Hg}}{\rho_{Hg} \cdot \pi \cdot h}} \qquad \text{(B-9)}$$

where: r is the capillary tube radius; w_{Hg} is the weight of the Mercury thread; ρ_{Hg} is the density of the Mercury; and h is the height of the Mercury thread. The uncertainty in the radius, δr , is given by:

$$\delta r = \frac{\frac{1}{2}\,\delta w_{Hg}}{\rho^{1/2}\,\pi\, w_{Hg}^{1/2}\, h^{1/2}} + \frac{\frac{1}{2}\, w_{Hg}^{1/2}\,\delta\rho}{\rho_{Hg}^{3/2}\,\pi\, h^{1/2}} + \frac{\frac{1}{2}\, w_{Hg}^{1/2}\,\delta h}{\rho_{Hg}^{1/2}\,\pi\, h^{3/2}} \,. \qquad \text{(B-10)}$$

The uncertainty in the weight of the Mercury thread was taken $\pm$ 0.00005 grams for the analytical balance and nominal weight was 0.84 gms. The uncertainty in the density of the Mercury was taken as $\pm$ 0.00005 grams/cc (40) and the density as 13.6 grams/cc nominal. The uncertainty in the height of Mercury thread was taken as $\pm$ 0.00005 cm, based upon reproducibility of the cathetometer reading, and the average length of Mercury was 1.0 cm. Substituting these values into B-10 we obtain:

$$\delta r = \frac{0.00005(0.5)}{(3.14)(.7)(1.)(3.6)} + \frac{(0.5)(0.7)(0.00005)}{(50.)(3.14)(1.0)} +$$

$$\frac{(0.5)(0.00005)(0.7)}{(3.6)(3.14)(1.0)} \,, \quad \text{or}$$

$\delta r = \pm 0.000049$ cm $\simeq \pm$ 0.00005 cm.

4. Bellows Cross Sectional Area

The calibration technique used to determine the cross sectional area of the bellows is described in Appendix C. The equation used to determine the bellows cross sectional area is:

$$A_{o,o} = \left(\frac{\Delta V}{\Delta L}\right)_B = A_c \frac{\Delta L_c}{\Delta L_B} \qquad \text{(B-11)}$$

where: ΔL_c is the change in liquid level in the capillary tube; ΔL_B is the change in bellows length required to produce a liquid displacement of ΔL_c within the capillary tube; A_c is the capillary tube cross sectional area; and $A_{o,o}$ is the 25.0°C and 1 atm. value of the bellows cross sectional area. Thus the uncertainty in $A_{o,o}$ is given by:

$$\delta A_{o,o} = A_c \frac{\Delta L_c}{\Delta L_B}\left(\frac{\delta A_c}{A_c} + \frac{\delta \Delta L_c}{\Delta L_c} + \frac{\delta \Delta L_B}{\Delta L_B}\right). \qquad \text{(B-12)}$$

For the 0.2 cm I.D. capillary tube A_c is 0.032 cm^2 and the uncertainty is given by:

$$\delta A_c = \delta(\pi r^2) = 2\pi r\, \delta r. \qquad \text{(B-13)}$$

Since the uncertainty in the radius of the capillary tube was $\pm$ 0.00005 cm, $\delta A_c = 2.0 \cdot 3.14 \cdot 0.1 \cdot 0.00005$ cm^2, or $\delta A_c = \pm$ 0.000032 cm^2. For a compression of 0.25 cm, ΔL_B, on the bellows the change in liquid level in the capillary tube will be 15.5 cm, ΔL_c. Both ΔL_B and ΔL_c were measured with cathotometers and the $\delta(\Delta L_B) = \delta(\Delta L_c) = \pm$ 0.00005 cm. Thus substitution into B-12 yields the uncertainty $\delta A_{o,o}$ as:

$$\delta A_{o,o} = 0.032 \frac{15.5}{0.25} \left(\frac{0.000032}{0.032} + \frac{0.00005}{15.5} + \frac{0.00005}{0.25}\right),$$

or

$$\delta A_{o,o} = \pm 0.0012 \text{ cc}.$$

APPENDIX C

EQUIPMENT CALIBRATION

During the course of this work it was found necessary to make a total of four equipment calibrations to determine: the capillary tube radius for use in determining the bellows cross sectional area, the bellows cross sectional area, the slide wire unit length, and the manganin cell pressure coefficient.

1. Capillary Tube Radius

The capillary tube radius and its uniformity were determined so that the cross sectional area of the bellows could be determined using the capillary tube liquid displacement method. (See section on bellows calibration below.) The mercury thread weight technique was used (30) to calibrate the capillary tube.

a. Apparatus

The capillary calibration apparatus is shown in Figure 59 and a detailed section of the injection system is shown in Figure 59. The temperature bath B in Figure 58 was used as a source of constant temperature fluid and

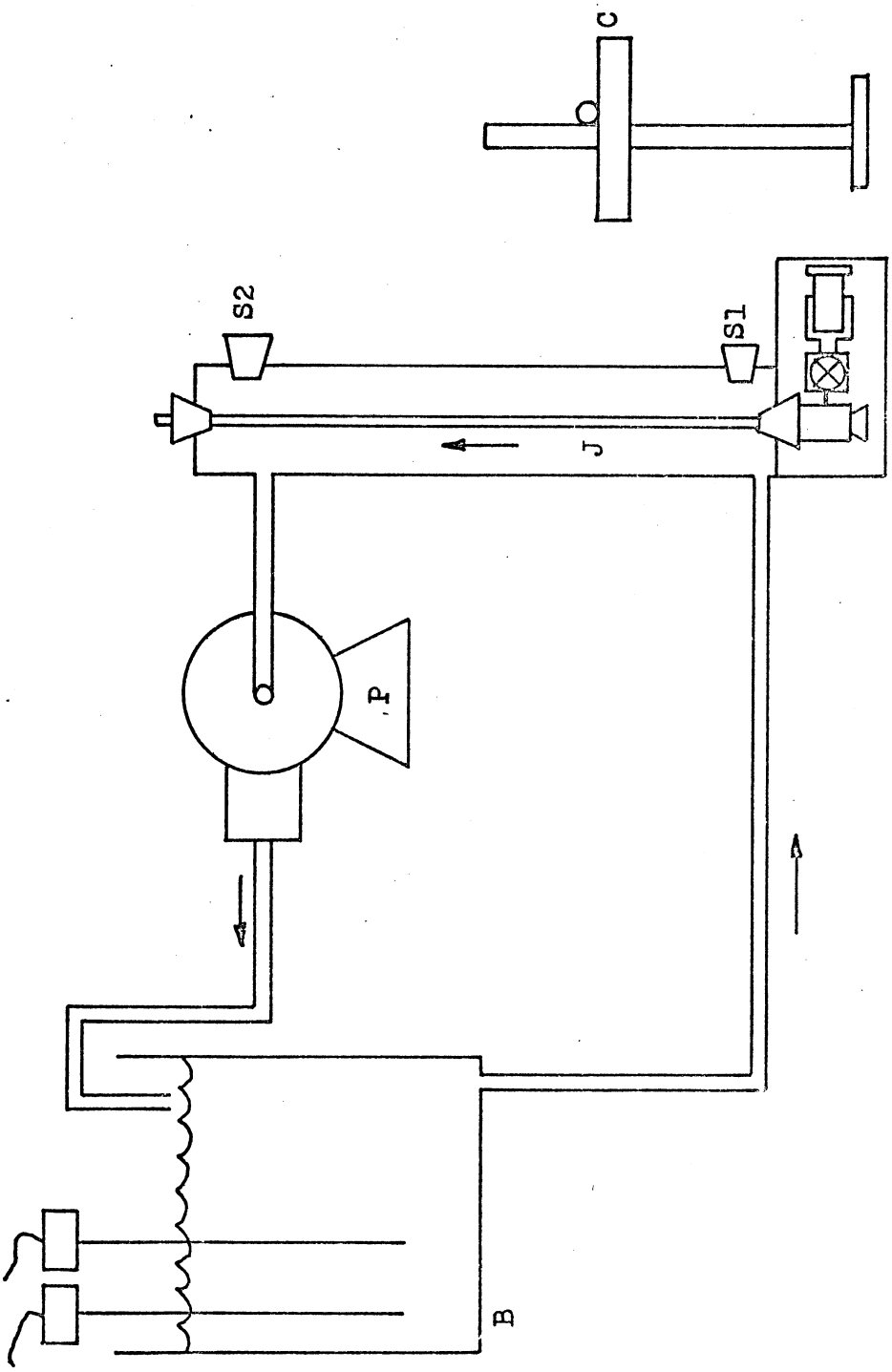

FIGURE 58. CAPILLARY CALIBRATION APPARATUS

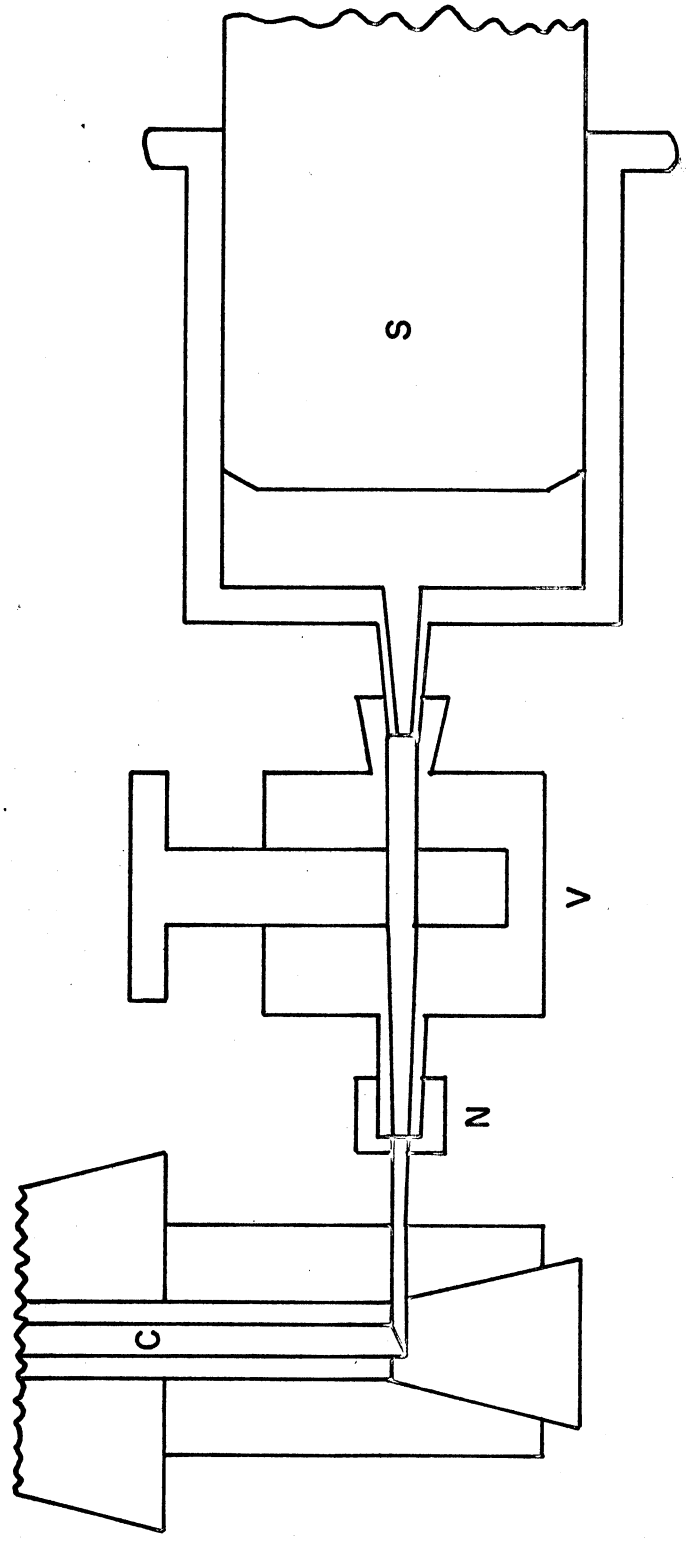

FIGURE 59. INJECTION SYSTEM DETAIL

was maintained at 25.00 ± 0.005°C during the course of the measurements. The bath fluid, distilled water, was continuously circulated in the flow loop indicated by arrows in Figure 58 by centrifugal pump P. The fluid flow rate was sufficiently high, that when a Philadelphia differential thermometer was inserted into the calibration jig J at points S1 and S2 it read 2.37 in both cases. This was also its reading when placed in bath B. Room temperature was monitored via an A.S.T.M. 90C thermometer and maintained at 25.0 ± 0.1°C during the course of measurements.

b. Procedure

Prior to calibrating a capillary tube a group of ten precision bore tubes, made of borosilicate glass, were inspected and the one with the most uniform bore was chosen for calibration. Then the capillary was cleaned in hot chromic acid, flushed with distilled water and vacuum dried.

The capillary tube was then mounted in calibration jig J in Figure 58. It was vertically aligned and it was also aligned to be parallel to the travel of cathetometer C.

To make a measurement, three threads of Mercury were introduced into the capillary tube. The central thread was the thread to be measured. The upper and lower

threads were used to protect the central thread. These threads were driven up the capillary tube by water injected into the capillary with a syringe S and valve V in Figure 50.

It was observed that the position and measurements of the central thread were not affected by time up to 24 hours as long as temperature control was maintained. Since water was used to drive the mercury measurements could be made only in the upwards direction. Once the walls of the tube were wetted with water it was impossible to obtain a reproducible reading at that point without cleaning and drying the tube.

c. Results and Method

Two different lengths of mercury threads were measured. One of one cm and the other of two cm nominal length. The two cm thread weight was 0.90526 gm and the one cm thread weight was 0.51263 gm. The density of Mercury used (40) was 13.5336348 gm/cc at 25.0°C.

The mercury thread contained in a capillary tube of uniform bore may be assumed to be right circular cylinder capped at each end by a volume element which has a volume larger than that of a paraboloid and smaller than that of a spherical segment Figure 60.

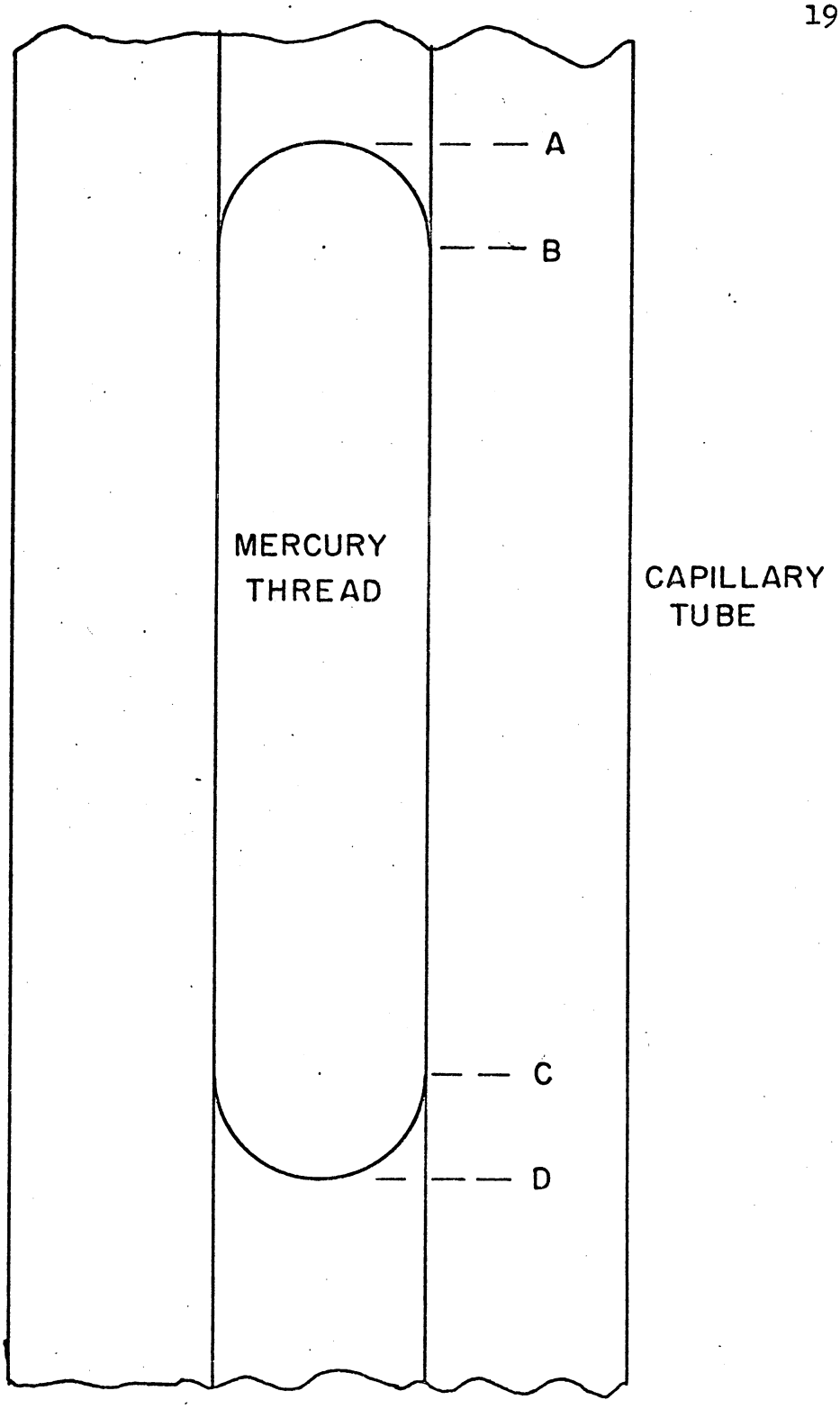

FIGURE 60. HYPOTHETICAL MERCURY THREAD

With B-C being the height of the right circular cylinder with A-B and C-D the height of the caps with R the radius of the capillary tube

Thus:

$$V_{Hemi} = \pi R^2 (B-C) + \tfrac{1}{6}\pi (A-B)((A-B)^2 + 3R^2 + \tfrac{1}{6}\pi (C-D)((C-D)^2 + 3R^2) \qquad (C-1)$$

$$V_{para.} = \pi R^2 (B-C) + \tfrac{1}{2}\pi R^2 (A-B) + \tfrac{1}{2}\pi R^2 (C-D) \qquad (C-2)$$

If the weight of the mercury thread is known and the density at the temperature that A,B,C,D are measured in the capillary tube the real volume of the thread can be computed. This may be used for V_{Hemi} or $V_{Para.}$ in equations C-1 or C-2 and then the only unknown is radius.

Rearranging equations C-1 and C-2 to solve for the radius:

$$R_{Hemi} = \left(\left(\frac{wt.}{\rho\pi} - \frac{1}{6}\left((A-B)^3 + (C-D)^3\right)\right) \Big/ \left((B-C) + \tfrac{1}{2}\left((A-B) + (C-D)\right)\right)\right)^{\frac{1}{2}} \qquad (C-3)$$

$$R_{para.} = \left(\frac{wt.}{\rho\pi} \Big/ \left((B-C) + \tfrac{1}{2}\left((A-B) + (C-D)\right)\right)\right)^{\frac{1}{2}}. \qquad (C-4)$$

By measuring two threads of mercury of different lengths the values of R_{Hemi} and $R_{Para.}$ calculated from equations C-3 and C-4 should be different for the two threads if the cap volume is not exactly described by a paraboloid or spherical segment. This was done for a thread 1 cm. in length and one 2 cm. in length. It was noted that the radius calculated with equations C-3 increases as the thread length increases. (Thus the postulated cap volumes are too small.) The value of the radius calculated with equation C-4 also decreases with thread length. Thus a correction of the cap volumes must be made. To do this equations C-3 and C-4 were modified;

$$R_{Hemi} = \left(\left(\frac{wt}{\rho\pi} - \frac{1}{6}\left((A-B)^3 + (C-D)^3\right)\right) / \left((B-C) + X\cdot\left((A-B) + (C-D)\right)\right)\right)^{1/2} \qquad (C\text{-}5)$$

$$R_{Para.} = \left(\frac{wt}{\rho\pi} / \left((B-C) + Y\left((A-B) + (C-D)\right)\right)\right)^{\frac{1}{2}} \qquad (C\text{-}6)$$

Then the values of X and Y were found such that the value of the radius for the 1 cm. and 2 cm. thread were the same. It was noted that the average value of R_{Hemi} varies from that of $R_{Para.}$ by .000002 cm. The average of these two will be used. Then R = .100320 ± .000035 cm. and the capillary cross sectional area is 0.0316167 cm^2.

From these measurements, the uniformity of the capillary tube bore was found to be better than that required by error analysis (± 0.00005 cm.) so no correction with position is required.

This calibrated precision bore Borosilicate glass capillary tube made it possible to determine the cross sectional area of the sylphon bellows.

2. Bellows Cross Sectional Area

This section deals with the determination of the bellows cross sectional area via the liquid displacement method.

a. Apparatus

The bellows calibration apparatus is shown in Figure 61 and a detailed section of the bellows and micrometer section are shown in Figure 62. The apparatus used in the bellows calibration was essentially the same as that used in the capillary calibration with the exception that the fluid displaced into the capillary tube was held in the sylphon bellows and the bellows was driven by a precision micrometer. One additional cathetometer was required to determine bellows displacement.

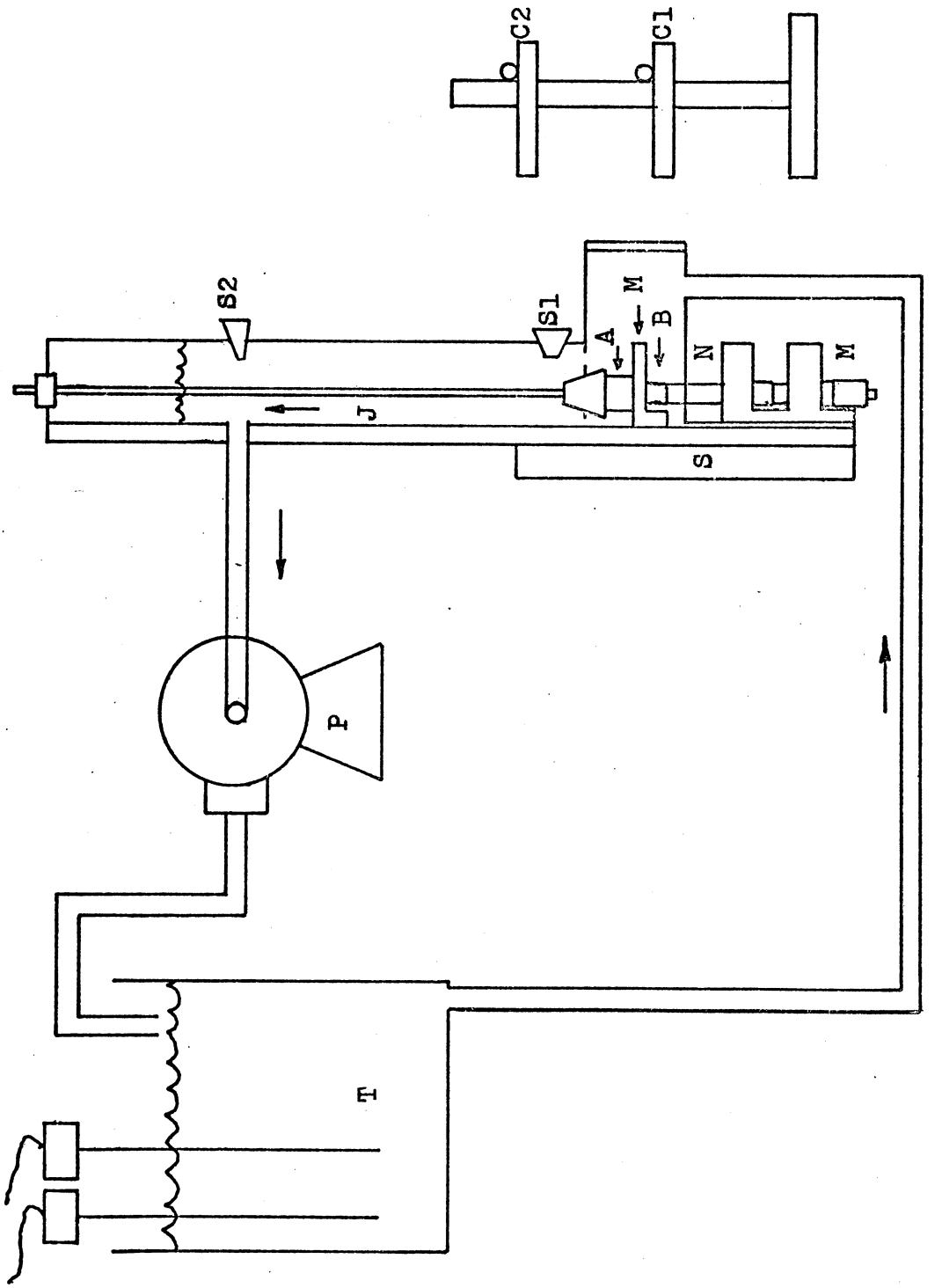

FIGURE 61. BELLOWS CALIBRATION APPARATUS

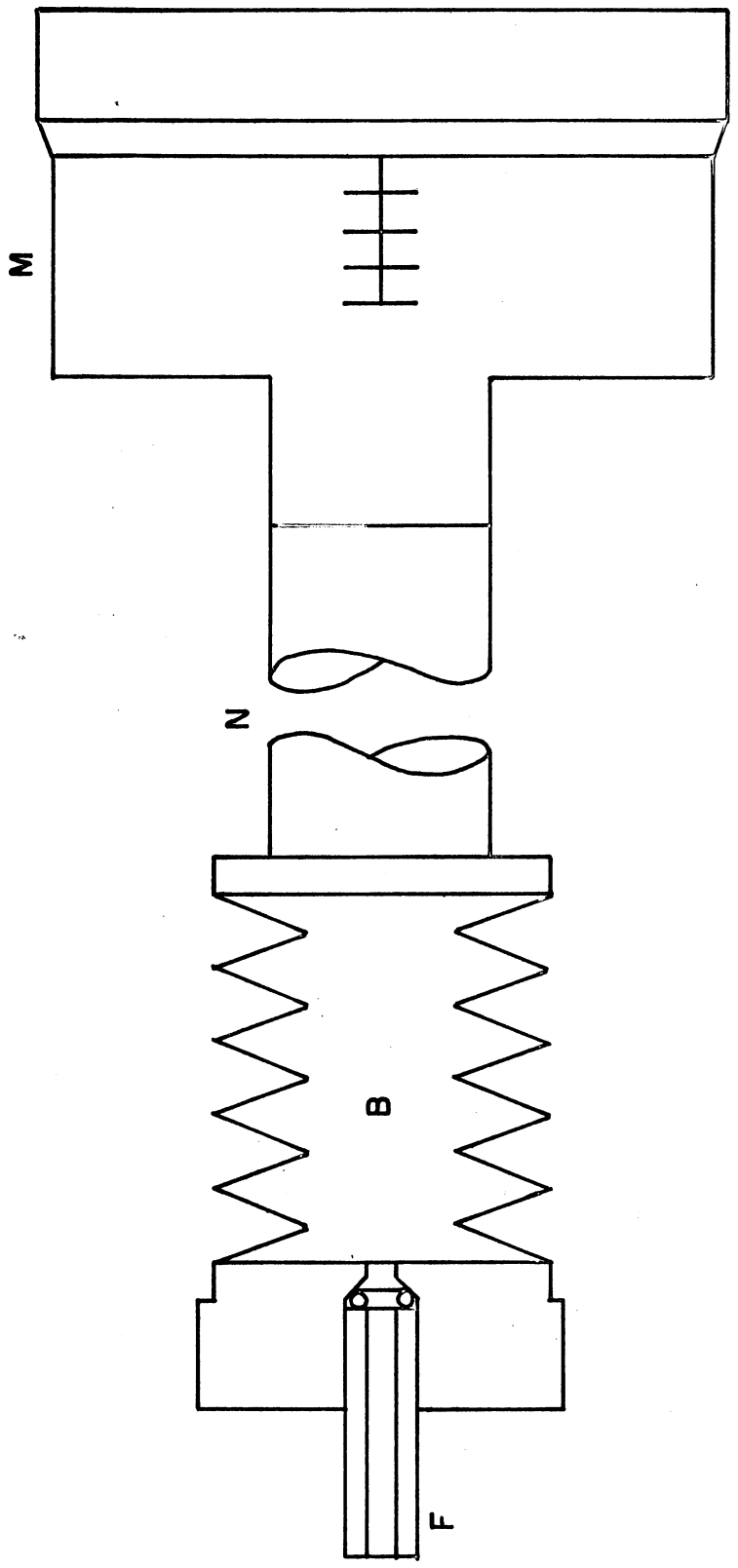

FIGURE 62. BELLOWS AND MICROMETER SECTION

b. Procedure

The temperature bath T in Figure 61 was used as a source of constant temperature fluid. It was maintained at 25.00 ± 0.005°C during the course of the measurements. The bath fluid, distilled water, was continuously circulated in the flow loop, indicated by arrows in Figure 61, by centrifugal pump P. As before, the temperature in calibration jig J was monitored at S1 and S2 and found to read 2.37 on the Philadelphia differential thermometer. Room temperature was maintained at 25.0 ± 0.1°C during the course of measurements.

Prior to filling of calibration jig J and bath T with fluid it was necessary to fill the bellows B with water, to mount and to align it in jig J, Figure 61. The bellows was filled by using the sample filling apparatus described in Appendix E. Alignment consisted of adjusting the flat face of the bellows and the face of driver N, Figure 62, until they were parallel using the two cathetometers. Then as in the capillary tube calibration above, the capillary tube and cathetometer travel were aligned to each other. The flow system was then filled.

Micrometer M, Figure 61 and 62, was advanced, driving the column of distilled water up the capillary tube. Cathetometers C1 and C2 were used to measure bellows and meniscus displacements respectively.

c. Results and Method

The bellows cross sectional area can be calculated from equation B-11:

$$A_{o,o} = A_c \frac{\Delta L_c}{\Delta L_B} . \qquad (C-7)$$

Where $A_{o,o}$ is the bellows cross sectional area at 25.00°C and one atmosphere, A_c is the cross sectional area of the capillary tube determined above, ΔL_c is the water meniscus displacement within the capillary tube caused by the bellows displacement ΔL_B. The average value for all measurements is 1.9815 $\pm$0.0011 cm^2. The maximum deviation in $A_{o,o}$ is slightly less than that required by the error analysis in Appendix B.

3. Slide Wire Unit Length

The slide wire unit length was determined by measuring the resistance over an accurately known distance.

a. Apparatus

The slide wire calibration apparatus is shown in Figure 63. The lower assembly is used to hold and position the wire for which the resistivity is being determined.

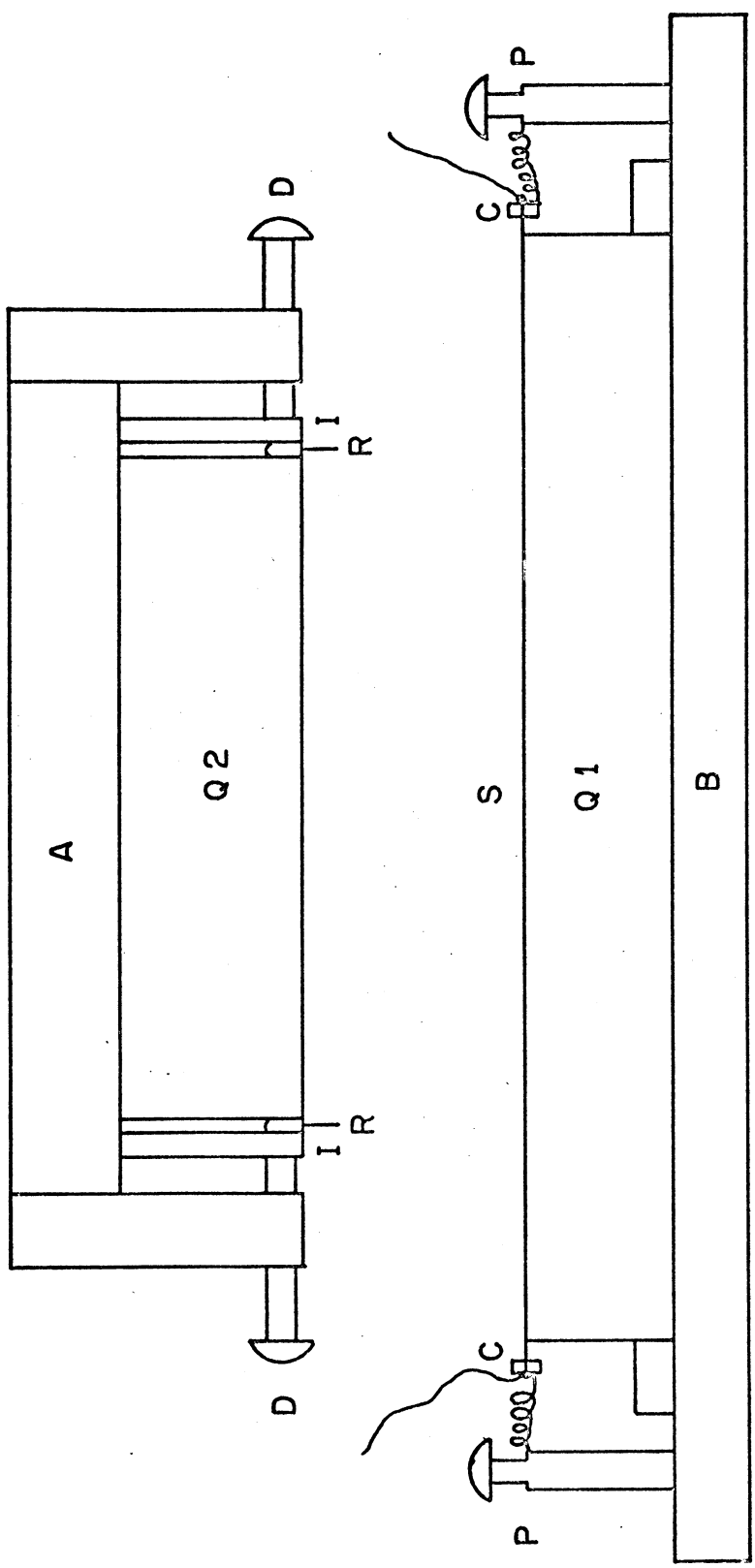

FIGURE 63. SLIDE WIRE CALIBRATION APPARATUS

The upper assembly is a spacer for the knife edge contacts R.

b. Procedure

The upper section in Figure 63 is lowered onto the lower section so that the knife edges R contact the slide wire S. The resistance between the knife edges is measured using the Mueller G-2 bridge.

The lower section was mounted vertically in front of the cathetometer and aligned to be paralled to the cathetometer travel as in the case of the capillary tube calibration. The distance between the scratches the knife edges make on the wire was measured.

c. Results and Method

With the resistance for a given length of slide wire, and that length known, the length per resistance is determined. Thus the unit length, Ω, is 3.8780 $\pm$ 0.00002 cm/ohm. Three different sections of wire were measured to obtain Ω. The manufacture, Driver-Harris (12), claims a linearity of $\pm$ 0.008% for their Karma wire.

4. Manganin Cell Pressure Coefficient

The manganin cell calibration against the 100,000 psi Aminco dead weight tester is described below.

a. Apparatus

The general apparatus is shown in Figure 64. The manganin cell was maintained at 25.00 ± 0.01°C during the course of the calibration and subsequent p-v-T measurements. Room temperature was maintained at 19.5± 0.1°C during calibration. This was done to minimize the temperature correction for the dead weight tester piston area.

b. Procedure

The zero point resistance was determined for the manganin cell. The time during which the dead weight gauge piston was floating varied from 2 minutes at 100,000 psi to over 60 minutes at 10,000 psi. Only the center of the piston floating time was used in the calibration for making resistance readings. Readings were taken every 5000 psi between 10,000 psi and 100,000 psi.

c. Results and Method

The pressure was calculated using the piston gauge pressure equation given in N.B.S. Monograph 65 (41).

$$P = \frac{M_A \left(\frac{g_L}{g_S}\right)\left(1.0 - \frac{\rho_A}{\rho_w}\right)}{A(1.0 - c\,\Delta t)(1.0+bP)} \qquad (C\text{-}7)$$

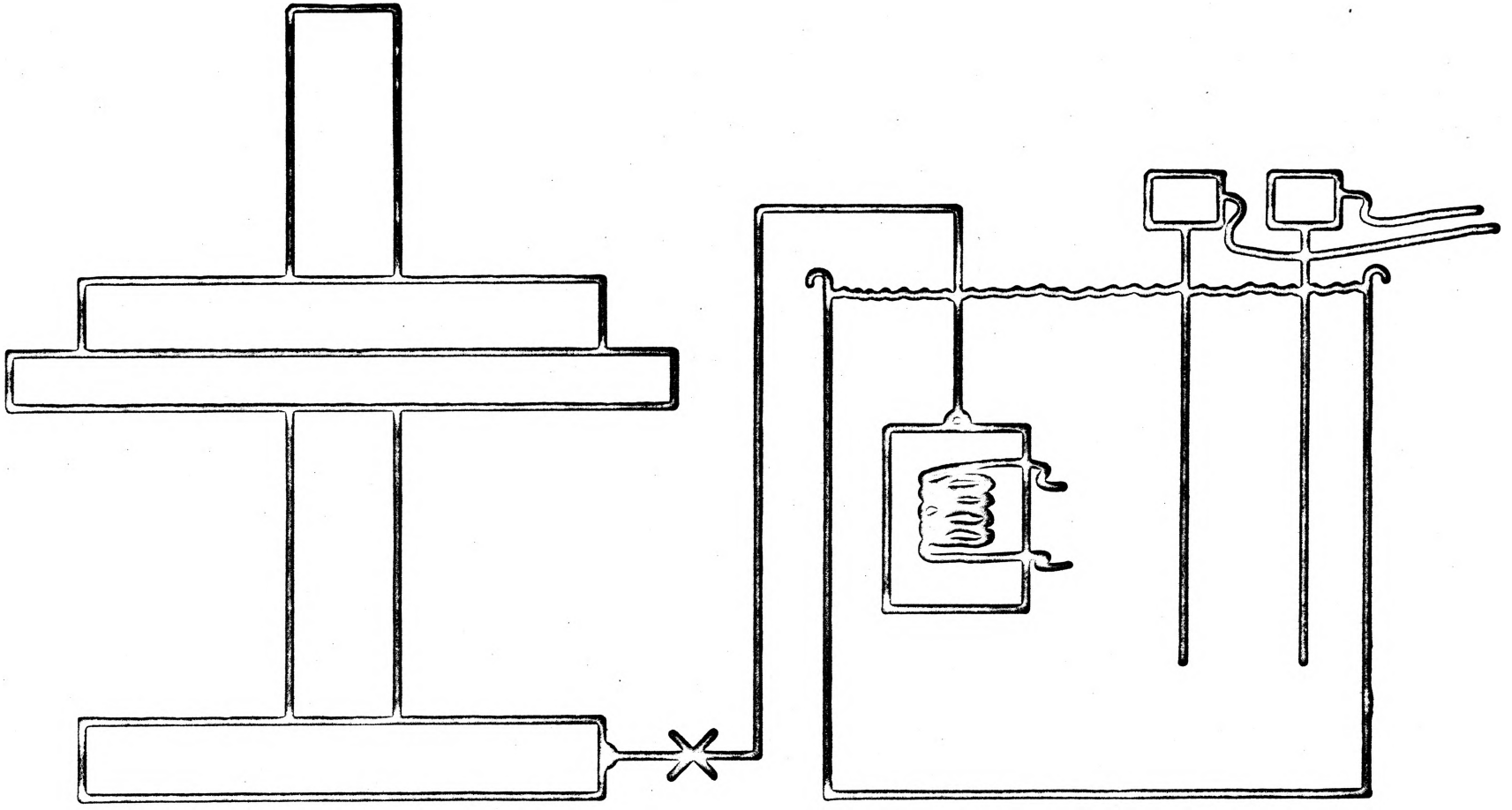

FIGURE 64. MANGANIN CELL CALIBRATION APPARATUS

Where P is the system pressure, M_A is the mass of the weights, g_L is the local gravity, g_S is the gravity at the point the weights were calibrated, ρ_A is the density of air at measurement conditions, ρ_w is the density of the weights, A is the cross sectional area of the piston as determined at 20.0°C and atmospheric pressure, c is the coefficient of thermal expansion of the piston, and b represents the fractional change in area as a result of elastic distortion.

The average cell factor for the manganin coil was found to be 58263. psi/ohm change.

APPENDIX D

COMPUTER PROGRAMS

The computer programs used are discussed in this appendix. The programs are: the initial data reduction program INDRN; the Tait equation program for J and L called TAITMN; the fitting program to determine characteristic volumes and pressures for the Flory or the Prausnitz liquid model called BMDX 85; the fitting program to determine characteristic temperatures for the Flory or the Prausnitz liquid model called STEPIT; and the fitting program for the Scaled Particle liquid model called SCLPRT.

1. Program INDRN

a. Use

This program converts raw resistance versus pressure readings into compression versus pressure data via equation A-12. It also punches out a data set of relative volume versus pressure.

2. Program TAITMN

a. Use

To determine the Tait coefficients J and L for a given data set.

b. Method

A least-squares regression analysis was written using the Tait equation and the relative volume:

$$\Psi = \sum_{i=1}^{N} \left(V_i - \left(V_o - J \ln \left(\frac{P_i + L}{P_o + L} \right) \right) \right)^2 . \qquad \text{(D-1)}$$

In D-1 V_1 is the experimental relative volume at pressure P_1 and V_o is the initial volume at the initial pressure P_o. The partial derivatives with respect to J and L of D-1 were taken, set equal to zero, and J was eliminated from the set of equations thus leaving one equation in one unknown. This equation is solved via the Newton-Raphson method of root finding. The program is double precision and it is in Fortran IV.

3. Program BMDX 85

a. Acknowledgement

The MAIN program and two subroutines MINIZ and STEP were obtained from the Health Sciences Computing Facility at the University of California at Los Angeles. This program is part of the Biomedical Package available from the Health Sciences Computing Facility.

b. Use

To determine characteristic volumes and pressures for either the Prausnitz or Flory partition function via regression analysis on the isothermal compressibility.

c. Method

A stepwise Gauss-Newton (28) iteration procedure is used. All parameters, in this case character volumes and pressures, are adjusted at each step. The program is double precision and written in Fortran IV.

4. Program STEPIT

a. Acknowledgement

The subroutine STEPIT was obtained from the Quantum Chemistry Program Exchange at Indiana University, Bloomington, Indiana. The programmer and copyrighter is Dr. J. P. Chandler of the Physics Department at Indiana.

b. Use

To determine characteristic temperatures for either the Flory or Prausnitz partition function via regression analysis on the molar volume of the liquid.

c. Method

The method is one of direct search until the root has been bracketed, then parabolic interpolation is used. The program is double precision and in Fortran IV.

5. Program SCLPRT

a. Use

To determine the scaled particle theory parameter A via regression analysis on the experimental isothermal compressibility.

b. Method

The method is one of direct search until the root has been bracketed, then parabolic interpolation is used. The program is double precision and in Fortran IV.

APPENDIX E

DETAILED APPARATUS AND SPECIFICATIONS

This appendix deals with the detailed description of all of the equipment used. It includes working arrangements and equipment specifications.

Figure 65 presents a schematic diagram of the apparatus used during the P-V-T measurements.

1. P-V-T Cell

Detailed views of the P-V-T cell, P-V-T C, in Figure 65 are shown in Figures 66 and 67. A detailed listing of the balloons in Figures 66 and 67 is given in Table XIV. The P-V-T cell design is that of Harwood Engineering, design number E1619.

a. Specifications

Cell Diameter: 6"

Cell Body Length: 10"

Temperature Range: Ambient to 300°F

Pressure Range: 0 to 200,000 PSIG

Pressure Fittings: Harwood 12H

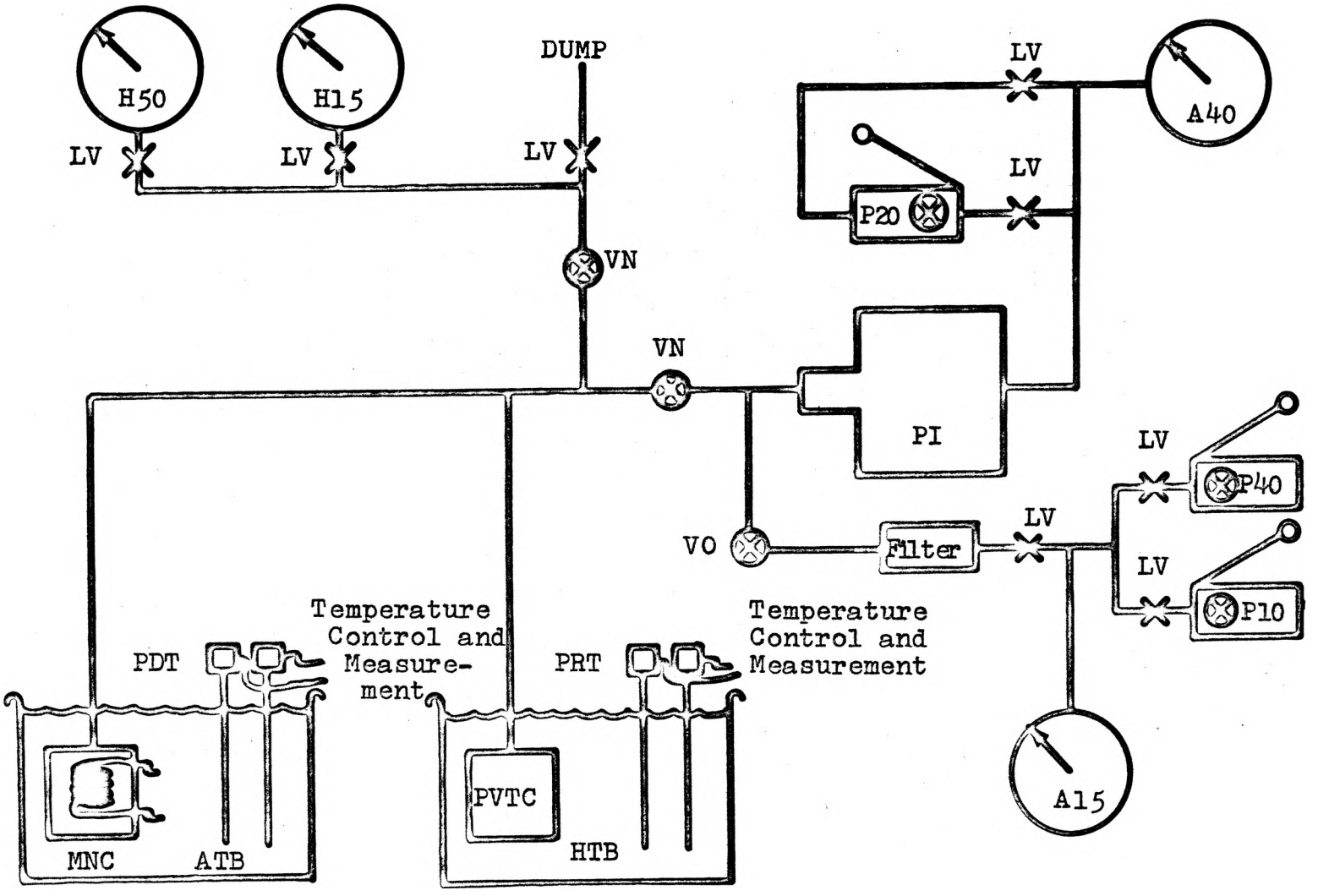

FIGURE 65. EXPERIMENTAL APPARATUS

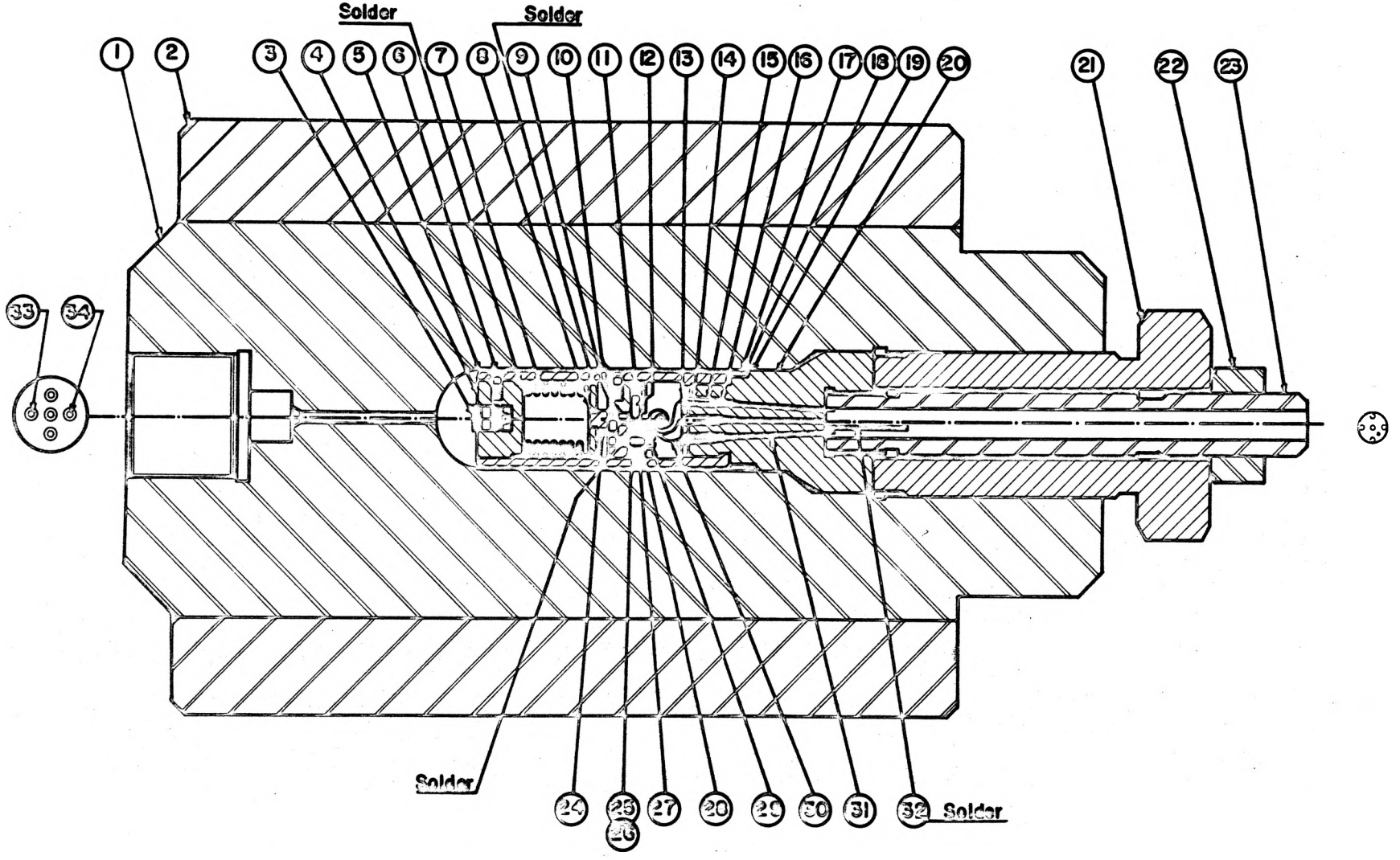

FIGURE 66. PVT CELL (Courtesy of Harwood Engineering Company)

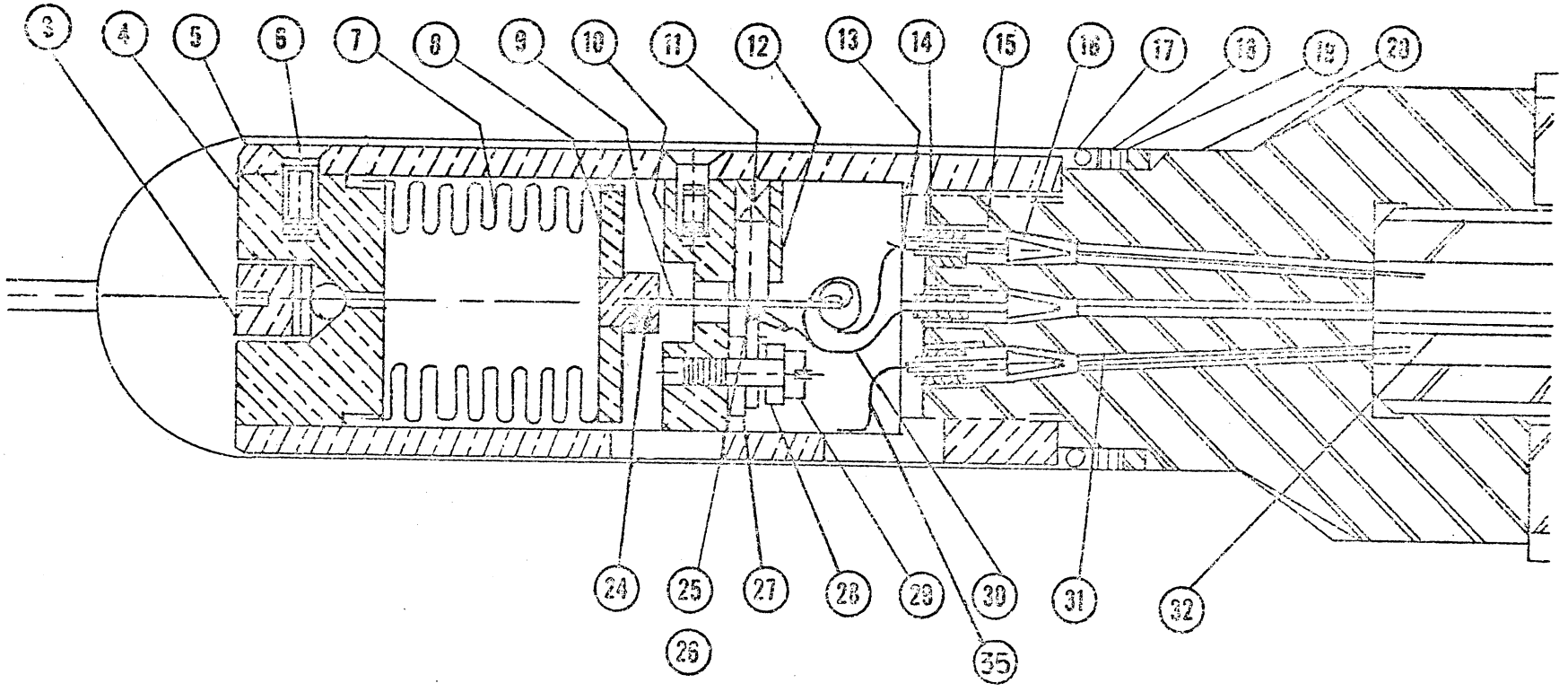

FIGURE 67. PVT CELL DETAIL (Courtesy of Harwood Engineering Company)

TABLE XIV

LISTING OF BALLOONS

1 - Vessel
2 - Sleeve
3 - Cap screw
4 - Front bellows end plate
5 - Retainer
6 - Set screws
7 - Syphon bellows
8 - Rear bellows end plate
9 - Karma wire
10 - Fixed connection housing
11 - Spring
12 - Teflon piston
13 - Electrical connection
14 - Teflon insulator
15 - Unsupported area seal
16 - Unsupported area seal
17 - O-ring
18 - Lead washer
19 - Steel ring
20 - Closure
21 - Drive plug
22 - Nut
23 - Closure bolt
24 - Set screw
25 - Fixed contact
26 - Fixed contact insulator
27 - Insulating spacer
28 - Insulating spacer
29 - Insulating spacer
30 - Electrical leads
31 - Electrical leads
32 - Ground
33 - Electrical lead
34 - Electrical lead

2. Hallikainen Temperature Bath

The Hallikainen temperature bath, HTB Figure 65, was used to control the temperature of the P-V-T cell.

a. Specifications

Model Number:	1128C
Serial Number:	13841
Temperature Controller:	Thermotrol 1253A
Serial Number:	13720
Resistance Thermometer:	1281D
Serial Number:	13735
Sensitivity:	0.001°C
Tank Diameter:	12"
Tank Depth:	18"
Tank Capacity:	8 1/2 gal.
Obtainable Control:	$\pm$ 0.002°C

3. Platinum Resistance Thermometer

The Leeds and Northrup platinum resistance thermometer, PRT, was used to set and monitor the temperature in the Hallikainen bath.

a. Specifications

Model Number:	8163-C
Serial Number:	1662272
Calibration Reference:	N.B.S. Test No. 180710
R_o:	25.5630 ohms absolute
α :	$0.0039266_7/^oC$
δ :	$1.49_1/^oC$
Minimum Immersion:	7"
Measurement Current:	2 ma.

4. AMINCO Bath

The American Instrument Company bath, ATB, was of the Mercury contact thermometer type. It was used to control the temperature of the Manganin cell and was always set at 25.00°C.

a. Specifications

Model Number :	R 4-1588
Tank Diameter:	20"
Tank Depth :	20"
Capacity :	20 gals.
Sensitivity :	$\pm 0.005^oC$
Obtainable Control:	$\pm 0.01^oC$

5. Philadelphia Differential Thermometer

The Philadelphia differential thermometer, PDT, was used to monitor the temperature in the Aminco bath.

a. Specifications

Serial Number : T46091

Range : 5°C

Divisions : 1/100°C

25.00°C Reading: 2.37

6. Manganin Cell

The Manganin cell, MNC, is a resistance type pressure transducer. The design was that of Harwood Engineering Co., number D1723.

a. Specifications

Pressure Range: 0 to 200,000 PSIG

Temperature Coefficient Zero Point: 25.0°C

7. High Pressure Valves

Three Harwood high pressure valves were used in the high pressure side of the system. Two were of the D-2286, VN, type and one of the D-1545, VO type. The D-2286 being a newer design with improved characteristics.

a. Specifications

Model : D2286

Pressure Range Closed: 0 to 200,000 PSIG

Pressure Range Open : 0 to 200,000 PSIG

Maximum Closing Pressure: 200,000 PSIG

Model : D-545

Pressure Range Closed: 0 to 200,000 PSIG

Pressure Range Open: 0 to 40,000 PSIG

Maximum Closing Pressure: 40,000 PSIG

8. Low Pressure Valves

All of the low pressure valves, LV, were from American Instrument Company.

a. Specifications

Model Number : 44-16106

Pressure Range: 0 to 60,000 PSIG

9. Piston Intensifier

The piston intensifier, PI, was of Harwood Engineering design number E1796.

a. Specifications

Area Ratio Low side/High side: 17:1

Maximum High Side Pressure: 200,000 PSIG

10. Heise 0-50,000 PSIG Gauge

The 0-50,000 PSIG gauge, H50, was used as the primary pressure measuring device for all runs up to 50,000 psi.

a. Specifications

Serial Number :	H43373
Pressure Range :	0-50,000 PSIG
Accuracy :	± 0.1% Full Scale
Maximum Hysteresis :	± 0.1% Full Scale
Thermal Compensation Range:	-25°F to 125°F

11. Heise 0-1500 PSIG Gauge

The 0-1500 PSIG gauge, H15, was used to obtain high accuracy pressures for the low pressure points taken.

a. Specifications

Serial Number :	C-51067R
Pressure Range :	0-1500 PSIG
Accuracy :	± 0.1% Full Scale
Maximum Hysteresis :	± 0.1% Full Scale
Thermal Compensation Range:	-25°F to 125°F

12. AMINCO 0-15,000 PSIG Gauge

The 0-15,000 psi gauge, A15, was used on the low pressure system to indicate system pressure while the intensifier was being reversed and also when the reversal process had been accomplished.

a. Specifications

Model Number: 47-18305

Accuracy : 1% Full Scale

13. AMINCO 0-40,000 PSIG Gauge

The 0-40,000 psi gauge, A40, was used on the low pressure side of the piston intensifier to indicate the pressure driving the intensifier and when it had reached the end or its stroke.

a. Specifications

Pressure Range: 0-40,000 PSIG

Model Number : 47-18340

Accuracy : 1.0% Full Scale

14. AMINCO 0-20,000 PSI Pump

The Aminco 0-20,000 psi pump, P20, was used to drive the piston intensifier forward. Its capacity was such that it required approximately six strokes per 1000 psi of system pressure increase.

a. Specifications

Model Number :	46-12155
Serial Number :	GG-0664
Displacement per stroke:	1.6 cc at 20,000 psi
Maximum Discharge Pressure:	20,000 psi

15. Blackhawk 0-10,000 PSI Pump

The Blackhawk 0-10,000 psi pump, P10, was used to reverse the piston intensifier.

a. Specifications

Model Number :	P39
Serial Number :	003J440
Displacement per stroke:	0.096 cu. in.
Maximum Discharge Pressure:	10,000 psi

16. Blackhawk 0-40,000 PSI Pump

The Blackhawk 0-40,000 psi pump, P40, was used when the reversal pressure on the piston intensifier exceeded 10,000 psi.

a. Specifications

Model Number :	P228
Serial Number :	FC3Y684
Displacement per stroke :	0.024 cu. in.
Maximum Discharge Pressure :	40,000 psi

17. Mueller G-2 Bridge

Figure 68 is a schematic diagram of the Mueller G-2 bridge used in the measurement; of slide wire total resistance, bellows to fixed contact resistance, P-V-T cell temperature via Platinum resistance thermometer, and system pressure via Manganin cell (above 50,000 psi). The four different measurements were made through use of a Leeds and Northrup Special Commutator.

a. Specifications

Range :	0 to 111.1111 ohms
Setability :	0.001 ohms
Absolute Accuracy:	$\pm$ 0.002%

18. Sartorius Balance

The Sartorius balance was used for all weight determinations.

a. Specifications

Model Number :	2603
Capacity :	150 grams
Optical Range :	1000 milligrams
Sensitivity :	0.1 milligram
Readability :	0.1 milligram
Reproducibility :	0.05 milligrams

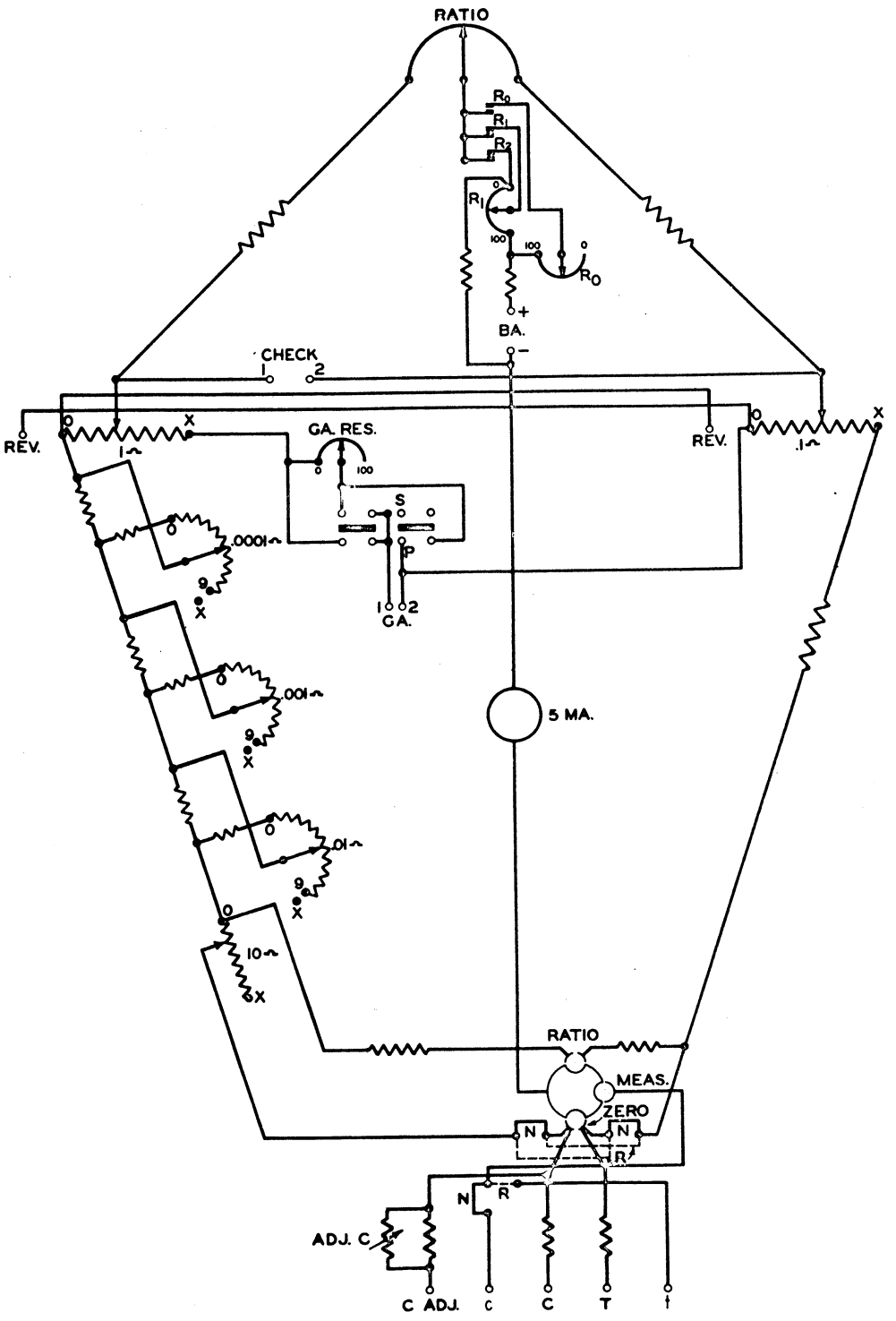

FIGURE 68. Schematic Diagram of the Bridge Circuit

19. Cathetometer 2.5 CM Travel

This unit was used for the majority of the optical distance measurements with the exception of those requiring a large travel.

a. Specifications

Model Number : M-300P

Serial Number : 3337-P

Range : 2.5 cm.

Direct Reading to : 0.0001 cm.

20. Cathetometer 10.0 CM Travel

a. Specifications

Model Number : M-303P

Serial Number : 2705-P

Range : 10.0 cm.

Direct Reading to : 0.0001 cm.

21. Sample Filling Apparatus

The sample filling apparatus is shown in Figure 69 . It was used to charge the liquid samples into the bellows. The three-way tee valve is arranged so that is is possible to evacuate the bellows, then close the system off and open the evacuated bellows to the liquid sample chamber. Thus allowing the bellows to be filled essentially in vacuum.

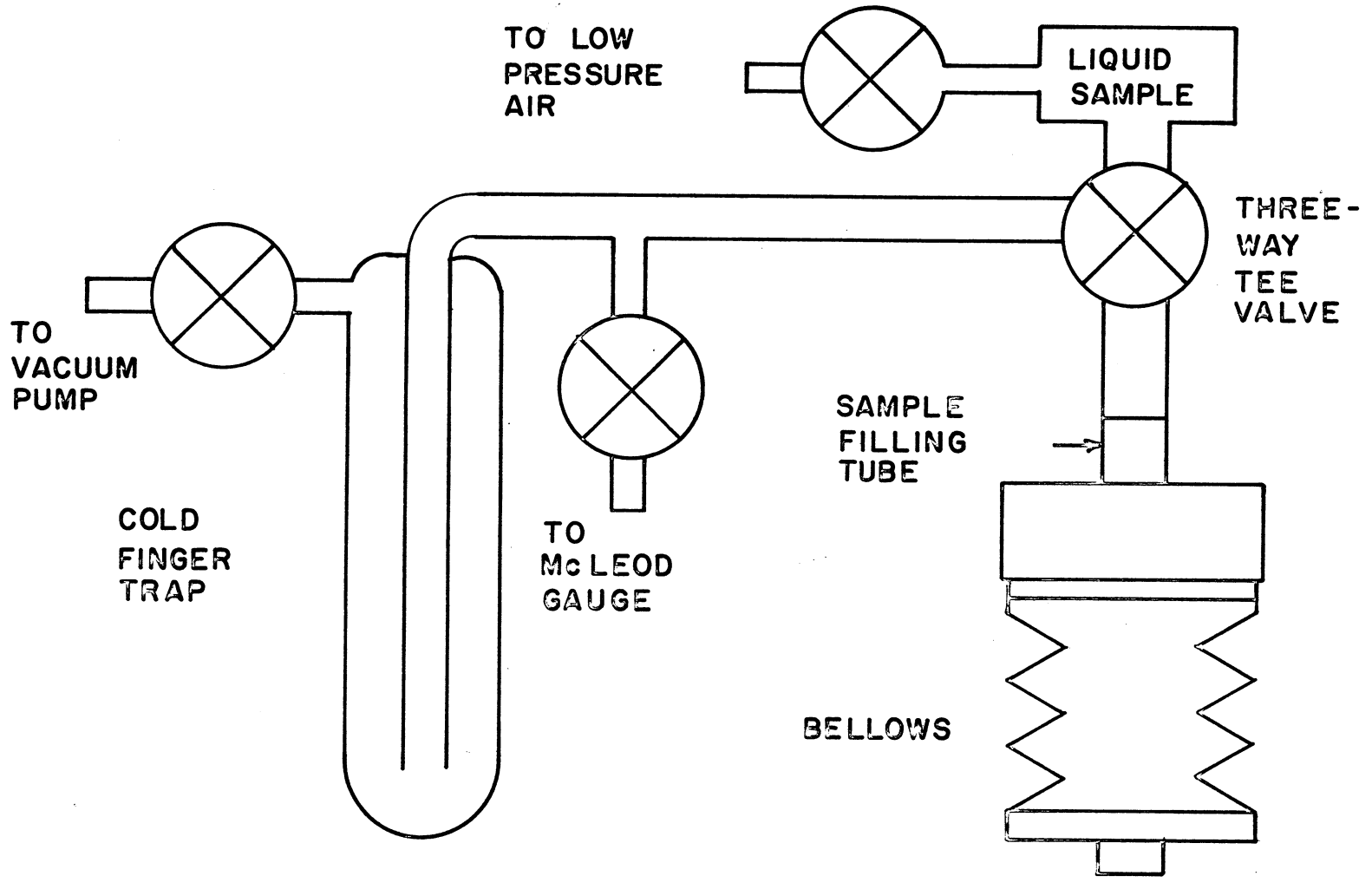

FIGURE 69. SAMPLE FILLING APPARATUS

APPENDIX F

RAW DATA

The raw resistance versus pressure data is listed in Table XV. Also listed are the manganin cell zero point and high pressure resistances in the cases where the data range extended beyond 50,000 psi. The table is ordered by compound or mixture and then by temperature for the compound or mixture, lowest first. The table order is: n-Decane, n-Dodecane, n-Tetradecane, n-Hexadecane, misture of 0.5000 mole fraction n-Decane and n-Tetradecane, mixture of 0.5000 mole fraction n-Dodecane and n-Hexadecane, and a mixture of 0.6000 mole fraction n-Decane and 0.2000 mole fraction n-Tetradecane and n-Hexadecane.

TABLE XV

N-DECANE AT 25.00 DEG. C.

DENSITY = .72588 GM./C.C. SAMPLE WEIGHT = 2.07530 GM.

RA (OHMNS)	RMN (OHMNS)	P (PSI)	P (PATM)
0.26800	104.38005	14.7	1.0
0.26879	0.0	292.7	19.9
0.26950	0.0	523.7	35.6
0.27081	0.0	1006.7	68.5
0.27180	0.0	1401.7	95.4
0.27313	0.0	1994.7	135.7
0.27618	0.0	3194.7	217.4
0.27902	0.0	4524.7	307.9
0.28224	0.0	6094.7	414.7
0.28498	0.0	7584.7	516.1
0.28750	0.0	9024.7	614.1
0.28994	0.0	10574.7	719.6
0.29224	0.0	12064.7	821.0
0.29423	0.0	13584.7	924.4
0.29623	0.0	15034.7	1023.0
0.29811	0.0	16534.7	1125.1
0.30018	0.0	18014.7	1225.8
0.30208	0.0	19994.7	1360.6
0.30454	0.0	22014.7	1498.0
0.30723	0.0	25194.7	1714.4
0.30993	0.0	27994.7	1904.9
0.31228	0.0	31014.7	2110.4
0.31469	0.0	33954.7	2310.5

TABLE XV (CONTINUED)

N-DECANE AT 45.00 DEG. C.

DENSITY = .71059 GM./C.C. SAMPLE WEIGHT = 2.07530 GM.

RA (OHMNS)	RMN (OHMNS)	P (PSI)	(PATM)
0.26001	104.37925	14.7	1.0
0.26103	0.0	300.7	20.5
0.26164	0.0	460.7	31.3
0.26339	0.0	1024.7	69.7
0.26490	0.0	1474.7	100.3
0.26619	0.0	2014.7	137.1
0.26913	0.0	3044.7	207.2
0.27290	0.0	4584.7	312.0
0.27613	0.0	5984.7	407.2
0.27956	0.0	7614.7	518.1
0.28226	0.0	9064.7	616.8
0.28510	0.0	10664.7	725.7
0.28739	0.0	12074.7	821.6
0.28975	0.0	13614.7	926.4
0.29206	0.0	15114.7	1028.5
0.29425	0.0	16794.7	1142.8
0.29590	0.0	18064.7	1229.2
0.29936	0.0	21084.7	1434.7
0.30268	0.0	24014.7	1634.1
0.30580	0.0	27184.7	1849.8
0.30843	0.0	30064.7	2045.8
0.31079	0.0	33054.7	2249.2
0.31326	0.0	36014.7	2450.6
0.31521	0.0	39014.7	2654.8
0.31733	0.0	41884.7	2850.1
0.31919	0.0	44994.7	3061.7
0.32129	0.0	48114.7	3274.0
0.32208	105.22900	49492.6	3367.8
0.32506	105.31290	54389.7	3701.0

TABLE XV (CONTINUED)

N-DECANE AT 65.00 DEG. C.

DENSITY = .69512 GM./C.C. SAMPLE WEIGHT = 2.07530 GM.

RA (OHMNS)	RMN (OHMNS)	P (PSI)	P (PATM)
0.25175	104.37840	14.7	1.0
0.25288	0.0	327.7	22.3
0.25386	0.0	492.7	33.5
0.25568	0.0	1009.7	68.7
0.25754	0.0	1444.7	98.3
0.25945	0.0	2094.7	142.5
0.26233	0.0	3084.7	209.9
0.26651	0.0	4534.7	308.6
0.27023	0.0	5994.7	407.9
0.27399	0.0	7604.7	517.5
0.27706	0.0	9084.7	618.2
0.28031	0.0	10674.7	726.4
0.28268	0.0	12114.7	824.4
0.28501	0.0	13474.7	916.9
0.28752	0.0	15039.7	1023.4
0.29007	0.0	16794.7	1142.8
0.29185	0.0	17994.7	1224.5
0.29564	0.0	21004.7	1429.3
0.29947	0.0	24034.7	1635.5
0.30235	0.0	27104.7	1844.4
0.30547	0.0	30144.7	2051.2
0.30824	0.0	33194.7	2258.8
0.31035	0.0	36024.7	2451.3
0.31265	0.0	39204.7	2667.7
0.31489	0.0	42064.7	2862.3
0.31676	0.0	45084.7	3067.8
0.31883	0.0	48014.7	3267.2
0.32140	105.28130	52594.5	3578.8
0.32381	105.34910	56553.3	3848.2
0.32491	105.38725	58781.7	3999.8
0.32809	105.48785	64661.3	4399.9
0.33110	105.59755	71077.8	4836.5

TABLE XV (CONTINUED)

N-DECANE AT 85.00 DEG. C.

DENSITY = .67945 GM./C.C. SAMPLE WEIGHT = 2.07530 GM.

RA (OHMNS)	RMN (OHMNS)	P (PSI)	(PATM)
0.24359	104.37705	14.7	1.0
0.24490	0.0	301.7	20.5
0.24577	0.0	529.7	36.0
0.24773	0.0	994.7	67.7
0.24983	0.0	1436.7	97.8
0.25144	0.0	1994.7	135.7
0.25596	0.0	3114.7	211.9
0.25904	0.0	4024.7	273.9
0.26207	0.0	5144.7	350.1
0.26452	0.0	6134.7	417.4
0.26705	0.0	7054.7	480.0
0.26959	0.0	8084.7	550.1
0.27416	0.0	10184.7	693.0
0.27604	0.0	11064.7	752.9
0.27782	0.0	12044.7	819.6
0.27997	0.0	13044.7	887.6
0.28159	0.0	14134.7	961.8
0.28316	0.0	15034.7	1023.0
0.28413	0.0	15664.7	1065.9
0.28635	0.0	17014.7	1157.8
0.28806	0.0	18134.7	1234.0
0.28935	0.0	19064.7	1297.3
0.29061	0.0	20134.7	1370.1
0.29218	0.0	21034.7	1431.3
0.29419	0.0	22934.7	1560.6
0.29701	0.0	25014.7	1702.1
0.29909	0.0	27244.7	1853.9
0.30124	0.0	29054.7	1977.0
0.30328	0.0	31284.7	2128.8
0.30565	0.0	33814.7	2300.9
0.30693	0.0	35164.7	2392.8
0.30874	0.0	37014.7	2518.7
0.30989	0.0	38954.7	2650.7
0.31185	0.0	40984.7	2788.8
0.31284	0.0	43144.7	2935.8
0.31460	0.0	45064.7	3066.5
0.31570	0.0	46934.7	3193.7
0.31730	0.0	49039.7	3336.9
0.31915	105.28345	52798.8	3592.7
0.32210	105.35725	57108.2	3886.0
0.32383	105.42440	61031.4	4152.9

TABLE XV (CONTINUED)

N-DECANE AT 85.00 DEG. C.

RA (OHMNS)	RMN (OHMNS)	P (PSI)	(PATM)
0.32383	105.42440	61031.4	4152.9
0.32764	105.55360	68585.5	4666.9
0.32846	105.56050	68989.1	4694.4
0.33066	105.64635	74013.1	5036.3
0.33107	105.67540	75713.8	5152.0
0.33913	106.00655	95128.2	6473.1

TABLE XV (CONTINUED)

N-DODECANE AT 25.00 DEG. C.

DENSITY = .74490 GM./C.C. SAMPLE WEIGHT = 2.18552 GM.

RA (OHMNS)	RMN (OHMNS)	P (PSI)	P (PATM)
0.25938	0.0	14.7	1.0
0.26008	0.0	252.7	17.2
0.26091	0.0	425.7	29.0
0.26165	0.0	999.7	68.0
0.26288	0.0	1462.7	99.5
0.26398	0.0	1974.7	134.4
0.26633	0.0	3014.7	205.1
0.26949	0.0	4524.7	307.9
0.27239	0.0	5984.7	407.2
0.27509	0.0	7544.7	513.4
0.27767	0.0	9054.7	616.1
0.27990	0.0	10554.7	718.2
0.28222	0.0	12034.7	818.9
0.28418	0.0	13614.7	926.4
0.28622	0.0	15024.7	1022.4
0.28794	0.0	16604.7	1129.9
0.28981	0.0	18024.7	1226.5
0.29130	0.0	19484.7	1325.9
0.29327	0.0	21014.7	1430.0

TABLE XV (CONTINUED)

N-DODECANE AT 45.00 DEG. C.

DENSITY = .73030 GM./C.C. SAMPLE WEIGHT = 2.18552 GM.

RA (OHMNS)	RMN (OHMNS)	P (PSI)	P (PATM)
0.25162	0.0	14.7	1.0
0.25241	0.0	253.7	17.3
0.25324	0.0	532.7	36.2
0.25471	0.0	1012.7	68.9
0.25613	0.0	1446.7	98.4
0.25716	0.0	2014.7	137.1
0.26064	0.0	3094.7	210.6
0.26346	0.0	4514.7	307.2
0.26670	0.0	6014.7	409.3
0.26969	0.0	7544.7	513.4
0.27235	0.0	9014.7	613.4
0.27505	0.0	10544.7	717.5
0.27725	0.0	11994.7	816.2
0.27960	0.0	13594.7	925.1
0.28177	0.0	15094.7	1027.1
0.28386	0.0	16654.7	1133.3
0.28560	0.0	18054.7	1228.5
0.28799	0.0	20074.7	1366.0
0.29018	0.0	21994.7	1496.6
0.29353	0.0	25284.7	1720.5
0.29602	0.0	27974.7	1903.6
0.29775	0.0	30014.7	2042.4
0.29950	0.0	32014.7	2178.5

TABLE XV (CONTINUED)

N-DODECANE AT 65.00 DEG. C.

DENSITY = .71563 GM./C.C. SAMPLE WEIGHT = 2.18552 GM.

RA (OHMNS)	RMN (OHMNS)	P (PSI)	(PATM)
0.24412	104.38100	14.7	1.0
0.24488	0.0	294.7	20.1
0.24563	0.0	530.7	36.1
0.24733	0.0	1040.7	70.8
0.24854	0.0	1398.7	95.2
0.25049	0.0	2014.7	137.1
0.25338	0.0	3064.7	208.5
0.25750	0.0	4584.7	312.0
0.26129	0.0	6064.7	412.7
0.26438	0.0	7564.7	514.7
0.26736	0.0	9094.7	618.9
0.27023	0.0	10534.7	716.8
0.27288	0.0	12064.7	821.0
0.27523	0.0	13664.7	929.8
0.27736	0.0	15044.7	1023.7
0.27957	0.0	16604.7	1129.9
0.28170	0.0	18064.7	1229.2
0.28407	0.0	20014.7	1361.9
0.28659	0.0	22114.7	1504.8
0.28966	0.0	24964.7	1698.7
0.29310	0.0	28104.7	1912.4
0.29546	0.0	31064.7	2113.8
0.29818	0.0	34104.7	2320.7
0.30043	0.0	36924.7	2512.6
0.30287	0.0	40114.7	2729.6
0.30485	0.0	42994.7	2925.6
0.30709	0.0	46114.7	3137.9
0.30895	0.0	49004.7	3334.6
0.31082	105.27230	51917.4	3532.8

TABLE XV (CONTINUED)

N-DODECANE AT 85.00 DEG. C.

DENSITY = .70082 GM./C.C. SAMPLE WEIGHT = 2.18552 GM.

RA (OHMNS)	RMN (OHMNS)	P (PSI)	(PATM)
0.23521	104.38145	14.7	1.0
0.23645	0.0	311.7	21.2
0.23763	0.0	548.7	37.3
0.23946	0.0	1037.7	70.6
0.24114	0.0	1459.7	99.3
0.24305	0.0	2034.7	138.5
0.24673	0.0	3114.7	211.9
0.25103	0.0	4544.7	309.2
0.25487	0.0	5964.7	405.9
0.25899	0.0	7544.7	513.4
0.26194	0.0	9034.7	614.8
0.26510	0.0	10554.7	718.2
0.26799	0.0	12064.7	821.0
0.27041	0.0	13464.7	916.2
0.27321	0.0	15064.7	1025.1
0.27780	0.0	18134.7	1234.0
0.28027	0.0	20134.7	1370.1
0.28294	0.0	21994.7	1496.6
0.28641	0.0	25144.7	1711.0
0.28968	0.0	28114.7	1913.1
0.29241	0.0	31144.7	2119.3
0.29515	0.0	33924.7	2308.4
0.29747	0.0	37094.7	2524.1
0.30021	0.0	39934.7	2717.4
0.30209	0.0	42994.7	2925.6
0.30459	0.0	46034.7	3132.5
0.30637	0.0	48974.7	3332.5
0.31062	105.34615	56202.9	3824.4
0.31335	105.41905	60461.6	4114.2

TABLE XV (CONTINUED)

N-HEXADECANE AT 25.00 DEG. C.

DENSITY = .75888 GM./C.C. SAMPLE WEIGHT = 2.24803 GM.

RA (OHMNS)	RMN (OHMNS)	P (PSI)	P (PATM)
0.25242	0.0	14.7	1.0
0.25261	0.0	129.7	8.8
0.25334	0.0	337.7	23.0
0.25374	0.0	484.7	33.0
0.25485	0.0	1030.7	70.1
0.25629	0.0	1467.7	98.5
0.25710	0.0	2054.7	139.8
0.25856	0.0	2534.7	172.5
0.25928	0.0	3064.7	208.5
0.26084	0.0	3564.7	242.6
0.26126	0.0	4064.7	276.6
0.26256	0.0	4574.7	311.3
0.26299	0.0	5044.7	343.3
0.26433	0.0	5564.7	378.7
0.26472	0.0	6074.7	413.4
0.26617	0.0	6544.7	445.3
0.26667	0.0	7044.7	479.4
0.26789	0.0	7474.7	508.6
0.26821	0.0	7984.7	543.3
0.26954	0.0	8584.7	584.2
0.27134	0.0	9594.7	652.9

TABLE XV (CONTINUED)

N-HEXADECANE AT 45.00 DEG. C.

DENSITY = .74477 GM./C.C. SAMPLE WEIGHT = 2.24803 GM.

RA (OHMNS)	RMN (OHMNS)	P (PSI)	P (PATM)
0.24535	0.0	14.7	1.0
0.24609	0.0	174.7	11.9
0.24639	0.0	344.7	23.5
0.24693	0.0	561.7	38.2
0.24839	0.0	1096.7	74.6
0.24959	0.0	1429.7	97.3
0.25089	0.0	2054.7	139.8
0.25222	0.0	2564.7	174.5
0.25335	0.0	3084.7	209.9
0.25459	0.0	3624.7	246.6
0.25556	0.0	4044.7	275.2
0.25679	0.0	4564.7	310.6
0.25748	0.0	5024.7	341.9
0.26154	0.0	7084.7	482.1
0.26334	0.0	7964.7	542.0
0.26515	0.0	9154.7	622.9
0.26692	0.0	10014.7	681.5
0.26826	0.0	11114.7	756.3
0.27010	0.0	12054.7	820.3
0.27145	0.0	13164.7	895.8
0.27290	0.0	14004.7	953.0
0.27406	0.0	15084.7	1026.4
0.27566	0.0	15994.7	1088.4
0.27654	0.0	16964.7	1154.4
0.27809	0.0	18034.7	1227.2
0.27955	0.0	19014.7	1293.9
0.28055	0.0	20034.7	1363.3
0.28167	0.0	21244.7	1445.6
0.28264	0.0	22054.7	1500.7
0.28373	0.0	22984.7	1564.0
0.28506	0.0	24084.7	1638.9

TABLE XV (CONTINUED)

N-HEXADECANE AT 65.00 DEG. C.

DENSITY = .73057 GM./C.C. SAMPLE WEIGHT = 2.24803 GM.

RA (OHMNS)	RMN (OHMNS)	P (PSI)	P (PATM)
0.23847	0.0	14.7	1.0
0.23902	0.0	199.7	13.6
0.24006	0.0	507.7	34.5
0.24179	0.0	1055.7	71.8
0.24475	0.0	2094.7	142.5
0.24741	0.0	3104.7	211.3
0.24999	0.0	4034.7	274.5
0.25208	0.0	5024.7	341.9
0.25431	0.0	6014.7	409.3
0.25677	0.0	7134.7	485.5
0.25861	0.0	7994.7	544.0
0.26078	0.0	9154.7	622.9
0.26247	0.0	10054.7	684.2
0.26424	0.0	11044.7	751.5
0.26572	0.0	12034.7	818.9
0.26739	0.0	13094.7	891.0
0.26875	0.0	14024.7	954.3
0.27046	0.0	15084.7	1026.4
0.27181	0.0	16084.7	1094.5
0.27326	0.0	17214.7	1171.4
0.27449	0.0	18064.7	1229.2
0.27572	0.0	19154.7	1303.4
0.27703	0.0	20104.7	1368.0
0.27821	0.0	21154.7	1439.5
0.27948	0.0	22134.7	1506.2
0.28036	0.0	23034.7	1567.4
0.28173	0.0	24084.7	1638.9
0.28268	0.0	25084.7	1706.9
0.28373	0.0	26044.7	1772.2
0.28440	0.0	27114.7	1845.0
0.28571	0.0	28094.7	1911.7
0.28642	0.0	29114.7	1981.1
0.28757	0.0	30134.7	2050.5
0.28811	0.0	31124.7	2117.9
0.28913	0.0	32034.7	2179.8
0.28978	0.0	33084.7	2251.3
0.29097	0.0	34114.7	2321.4
0.29175	0.0	35064.7	2386.0
0.29269	0.0	36004.7	2450.0

TABLE XV (CONTINUED)

N-HEXADECANE AT 85.00 DEG. C.

DENSITY = .71625 GM./C.C. SAMPLE WEIGHT = 2.24803 GM.

RA (OHMNS)	RMN (OHMNS)	P (PSI)	(PATM)
0.23031	104.37510	14.7	1.0
0.23077	0.0	139.7	9.5
0.23253	0.0	566.7	38.6
0.23404	0.0	1005.7	68.4
0.23579	0.0	1466.7	99.8
0.23740	0.0	1994.7	135.7
0.24100	0.0	3164.7	215.3
0.24342	0.0	4039.7	274.9
0.24625	0.0	5064.7	344.6
0.24860	0.0	6054.7	412.0
0.25306	0.0	8024.7	546.0
0.25524	0.0	9064.7	616.8
0.25744	0.0	10114.7	688.3
0.25920	0.0	11044.7	751.5
0.26106	0.0	12114.7	824.4
0.26255	0.0	13014.7	885.6
0.26420	0.0	14154.7	963.2
0.26577	0.0	15064.7	1025.1
0.26745	0.0	16144.7	1098.6
0.26880	0.0	17024.7	1158.5
0.27032	0.0	18114.7	1232.6
0.27175	0.0	19084.7	1298.6
0.27297	0.0	20214.7	1375.5
0.27428	0.0	21074.7	1434.0
0.27611	0.0	23174.7	1576.9
0.27899	0.0	25014.7	1702.1
0.28082	0.0	27014.7	1838.2
0.28336	0.0	29114.7	1981.1
0.28513	0.0	31214.7	2124.0
0.28710	0.0	33014.7	2246.5
0.28847	0.0	35234.7	2397.6
0.29046	0.0	37014.7	2518.7
0.29175	0.0	39039.7	2656.5
0.29367	0.0	41024.7	2791.6
0.29507	0.0	43154.7	2936.5
0.29663	0.0	45114.7	3069.9
0.29716	0.0	47104.7	3205.3
0.29915	0.0	49044.7	3337.3
0.30018	105.24570	50709.3	3450.5
0.30176	105.28825	53192.9	3619.5

TABLE XV (CONTINUED)

N-TETRADECANE AT 25.00 DEG. C.

DENSITY = .76968 GM./C.C. SAMPLE WEIGHT = 2.26350 GM.

RA (OHMNS)	RMN (OHMNS)	P (PSI)	(PATM)
0.25315	0.0	14.7	1.0
0.25368	0.0	91.7	6.2
0.25386	0.0	164.7	11.2
0.25412	0.0	244.7	16.7
0.25449	0.0	312.7	21.3
0.25453	0.0	395.7	26.9
0.25474	0.0	470.7	32.0
0.25505	0.0	646.7	44.0
0.25498	0.0	688.7	46.9
0.25548	0.0	770.7	52.4
0.25542	0.0	871.7	59.3
0.25585	0.0	936.7	63.7
0.25590	0.0	1070.7	72.9
0.25662	0.0	1230.7	83.7
0.25629	0.0	1237.7	84.2
0.25721	0.0	1516.7	103.2
0.25709	0.0	1734.7	118.0
0.25826	0.0	2084.7	141.9
0.25810	0.0	2184.7	148.7
0.25932	0.0	2564.7	174.5
0.26009	0.0	2994.7	203.8
0.25990	0.0	3194.7	217.4
0.26120	0.0	3514.7	239.2
0.26214	0.0	4064.7	276.6

TABLE XV (CONTINUED)

N-TETRADECANE AT 45.00 DEG. C.

DENSITY = .75586 GM./C.C. SAMPLE WEIGHT = 2.26350 GM.

RA (OHMNS)	RMN (OHMNS)	P (PSI)	P (PATM)
0.24667	0.0	14.7	1.0
0.24700	0.0	152.7	10.4
0.24726	0.0	274.7	18.7
0.24828	0.0	548.7	37.3
0.24915	0.0	1034.7	70.4
0.25163	0.0	1984.7	135.1
0.25413	0.0	3094.7	210.6
0.25633	0.0	4044.7	275.2
0.25796	0.0	5064.7	344.6
0.26004	0.0	6024.7	410.0
0.26183	0.0	7144.7	486.2
0.26374	0.0	8064.7	548.8
0.26515	0.0	9114.7	620.2
0.26677	0.0	10014.7	681.5
0.26834	0.0	11084.7	754.3
0.26991	0.0	12084.7	822.3
0.27090	0.0	13084.7	890.4
0.27252	0.0	14094.7	959.1
0.27344	0.0	15034.7	1023.0
0.27548	0.0	16014.7	1089.7

TABLE XV (CONTINUED)

N-TETRADECANE AT 65.00 DEG. C.

DENSITY = .74202 GM./C.C. SAMPLE WEIGHT = 2.26350 GM.

RA (OHMNS)	RMN (OHMNS)	P (PSI)	(PATM)
0.23953	0.0	14.7	1.0
0.23990	0.0	108.7	7.4
0.24018	0.0	215.7	14.7
0.24120	0.0	484.7	33.0
0.24243	0.0	1005.7	68.4
0.24526	0.0	2034.7	138.5
0.24799	0.0	3114.7	211.9
0.25030	0.0	4014.7	273.2
0.25229	0.0	5034.7	342.6
0.25465	0.0	6014.7	409.3
0.25655	0.0	7114.7	484.1
0.25878	0.0	8064.7	548.8
0.26032	0.0	9114.7	620.2
0.26207	0.0	10034.7	682.8
0.26381	0.0	11194.7	761.8
0.26519	0.0	12034.7	818.9
0.26645	0.0	13044.7	887.6
0.26844	0.0	14044.7	955.7
0.26980	0.0	15134.7	1029.9
0.27112	0.0	16014.7	1089.7
0.27347	0.0	18134.7	1234.0
0.27644	0.0	20124.7	1369.4
0.27844	0.0	22184.7	1509.6
0.28062	0.0	24064.7	1637.5
0.28255	0.0	26254.7	1786.5
0.28452	0.0	28024.7	1907.0
0.28632	0.0	30064.7	2045.8

TABLE XV (CONTINUED)

N-TETRADECANE AT 85.00 DEG. C.

DENSITY = .72810 GM./C.C. SAMPLE WEIGHT = 2.26350 GM.

RA (OHMNS)	RMN (OHMNS)	P (PSI)	P (PATM)
0.23184	0.0	14.7	1.0
0.23215	0.0	55.7	3.8
0.23268	0.0	132.7	9.0
0.23372	0.0	534.7	36.4
0.23533	0.0	939.7	63.9
0.23851	0.0	2084.7	141.9
0.24175	0.0	3094.7	210.6
0.24504	0.0	4504.7	306.5
0.24695	0.0	5064.7	344.6
0.24901	0.0	6074.7	413.4
0.25137	0.0	7114.7	484.1
0.25323	0.0	8104.7	551.5
0.25559	0.0	9174.7	624.3
0.25708	0.0	10094.7	686.9
0.25943	0.0	11024.7	750.2
0.26045	0.0	12114.7	824.4
0.26246	0.0	13114.7	892.4
0.26372	0.0	14114.7	960.4
0.26551	0.0	15194.7	1033.9
0.26740	0.0	16584.7	1128.5
0.26979	0.0	18014.7	1225.8
0.27215	0.0	20094.7	1367.4
0.27506	0.0	22114.7	1504.8
0.27697	0.0	24164.7	1644.3
0.27947	0.0	26134.7	1778.4
0.28102	0.0	28114.7	1913.1
0.28308	0.0	30104.7	2048.5
0.28532	0.0	32154.7	2188.0
0.28659	0.0	34214.7	2328.2
0.28844	0.0	36194.7	2462.9
0.28989	0.0	38234.7	2601.7
0.29161	0.0	40094.7	2728.3
0.29287	0.0	42084.7	2863.7

TABLE XV (CONTINUED)

MIXTURE 0.5000 MOLE FRACTION N-DECANE AND N-TETRADECANE
AT 25.00 DEG. C.

DENSITY = .74490 GM./C.C. SAMPLE WEIGHT = 2.18239 GM.

RA (OHMNS)	RMN (OHMNS)	P (PSI)	(PATM)
0.25833	0.0	14.7	1.0
0.25867	0.0	253.7	17.3
0.25918	0.0	545.7	37.1
0.26037	0.0	1036.7	70.5
0.26154	0.0	1456.7	99.1
0.26258	0.0	2014.7	137.1
0.26404	0.0	2594.7	176.6
0.26483	0.0	3064.7	208.5
0.26603	0.0	3524.7	239.8
0.26676	0.0	4024.7	273.9
0.26827	0.0	4594.7	312.6
0.26989	0.0	5544.7	377.3
0.27221	0.0	6594.7	448.7
0.27346	0.0	7554.7	514.1
0.27548	0.0	8604.7	585.5
0.27653	0.0	9494.7	646.1
0.27851	0.0	10544.7	717.5
0.27971	0.0	11564.7	786.9
0.28130	0.0	12524.7	852.3
0.28245	0.0	13534.7	921.0
0.28412	0.0	14564.7	991.1
0.28518	0.0	15554.7	1058.4
0.28668	0.0	16624.7	1131.2
0.28760	0.0	17384.7	1183.0
0.28880	0.0	18484.7	1257.8

TABLE XV (CONTINUED)

MIXTURE 0.5000 MOLE FRACTION N-DECANE AND N-TETRADECANE
AT 45.00 DEG. C.

DENSITY = .73030 GM./C.C. SAMPLE WEIGHT = 2.18239 GM.

RA (OHMNS)	RMN (OHMNS)	P (PSI)	(PATM)
0.25031	0.0	14.7	1.0
0.25095	0.0	249.7	17.0
0.25187	0.0	488.7	33.3
0.25332	0.0	999.7	68.0
0.25473	0.0	1445.7	98.4
0.25627	0.0	2024.7	137.8
0.25880	0.0	3094.7	210.6
0.26185	0.0	4474.7	304.5
0.26541	0.0	6044.7	411.3
0.26795	0.0	7414.7	504.5
0.27106	0.0	9004.7	612.7
0.27355	0.0	10634.7	723.6
0.27605	0.0	12094.7	823.0
0.27826	0.0	13704.7	932.5
0.28019	0.0	14964.7	1018.3
0.28222	0.0	16614.7	1130.6
0.28431	0.0	18084.7	1230.6
0.28754	0.0	21034.7	1431.3
0.29082	0.0	23994.7	1632.7
0.29360	0.0	27014.7	1838.2
0.29686	0.0	30094.7	2047.8

TABLE XV (CONTINUED)

MIXTURE 0.5000 MOLE FRACTION N-DECANE AND N-TETRADECANE
AT 65.00 DEG. C.

DENSITY = .71563 GM./C.C. SAMPLE WEIGHT = 2.18239 GM.

RA (OHMNS)	RMN (OHMNS)	P (PSI)	(PATM)
0.24251	0.0	14.7	1.0
0.24334	0.0	263.7	17.9
0.24416	0.0	479.7	32.6
0.24600	0.0	1031.7	70.2
0.24756	0.0	1490.7	101.4
0.24880	0.0	1984.7	135.1
0.25235	0.0	3144.7	214.0
0.25632	0.0	4484.7	305.2
0.26293	0.0	7624.7	518.8
0.26581	0.0	9024.7	614.1
0.26865	0.0	10614.7	722.3
0.27144	0.0	12094.7	823.0
0.27354	0.0	13634.7	927.8
0.27592	0.0	15084.7	1026.4
0.27791	0.0	16624.7	1131.2
0.28034	0.0	18144.7	1234.7
0.28248	0.0	21124.7	1437.4
0.28518	0.0	22054.7	1500.7
0.28832	0.0	25284.7	1720.5
0.29130	0.0	27944.7	1901.5
0.29383	0.0	31144.7	2119.3
0.29708	0.0	34134.7	2322.7
0.29971	0.0	37114.7	2525.5
0.30157	0.0	40054.7	2725.6
0.30350	0.0	43014.7	2927.0
0.30591	0.0	46014.7	3131.1

TABLE XV (CONTINUED)

MIXTURE 0.5000 MOLE FRACTION N-DECANE AND N-TETRADECANE
AT 85.00 DEG. C.

DENSITY = .70082 GM./C.C. SAMPLE WEIGHT = 2.18239 GM.

RA (OHMNS)	RMN (OHMNS)	P (PSI)	(PATM)
0.23427	104.38270	14.7	1.0
0.23467	0.0	144.7	9.8
0.23492	0.0	225.7	15.4
0.23523	0.0	265.7	18.1
0.23528	0.0	306.7	20.9
0.23583	0.0	394.7	26.9
0.23624	0.0	520.7	35.4
0.23683	0.0	616.7	42.0
0.23725	0.0	717.7	48.8
0.23758	0.0	818.7	55.7
0.23820	0.0	938.7	63.9
0.23838	0.0	1041.7	70.9
0.23850	0.0	1042.7	71.0
0.23953	0.0	1267.7	86.3
0.24035	0.0	1490.7	101.4
0.24184	0.0	2014.7	137.1
0.24534	0.0	3064.7	208.5
0.24966	0.0	4524.7	307.9
0.25431	0.0	6134.7	417.4
0.25813	0.0	7624.7	518.8
0.26067	0.0	9014.7	613.4
0.26391	0.0	10704.7	728.4
0.26676	0.0	12114.7	824.4
0.26934	0.0	13614.7	926.4
0.27193	0.0	15164.7	1031.9
0.27356	0.0	16644.7	1132.6
0.27620	0.0	18024.7	1226.5
0.27879	0.0	20184.7	1373.5
0.28179	0.0	22194.7	1510.3
0.28352	0.0	24034.7	1635.5
0.28610	0.0	26024.7	1770.9
0.28899	0.0	29244.7	1990.0
0.29207	0.0	32014.7	2178.5
0.29430	0.0	35094.7	2388.0
0.29752	0.0	37944.7	2582.0
0.29908	0.0	41084.7	2795.6
0.30229	0.0	43994.7	2993.7
0.30338	0.0	46954.7	3195.1
0.30599	0.0	49914.7	3396.5
0.30721	105.29030	52868.9	3597.5
0.30944	105.34375	55989.7	3809.9

TABLE XV (CONTINUED)

MIXTURE 0.5000 MOLE FRACTION N-DECANE AND N-TETRADECANE
AT 85.00 DEG. C.

RA (OHMNS)	RMN (OHMNS)	P (PSI)	(PATM)
0.30944	105.34375	55989.7	3809.9
0.31101	105.39165	58787.6	4000.2
0.31286	105.45315	62381.4	4244.8

TABLE XV (CONTINUED)

MIXTURE 0.5000 MOLE FRACTION N-DODECANE AND N-HEXADECANE
AT 25.00 DEG. C.

DENSITY = .75888 GM./C.C. SAMPLE WEIGHT = 2.23155 GM.

RA (OHMNS)	RMN (OHMNS)	P (PSI)	(PATM)
0.26218	0.0	14.7	1.0
0.26281	0.0	258.7	17.6
0.26358	0.0	505.7	34.4
0.26419	0.0	752.7	51.2
0.26484	0.0	1066.7	72.6
0.26515	0.0	1264.7	84.7
0.26587	0.0	1485.7	101.1
0.26681	0.0	1994.7	135.7
0.26817	0.0	2584.7	175.9
0.26898	0.0	3014.7	205.1
0.26991	0.0	3514.7	239.2
0.27093	0.0	3984.7	271.1
0.27196	0.0	4534.7	308.6
0.27297	0.0	5064.7	344.6
0.27397	0.0	5584.7	380.0
0.27491	0.0	6044.7	411.3
0.27568	0.0	6564.7	446.7
0.27662	0.0	7064.7	480.7
0.27727	0.0	7524.7	512.0
0.27821	0.0	8084.7	550.1

TABLEXV (CONTINUED)

MIXTURE 0.5000 MOLE FRACTION N-DODECANE AND N-HEXADECANE
AT 45.00 DEG. C.

DENSITY = .74477 GM./C.C. SAMPLE WEIGHT = 2.23155 GM.

RA (OHMNS)	RMN (OHMNS)	P (PSI)	(PATM)
0.25500	0.0	14.7	1.0
0.25595	0.0	265.7	18.1
0.25674	0.0	513.7	35.0
0.25860	0.0	1262.7	85.9
0.25905	0.0	1450.7	98.7
0.26056	0.0	1984.7	135.1
0.26345	0.0	3134.7	213.3
0.26499	0.0	4044.7	275.2
0.26700	0.0	4984.7	339.2
0.26924	0.0	6024.7	410.0
0.27155	0.0	7114.7	484.1
0.27300	0.0	8064.7	548.8
0.27476	0.0	9094.7	618.9
0.27648	0.0	10064.7	684.9
0.27797	0.0	11084.7	754.3
0.27960	0.0	12084.7	822.3
0.28092	0.0	13064.7	889.0
0.28237	0.0	14084.7	958.4
0.28360	0.0	14984.7	1019.6
0.28478	0.0	15914.7	1082.9
0.28615	0.0	17044.7	1159.8
0.28732	0.0	18014.7	1225.8

TABLE XV (CONTINUED)

MIXTURE 0.5000 MOLE FRACTION N-DODECANE AND N-HEXADECANE
AT 65.00 DEG. C.

DENSITY = .73057 GM./C.C. SAMPLE WEIGHT = 2.23155 GM.

RA (OHMNS)	RMN (OHMNS)	P (PSI)	(PATM)
0.24782	0.0	14.7	1.0
0.24844	0.0	252.7	17.2
0.24943	0.0	514.7	35.0
0.25094	0.0	1009.7	68.7
0.25217	0.0	1426.7	97.1
0.25374	0.0	2014.7	137.1
0.25676	0.0	3064.7	208.5
0.26033	0.0	4524.7	307.9
0.26381	0.0	6014.7	409.3
0.26695	0.0	7574.7	515.4
0.26995	0.0	9074.7	617.5
0.27231	0.0	10594.7	720.9
0.27479	0.0	11934.7	812.1
0.27718	0.0	13584.7	924.4
0.27922	0.0	14964.7	1018.3
0.28165	0.0	16614.7	1130.6
0.28349	0.0	17954.7	1221.7
0.28610	0.0	20114.7	1368.7
0.28825	0.0	22014.7	1498.0
0.29046	0.0	24104.7	1640.2
0.29224	0.0	25764.7	1753.2
0.29535	0.0	28974.7	1971.6
0.29806	0.0	31874.7	2168.9

TABLE XV (CONTINUED)

MIXTURE 0.5000 MOLE FRACTION N-DODECANE AND N-HEXADECANE
AT 85.00 DEG. C.

DENSITY = .71625 GM./C.C. SAMPLE WEIGHT = 2.23155 GM.

RA (OHMNS)	RMN (OHMNS)	P (PSI)	(PATM)
0.23993	0.0	14.7	1.0
0.24057	0.0	250.7	17.1
0.24192	0.0	534.7	36.4
0.24347	0.0	1014.7	69.0
0.24507	0.0	1434.7	97.6
0.24694	0.0	2024.7	137.8
0.25000	0.0	3024.7	205.8
0.25423	0.0	4554.7	309.9
0.25785	0.0	5934.7	403.8
0.26165	0.0	7604.7	517.5
0.26484	0.0	9064.7	616.8
0.26772	0.0	10564.7	718.9
0.27051	0.0	12124.7	825.0
0.27303	0.0	13654.7	929.1
0.27510	0.0	14964.7	1018.3
0.27746	0.0	16664.7	1134.0
0.27954	0.0	18044.7	1227.9
0.28212	0.0	20124.7	1369.4
0.28455	0.0	22004.7	1497.3
0.28713	0.0	24194.7	1646.3
0.28916	0.0	26014.7	1770.2
0.29118	0.0	28124.7	1913.8
0.29312	0.0	30054.7	2045.1
0.29587	0.0	33054.7	2249.2
0.29838	0.0	35914.7	2443.8
0.30080	0.0	39154.7	2664.3
0.30288	0.0	42194.7	2871.2
0.30538	0.0	45214.7	3076.7
0.30722	0.0	48044.7	3269.2

TABLE XV (CONTINUED)

MIXTURE 0.6000 MOLE FRACTION N-DECANE, 0.2000 MOLE FRACTION N-TETRADECANE AND N-HEXADECANE AT 25.00 DEG. C.

DENSITY = .74490 GM./C.C. SAMPLE WEIGHT = 2.14735 GM.

RA (OHMNS)	RMN (OHMNS)	P (PSI)	(PATM)
0.26695	0.0	14.7	1.0
0.26765	0.0	244.7	16.7
0.26823	0.0	513.7	35.0
0.26967	0.0	1012.7	68.9
0.27051	0.0	1473.7	100.3
0.27185	0.0	2014.7	137.1
0.27407	0.0	3034.7	206.5
0.27636	0.0	4054.7	275.9
0.27833	0.0	5174.7	352.1
0.28029	0.0	6034.7	410.6
0.28152	0.0	6944.7	472.6
0.28379	0.0	8094.7	550.8
0.28518	0.0	9064.7	616.8
0.28692	0.0	10114.7	688.3
0.28814	0.0	11054.7	752.2
0.28981	0.0	12054.7	820.3
0.29092	0.0	13034.7	887.0
0.29237	0.0	14014.7	953.6
0.29342	0.0	15074.7	1025.8
0.29451	0.0	15814.7	1076.1
0.29591	0.0	16964.7	1154.4

TABLE XV (CONTINUED)

MIXTURE 0.6000 MOLE FRACTION N-DECANE, 0.2000 MOLE FRACTION N-TETRADECANE AND N-HEXADECANE AT 45.00 DEG. C.

DENSITY = .73030 GM./C.C. SAMPLE WEIGHT = 2.14735 GM.

RA (OHMNS)	RMN (OHMNS)	P (PSI)	(PATM)
0.25938	0.0	14.7	1.0
0.26015	0.0	272.7	18.6
0.26136	0.0	544.7	37.1
0.26260	0.0	985.7	67.1
0.26369	0.0	1432.7	97.5
0.26500	0.0	2024.7	137.8
0.26770	0.0	3094.7	210.6
0.27129	0.0	4534.7	308.6
0.27382	0.0	5924.7	403.2
0.27757	0.0	7614.7	518.1
0.28000	0.0	9084.7	618.2
0.28272	0.0	10634.7	723.6
0.28475	0.0	12014.7	817.5
0.28734	0.0	13694.7	931.9
0.28904	0.0	15014.7	1021.7
0.29131	0.0	16614.7	1130.6
0.29280	0.0	18014.7	1225.8
0.29574	0.0	20194.7	1374.2
0.29752	0.0	22034.7	1499.4
0.29970	0.0	24054.7	1636.8
0.30142	0.0	26154.7	1779.7
0.30317	0.0	27914.7	1899.5
0.30480	0.0	30004.7	2041.7

TABLE XV (CONTINUED)

MIXTURE 0.6000 MOLE FRACTION N-DECANE, 0.2000 MOLE FRACTION N-TETRADECANE AND N-HEXADECANE AT 65.00 DEG. C.

DENSITY = .71563 GM./C.C. SAMPLE WEIGHT = 2.14735 GM.

RA (OHMNS)	RMN (OHMNS)	P (PSI)	(PATM)
0.25167	0.0	14.7	1.0
0.25272	0.0	261.7	17.8
0.25344	0.0	463.7	31.6
0.25528	0.0	1002.7	68.2
0.25857	0.0	2014.7	137.1
0.26123	0.0	2954.7	201.1
0.26509	0.0	4534.7	308.6
0.26857	0.0	6044.7	411.3
0.27164	0.0	7314.7	497.7
0.27496	0.0	9054.7	616.1
0.27778	0.0	10544.7	717.5
0.27984	0.0	12064.7	821.0
0.28276	0.0	13614.7	926.4
0.28475	0.0	15014.7	1021.7
0.28697	0.0	16614.7	1130.6
0.28886	0.0	17974.7	1223.1
0.29159	0.0	20174.7	1372.8
0.29374	0.0	22004.7	1497.3
0.29626	0.0	24174.7	1645.0
0.29790	0.0	25914.7	1763.4
0.30022	0.0	28214.7	1919.9
0.30185	0.0	29974.7	2039.6
0.30471	0.0	33294.7	2265.6
0.30673	0.0	36014.7	2450.6
0.30933	0.0	39134.7	2662.9
0.31146	0.0	42344.7	2881.4
0.31263	0.0	43814.7	2981.4
0.31396	0.0	45944.7	3126.3

TABLEXV (CONTINUED)

MIXTURE 0.6000 MOLE FRACTION N-DECANE, 0.2000 MOLE FRACTION N-TETRADECANE AND N-HEXADECANE AT 85.00 DEG. C.

DENSITY = .70082 GM./C.C. SAMPLE WEIGHT = 2.14735 GM.

RA (OHMNS)	RMN (OHMNS)	P (PSI)	(PATM)
0.24358	104.38525	14.7	1.0
0.24458	0.0	251.7	17.1
0.24593	0.0	593.7	40.4
0.24749	0.0	996.7	67.8
0.24924	0.0	1406.7	95.7
0.25100	0.0	2024.7	137.8
0.25424	0.0	2964.7	201.7
0.25936	0.0	4684.7	318.8
0.26293	0.0	6034.7	410.6
0.26669	0.0	7604.7	517.5
0.27006	0.0	9174.7	624.3
0.27302	0.0	10594.7	720.9
0.27575	0.0	12114.7	824.4
0.27816	0.0	13614.7	926.4
0.28052	0.0	15014.7	1021.7
0.28298	0.0	16594.7	1129.2
0.28502	0.0	18114.7	1232.6
0.28776	0.0	20114.7	1368.7
0.29024	0.0	22084.7	1502.8
0.29265	0.0	24164.7	1644.3
0.29471	0.0	26024.7	1770.9
0.29799	0.0	29264.7	1991.3
0.30064	0.0	32014.7	2178.5
0.30341	0.0	35124.7	2390.1
0.30552	0.0	37974.7	2584.0
0.30797	0.0	41064.7	2794.3
0.31000	0.0	43934.7	2989.6
0.31204	0.0	46834.7	3186.9
0.31393	0.0	49764.7	3386.3
0.31539	105.27930	52077.9	3543.7
0.31746	105.34590	55966.4	3808.3
0.31791	105.35905	56734.4	3860.5
0.32045	105.44080	61510.5	4185.5

APPENDIX G

EDULJEE ERROR ANALYSIS

Described below is a detailed error analysis on the experimental method of Eduljee (17). Several experimental uncertainties are not reported by Eduljee. These have been estimated and are based upon accuracies obtainable at present and thus should be conservative. It will also be assumed that all errors due to temperature and pressure effects, introduced no error into the final results.

1. Error Analysis

The apparatus used was of the mercury contact displacement type. Writing the data reduction equation:

$$\frac{\Delta V}{V_o} = \frac{A_o \cdot \Delta L \cdot \rho_o}{W} \qquad \text{(G-1)}$$

Where: $\frac{\Delta V}{V_o}$ is the compression, A_o is the cross sectional area of the capillary tube containing the contacts, W is the sample weight, ρ_o is the fiducial density, and ΔL is the distance between contacts in the capillary tube.

Thus the error in the compression is:

$$\delta\left(\frac{\Delta V}{V_o}\right) = \frac{A_o \cdot \Delta L \cdot \rho_o}{w}\left[\frac{\delta A_o}{A_o} + \frac{\delta \Delta L}{\Delta L} + \frac{\delta \rho_o}{\rho_o} + \frac{\delta w}{w}\right] \qquad \text{(G-2)}$$

Each of the four quantities on the right hand side of G-1 will be considered separately.

a. Sample Weight

The reported sample weight is 1.67 grams. Assume an error of $\pm$ 0.0001 grams in the sample weight.

b. Sample Desnity

The reported fiducial densities are 0.67 gm/cc nominal. Assume an error of $\pm$ 0.0001 gm/cc in the fiducial density.

c. Distance Between Contacts

The reported distance between contacts is 1.13 cm. Assume the contact make to break error on the mercury contact is $\pm$ 0.001 cm.

d. Capillary Cross Sectional Area

The capillary tube had a diameter of 4 mm. Thus its area was 0.126 cm^2. The uncertainty in the cross sectional area was determined via a mercury weight technique. The equation for A_o is:

$$A_o = \frac{w}{\rho_{Hg} \cdot \Delta L} \qquad \text{(G-3)}$$

The error in A_o is:

$$\delta A_o = \frac{W}{\rho_{Hg} \Delta L} \cdot \left[\frac{\delta w}{w} + \frac{\delta \Delta L}{\Delta L} \right] . \qquad (G-4)$$

The error in ρ_{Hg} was assumed to be 0.0. The volume between contacts was approximately 0.143 cc. Thus the mercury weight was W = 0.143 cc · 13.6 gm/cc = 1.95 gm. Assume an error of ± 0.0001 gm in the weighing. Then

$$\delta A_o = .126 \left[\frac{10^{-4}}{1.95} + \frac{10^{-3}}{1.13} \right], \text{ or}$$

$$\delta A_o = 1.16 \times 10^{-4} \text{ cm.}$$

e. Evaluating the Error in Compression

Substitution into equation G-2 yields:

$$\delta\left(\frac{\Delta V}{V_o}\right) = \frac{(0.126)(1.13)(.67)}{1.67} \left[\frac{1.16 \times 10^{-4}}{.126} + \frac{1. \times 10^{-3}}{1.13} + \frac{1. \times 10^{-4}}{.67} + \frac{1. \times 10^{-4}}{1.67} \right],$$

or

$$\delta\left(\frac{\Delta V}{V_o}\right) = \pm 1.35 \times 10^{-3} \text{ cc/cc.}$$

2. Conclusion

From the above it appears the Eduljee reported experimental reproducibility not actual absolute error. His data is absolute to ± 0.001 compression or relative volume.

ADDENDUM

The buoyancy correction was omitted in the weighing of the mercury for the capillary tube radius determination. This changes the capillary tube radius from 0.100319 cm, which was rounded to 0.100320 cm, to 0.100317 cm which is rounded to 0.100320 cm.

The buoyancy correction was also omitted in the differential weighing to determine the amount of sample contained within the bellows. This correction amounts to about 0.15% of the sample weight. The corrected sample weights are tabulated below. The compression data ($\Delta V/V_o$) maybe corrected by multiplying by the uncorrected weight and dividing by the corrected weight.

Compound or Mixture	Old Weight (gm.)	Corrected Weight (gm.)
A	2.07530	2.07833
B	2.18552	2.18559
C	2.24803	2.25111
D	2.26350	2.26656
FU	2.18239	2.18546
IU	2.23155	2.23466
Tl	2.14735	2.15037

In the case of n-Decane at 85.00°C and 6473 atmospheres this changes the compression from 0.2396 cc/cc to 0.2392 cc/cc. This is maximum correction. The correction in turn changes the Tait coefficient J by about 0.15%. This correction is small enough that it is within the experimental error on the isothermal compressibility and cannot be seen on the plots.

The tabulated Prausnitz, Flory, and Scaled particle parameters are all slightly in err due to this and should be redetermined as covered above.

The undersigned, appointed by the Dean of the Graduate Faculty, have examined a thesis entitled

The Pressure, Volume, Temperature, and Composition Properties of Liquid n-Alkane Mixtures at Elevated Pressures.

presented by Phillip Sidney Snyder

a candidate for the degree of Doctor of Philosophy

and hereby certify that in their opinion it is worthy of acceptance.

Jack Winnick

Truman Storvick

Robert E Harris

VITA

The author was born on November 10, 1941 in Melrose Park, Illinois. He obtained an A.A. degree from Fullerton Junior College in Fullerton, California in 1962. He married Linda Ruth Brown in August of 1963. He obtained a B.S. degree from the University of California at Berkeley in 1965. In 1965 he enrolled in the Ph.D. program at the University of Missouri at Columbia. In July of 1965 he became the father of twin sons, Thomas and John.

University Libraries
University of Missouri

Digitization Information Page

Local identifier	Snyder1969

Source information

Format	Book
Content type	Text with images
Source ID	department copy
Notes	

Capture information

Date captured	April 2023
Scanner manufacturer	Fujitsu
Scanner model	fi-7460
Scanning system software	ScandAll Pro v. 2.1.5 Premium
Optical resolution	600 dpi
Color settings	8 bit grayscale
File types	tiff
Notes	

Derivatives - Access copy

Compression	Tiff: LZW compression
Editing software	Adobe Photoshop
Resolution	600 dpi
Color	grayscale
File types	tiff/pdf
Notes	Images cropped, straightened, brightened